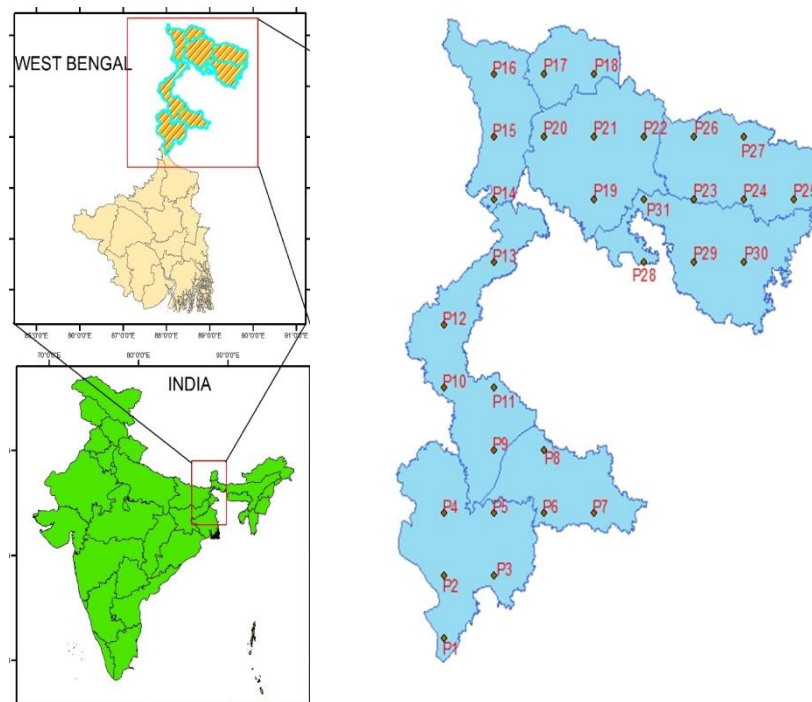


RAINFALL TREND ANALYSIS IN NORTHERNWEST BENGAL FROM 1901-2015

A thesis submitted toward partial fulfilment of the requirements for the degree of

MASTER OF ENGINEERING

in Water Resources and Hydraulic Engineering
Course affiliated to Faculty of Engineering & Technology, Jadavpur University



submitted by

SANTOSH KUMAR

Roll No:M4WRE22002

Under the guidance of

Dr. RAJIB DAS

Assistant Professor

School of Water Resources Engineering, Jadavpur University

School of Water Resources Engineering
Jadavpur University
Kolkata 700032, India

2022

RAINFALL TREND ANALYSIS IN NORTHERNWEST BENGAL FROM 1901-2015

A thesis submitted toward partial fulfilment of the requirements for the degree
of

MASTER OF ENGINEERING

in Water Resources and Hydraulic Engineering

Course affiliated to Faculty of Engineering & Technology

Jadavpur University

submitted by

SANTOSH KUMAR

Roll No: M4WRE22002

Under the guidance of

Dr. RAJIB DAS

Assistant Professor

School of Water Resources Engineering, Jadavpur University

School of Water Resources Engineering

M.E. (Water Resources & Hydraulic Engineering) course affiliated to

Faculty of Engineering & Technology

Jadavpur University

Kolkata 700032, India

2022



Declaration of Originality and Compliance of Academic Ethics

I hereby declare that this thesis contains literature survey and original research work by the undersigned candidate, as part of my Master of Engineering degree in Water Resources & Hydraulic Engineering, in the Faculty of Engineering & Technology, Jadavpur University during the academic session 2020-22.

All information in this document has been obtained and presented in accordance with academic rules and ethical conduct.

I also declare that, as required by these rules and conduct, I have fully cited and referred all materials and results that are not original to this work.

Name : SANTOSH KUMAR

Roll No : M4WRE22002

**Thesis Title : RAINFALL TREND ANALYSIS IN NORTHERN WEST BENGAL FROM
1901-2015**

Date:

Place: S.W.R.E, Jadavpur University

SANTOSH KUMAR

Roll. No:M4WRE22002

M.E. (Water Resources and Hydraulic Engineering) Course affiliated to
Faculty of Engineering and Technology
Jadavpur University
Kolkata – 700032, India

CERTIFICATE OF RECOMMENDATION

This is to certify that the thesis entitled “**RAINFALL TREND ANALYSIS IN NORTHERN WEST BENGAL FROM 1901-2015**” is Bona-fide work carried out by Santosh Kumar under our supervision and guidance of Dr.Rajib Das for partial fulfilment of the requirements for the Post Graduate degree of Master of Engineering in Water Resources & Hydraulic Engineering during the academic session 2020-2022 in the department of School of Water Resources Engineering, Jadavpur University, Kolkata – 700032.

THESIS ADVISOR

Dr.Rajib Das

Assistant Professor

School of Water Resources Engineering

Jadavpur University

DIRECTOR

School of Water Resources Engineering

Jadavpur University

DEAN

Faculty of Interdisciplinary Studies, Law & Management

Jadavpur University



**M.E. (Water Resources and Hydraulic Engineering) Course affiliated to
Faculty of Engineering and Technology
Jadavpur University
Kolkata – 700032, India**

CERTIFICATE OF APPROVAL

This foregoing thesis is hereby approved as a credible study of an Engineering subject carried out and presented in a manner satisfactorily to warrant its acceptance as a prerequisite to the degree for which it has been submitted. It is understood that by this approval the undersigned do not endorse or approve any statement made or opinion expressed, or conclusion drawn therein but approve the thesis only for the purpose for which it has been submitted.

**Committee of final examination for the
evaluation of the thesis**

DEDICATION

This thesis is dedicated to my parents and my respected teachers, who never stopped encouraging me throughout this endeavour and constantly inspired me to keep working hard and encouraged me to never stop learning.



ACKNOWLEDGEMENT

I express my sincere gratitude to my supervisor **Dr.Rajib Das**, Assistant professor, School of Water Resources Engineering, Jadavpur University under whose supervision and guidance this work has been carried out. I am deeply indebted to him for his valuable suggestions, inspiring guidance and continuous help, which made possible the completion of the present work. It would have been impossible to carry out this thesis work with confidence without his wholehearted involvement, advice, support and constant encouragement throughout.

I also express my sincere gratitude to **Prof. (Dr.) Pankaj Kumar Roy, Director**, School of Water Resources Engineering, Jadavpur University; **Prof. (Dr.) Asis Mazumdar**, Professor, SWRE, Jadavpur University; **Dr. Subhashish Das**, Associate Professor, SWRE, Jadavpur University and **Dr. Gourab Banerjee**, Assistant Professor, SWRE, Jadavpur University and Gaurav Patel, AICTE Doctoral Fellow, Jadavpur University for their valuable suggestions. Thanks, are also due to all the faculties and staffs of School of Water Resources Engineering Jadavpur University for their direct and indirect help and support.

Date:

Place:

SANTOSH KUMAR

ROLL NO - M4WRE22002

ABSTRACT

India is home to an extraordinary variety of climatic regions, ranging from tropical in the south to temperate and alpine in the Himalayan north, where elevated regions receive sustained winter snowfall. The nation's climate is strongly influenced by the Himalayas and the Thar Desert. The Thar Desert plays a role in attracting moisture-laden southwest summer monsoon winds that, between June and October, provide the majority of India's rainfall. Being a very big geographical area India experience much variation in the rainfall pattern as northern India get rainfall during the monsoon season while south India get rainfall on the time of Retreating monsoon. In the same we can observe difference in rainfall in the northern part of west Bengal and southern part of west Bengal because northern part of west Bengal is near to The Himalayas while south Bengal is near to Bay of Bengal. But in the current study we are working on northern eight districts of West Bengal. The thesis brings the result of the analysis based on the recent 115 years of data (1901-2015) on the mean spatial rainfall pattern. The study aims to investigate rainfall trends in Northern part of West Bengal comprising of eight districts. The study is carried out to understanding the underlying feature for the purpose of forecasting and in identifying the changes and impact that are very crucial for an Agro-based economy like the one of West Bengal, India. Here we studied using monthly data series of last 115 years (1901-2015). The present study, based on the data for the period 1901-2015, examines the seasonal and annual mean precipitation by the method of Mann-Kendall analysis, Sen-slope estimator and Innovative trend analysis (ITA).

TABLE OF CONTENTS

Declaration.....	ii
Certificate of Recommendation.....	iii
Certificate of Approval.....	iv
Dedication.....	v
Acknowledgement	vi
Abstract	vii
1. CHAPTER 1	
1.1. INTRODUCTION	1
1.1.1. HYDROLOGIC CYCLE.....	1-3
1.1.2. CHARACTERISTICS OF RAINFALL IN INDIA.....	3-7
2. CHAPTER 2	
2.1 LITERATURE REVIEW.....	8-13
3. CHAPTER 3	
3.1 OBJECTIVE.....	14
3.2 METHODOLOGY.....	14
3.3 DATA AND STUDY AREA.....	14-17
4. CHAPTER 4	
4.1 RESULT AND DISCUSSION	
4.1.1 INNOVATIVE TREND ANALYSIS.....	18-70
4.1.2 SEN SLOPE ANALYSIS.....	71-152
4.1.3 MAN-KENDALL ANALYSIS.....	153-159
4.2 DISTRICT-WISE DISCUSSION OF THE RESULTS.....	160-164
5. CHAPTER 5	
5.1 CONCLUSION	165
6. CHAPTER 6	
6.1 FUTURE SCOPE	166
7. CHAPTER 5	
7.1 REFERENCES.....	167-168

CHAPTER 1

1.1.1 INTRODUCTION

The Indian subcontinent is home to 1.3 billion people and major part its economy depends on agriculture-based production. Summer monsoon precipitation in India which spans generally from June to September (JJAS) each year, plays a critical parameter in providing water for agricultural purposes and other necessities. Monsoon precipitation is highly variable in terms of its temporal and spatial distribution, which can lead to extreme events such as droughts and floods. Apart from the land-sea contrast, the spatial variability of precipitation is also governed by the local drivers. These also include the orography, land use, and land cover, terrestrial moisture sources, anthropogenic emissions, aerosols, etc. (Shastri et al., 2015; Das et al., 2016; Pathak et al., 2017; Salvi and Ghosh, 2019). A thorough understanding of both global and local drivers is extremely crucial to study the complexities associated with the rainfall pattern over a particular region and its possible variations in the future. Some knowledge about Hydrological cycle is also important to understand all these complex phenomena.

Hydrology is the scientific study of the movement, distribution, and management of water on Earth and other planets, including the water cycle, water resources, and environmental watershed sustainability. Hydrology has been a subject of investigation and engineering for millennia. Marcus Vitruvius, in the first century BC, described a philosophical theory of the hydrologic cycle, in which precipitation falling in the mountains infiltrated the Earth's surface and led to streams and springs in the lowlands. With the adoption of a more scientific approach, Leonardo da Vinci and Bernard Palissy independently reached an accurate representation of the hydrologic cycle. It was not until the 17th century that hydrologic variables began to be quantified.

1.1.2 HYDROLOGIC CYCLE

The water, or hydrologic, cycle describes the pilgrimage of water as water molecules make their way from the Earth's surface to the atmosphere and back again, in some cases to below the surface. This gigantic system, powered by energy from the Sun, is a continuous exchange of moisture between the oceans, the atmosphere, and the land.

Studies have revealed that evaporation—the process by which water changes from a liquid to a gas—from oceans, seas, and other bodies of water (lakes, rivers, streams) provides nearly 90% of the

moisture in our atmosphere. Most of the remaining 10% found in the atmosphere is released by plants through transpiration. Plants take in water through their roots, then release it through small pores on the underside of their leaves called stomata. In addition, a very small portion of water vapor enters the atmosphere through sublimation, the process by which water changes directly from a solid (ice or snow) to a gas. The gradual shrinking of snow banks in cases when the temperature remains below freezing results from sublimation.

Together, evaporation, transpiration, and sublimation, plus volcanic emissions, account for almost all the water vapor in the atmosphere that isn't inserted through human activities. While evaporation from the oceans is the primary vehicle for driving the surface-to-atmosphere portion of the hydrologic cycle, transpiration is also significant. For example, a cornfield 1 acre in size can transpire as much as 4,000 gallons of water every day.

After the water enters the lower atmosphere, rising air currents carry it upward, often high into the atmosphere, where the air is cooler. In the cool air, water vapor is more likely to condense from a gas to a liquid to form cloud droplets. Cloud droplets can grow and produce precipitation (including rain, snow, sleet, freezing rain, and hail), which is the primary mechanism for transporting water from the atmosphere back to the Earth's surface.

When precipitation falls over the land surface, it follows various routes in its subsequent paths. Some of it evaporates, returning to the atmosphere; some seeps into the ground as soil moisture or groundwater; and some runs off into rivers and streams. Almost all of the water eventually flows into the oceans or other bodies of water, where the cycle continues. At different stages of the cycle, some of the water is intercepted by humans or other life forms for drinking, washing, irrigating, and a large variety of other uses.

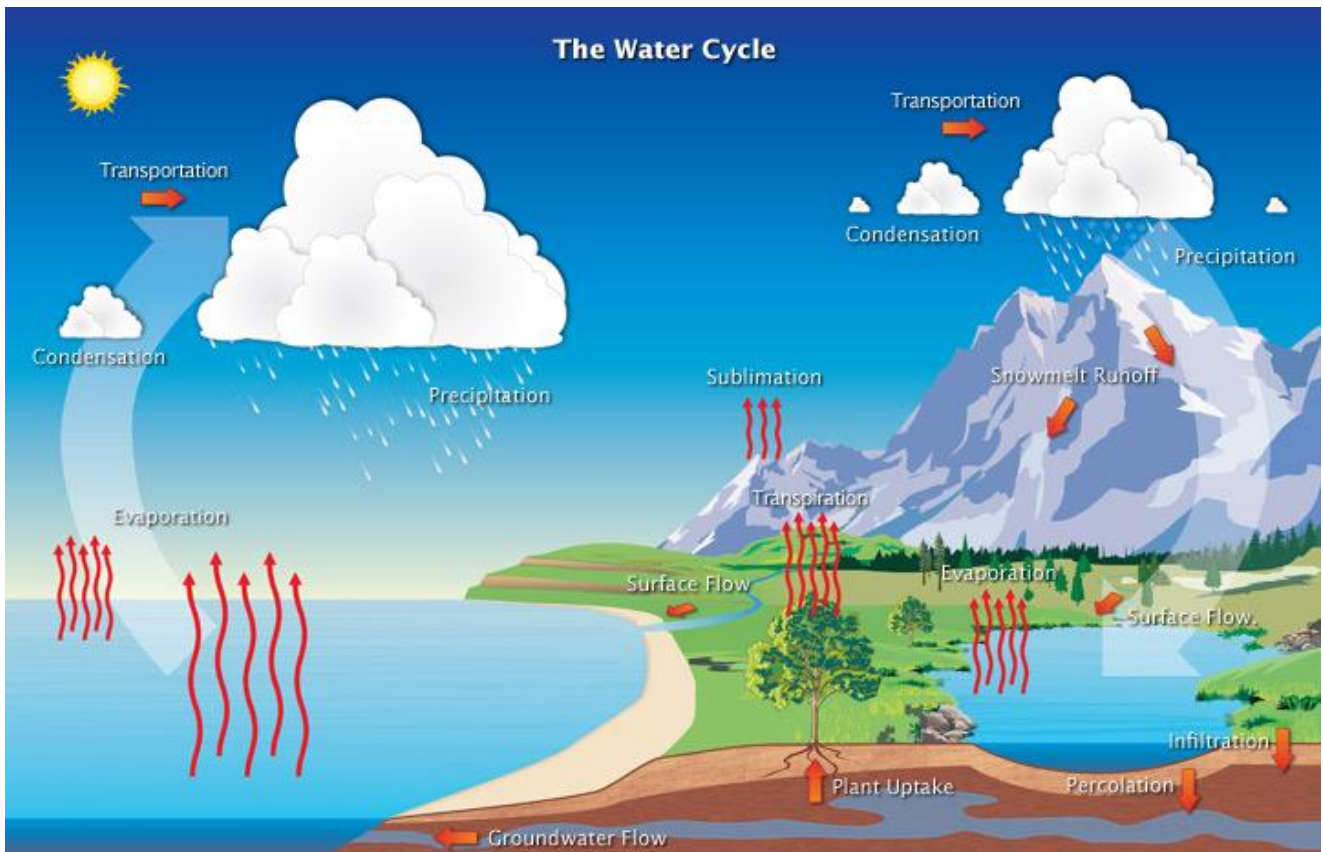


Fig 1: Diagram of water cycle

1.1.3 CHARACTERISTICS OF RAINFALL IN INDIA

From the point of view of climate, the Indian subcontinent can be considered to have two major seasons

- South-west monsoon (June-September)
- Winter season (December-February)

two transitional period as:

- Transition-1, post monsoon (October-November)
- Transition-2, summer, (march, may)

South-West monsoon (June-September)

The reversal of winds starts taking place over the Indian sub-continent during the summer season, when cold and dry continental north-westerly winds are replaced by warm and moist south-westerly winds. These winds originate in the Southern Hemisphere, cross the Equator (trade winds) and gets deflected to the right by the Coriolis force in the Northern Hemisphere.

The trade winds then approach the India sub-continent in two separate branches – the Bay of Bengal and the Arabian Sea

The four-month long Monsoon season, which runs from June to September, brings 70% of the country's annual rainfall. It holds a Long Period Average (LPA) of 89 cm of rain but never behaves in a normal manner. In fact, rainfall distribution mostly remains uneven both in space and time.

During the Monsoon season, low-pressure areas and depressions form on either side of the Indian Ocean – the Arabian Sea and the Bay of Bengal. However, these weather systems are more frequent in the Bay of Bengal. They are responsible for rainfall activity over the country during the Monsoon season. These systems lead to the commencement and further progress of Southwest Monsoon.

Southwest Monsoon in India is conceived as a complex phenomenon. A cautious approach is generally taken before announcing onset or withdrawal of Monsoon in India.

July and August are generally the active Monsoon months for the entire country. June is the onset month which witnesses an outburst of rain while, September is the withdrawal month, receiving more of sporadic rain.

Withdrawal is generally not attempted before September 1 and commences from extreme west Rajasthan. As Southwest Monsoon approaches the withdrawal phase from a particular region, certain conditions become prevalent. These include change of wind pattern, reduction in cloud cover, decrease in humidity, cessation of rain or sporadic rain, and temporary rising tendency of temperatures.

Winter season (December-February)

By about mid-December, disturbances of extra tropical origin travel eastwards across Afghanistan and Pakistan. Known as western disturbances, they cause moderate to heavy rain and snowfall (about 25cm) in the Himalayas, and, Jammu and Kashmir. Some light rainfall also occurs in the northern plane. Low-pressure areas in the Bay of Bengal formed in these months cause 10-12 cm of rainfall in the southern parts of Tamilnadu.

Post-monsoon (October-November)

The months of October-November form a period of transition from the hot rainy season to the dry winter conditions

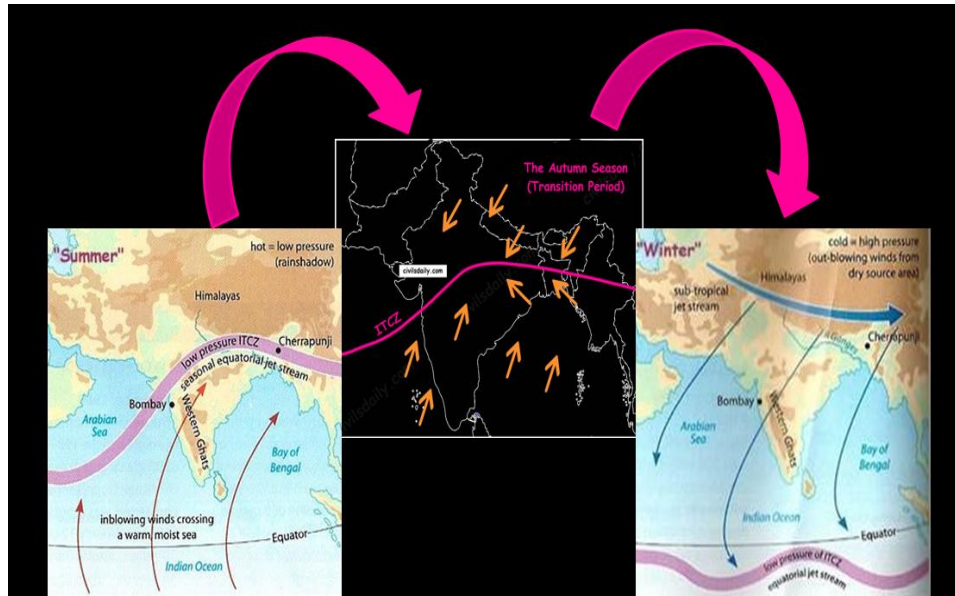


Fig 2: Post-Monsoon season

The withdrawal of the south-west monsoon and the onset of north-east monsoon are both gradual phenomena. They take place almost at the same time and tend to merge. This explains the popularity of the phrase “**Retreating Monsoon**”. The retreat takes place due to the weakening of the low-pressure area over the north-western parts of India (and thus a gradual transition of ITCZ towards the south). This happens due to:

- The apparent shift of sun towards the equator
- Reduction in temperature due to widespread rains.

Consequently, the air pressure starts decreasing. Such changes in the atmospheric pressure cause the south-west monsoons to withdraw.

The Retreat of Monsoons is a process much slower than its arrival. It does not imply a right about turn but a gradual change of comparative pressure positions, thus gradually weakening and reducing the area of coverage and influence

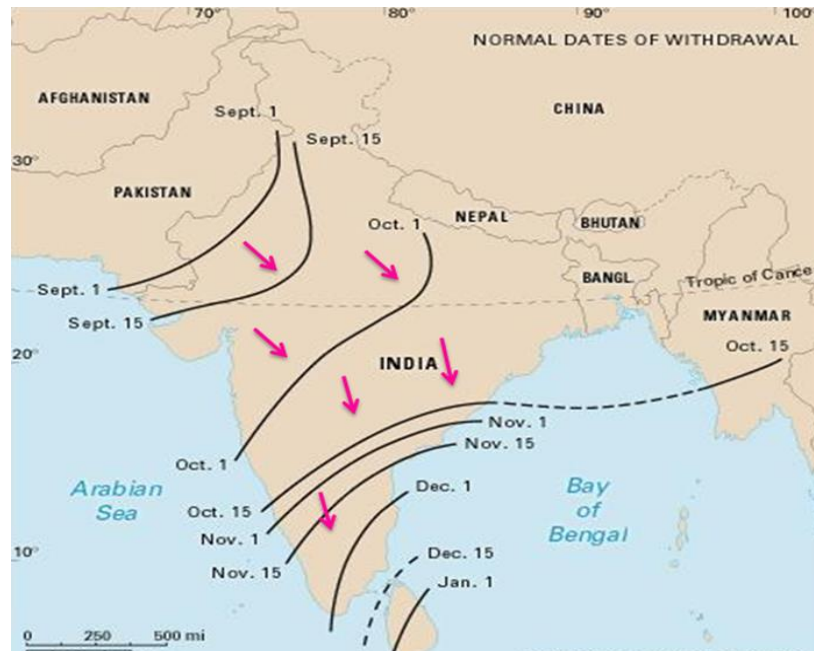


Fig 3: Post-Monsoon pattern

The south-west monsoons start retreating in the first week of September from Pakistan's border in North-West India. Thus, these winds withdraw earlier from the regions they reached the last.

The monsoon retreats from the western Rajasthan by the first week of September. It withdraws from Rajasthan, Gujarat, Western Ganga plain and the Central Highlands by the end of the month. By the beginning of October, the low pressure covers northern parts of the Bay of Bengal and by early November, it moves over Karnataka and Tamil Nadu. By the middle of December, the centre of low pressure is completely removed from the Peninsula.

Summer (Pre-monsoon) (March-May)

There is very little rainfall in India in this season. Convective cells cause some thunderstorms mainly in Kerala, West Bengal and Assam. Some cyclone activity, dominantly on the east coast, also occurs.

This thesis has been carried out to find the trend in the rainfall over the northern districts (Malda, Dakshin Dinajpur, Uttar Dinajpur, Alipurduar, Darjeeling, Kalimpong, Cooch Behar, Jalpaiguri) of the west-Bengal over a duration of 115 years i.e., 1901-2015. These eight districts have 31 different stations to collect rainfall data. Three different methods have been used to carry out the analysis. The methods used are

- Innovative trend analysis
- Man-Kendall Analysis
- Sen-slope

CHAPTER 2

2.1 Literature Review

Chung and Ramanathan (2006) Sea surface temperatures (SSTs) in the equatorial Indian Ocean have warmed by about 0.6–0.8 K since the 1950s, accompanied by very little warming or even a slight cooling trend over the northern Indian Ocean (NIO). It is reported that this differential trend has resulted in a substantial weakening of the meridional SST gradient from the equatorial region to the South Asian coast during summer, to the extent that the gradient has nearly vanished recently. Based on simulations with the Community Climate Model Version 3 (CCM3), it is shown that the summertime weakening in the SST gradient weakens the monsoon circulation, resulting in less monsoon rainfall over India and excess rainfall in sub-Saharan Africa. The observed trend in SST is decomposed into a hypothetical uniform warming and a reduction in the meridional gradient. The uniform warming of the tropical Indian Ocean in the authors' simulations increases the Indian summer monsoon rainfall by 1–2 mm day⁻¹, which is opposed by a larger drying tendency due to the weakening of the SST gradient. The net effect is to decrease the Indian monsoon rainfall, while preventing the sub-Saharan region from becoming too dry.

P. Guhathakurta and M. Rajeevan (2008) They examined the New monthly, seasonal and annual rainfall time series of 36 meteorological subdivisions of India were constructed using the monthly rainfall data for the period 1901 – 2003 of fixed network of 1476 rain gauge stations. In the new network, on an average, there is one rain gauge station for every 3402 Sq. km area. The new rainfall series is temporally as well as spatially homogenous. Linear trend analysis was carried out to examine the long-term trends in rainfall over different subdivisions and monthly contribution of each of the monsoon months to annual rainfall. During the south-west monsoon season, three subdivisions viz. Jharkhand, Chhattisgarh, Kerala showed significant decreasing trend and eight subdivisions viz. Gangetic WB, West UP, Jammu and Kashmir, Konkan and Goa, Madhya Maharashtra subdivision, Rayalaseema, Coastal AP and North Interior Karnataka showed significant increasing trends. It has been found that the contribution of June, July and September rainfall to annual rainfall is decreasing for few subdivisions while contribution of August rainfall is increasing in few other subdivisions. EOF analysis is also done to know the spatial distribution of rainfall. The all India Monthly, seasonal and annual rainfall series constructed based on the 1476 stations are also reported.

Pal et al. (2015) They estimate long-term trend in the amount of rainfall for Gangetic West Bengal (GWB) meteorological sub-division of India and each of the 13 districts under GWB separately. Monthly rain-fall time series data of 100 years (1901-2000) were analysed to measure monotonous trend of rainfall employing Sen's slope estimator. Statistical significance of the trend was determined using non-parametric Mann-Kendall test. An important result derived from the analysis was that the GWB sub-division and South 24 Parganas (S24P) district showed significant increasing trend (mm/year) of annual rainfall measuring 2.025 and 4.99 respectively. An inclining trend of monsoon precipitation, which was significant, found in four districts viz. Bankura, North 24 Parganas(N24P), S24P and West Midnapore along with GWB itself. A major finding of the study revealed that six districts and GWB had significant increasing trend in September rainfall with a maximum value of 1.324 mm/year in S24P district. Contribution of rainfall in October and post-monsoon season as well increased considerably in Kolkata and S24P districts while in December, similar trend was observed for Birbhum and Howrah districts. Murshidabad, S24P and East Midnapore districts experienced significant rising trend of precipitation in July, August and November respectively. On the contrary, Burdwan and Nadia districts, in the month of May and pre-monsoon season, had considerable declining trend of rainfall. Significant decreasing trend (mm/year) of precipitation, a concern for Nadia district, with magnitude of 0.127 and 0.293, was observed in the months of March and April respectively. Soumendu Chatterjee, Ansar Khan, Hashem Akbari, Yupeng Wang (2016) They investigate spatiotemporal monotonic trend and shift in concentration of monsoon precipitation across West Bengal, India, by analysing the time series of monthly precipitation from 18 weather stations during the period from 1901-2002. In dealing with, the in homogeneity in the precipitation series, RHtestsV4 software package is used to detect, and adjust for, multiple change points (shifts) that could exist in data series. Finally, the cumulative deviation test was applied at 5% significant level to check the homogeneity (presence of historic changes by cumulative deviations test). Afterward non-parametric Mann Kendal (MK) test and Theil-Sen estimator (TSE) was applied to detect of nature and slope of trends; and, Sequential Mann Kendall (SQMK) test was applied for detection of turning point and magnitude of change in trends. Prior to the application of statistical tests, the pre-whitening technique was used to eliminate the effect of auto correlation of precipitation data series. Four indices precipitation concentration index (PCI), precipitation concentration degree (PCD) and precipitation concentration period (PCP) and Fulcrum (Centre of gravity) were used to detect precipitation concentration and the spatial pattern in it. The application of the abovementioned procedures has shown very notable state wide monotonic trend for monsoon precipitation time series. Regional cluster analysis by SQMK found increasing precipitation in mountain and coastal regions in general except during the non- monsoon seasons. The results show that higher PCI values were mainly observed in South Bengal, whereas lower PCI values were mostly detected in North Bengal. The PCI values are noticeably larger in places where both monsoon total precipitation and span of rainy season are lower. The results of PCP reveal that precipitation in Gangetic Bengal mostly occurs in summer (monsoon

season), and the rainy season arrives earlier in North Bengal than South Bengal, whereas the results of PCD also indicate that the precipitation in North Bengal was more dispersed within a year than that in South Bengal. The concentration characteristic of precipitation could be detected by fulcrum analysis, and significant concentration over most of West Bengal was obvious within July month band. Precipitation trend observed in west Bengal is compared with that in CI region and comparison of precipitation departure with Indian monsoon and Gangetic Bengal can be explained by forecasting ensemble.

PulakGuhathakurta and Jayashree Revadekar (2017) Long-term (1901–2010) district data have been used to examine the observed variability and trends in rainfall during the south-west monsoon season (June–September) and north-east monsoon season (October–December) over India. South-west monsoon rainfall averaged over the country as a whole does not show any significant long-term trend during the period 1901–2010, suggesting that south-west monsoon system is stable. However, there is a significant multi-decadal epochal variability over the country and the four homogenous regions over India. The recent decades from 1971 onwards are found to be drier than normal with the recent decade 2001–2010 being the driest. Rainfall during the month of July shows a decreasing trend over most parts of the central India. However, rainfall during June and August shows increasing trend over the central and south-western parts of the country. Significant decreasing trends are observed in the seasonal rainfall over three subdivisions, and significant increasing trends are observed over eight other subdivisions. The analysis of the north-east monsoon (October–December) rainfall over the five met subdivisions of Peninsular India reveals no significant long-term trend. However, the presence of decadal variability in north-east monsoon rainfall is clearly observed.

Yingying Yuet al. (2019) Climate is one of the most important factors in agricultural production and livelihood of the coastal zone of Bangladesh and the bay of West Bengal, India. They studied, nearly 40 years (1970 – 2017) of historical rainfall and temperature data from six weather stations located in the coastal zone were analysed to assess their key characteristics influencing crop growth and yield. The results revealed that the rainfall in the coastal zone varied both spatially and seasonally. The total annual rainfall generally increased from the west to east and from north to south, resulting in rainfall difference up to 1000 mm year⁻¹. In addition to spatial variations, the rainfall varied seasonally, with the wettest 25% of days during the wet season contributing to more than 70% of the annual total precipitation. Heavy rainfall (> 40 mm day⁻¹) was found to occur in the dry season (from December to February), including around the sowing time of Rabi crops, resulting in a risk of waterlogging. Daily temperature and rainfall were also investigated to detect linear trends over the 40-year period.

Maximum temperature was found to have increased at five weather stations with an average rate of $0.04^{\circ}\text{C year}^{-1}$ except at Canning, West-Bengal showing that the coastal zone has been experiencing hotter and longer summers. The rainfall behaviour was more varied, although it exhibited a general increase in the recent decade.

Singh et al. (2020) They examined the Spatio-temporal trends and variability of seasonal and annual rainfall for 36 districts of Maharashtra, India. For this purpose, 118 years (1901 to 2018) gridded rainfall data of India Meteorological Department (IMD) were analysed using Mann-Kendall (MK), modified Mann-Kendall (MMK), Sen's slope (SS), Spearman's rank correlation (SRC), simple linear regression (SLR), and innovative trend analysis (ITA). Auto-correlation coefficient was calculated at lag-1 and tested at 5% level of significance. Rainfall variability was examined using the coefficient of variation (CV). The analysis revealed significantly decreasing trends for winter and premonsoon rainfall in districts of Maharashtra. Monsoon, post-monsoon, and annual rainfall had both increasing and decreasing trends. Out of 185 time series analysed, ITA detected trends in 168 (90.8%) time series. All the trends detected by MK/MMK, SRC, and SLR were captured by ITA, along with trends in additional 103(55.6%) time series which were not captured by any of the aforesaid methods. Rainfall variability was very high in all the districts for winter, pre-monsoon, and post-monsoon seasons. The trends and variability analysis of rainfall in the state along with their maps would be useful for the local stakeholders for planning efficient use of water resources

Denzil et al Meghalaya is known to receive the most torrential rainfall in the world, but the region suffers from water shortage as soon as the rain recedes, and the dry season starts. Changes in rainfall patterns and distribution can have a profound impact on water availability in a watershed, and therefore, examining spatial and temporal variations in rainfall is essential. However, the long-term rainfall variations in Meghalaya are not well explored. In this study, we take up two important watersheds in Meghalaya, i.e. Umiam and Umtru watersheds, to study the spatial and temporal rainfall variations. Using the gridded rainfall data from the Indian Meteorological Department from 1901 to 2018, we show that annual, winter, pre-monsoon, and monsoon rainfall is decreasing, whereas the post-monsoon rainfall is increasing. We use the innovative trend analysis (ITA) method to identify the trends in low-, medium-, and high-intensity rainfall. We find that low- and medium-intensity rainfall is in decreasing trend while high-intensity rainfall is increasing across annual and seasonal time scales. Lastly, we cross-check the trends detected using the innovative trend analysis method with a widely accepted Mann-Kendall (MK) test. We find that the results obtained by using the two methods generally concur; however, the ITA can detect non-

monotonic trends in different rainfall intensities and is more sensitive to hidden patterns than the MK test.

Malik et al Under the climate change scenario, the identification of drought trends is primarily essential for the efficient utilization of water resources. In this paper, two methods, including traditional Mann-Kendall (MK) and graphical Şen-Innovative Trend (ŞIT), were utilized for Effective Drought Index (EDI) trend detection at 13 meteorological stations situated in the State of Uttarakhand, India. The EDI was computed for 54 years from 1962 to 2015 using monthly rainfall data at the study stations. The magnitude (mm/year) of the EDI was derived by Sen's-Slope Estimator (SSE) method. In total, 156 series of data were analyzed, and the results showed that the ŞIT method detected a significantly negative/positive trend in 71/60 time series, while the MK method detected a significantly negative/positive trend in 25/9 time series from January to December at the study stations. Magnitude (mm/year) varies from – 0.0275 to 0.0256 (January), – 0.0352 to 0.0343 (February), – 0.0312 to 0.0312 (March), – 0.0343 to 0.0276 (April), – 0.0359 to 0.0237 (May), – 0.0293 to 0.0205 (June), – 0.0234 to 0.0235 (July), – 0.0277 to 0.0405 (August), – 0.0297 to 0.0247 (September), – 0.0288 to 0.0227 (October), – 0.0290 to 0.0241 (November), and – 0.0298 to 0.0236 (December) over the study region. Additionally, the results indicated the supremacy of the ŞIT method by examining the unobserved trend that cannot be detected by the MK method over the study region in the EDI data series. In general, the EDI trend was found negative (decreasing) and positive (increasing), which suggested that more attention should be paid towards drought and wet (i.e., moderate, severe, extreme) at the study stations. The results of this research can be employed for water resource management and understanding the characteristics of climate variation over the study area.

Malik et al This study investigates the spatial and temporal patterns of trends on seasonal (pre-monsoon, monsoon, post-monsoon, and winter) and annual rainfall time series data (1966–2015) at 13 stations located in the central Himalayan region of the Uttarakhand State of India. The temporal trend was analyzed using recently proposed innovative trend analysis (ITA) method with significance test. The results of the ITA method were compared with the Mann-Kendall (MK) test at 5% significance level. The spatial variation of the trends in seasonal and annual rainfall series was interpolated using the Thiessen polygon (TP) method in ArcGIS 10.2 environment. The results of comparison revealed that the trend detected by MK test (significantly positive in 3-time series and significantly negative in 6-time series) can be effectively identified using ITA (significantly positive in 19-time series and significantly negative in 32-time series). The ITA method could detect some trends that cannot be observed by the MK test. According to the spatial distribution of MK-test, significantly increasing (decreasing) trends were observed in 1 (0), 1 (2), 0 (1), 1 (1), and 1 (1) polygons in pre-monsoon, monsoon, post-monsoon, winter, and annual rainfall data, while the ITA method detected significant

trends in 3 (7), 6 (5), 1 (9), 4 (5), and 5 (6) polygons in the study region. The developed maps of spatial variability of rainfall trends may help the stakeholders and/or water resource managers to figure out the risk and vulnerability related to climate change in the study region.

Maharana et al This work examines the changes in precipitation characteristics over the Indian region using the latest high-resolution CORDEX-CORE model simulations. Individual RCM (COSMO, RegCM4.7, and REMO) experiments, their ensembles, and all RCM ensembles are examined to evaluate their performance using various statistical metrics. It aims to provide a holistic idea for choosing better models for specific analysis (variability, climatology, temporal evolution, indices, etc.) of precipitation distribution over India. The COSMO model experiments show lesser mean bias and have a high correlation coefficient (>0.8) compared to REMO and RegCM4. Each RCM ensemble performs better than its members in representing the spatial patterns of precipitation. Interestingly, the RCM experiments downscaling the forcings from MPI_ESM GCMs and ERA-Interim outperforms other RCM experiments in the recent day period. The probability distribution function reflects that the mean frequency and the intensity of Precipitation are best represented in the RegCM4 ensemble. Further, most RCMs agree to a robust increase in low-intensity rainfall ($>0.1\text{--}4\text{ mm}_{\text{day}}^{-1}$) in the future under the RCP8.5 scenario. The intra-seasonal variability in terms of active and break spells are best represented in the RegCM4 ensemble. There exists uncertainty in terms of projection of active phases, while all model experiments agree to the decrease in the break phases in the near future compared to the present day. The projected consecutive dry (wet) days and their spells will decrease (increase) over India. The heavy precipitation events are expected to increase (by 18–32 days) along with its contribution (by 14–48%) towards the total precipitation over entire India indicating a possible increase in flooding events in the future. The present-day ISM characteristics is well captured in the model ensemble compared to individual experiments. The model ensemble indicates towards a robust increase in low-intensity rainfall in the future. The very heavy precipitation events and its contribution towards total precipitation are increasing in the future.

CHAPTER 3

3.1 OBJECTIVE

The study has been carried out to find the rainfall trend over the districts of the west-Bengal over a duration of 115 years i.e., 1901-2015. The objective is to analyse the rainfall trend using three different methods. The different methods used are as follows:

- Innovative trend analysis
- Man-Kendall Analysis
- Sen-slope

Our prime objective is to find the rainfall trend of eight districts (Malda, Dakshin Dinajpur, Uttar Dinajpur, Darjeeling, Kalimpong, Jalpaiguri, Alipurduar, Cooch Behar) using these three different methods.

3.2 METHODOLOGY

Steps

1. Collection of data from IMD Pune (IMD website)
2. Extraction of DATA for the present study area (eight districts of the west Bengal which includes (Malda, Dakshin Dinajpur, Uttar Dinajpur, Alipurduar, Cooch Behar, Darjeeling, Kalimpong, Jalpaiguri)
3. Point wise analysis of data using the method of ITA (Innovative Trend Analysis), Mann-Kendall analysis and Sen slope estimator of 31 stations of eight districts of the given study area.
4. Seasonal break
5. Discussion of the result pointwise and district-wise.
6. Finally, we came on the result of trend in rainfall of the given study area.

3.3 STUDY AREA AND DATA

The northern region of west Bengal covers 8 districts. West Bengal lies roughly between 21°30'N and 27°11'N latitude and 85°49'30" E and 89°54'E longitude. Observed monthly precipitation data for 115 years (1901–2015) have been collected from the Indian Meteorological Department (IMD) for 31 rain gauge stations of north Bengal. Historical monthly precipitation data from 1901 to 2015 have been chosen to perform the analysis.

The analysis was conducted for 31 stations in West Bengal. Different seasons considered for this study are: Pre-Monsoon (Mar- May), Monsoon (June -Sept), post-monsoon (Oct-Nov) and winter (Dec-Feb). For all these analyses we have used the monthly precipitation data for the period of 115 years (1901-2015) generated by the India Meteorological Department (IMD), Pune.

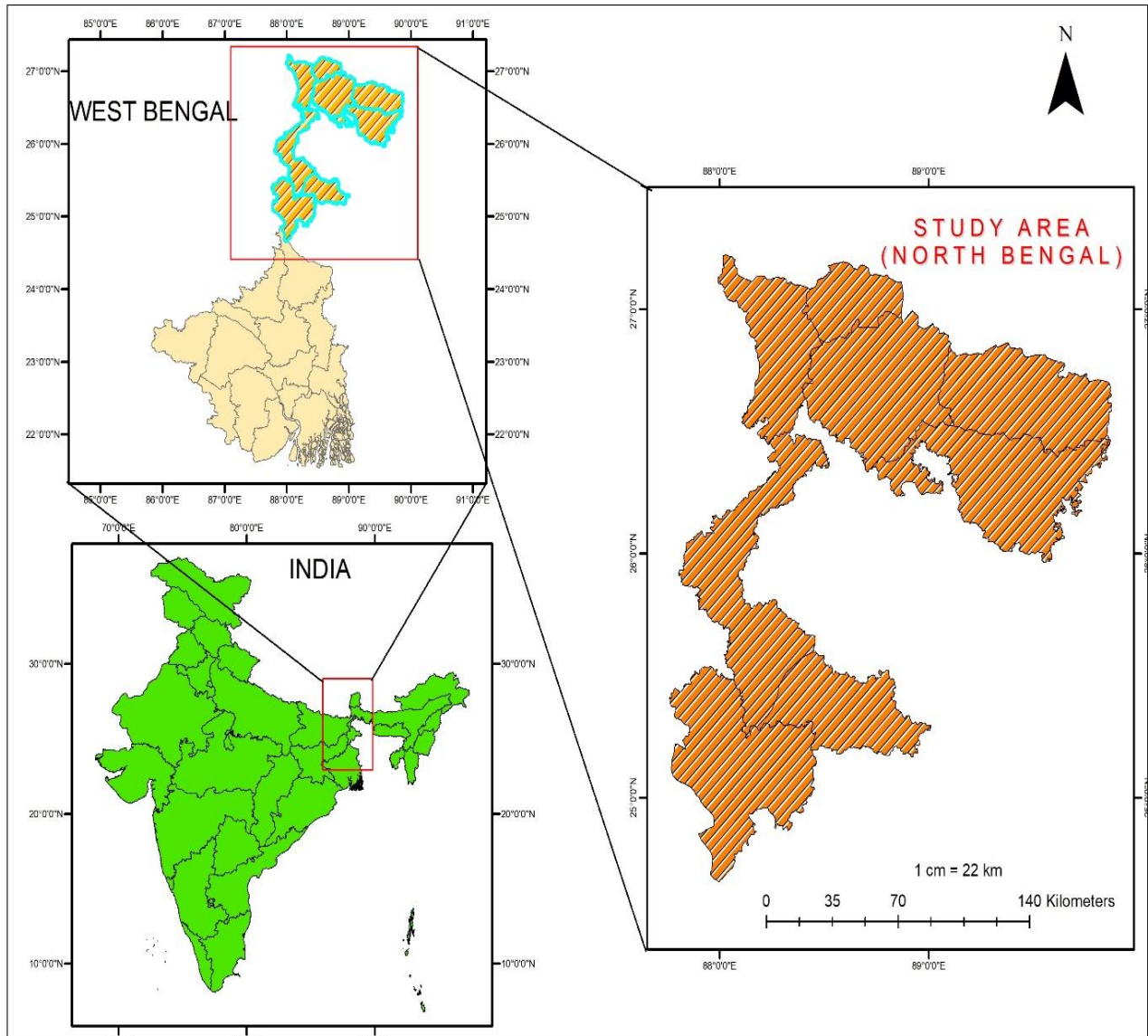


Fig 4: Study area map



Fig 5: Political Map of West Bengal

Coordinates of Different Points and Its Representation on The Map

Table 1: Coordinates of stations

Points	Longitude	Latitude
P1	88	24.75
P2	88	25
P3	88.25	25
P4	88	25.25
P5	88.25	25.25
P6	88.5	25.25
P7	88.75	25.25
P8	88.5	25.5
P9	88.25	25.5
P10	88	25.75
P11	88.25	25.75
P12	88	26
P13	88.25	26.25
P14	88.25	26.5
P15	88.25	26.75
P16	88.25	27
P17	88.5	27
P18	88.75	27
P19	88.75	26.5
P20	88.5	26.75
P21	88.75	26.75
P22	89	26.75
P23	89.25	26.5
P24	89.5	26.5
P25	89.75	26.5
P26	89.25	26.75
P27	89.5	26.75
P28	89	26.25
P29	89.25	26.25
P30	89.5	26.25
P31	89	26.5

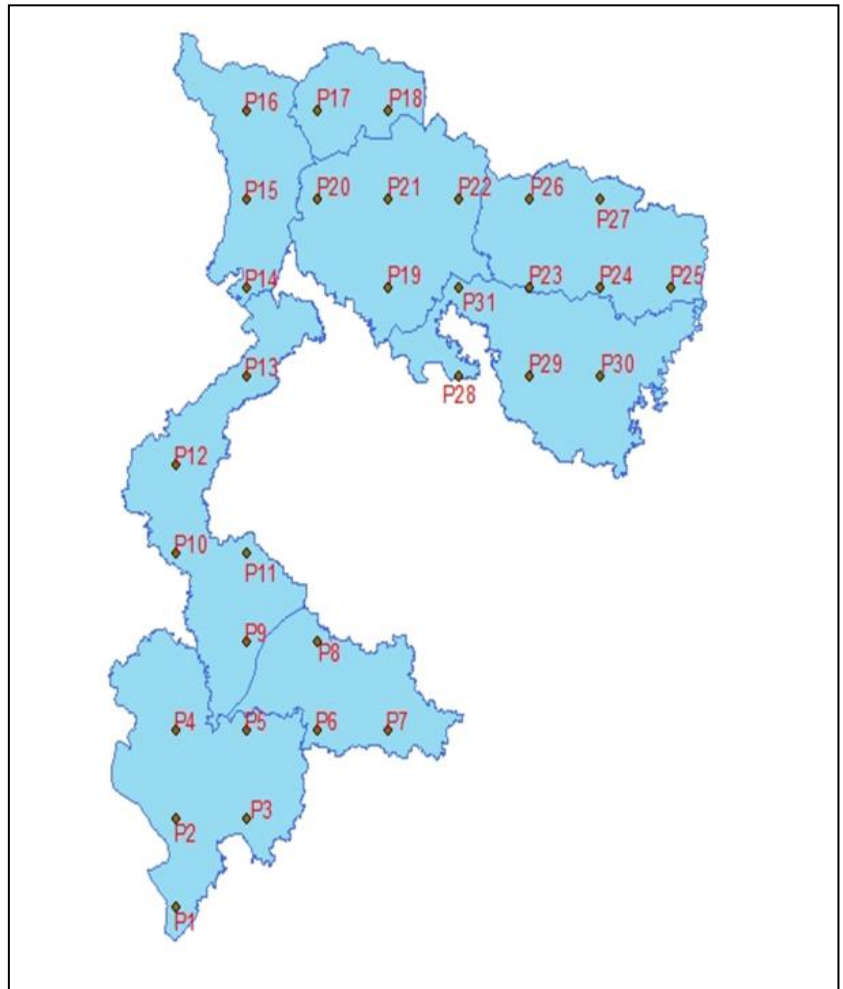


Fig 6: Rainfall Stations of Study Area

CHAPTER 4

4.1 Results and Discussion

In this study we have done analysis of the rainfall trend based on the 31 stations of the study area using three methods

- Innovative trend analysis
- Mann-Kendall Analysis
- Sen Slope

A year of Indian Subcontinent can be divided into four different seasons

1. Winter – Dec, Jan, Feb
2. Pre-Monsoon or Summer -Mar, Apr, May
3. Monsoon- June, July, Aug, Sep
4. Post-Monsoon – Oct, Nov

4.1.1 Innovative Trend Analysis Method

Sen (2012) proposed the concept of innovative trend analysis (ITA) and later used by Kisi and Ay (2014), Şen (2014), Ay and Kisi (2015), Kisi (2015), Dabanli et al. (2016), Cui et al. (2017), Mohorji et al. (2017), Wu and Qian (2017), Güçlü et al. (2018), Kisi et al. (2018), Wu et al. (2018), and Zhou et al. (2018)). In this method, a time series of data is divided into two equal halves from the first date to the end date, if there is an odd number of years then we will have to remove one year data that may be middle one or the last one (In this calculation we have neglected middle year i.e., 1958).

Both the sub-series are sorted in ascending order; the first half series ($X_i: i = 1, 2, \dots, n/2$) is located on horizontal axis (X-axis) and the second half series ($X_j: j = n/2 + 1, n/2 + 2, \dots, n$) is located on the vertical axis (Y-axis) of the Cartesian coordinate system.

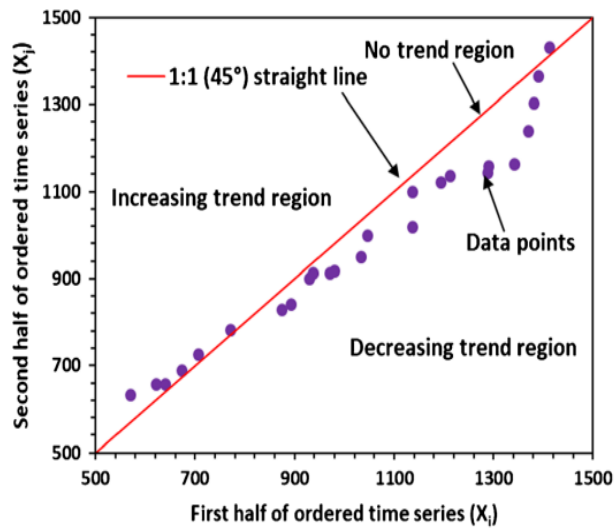


Fig 7: The innovative trend slope

The range of both the axis should be equal. The 1:1 (45°) line divides the diagram into two equal triangles, where the area of the upper and lower triangle indicate increasing and decreasing trends into the time series data (Şen 2012, 2014). If the points in scatter plot accumulate on 1:1 (45°) line or close to this line, this indicates no significant trend in the time series. If the points in scatter plot fall above and below the 1:1 (45°) line, this indicates the non-monotonic trends (may be positive or negative) in the time series. Then, it is possible to categorize the variation domain of each half series in several groups (low, medium, and high). Such plot represents first visual inspection of the type of trends. The range of each group can be determined either by an expert view or quantitatively by splitting the domain of variation into some sub-classes (Dabanli et al. 2016). The closer the scatter points to the 1:1 (45°) line, the weaker the trend slope (Şen 2012). Şen (2017) tested the ITA method at 1%, 5%, and 10% significance levels for a better understanding of existing trend nature into the time series of data. The trend slope is computed using the following expression (Şen 2017)

$$s = \frac{2 \left(\bar{y}_2 - \bar{y}_1 \right)}{n}$$

where s is the slope of trend line; y₂ and y₁ are the arithmetic averages of the first and second halves of the dependent variable (y, sequence); and n is the number of data year. Figure 4 is the graphical presentation for understanding the concept of trend slope. After the calculation of slope of the trend line, the standard deviation of sampling slope is calculated as:

$$\sigma_s = \frac{2\sqrt{2}}{n\sqrt{n}} \sigma \sqrt{1 - \rho_{\bar{y}_1 \bar{y}_2}}$$

where σ_s is the standard deviation of sampling slope; σ is the standard deviation of whole data series; and $\rho_{\bar{y}_1 \bar{y}_2}$ is the cross-correlation coefficient between the ascendingly sorted two halves' arithmetic averages.

Table2: ITA test result (Winter)

Points	standard deviation	$\rho_{\bar{x}_i \bar{x}_j}$	slope std deviation	slope ITA
P1	12.54334235	0.990774426	0.002799611	-0.112784627
P2	12.93877751	0.991939119	0.002699431	-0.094503162
P3	13.27740794	0.987524513	0.003446115	-0.085469034
P4	13.45108653	0.994084478	0.00240404	-0.08368536
P5	13.14387448	0.99311607	0.002534133	-0.078881069
P6	14.17389421	0.93607787	0.008327268	-0.069607811
P7	12.85852425	0.962008522	0.005824008	-0.070328542
P8	12.30707203	0.981387585	0.00390161	-0.058130358
P9	12.66645571	0.993866791	0.002305084	-0.068628328
P10	11.23533209	0.969296157	0.004574778	-0.076331503
P11	10.95313365	0.9938978	0.001988242	-0.046550613
P12	10.17238424	0.989435439	0.002429608	-0.086781438
P13	10.6347854	0.953997362	0.00530039	-0.049570355
P14	11.22255255	0.958085438	0.005339023	-0.022527809
P15	13.06323782	0.948064592	0.006917837	-0.047283422
P16	19.78047589	0.873012141	0.016379685	0.036253371
P17	14.58308624	0.89513753	0.010973551	-0.04398615
P18	40.71660643	0.587811696	0.060744523	0.04360481
P19	11.92734933	0.983733049	0.003534962	-0.038772936
P20	12.25542698	0.984261704	0.003572687	-0.019010577
P21	24.03343565	0.741620629	0.028387849	0.037638832
P22	16.76710804	0.983490493	0.005006255	-0.050372175
P23	12.70892568	0.975632915	0.004609973	-0.044354382
P24	16.81715221	0.966118317	0.007193209	-0.100059913
P25	15.64721553	0.954542784	0.007752222	-0.102125678
P26	34.82881791	0.75352341	0.040180403	-0.083437578
P27	19.97201463	0.875547675	0.016372353	-0.071346651
P28	11.48377577	0.984712209	0.003299475	-0.042666061
P29	12.85958437	0.979605516	0.004267475	-0.06709927
P30	12.68155661	0.97770242	0.004400369	-0.000428653
P31	12.07703397	0.98543637	0.003386748	-0.03296876

Table 3: ITA test result(pre-monsoon)

Points	standard deviation	$\rho_{\bar{x}_i \bar{x}_j}$	slope std deviation	slope ITA
P1	25.83484724	0.957320726	0.012402297	0.024845
P2	29.01843234	0.960536347	0.013395542	0.096267
P3	32.16996823	0.967783209	0.013417743	0.196555
P4	31.95087985	0.976769855	0.011316093	0.152333
P5	32.63760578	0.96313934	0.014560878	0.224285
P6	36.22136522	0.985289199	0.010208706	0.290749
P7	33.62792383	0.987081001	0.008881825	-0.24071
P8	30.81263816	0.968286977	0.012750741	-0.04944
P9	31.28762099	0.947951719	0.016586832	0.216539
P10	29.30787767	0.957836734	0.013984251	-0.05437
P11	31.42038853	0.961103617	0.014399714	-0.07222
P12	36.80504069	0.951852254	0.018766488	0.171532
P13	43.4576406	0.989766774	0.010215512	-0.31181
P14	45.84703839	0.981429005	0.014518327	-0.10136
P15	67.43771609	0.790902318	0.071658082	0.239896
P16	60.42652585	0.936985067	0.035248211	0.471262
P17	49.45085199	0.975911245	0.017834818	0.551667
P18	63.76566811	0.968483759	0.026305214	-0.22174
P19	53.8697591	0.991677188	0.011420044	-0.14345
P20	46.76297396	0.98337618	0.014010552	0.17701
P21	64.54820727	0.952700043	0.032621376	-0.43823
P22	69.14142123	0.981950926	0.021585071	-0.54082
P23	81.36980991	0.955198028	0.040022073	-0.35593
P24	86.7710597	0.961907598	0.039353358	-0.51092
P25	97.64197691	0.978453866	0.033304963	-0.80892
P26	98.76258525	0.988065885	0.025071209	-1.01285
P27	90.63536773	0.98663721	0.024346357	-0.408
P28	64.05506042	0.985627905	0.017844369	-0.17223
P29	71.90729466	0.963606449	0.031876665	-0.20417
P30	69.75387674	0.982973931	0.021150141	-0.17781
P31	60.13294863	0.983218991	0.018101278	0.038348

Table4: ITA test result(monsoon)

Points	standard deviation	ρ_{x_i, x_j}	slope std deviation	slope ITA
P1	66.47707645	0.987278092	0.017423514	0.022982
P2	78.46494316	0.983747681	0.023244545	0.049195
P3	79.53480622	0.985865241	0.02197299	0.113245
P4	88.92221353	0.983595909	0.026465132	0.321779
P5	83.57406979	0.985122699	0.023687616	0.172398
P6	84.92868951	0.992547392	0.017037124	-0.01334
P7	83.61163194	0.978973749	0.028173146	-0.75733
P8	87.16020188	0.97771422	0.030235689	-0.84934
P9	78.23117325	0.965785708	0.033625701	0.170491
P10	67.29988059	0.985331089	0.018940914	-0.69666
P11	90.42545776	0.972866827	0.034612161	-0.56944
P12	107.4667183	0.975009792	0.039477227	0.483879
P13	110.80157	0.966441504	0.047166633	-0.8587
P14	118.2441532	0.965283652	0.051195809	-0.28257
P15	109.8037928	0.980737946	0.035412481	0.313178
P16	90.79156522	0.957235203	0.043629117	0.072222
P17	126.0775668	0.968379989	0.05209626	1.804089
P18	138.2762061	0.973107713	0.052692529	0.074566
P19	139.1158631	0.973438271	0.052685674	0.074798
P20	115.8021003	0.975136685	0.042431039	0.295313
P21	205.2516312	0.96152598	0.093553086	-1.53303
P22	160.3160022	0.985567193	0.044754838	-0.77193
P23	135.8040097	0.98170959	0.042678783	-0.17973
P24	161.600734	0.964904983	0.070348327	-1.42069
P25	169.499943	0.988749886	0.041776854	-2.28264
P26	273.7257998	0.868632826	0.230540313	-2.94971
P27	171.5152468	0.968550918	0.070679657	-0.96209
P28	163.3965787	0.861780569	0.141161163	0.983994
P29	132.7945664	0.980073055	0.043560052	0.662191
P30	131.0245257	0.971014092	0.051836273	0.070118
P31	135.9127033	0.981969395	0.042408501	0.939437

Table 5: ITA test result(post-monsoon)

Points	standard deviation	ρ_{x_i, x_j}	slope std deviation	slope ITA
P1	33.90248925	0.991552097	0.00724092	0.02929856
P2	35.27378267	0.993729092	0.006490901	0.03806957
P3	35.45156744	0.987806007	0.009096957	0.00746195
P4	36.63493706	0.985581142	0.0102223	0.00470139
P5	34.56697047	0.977158552	0.012139781	-0.01156254
P6	35.6591014	0.966759418	0.015107494	0.01577732
P7	35.52629476	0.983049926	0.010747895	-0.05736327
P8	33.89736064	0.981045313	0.010844559	-0.04931923
P9	32.83351948	0.955548873	0.016085944	-0.01531608
P10	33.41901108	0.975780244	0.012085544	-0.03115906
P11	32.60475463	0.973490668	0.012335821	-0.07335124
P12	34.99880511	0.982378752	0.01079591	-0.0075331
P13	42.32199502	0.982335928	0.013070712	-0.04660344
P14	43.8470844	0.98674181	0.01173196	0.08493393
P15	46.18592017	0.98484604	0.013211751	0.22341029
P16	42.37229796	0.969039802	0.017324934	0.26751634
P17	43.40863503	0.967968421	0.018053151	0.33921754
P18	38.56256638	0.981814741	0.012084074	0.09646099
P19	38.406929	0.982045976	0.011958541	0.04329397
P20	43.00483399	0.982037652	0.013393267	0.22511652
P21	39.20612628	0.975964299	0.014124401	-0.02607711
P22	37.77932361	0.987469543	0.009827099	-0.11359499
P23	43.64816575	0.994127173	0.007772797	-0.12265032
P24	37.98999943	0.974194104	0.014181314	-0.14579253
P25	39.54957352	0.983261068	0.011890316	-0.12253767
P26	55.89406324	0.950173566	0.028992342	-0.30597165
P27	46.57303965	0.895764955	0.034940505	-0.05305695
P28	42.1111326	0.986737274	0.011269406	-0.0789508
P29	44.61190275	0.966962781	0.018842573	-0.119643
P30	39.64408642	0.985051808	0.011263165	-0.06767218
P31	39.15114505	0.98163114	0.01233029	0.00269715

Table6: ITA test result (Annual)

Points	standard deviation	ρ_{x_i, x_j}	slope std deviation	slope ITA
P1	289.3620431	0.990178512	0.066637383	0.0287899
P2	336.3286517	0.987918039	0.085905368	0.4107828
P3	342.2731847	0.981997069	0.106716654	0.8940917
P4	379.3164163	0.986149497	0.103734239	1.5908494
P5	357.9896652	0.981830893	0.112130819	1.1699952
P6	364.4024541	0.98229589	0.11266942	0.7270137
P7	366.3674265	0.956479519	0.177603456	-4.064205
P8	377.0227136	0.982853371	0.114721443	-3.809883
P9	339.9266296	0.966556615	0.144453483	1.148377
P10	370.7845379	0.983572025	0.110433629	-3.809775
P11	388.8895906	0.971123351	0.153563298	-2.807594
P12	466.5820178	0.96622152	0.199267176	2.2539475
P13	470.9403786	0.97509275	0.172709623	-4.609165
P14	505.5302373	0.961811069	0.229563905	-1.224611
P15	528.1271498	0.969337548	0.214896654	2.5480632
P16	453.3205166	0.985401608	0.127275732	2.577732
P17	615.86759	0.982682685	0.188328193	9.8010377
P18	704.8272923	0.981814741	0.220866667	0.0096481
P19	654.7386738	0.992313742	0.133386904	-0.078835
P20	527.0647623	0.978785137	0.178390536	2.3496116
P21	997.8311819	0.936055489	0.586335817	-7.449784
P22	776.2094932	0.975810365	0.280531298	-5.151727
P23	687.4738565	0.987262048	0.180299163	-2.243359
P24	759.7116699	0.969535349	0.308130447	-7.85303
P25	823.997318	0.989197082	0.199014194	-12.12919
P26	1356.505289	0.839810863	1.26161179	-15.92219
P27	845.072279	0.946590523	0.453827424	-5.374224
P28	711.1201266	0.927535803	0.444828321	3.0970955
P29	622.6913821	0.98326027	0.187212479	1.5431418
P30	621.0094283	0.99235812	0.12614964	-0.63197
P31	637.7977472	0.982152435	0.197997715	3.8149457

Here we are discuss each station season wise

Winter season

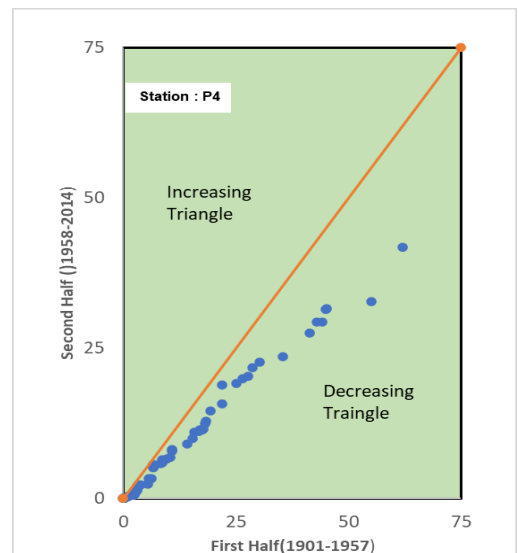
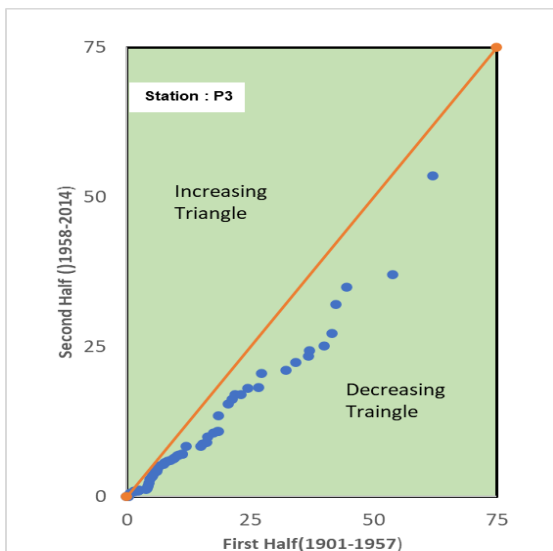
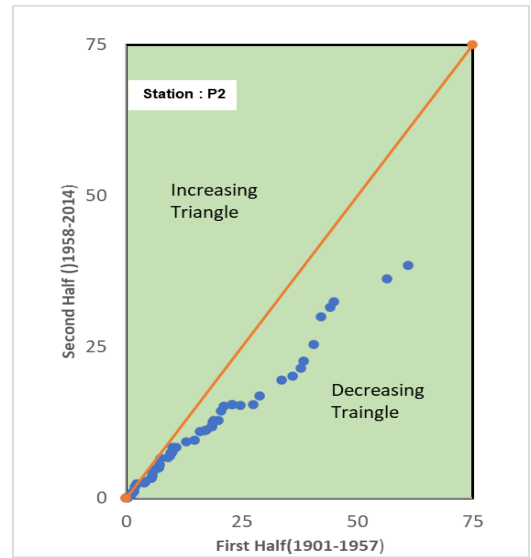
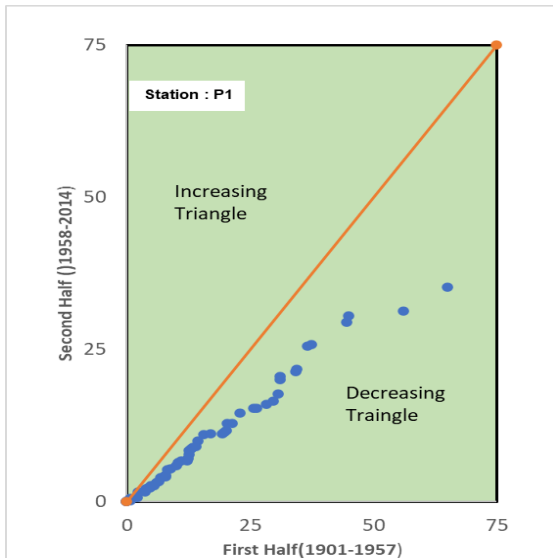


Fig 8: Trend Analysis of Points P1, P2, P3, P4

Result:

- Points P1, P2, P3, P4 are showing decreasing trend

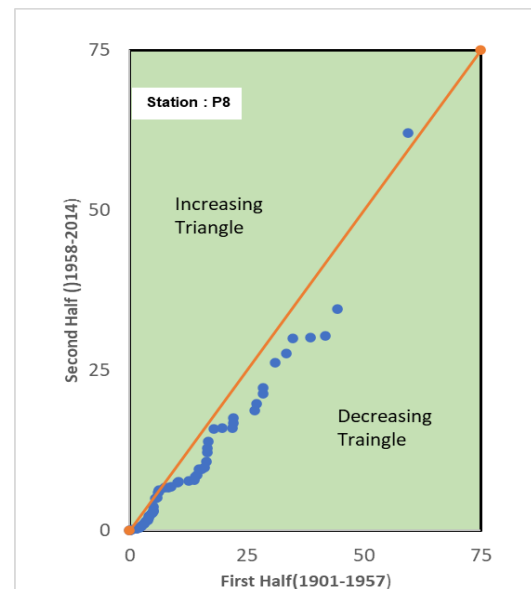
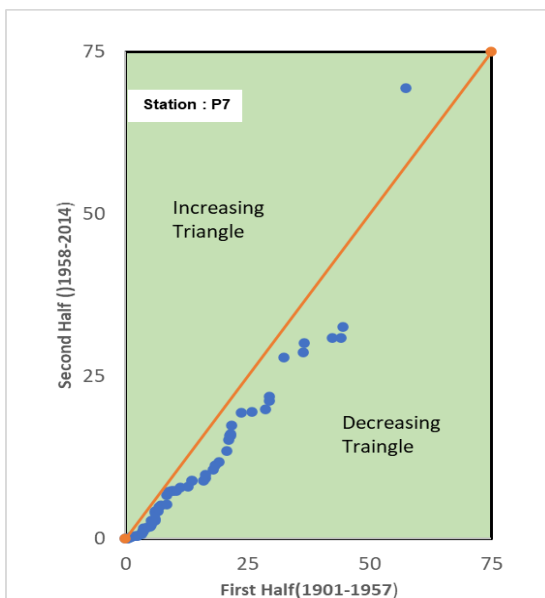
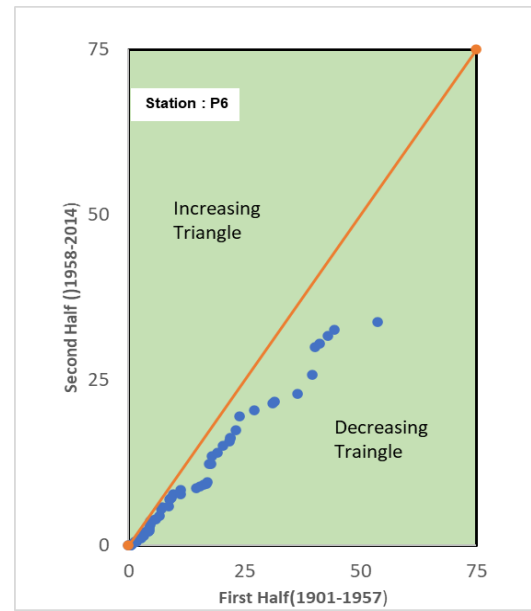
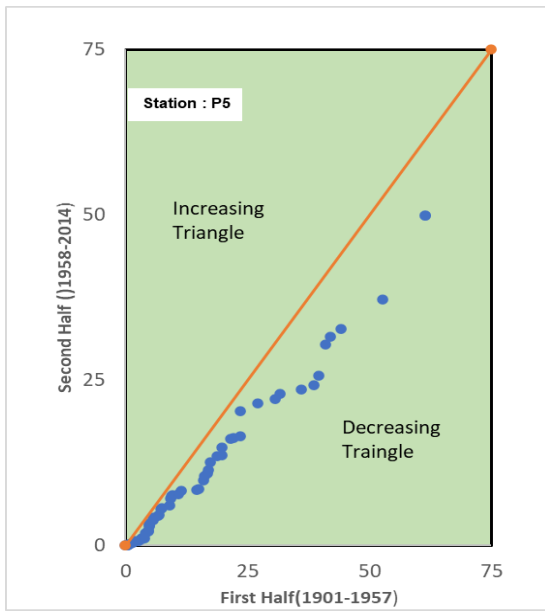


Fig 9: Trend Analysis of Points P5, P6, P7, P8

Result:

- Points P5, P6, P7, P8 are showing decreasing trend

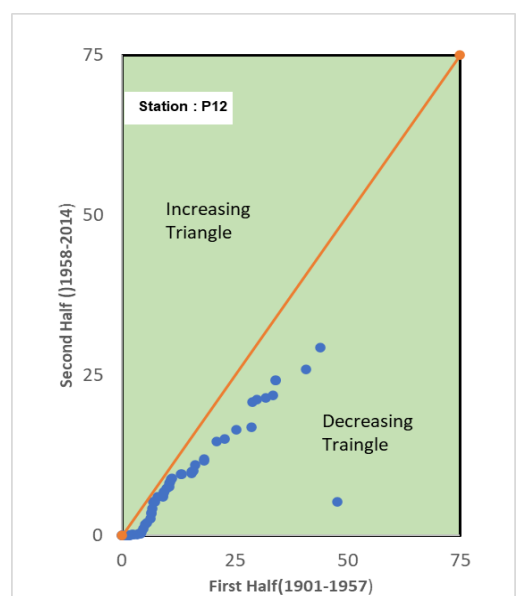
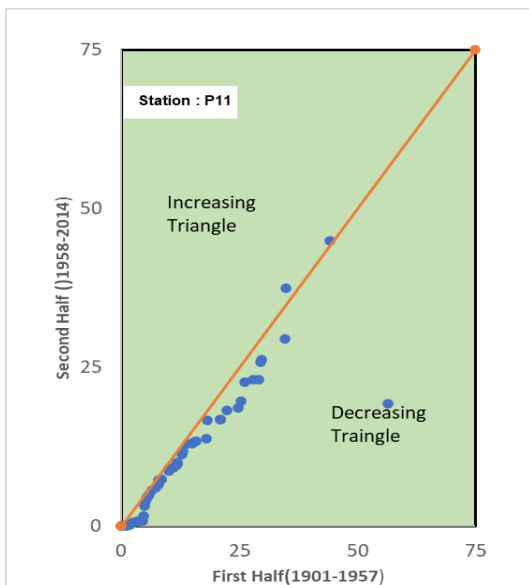
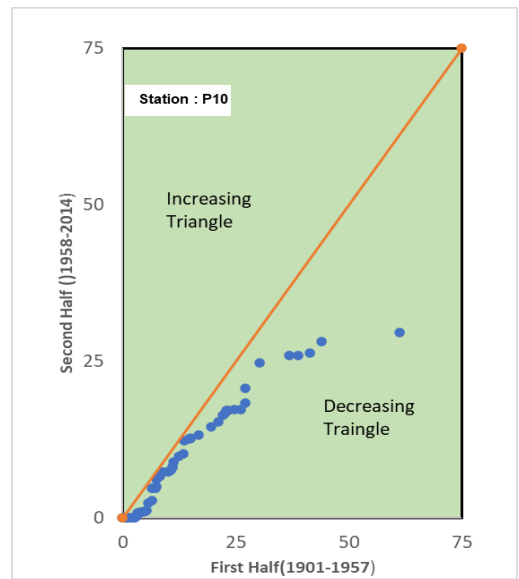
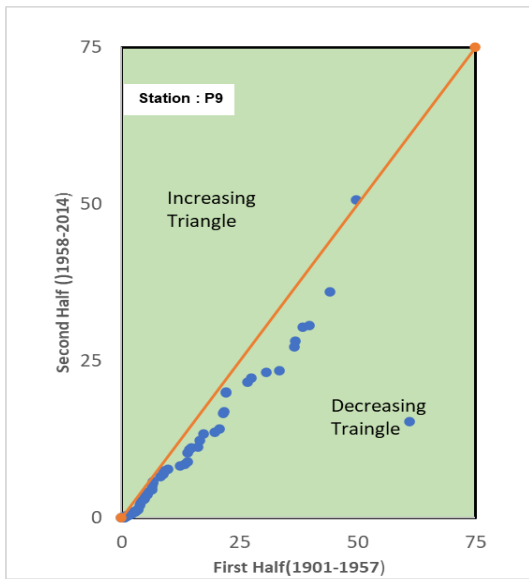


Fig 10: Trend Analysis of Points P9, P10, P11, P12

Result:

Points P9, P10, P11, P12 are showing decreasing trend

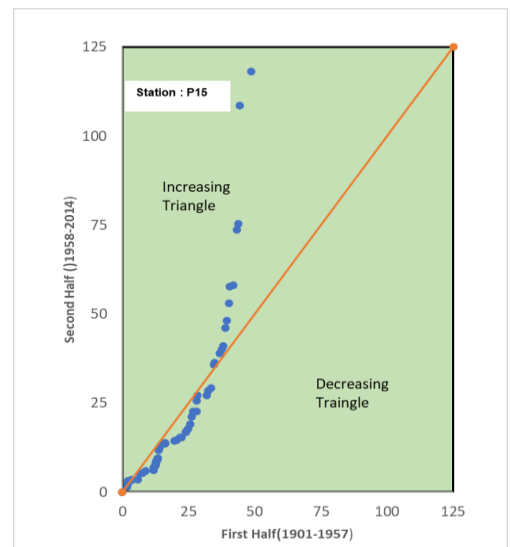
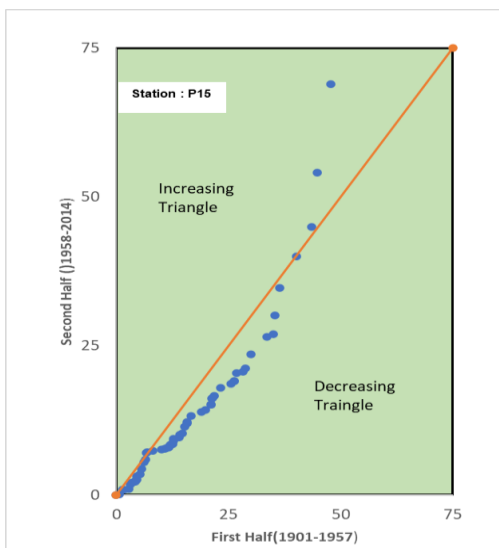
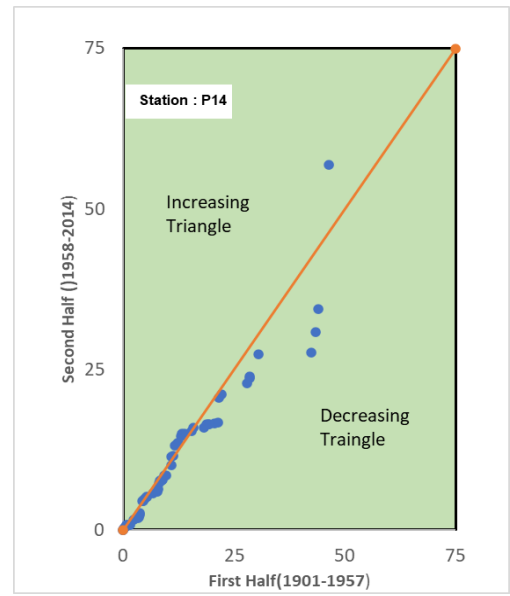
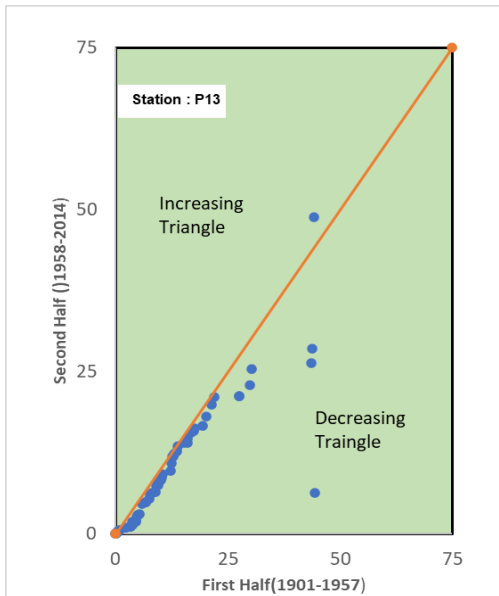


Fig 11: Trend Analysis of Points P13, P14, P15, P16

Result:

- Points P13, P14, P15 are showing decreasing trend
- Point P16 is showing increasing trend

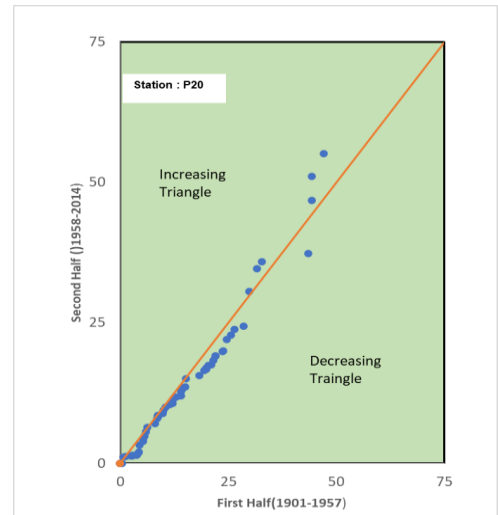
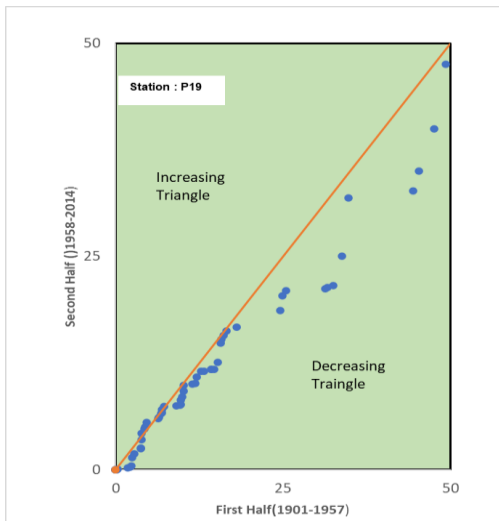
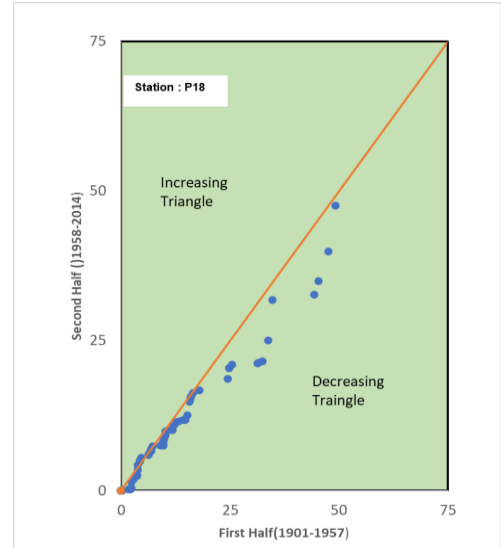
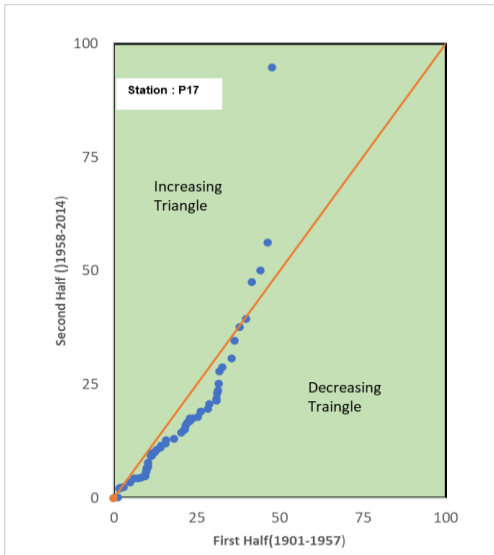


Fig 12: Trend Analysis of Points P17, P18, P19, P20

Result:

- Points P17, P18 , P19, P20 are showing decreasing trend

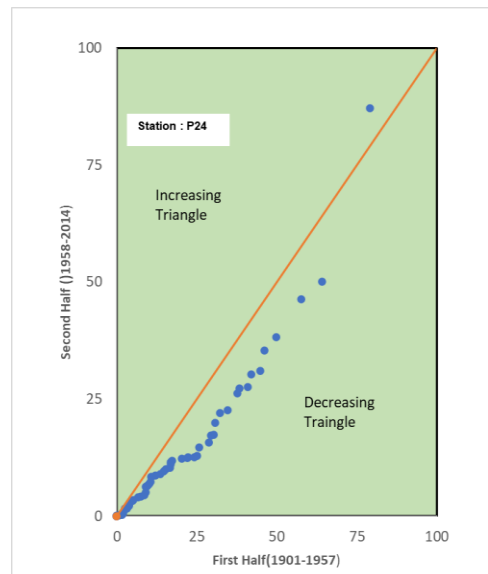
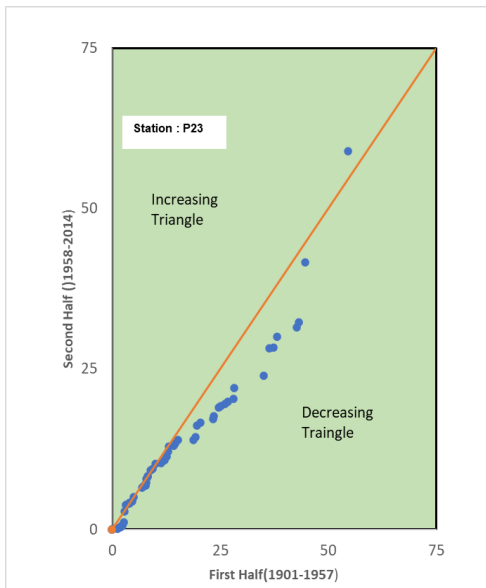
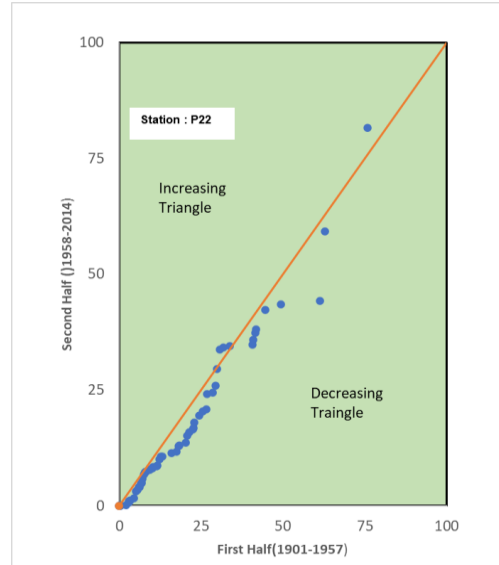
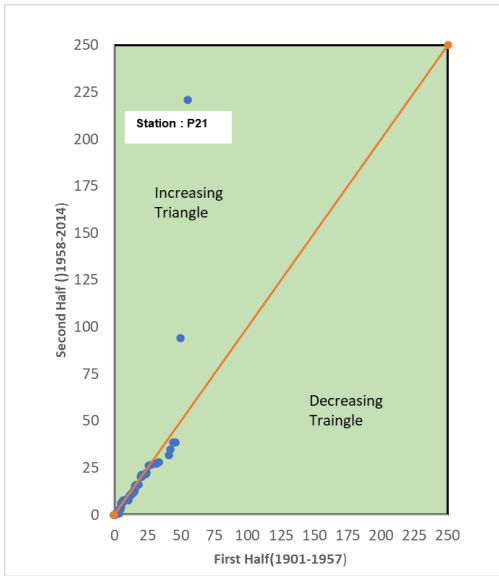


Fig 13: Trend Analysis of Points P21, P22, P23, P24

Result:

- Points P22, P23, P24 are showing decreasing trend
- Point P21 is showing increasing trend

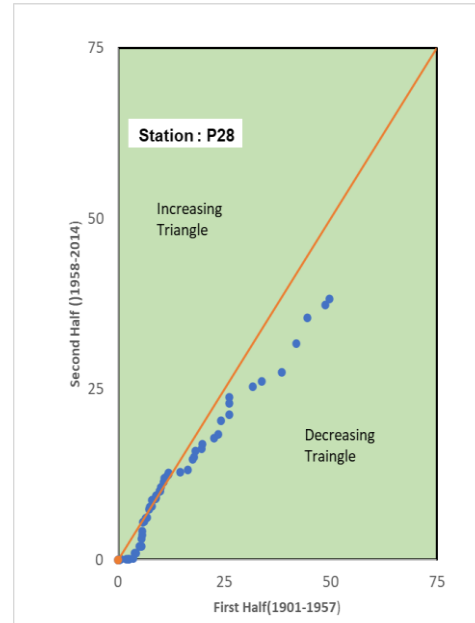
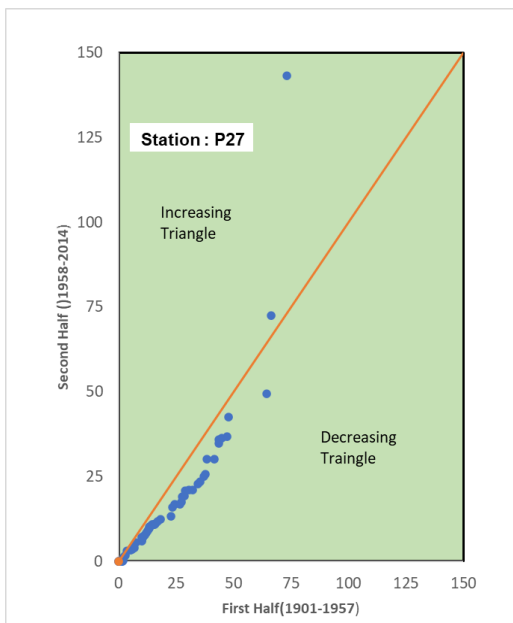
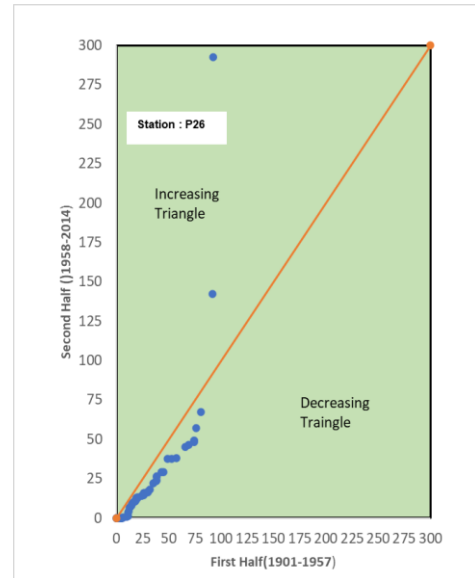
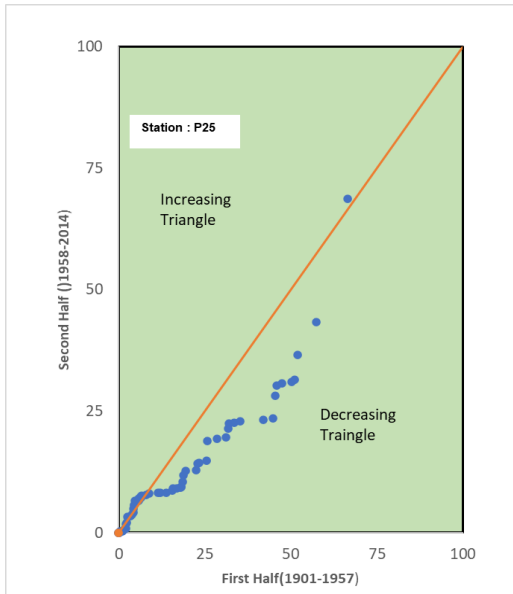


Fig 14: Trend Analysis of Points P25, P26, P27, P28

Result:

- Points P25, P26, P27, P28 are showing decreasing trend

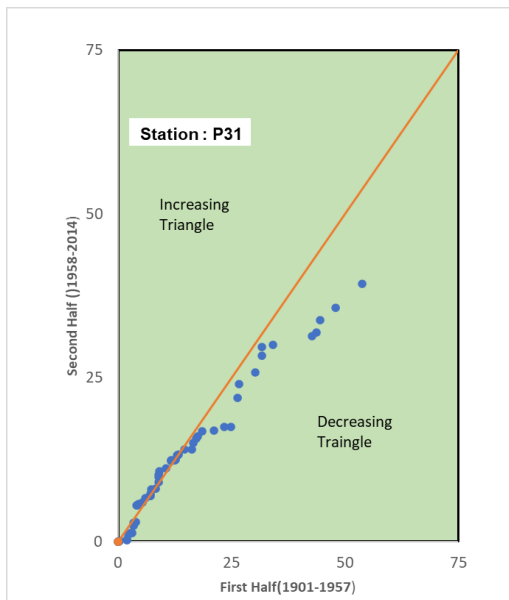
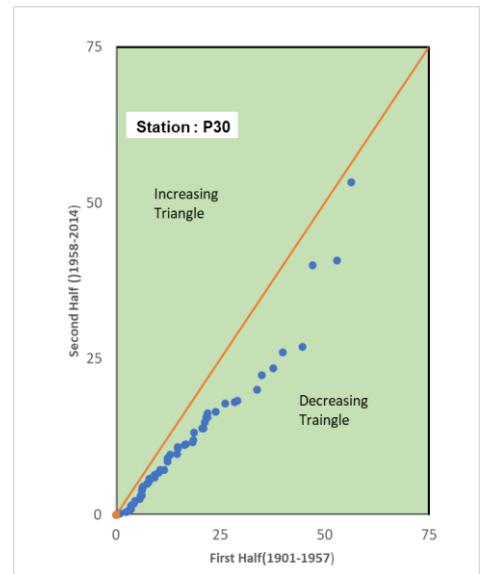
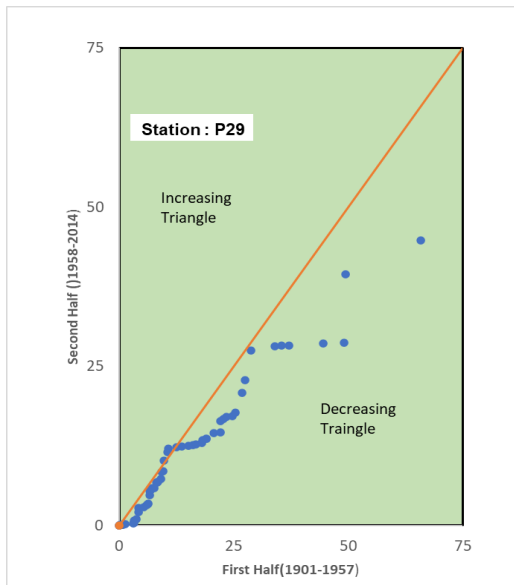


Fig 15: Trend Analysis of Points P29, P30, P31

Result:

- Points P29, P30, P31 are showing decreasing trend

Discussion

Winter is generally showing a decreasing trend although some point such as P16, P18, P21 are showing slight increasing trend.

PRE-MONSOON

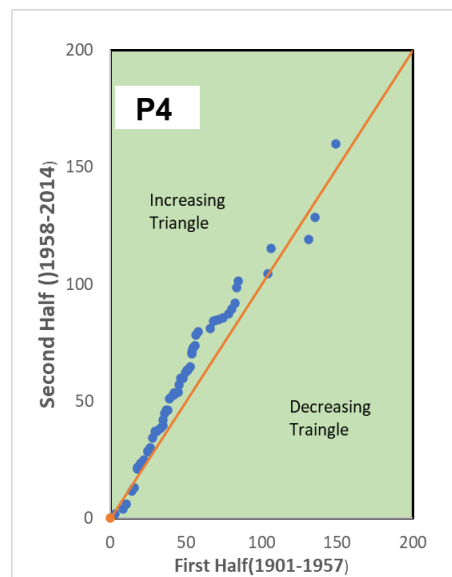
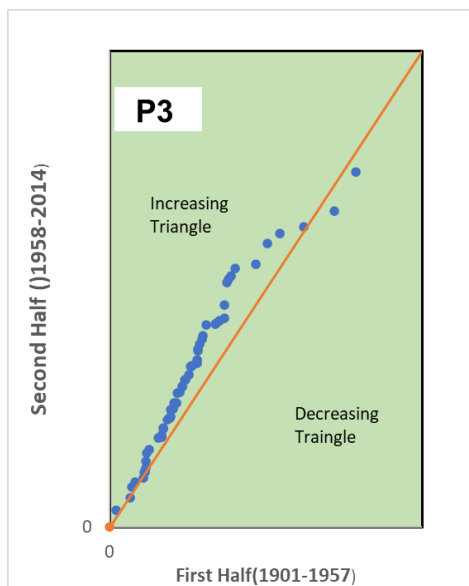
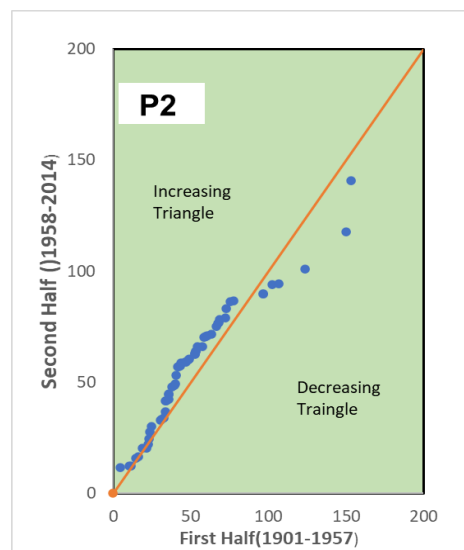
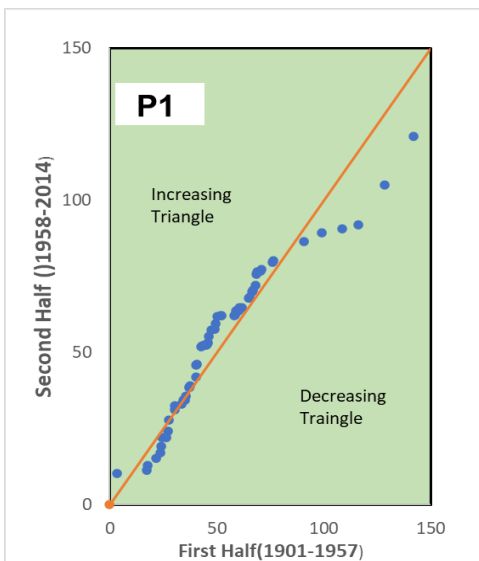


Fig 16: Trend Analysis of Points P1, P2, P3, P4

Result:

- Points P1, P2, P3, P4 are showing increasing trend

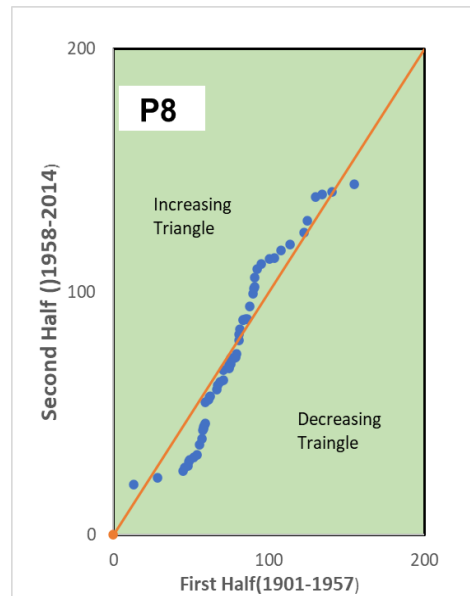
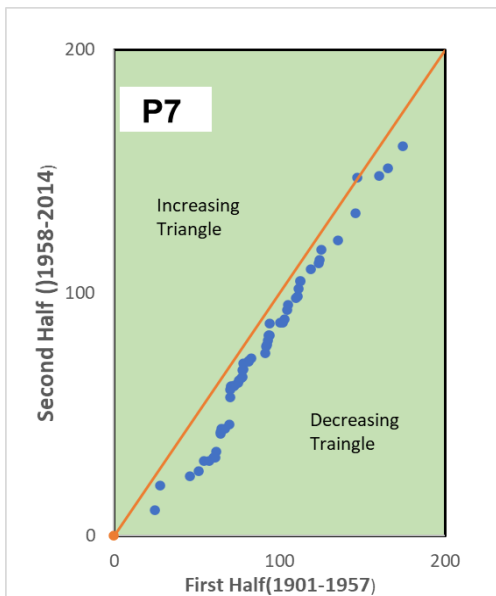
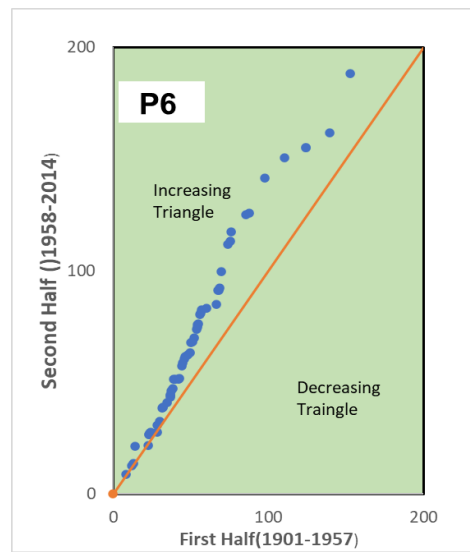
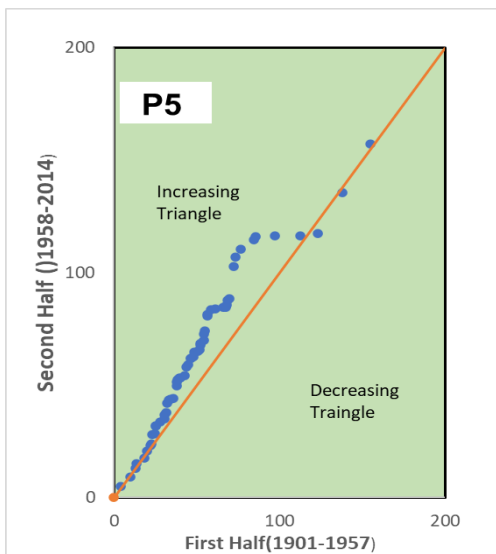


Fig 17: Trend Analysis of Points P5, P6, P7, P8

Result:

- Points P5, P6 are showing increasing trend
- Points P7, P8 are showing decreasing trend

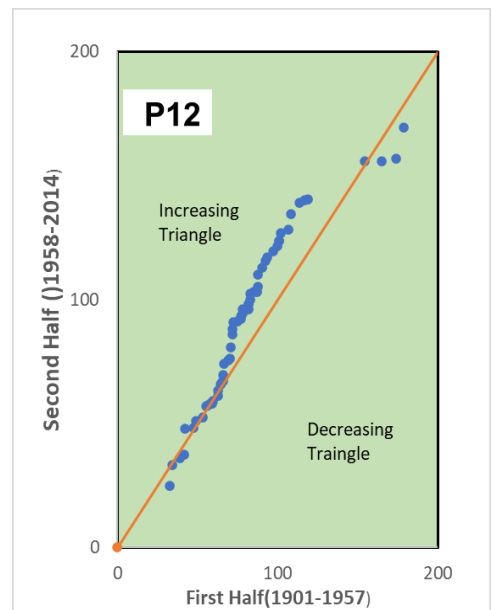
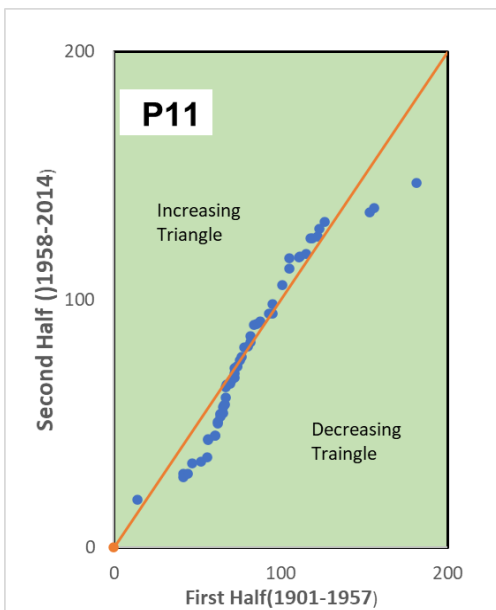
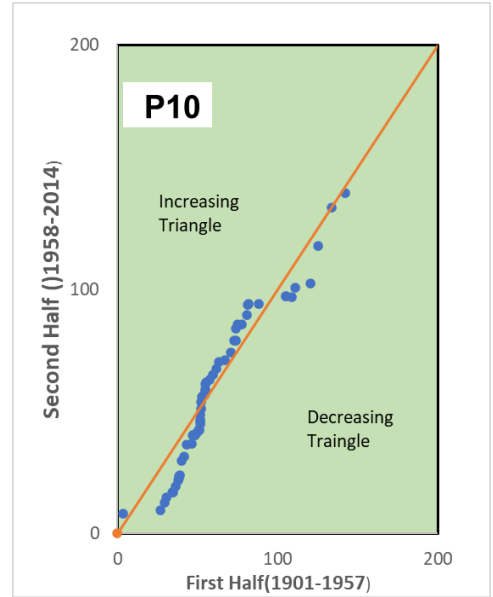
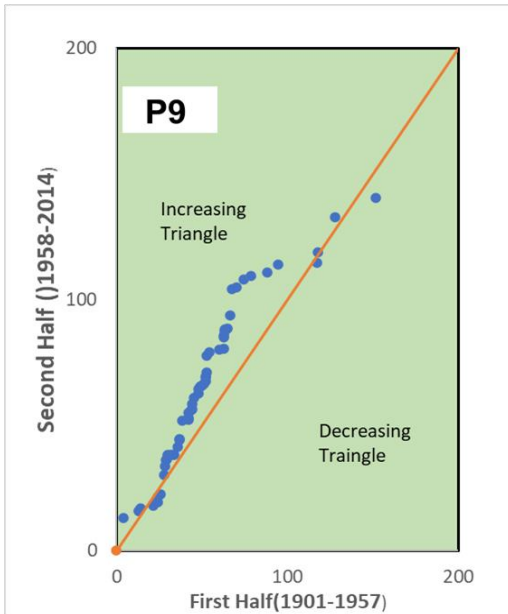


Fig 18: Trend Analysis of Points P9, P10, P11, P12

Result:

- Points P9, P12 are showing increasing trend
- Points P10, P11 are showing a decreasing trend

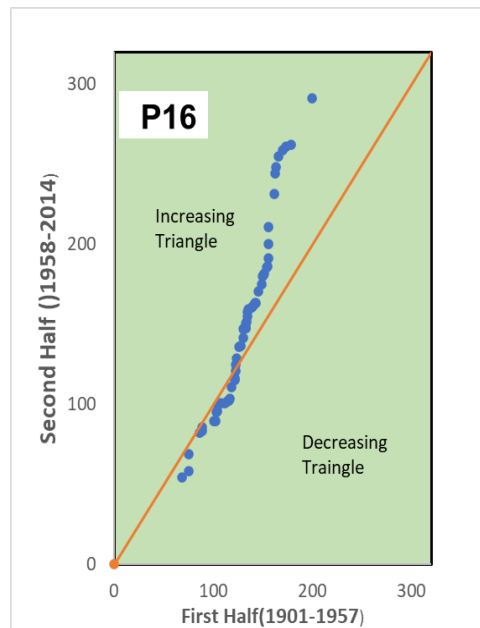
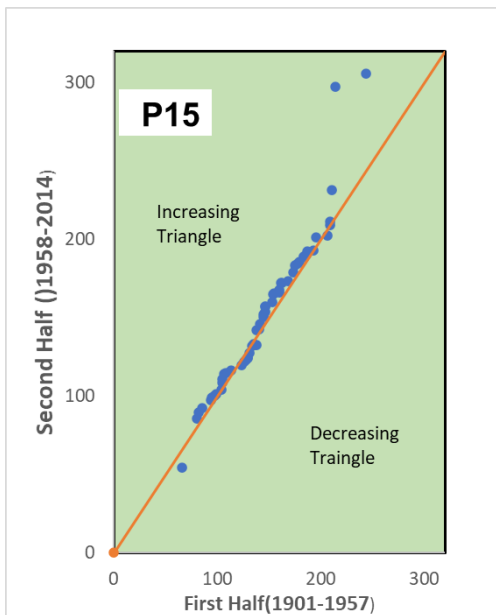
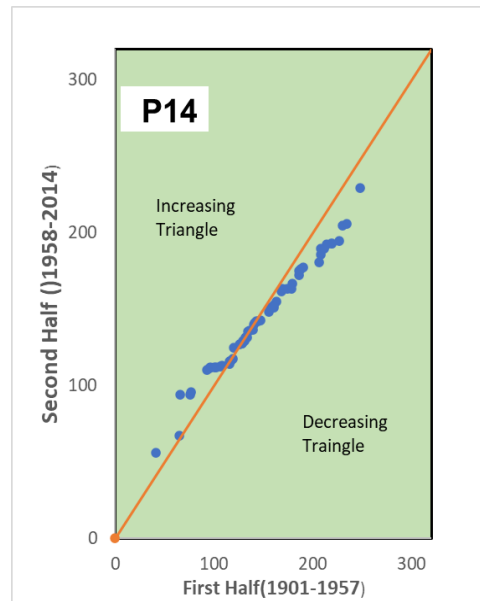
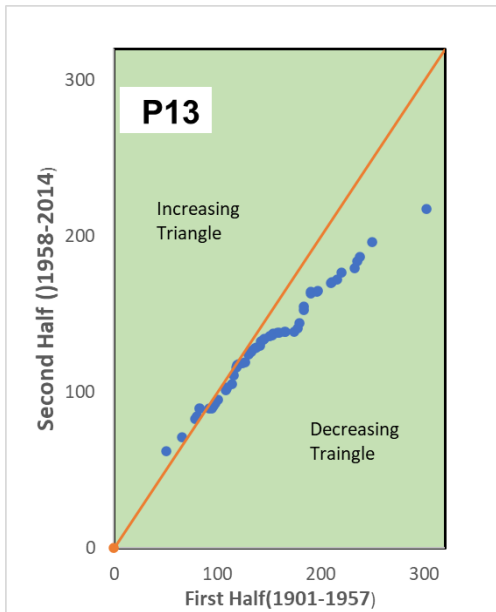


Fig 19: Trend Analysis of Points P13, P14, P15, P16

Result:

- Points P13, P14 are showing increasing trend
- Points P15, P16 are showing decreasing trend

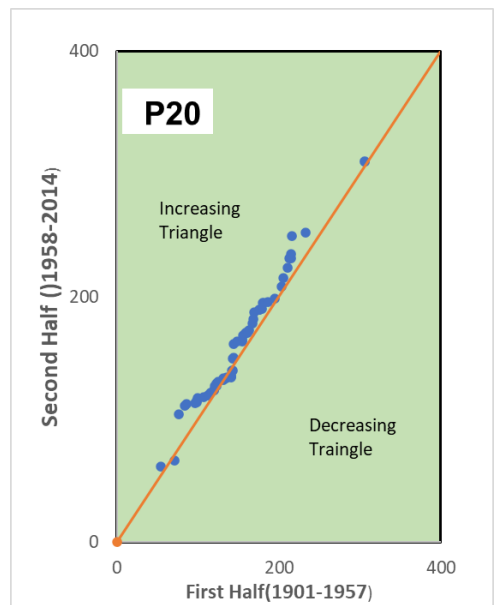
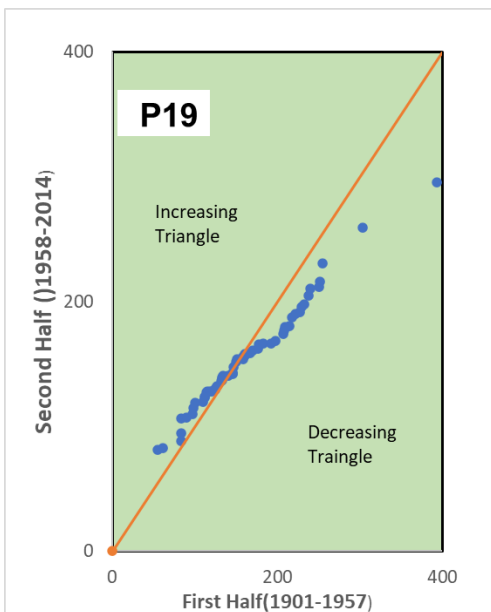
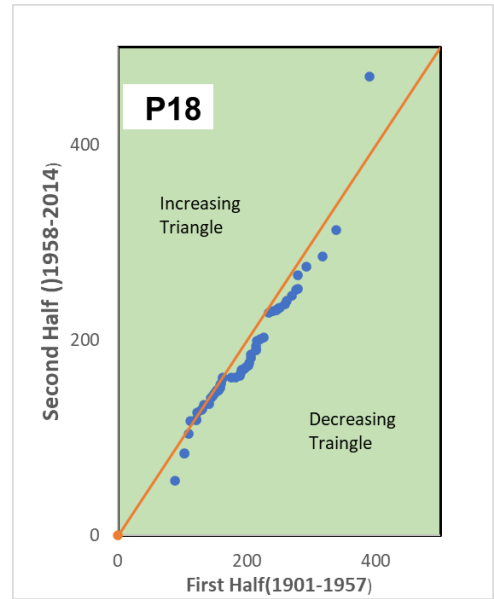
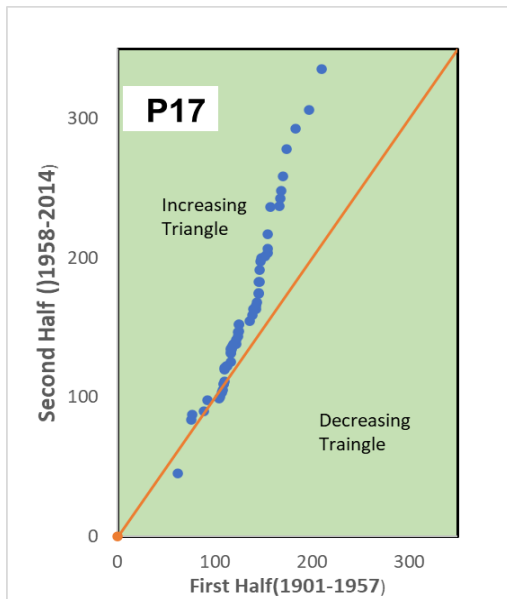


Fig 20: Trend Analysis of Points P17, P18, P19, P20

Result:

- Points P17, P20 are showing increasing trend
- Points P18, P19 are showing decreasing trend

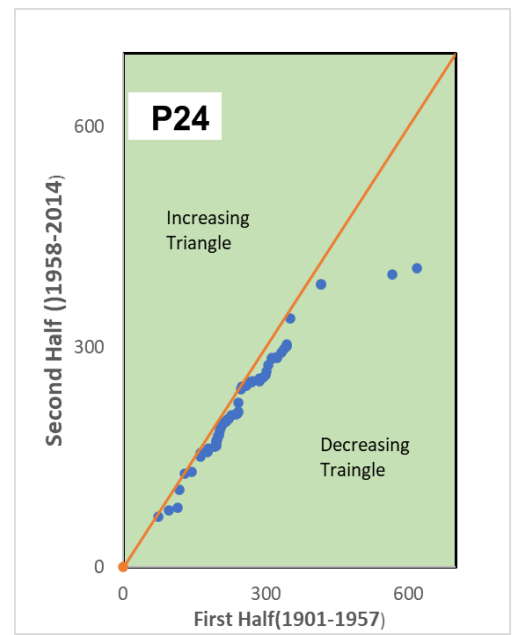
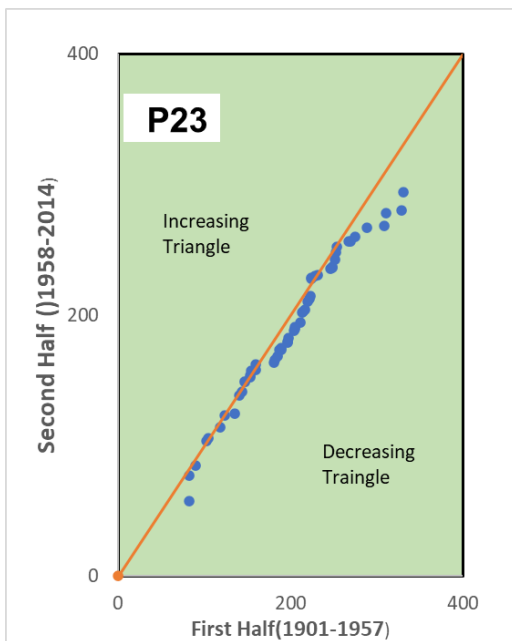
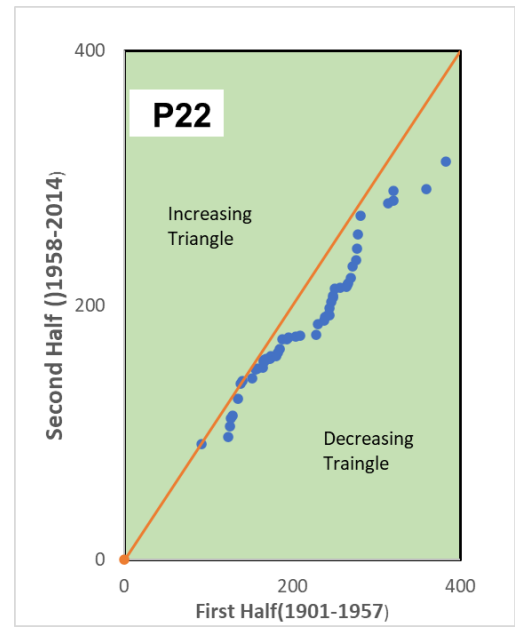
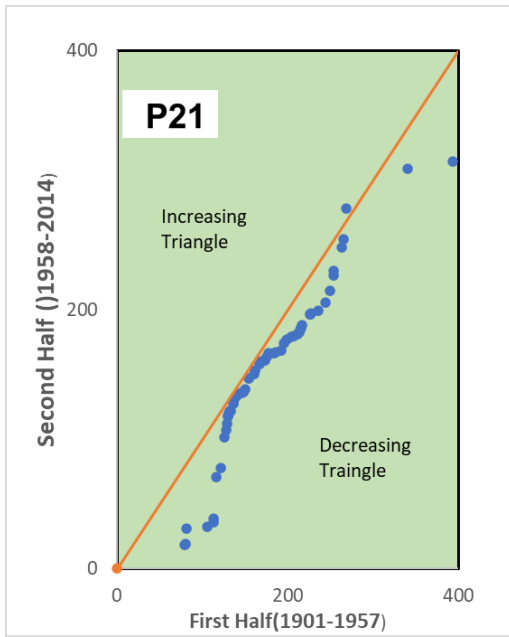


Fig 21: Trend Analysis of Points P21, P22, P23, P24

Result:

- Points P21, P22, P23, P24 are showing decreasing trend

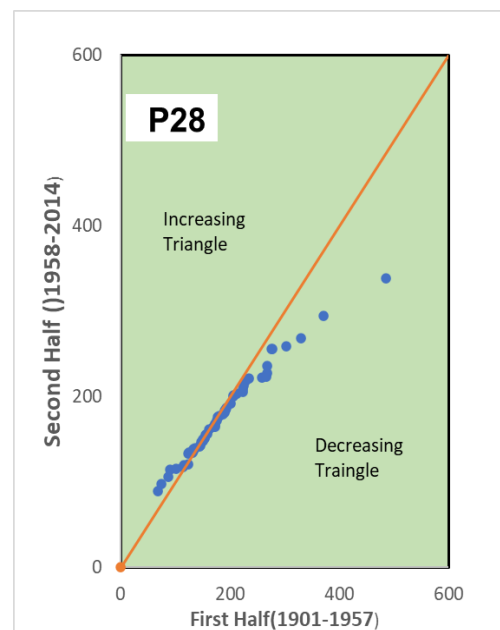
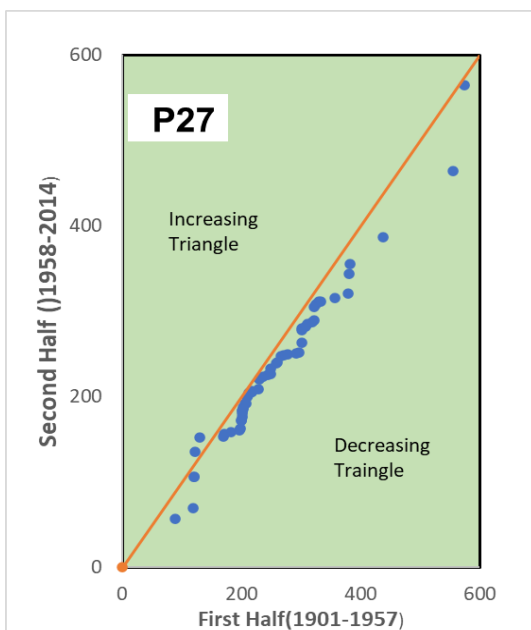
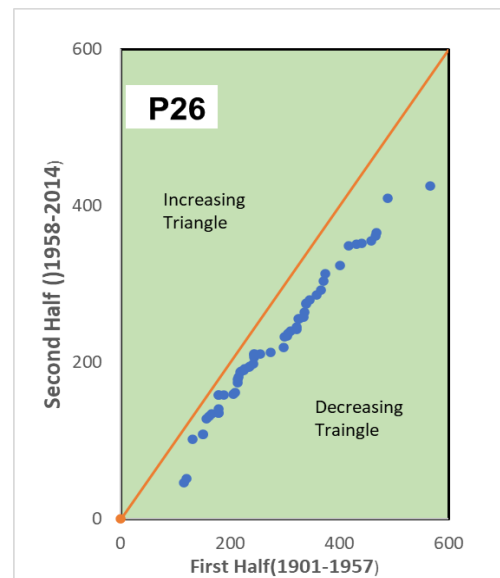
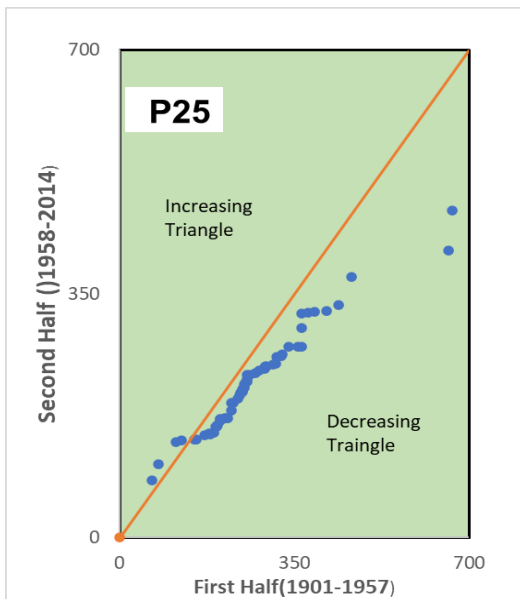


Fig 22: Trend Analysis of Points P25, P26, P37, P28

Result:

- Points P25, P26, P27, P28 are showing decreasing trend

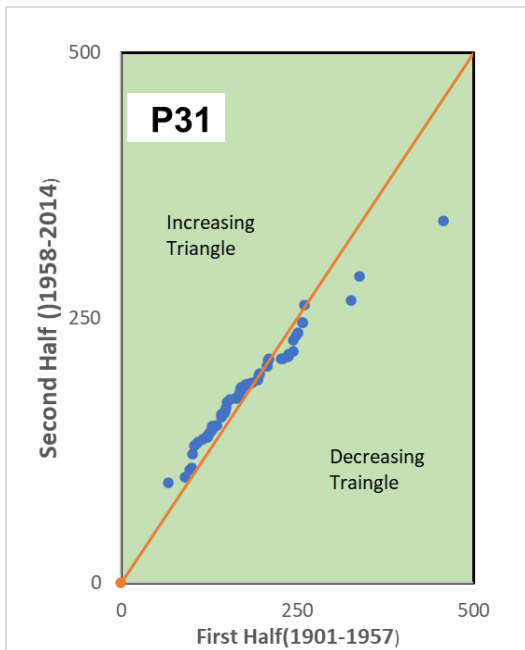
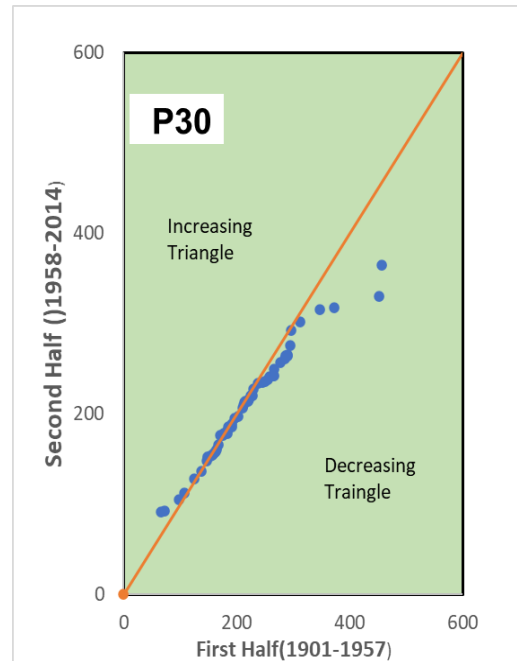
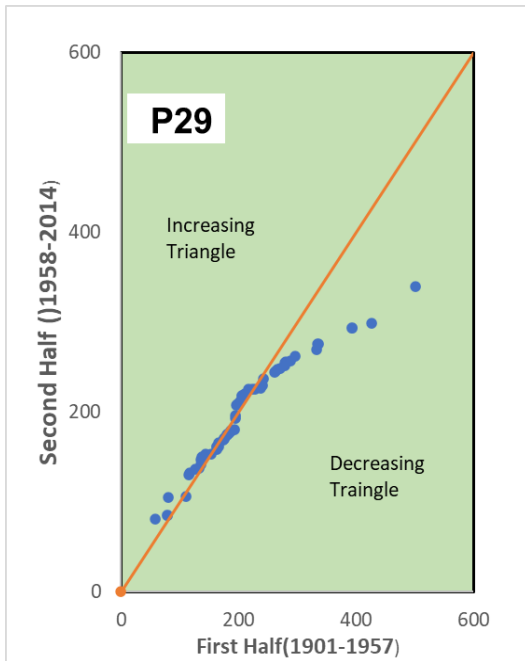


Fig 23: Trend Analysis of Points P29, P30, P31

Result:

- Points P29, P30 are showing decreasing trend
- Points P31 is showing increasing trend

Discussion

There is a mix trend in the pre-monsoon season but decreasing trend is significant

We can observe a decreasing trend in the Himalayan (extreme north) areas.

MONSOON

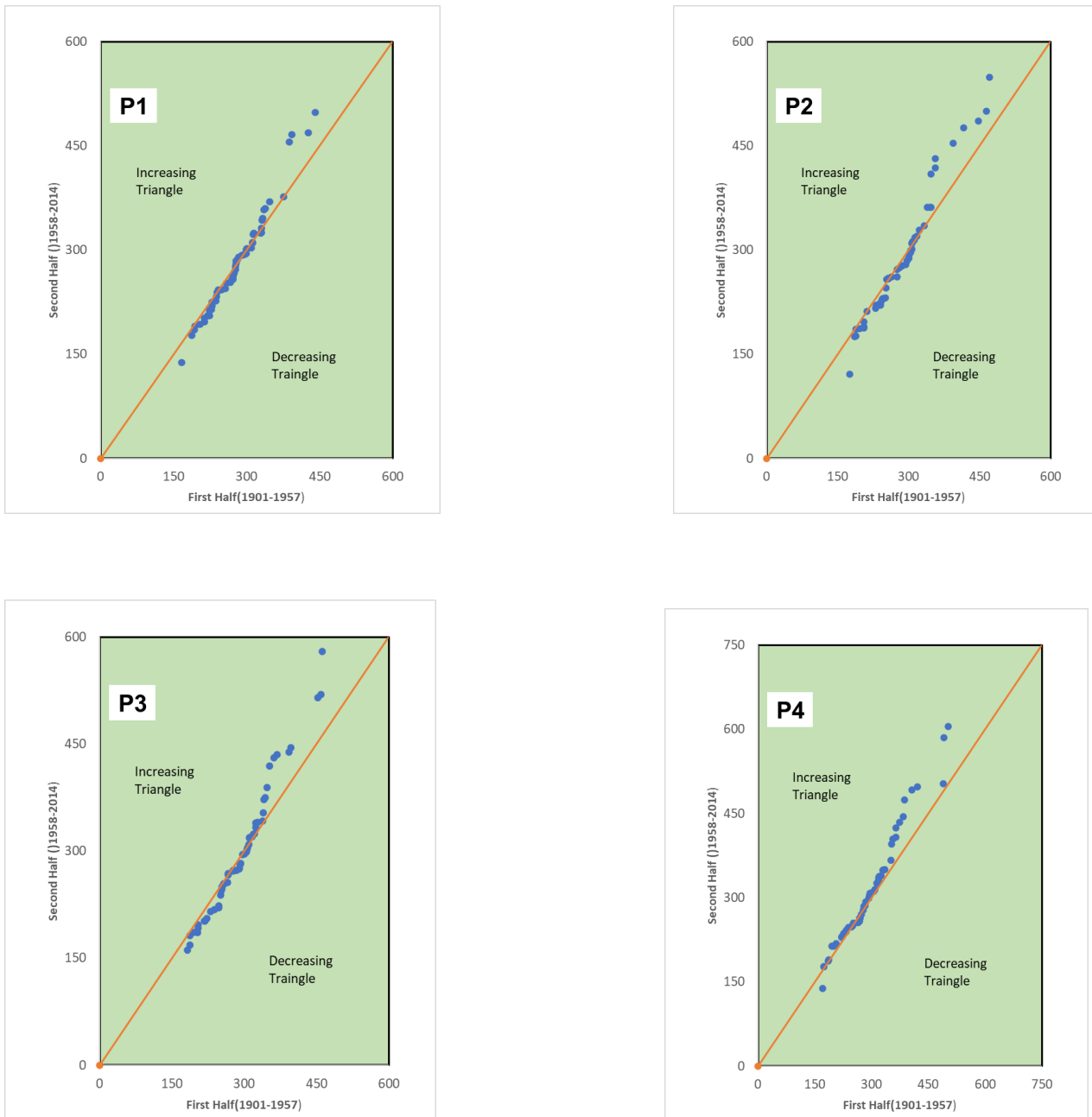


Fig 24: Trend Analysis of Points P1, P2, P3, P4

Result:

- Points P1, P2, P3, P4 are showing increasing trend

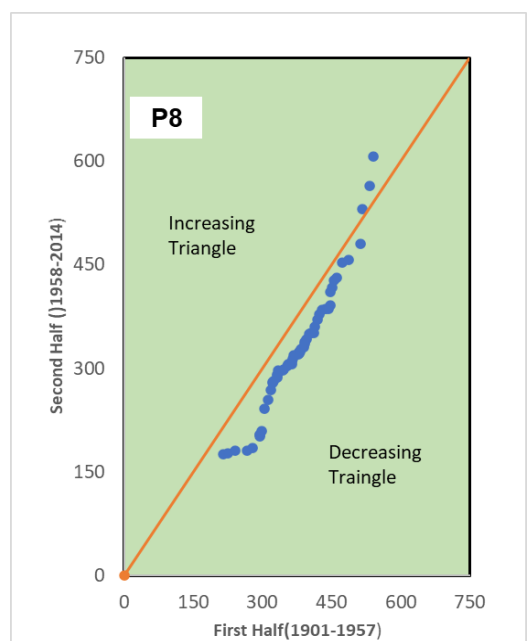
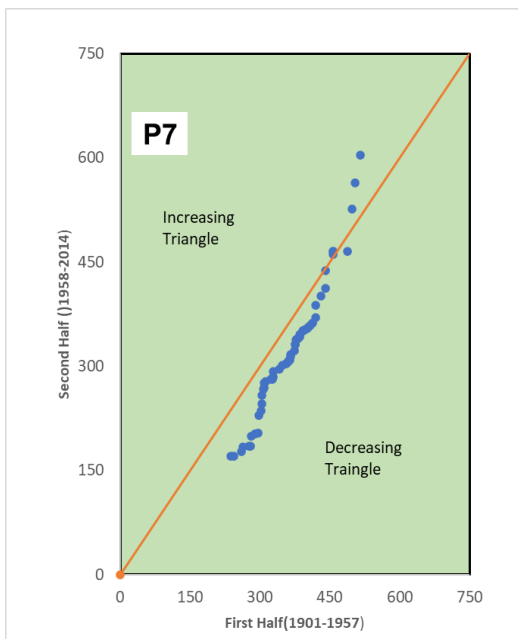
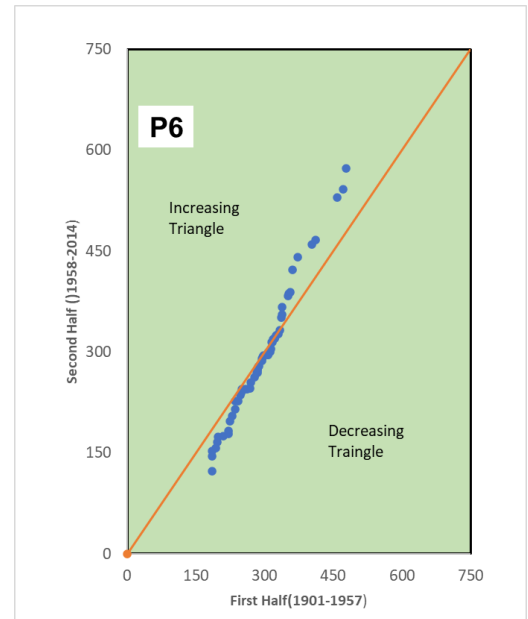
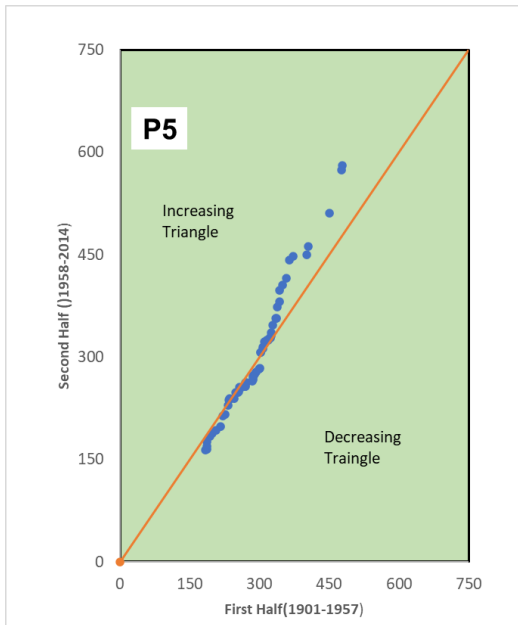


Fig 25: Trend Analysis of Points P6, P7, P8, P9

Result:

- Points P5 is showing increasing trend
- Points P6, P7, P8 are showing decreasing trend

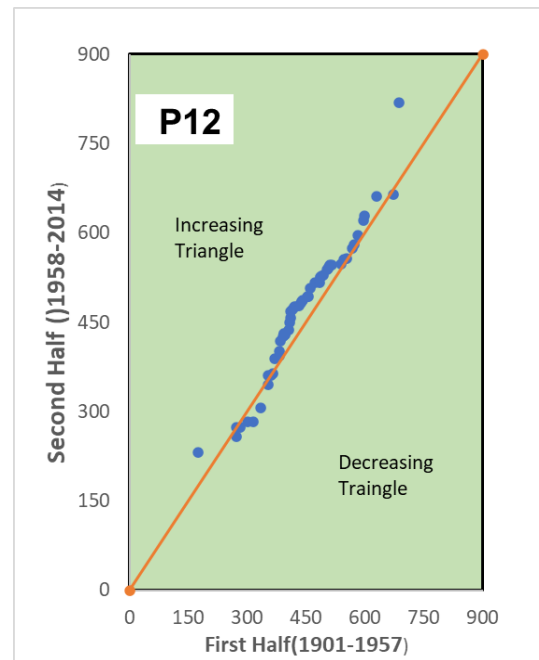
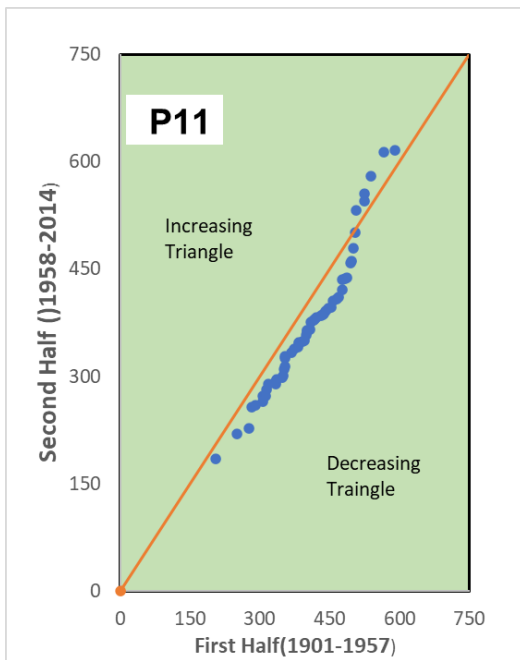
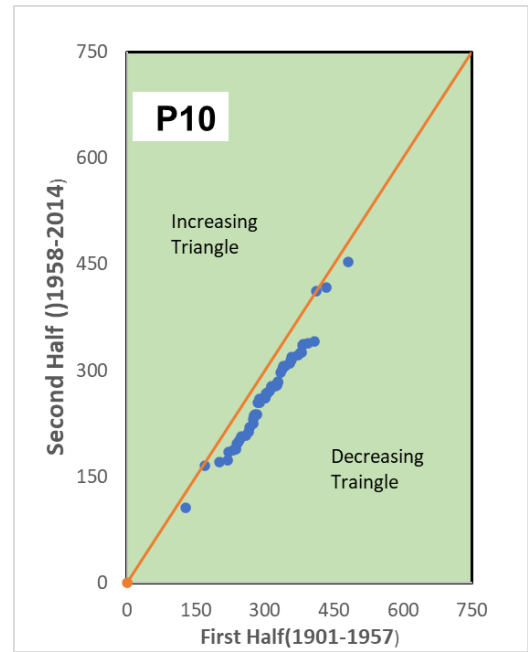
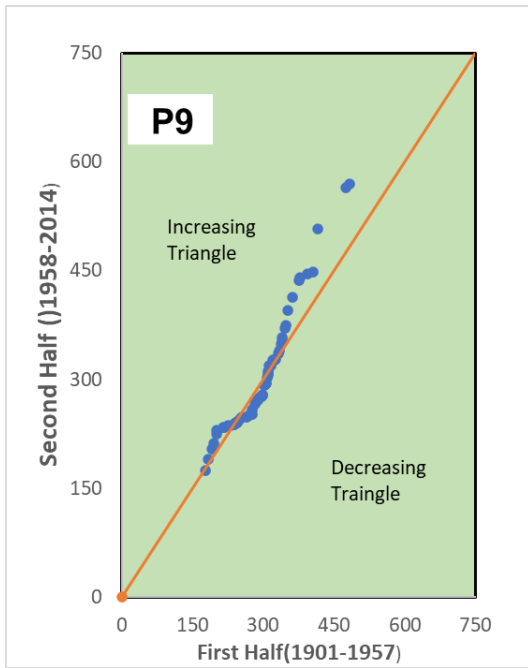


Fig 26: Trend Analysis of Points P9, P10, P11, P12

Result:

- Points P9, P12 are showing increasing trend
- Points P10, P11 are showing decreasing trend

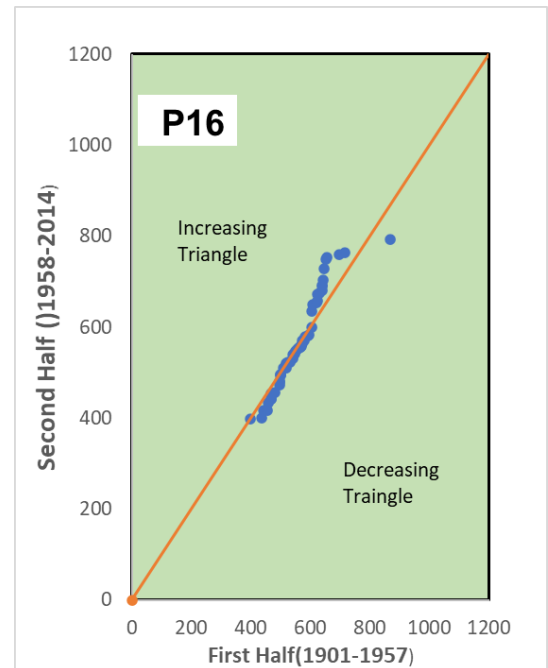
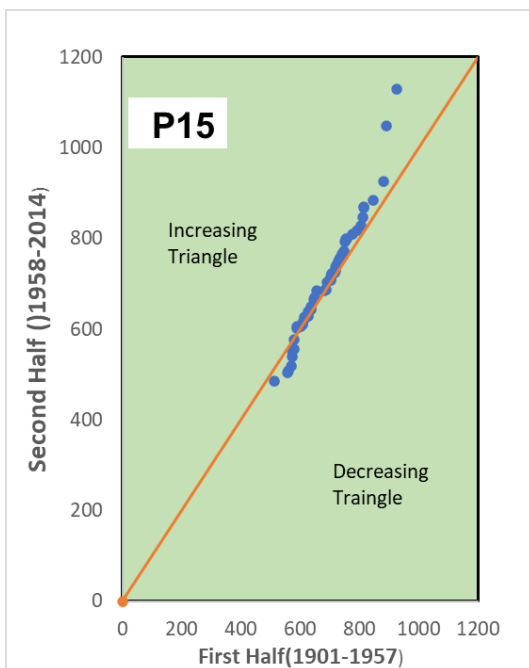
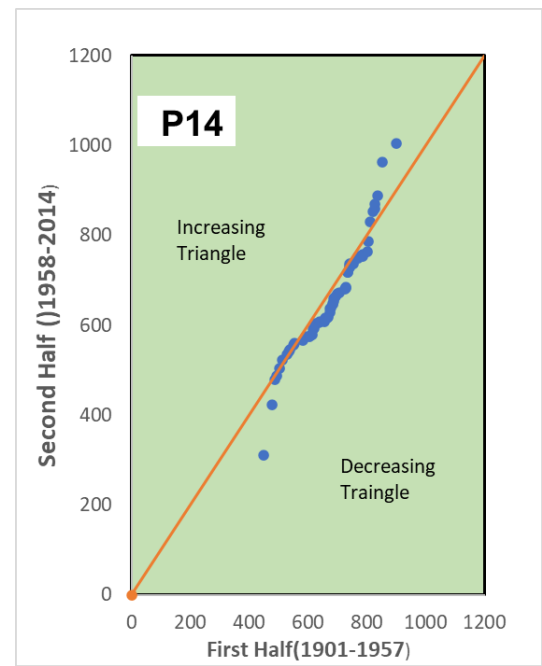
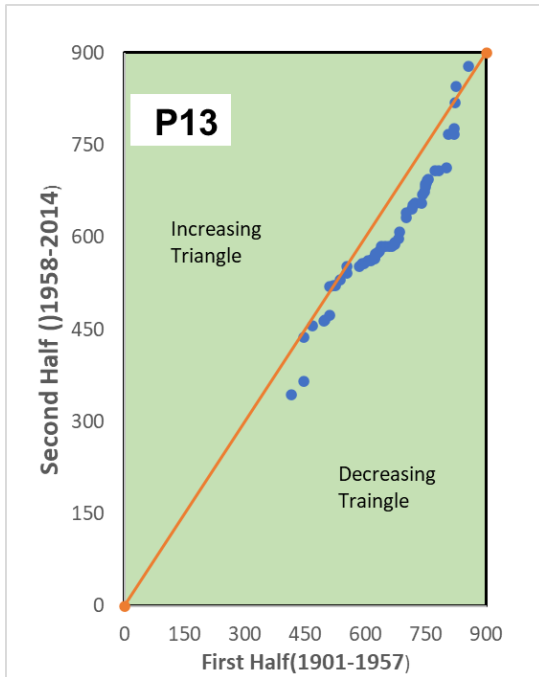


Fig 27: Trend Analysis of Points P13, P14, P15, P16

Result:

- Points P13, P14 are showing decreasing trend
- Points P15, P16 are showing increasing trend

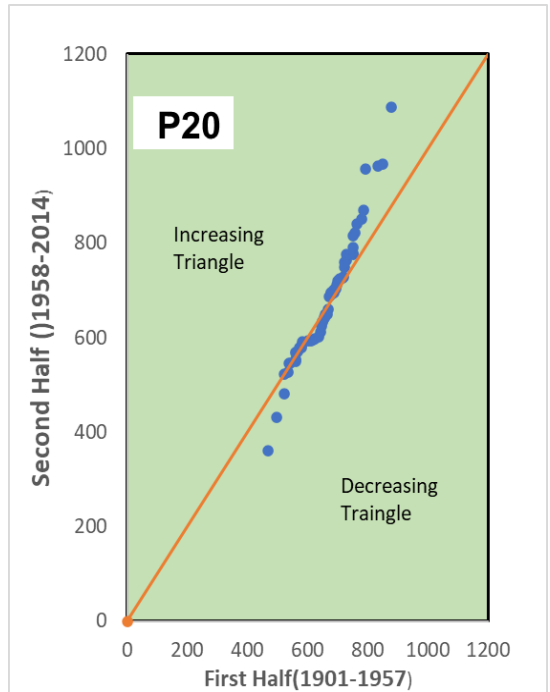
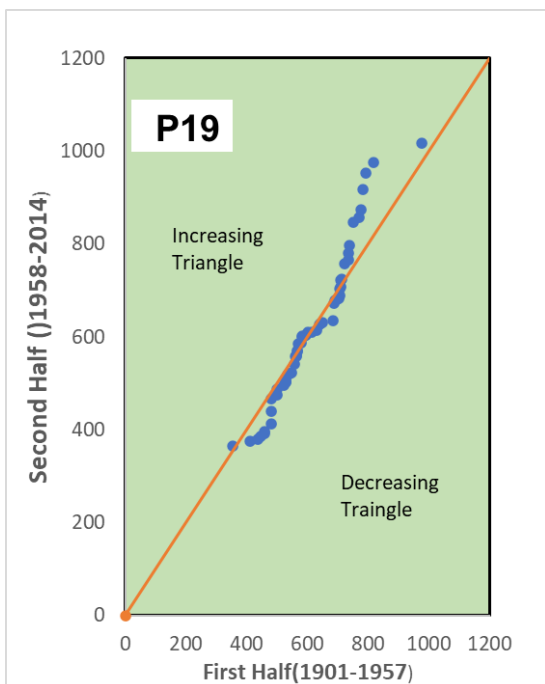
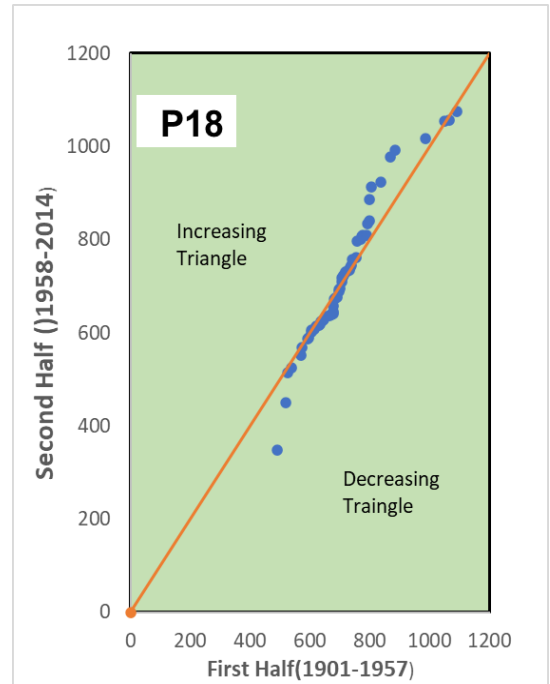
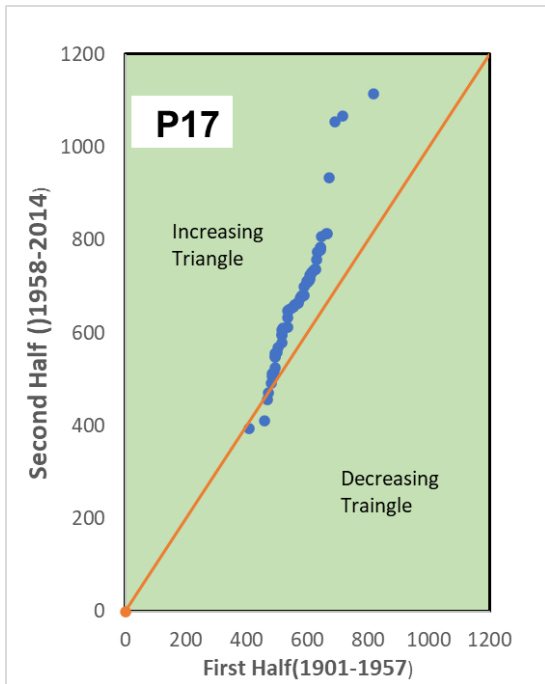


Fig 28: Trend Analysis of Points P17, P18, P19, P20

Result:

- Points P17, P18, P19, P20 are showing increasing trend

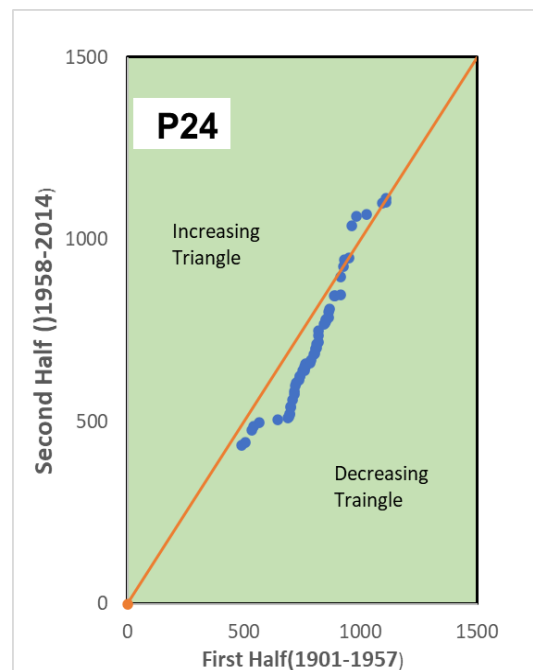
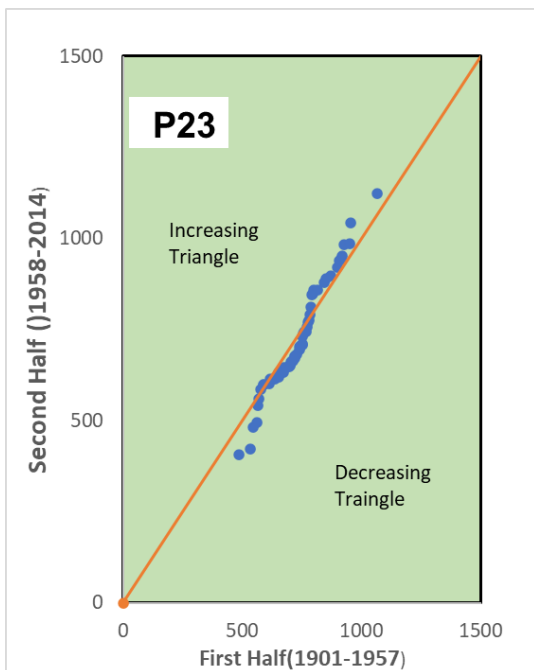
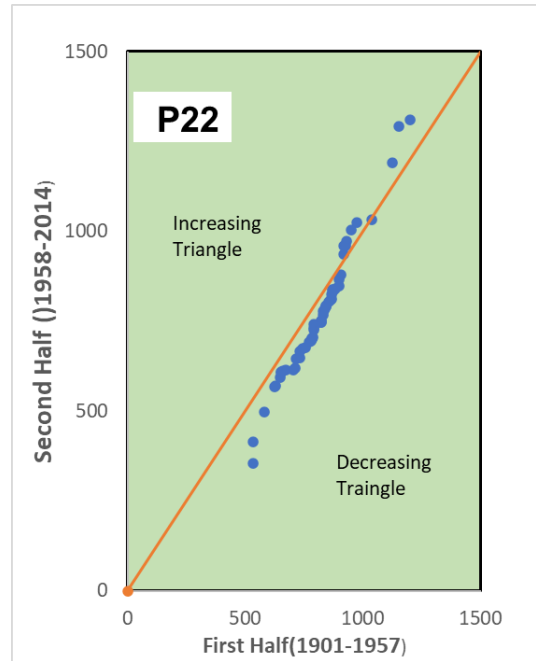
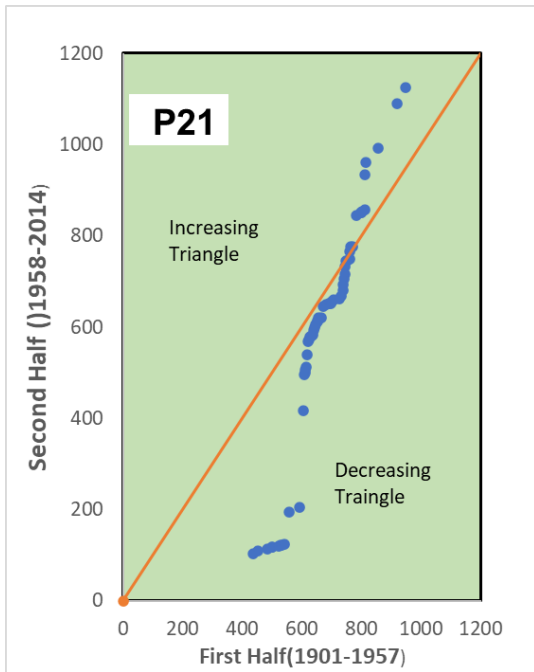


Fig 29: Trend Analysis of Points P21, P22, P23, P24

Result:

- Points P21, P22, P23, P24 are showing decreasing trend

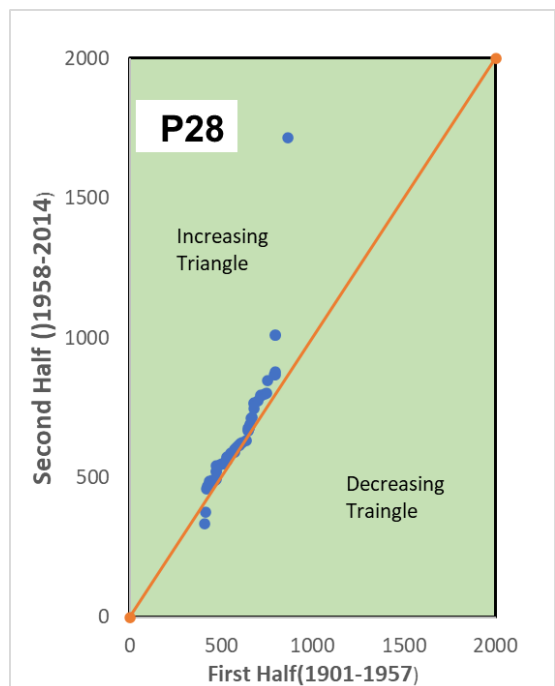
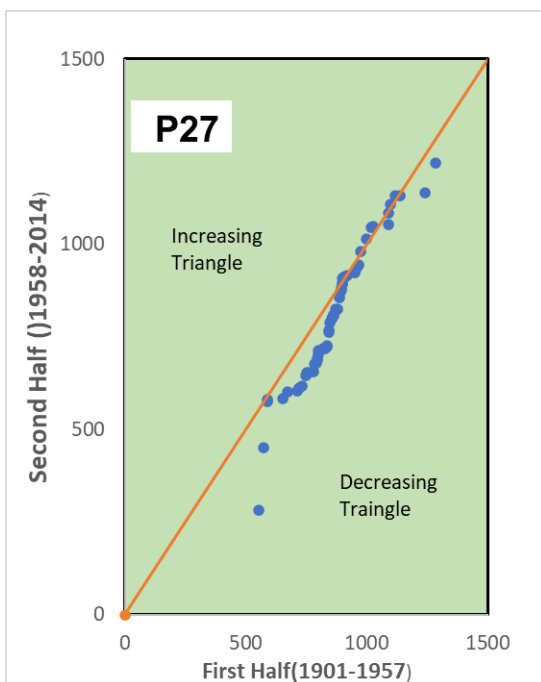
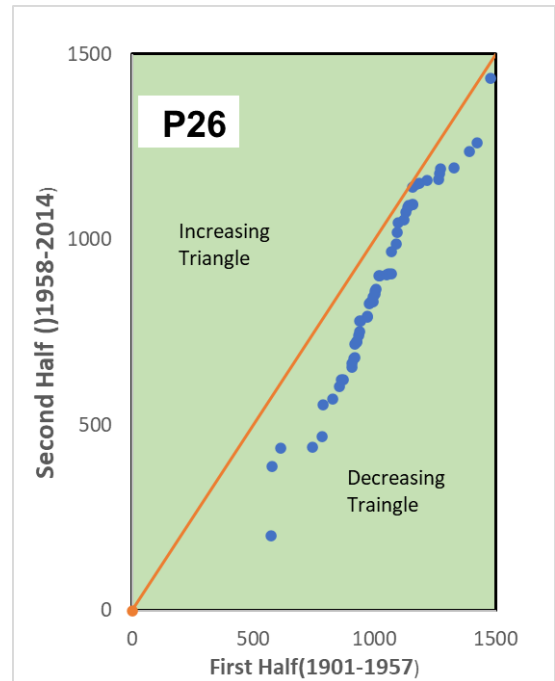
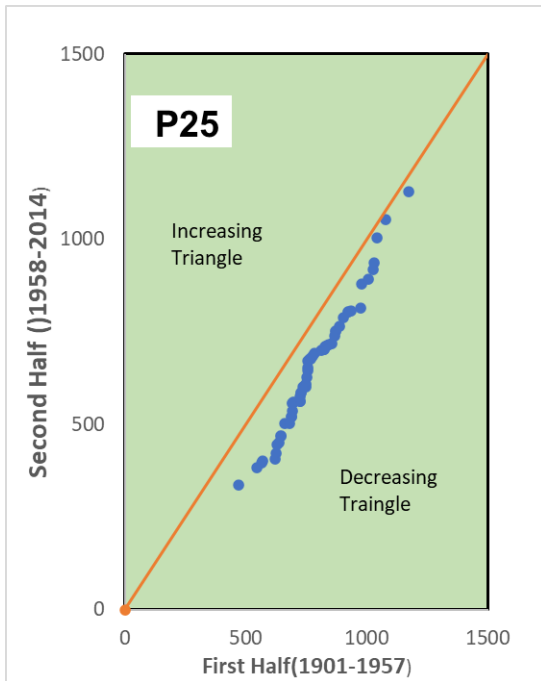


Fig 30: Trend Analysis of Points P25, P26, P27, P28

Result:

- Points P25, P26, P27 are showing decreasing trend
- Points P28 is showing increasing trend

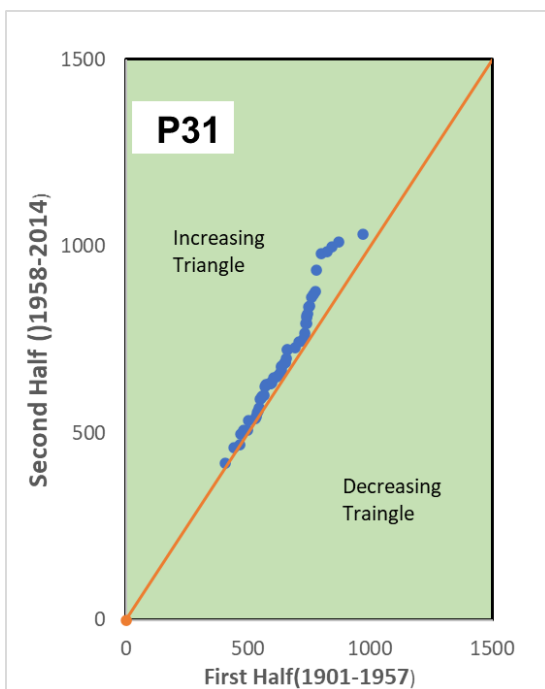
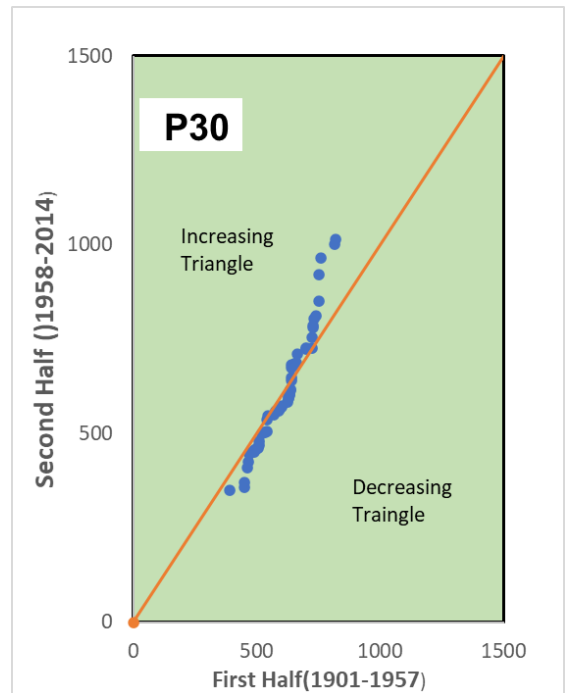
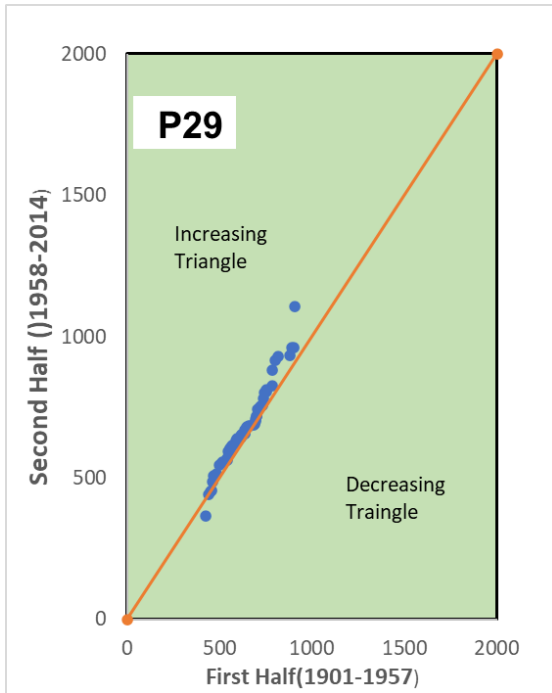


Fig 31: Trend Analysis of Points P29, P30, P31

Result:

- Points P29, P30, 31 are showing increasing trend

Discussion

There is a mix trend in the monsoon season but increasing trend is significant

17 stations are showing increasing trend while 14 stations are showing decreasing trend.

POST MONSOON

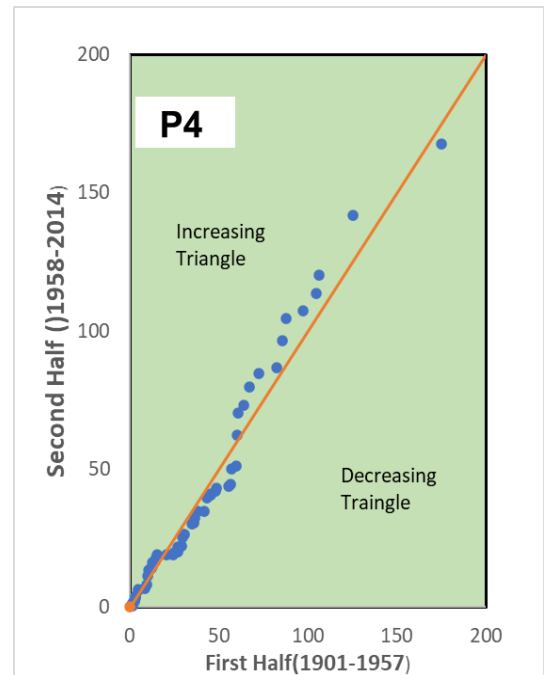
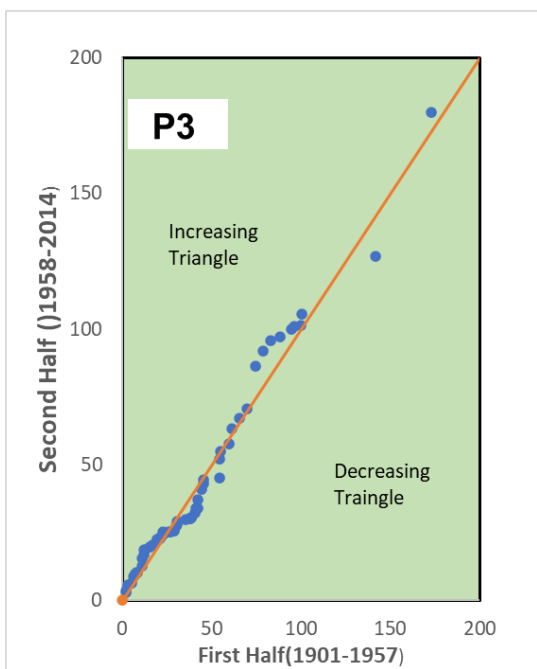
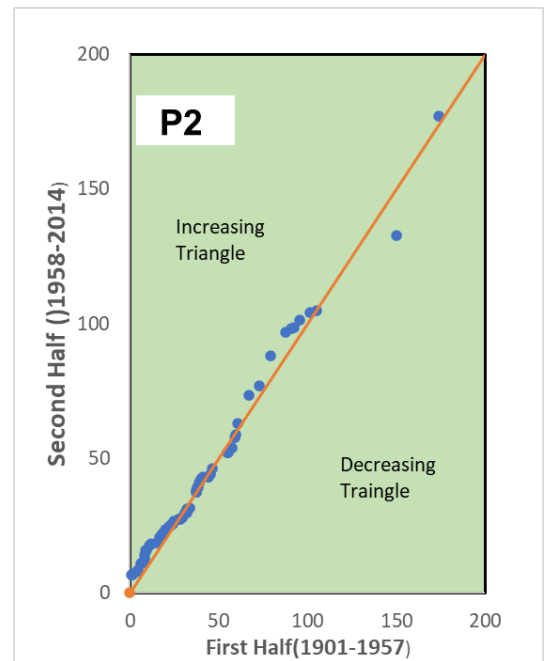
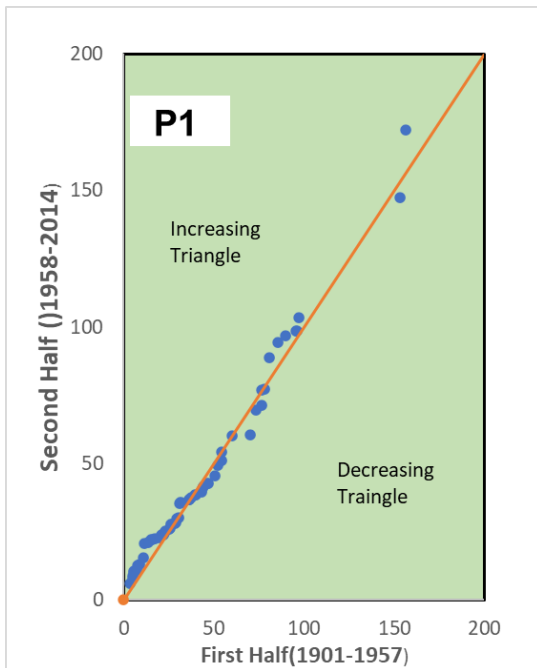


Fig 32: Trend Analysis of Points P1, P2, P3, P4

Result:

- Points P1, P2, P3, P4 are showing increasing trend

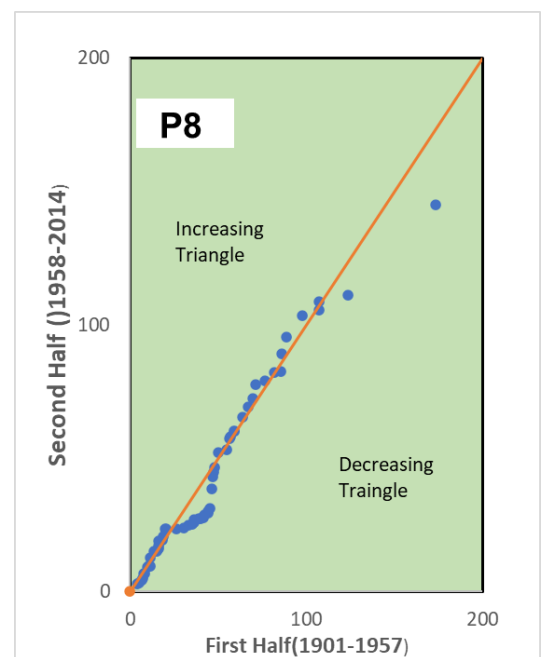
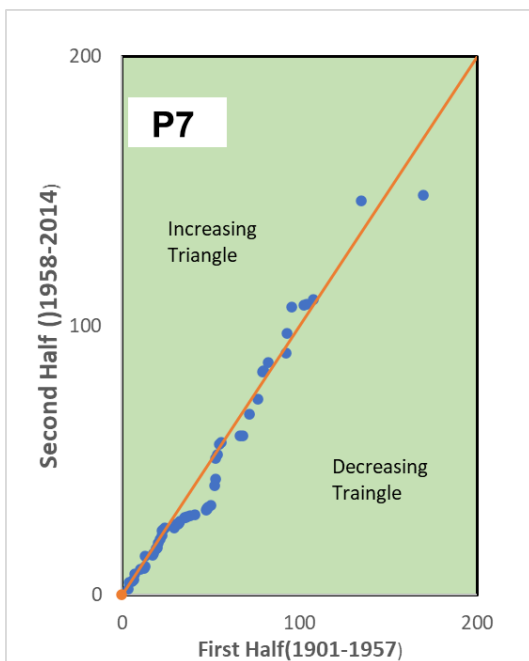
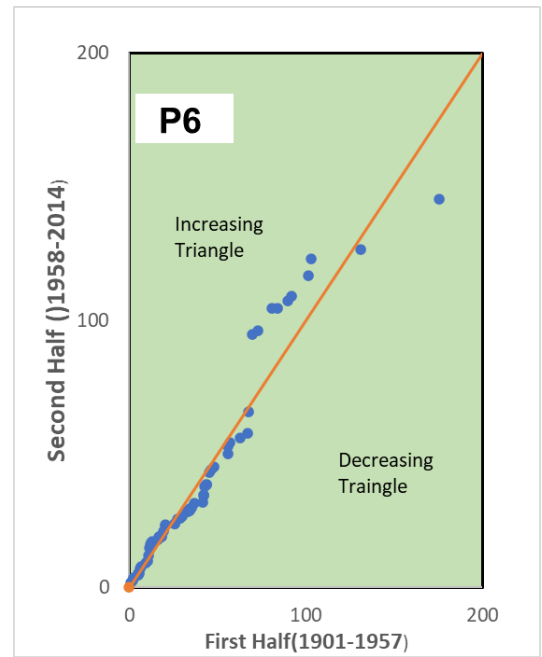
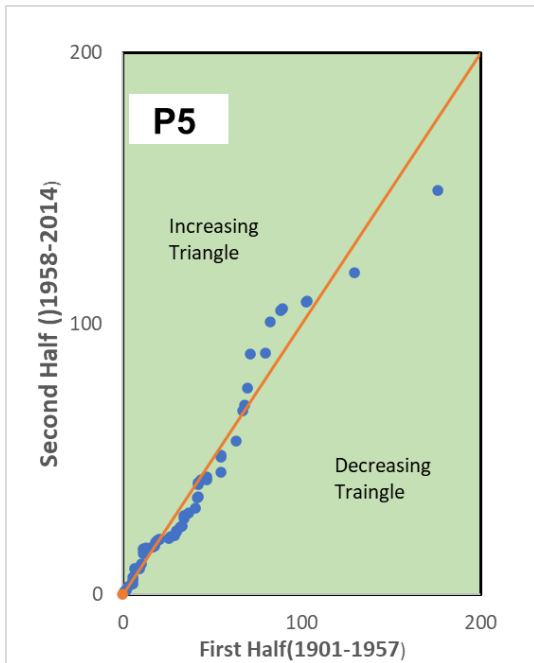


Fig 33: Trend Analysis of Points P5, P6, P7, P8

Result:

- Points P5, P7, P8 are showing decreasing trend
- Points P6 is showing increasing trend

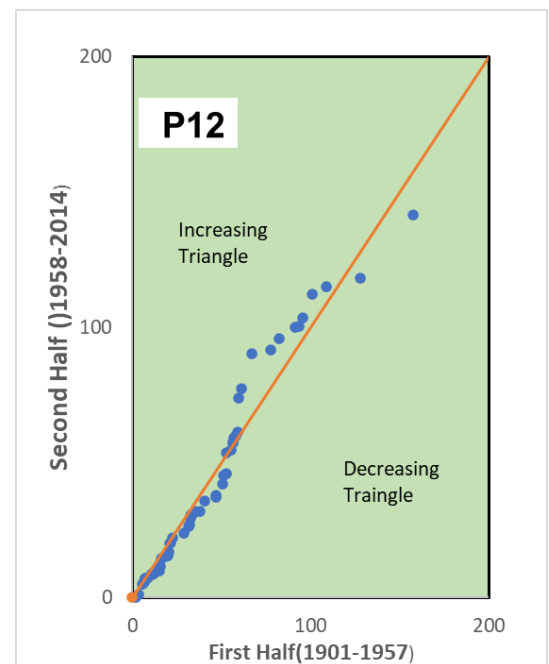
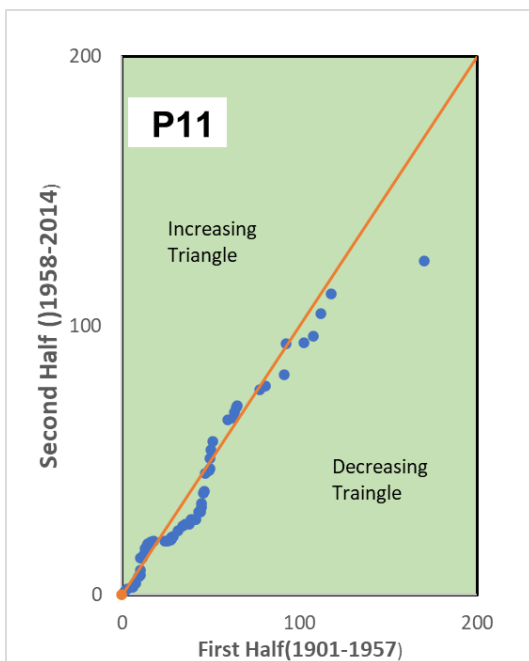
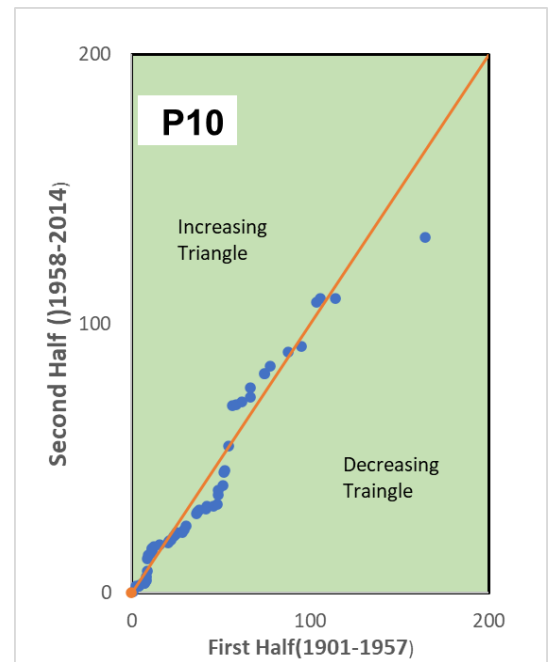
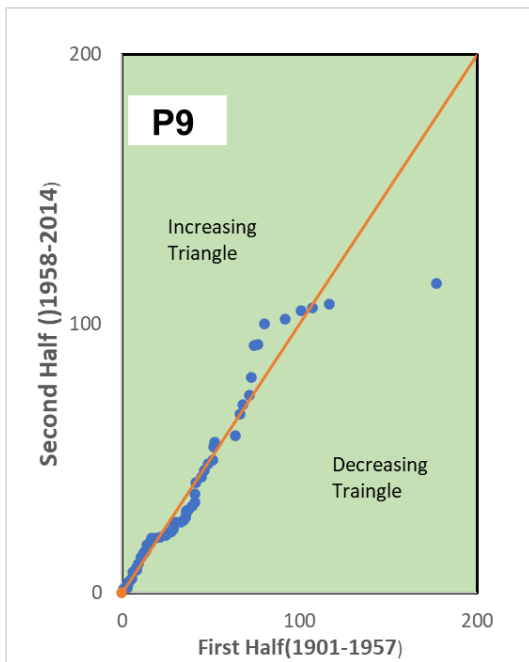


Fig 34: Trend Analysis of Points P9, P2, P3, P4

Result:

- Points P9, P10, P11, P12 are showing decreasing trend

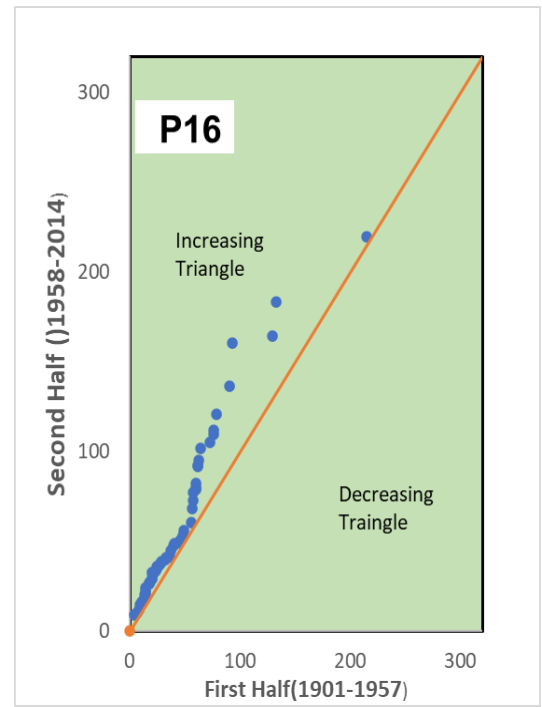
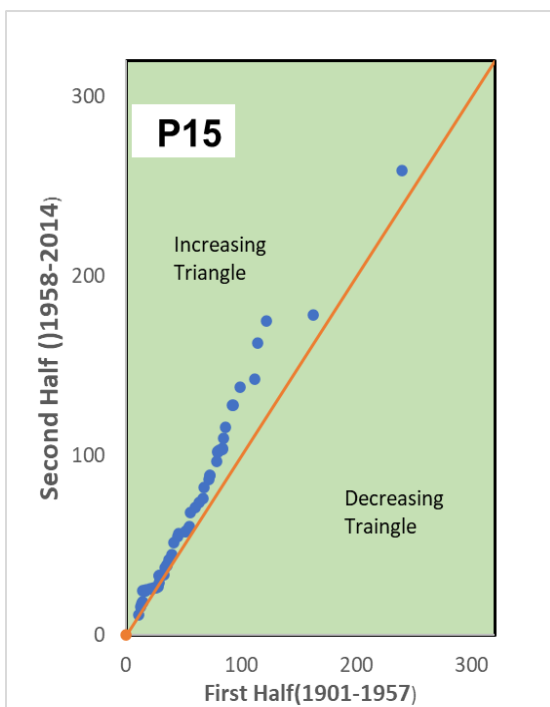
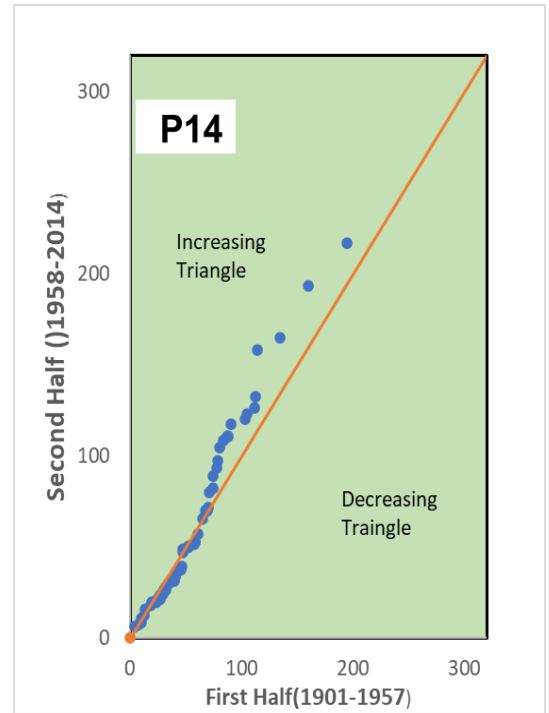
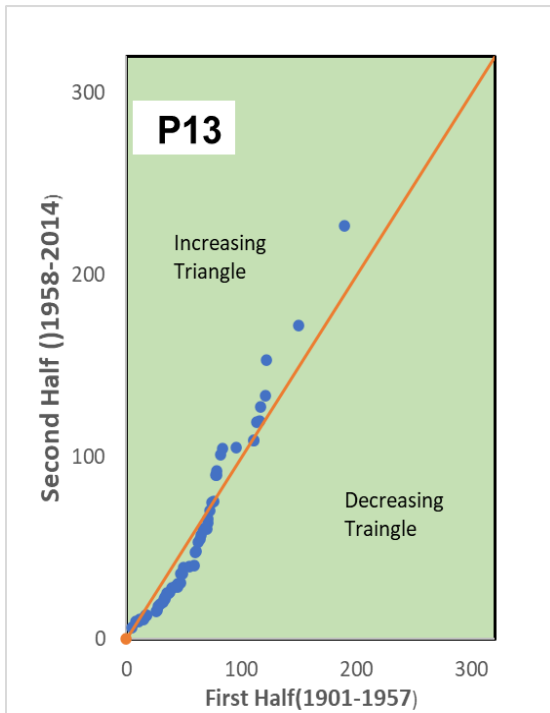


Fig 35: Trend Analysis of Points P1, P2, P3, P4

Result:

- Points P13 is showing decreasing trend
- Points P14, P15, P16 are showing increasing trend

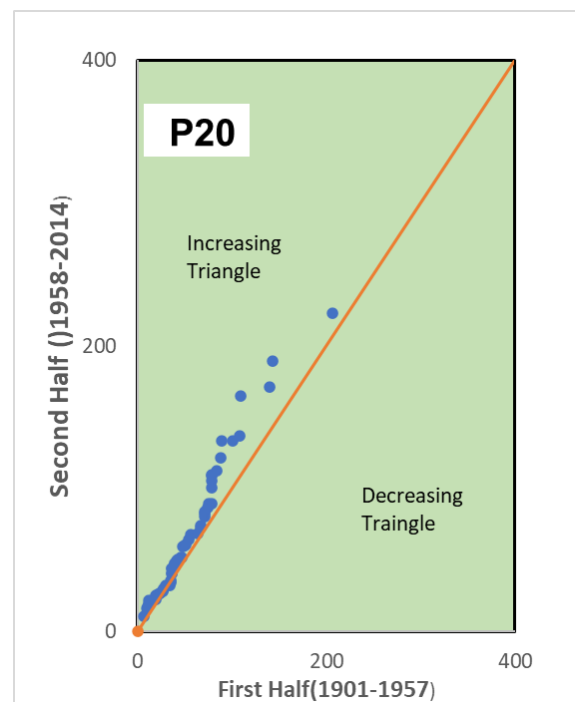
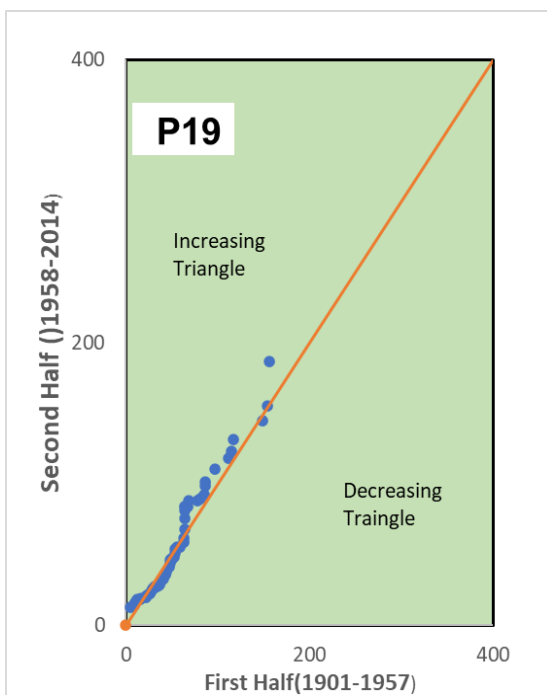
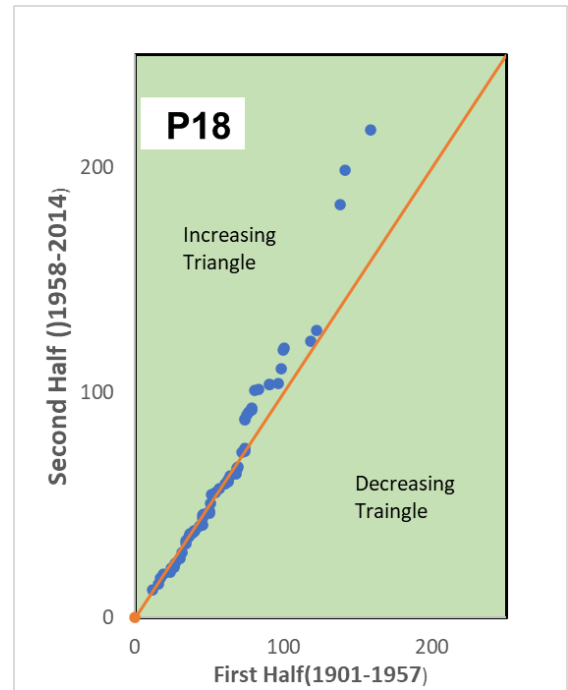
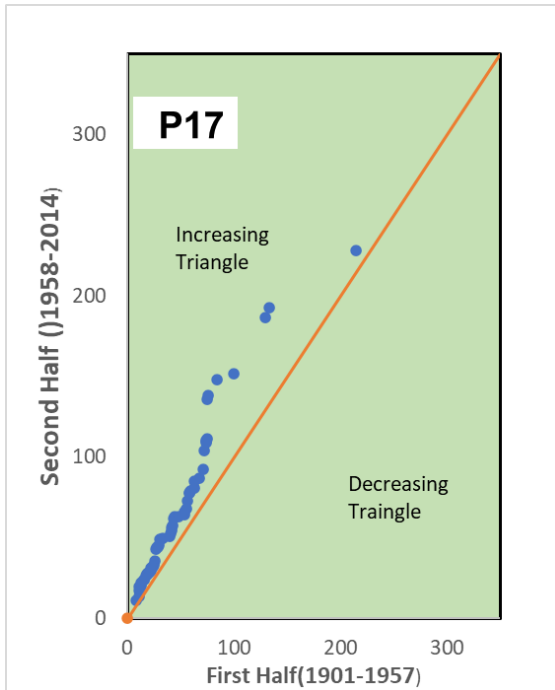


Fig 36: Trend Analysis of Points P17, P18, P19, P20

Result:

- Points P17, P18, P19, P20 are showing increasing trend

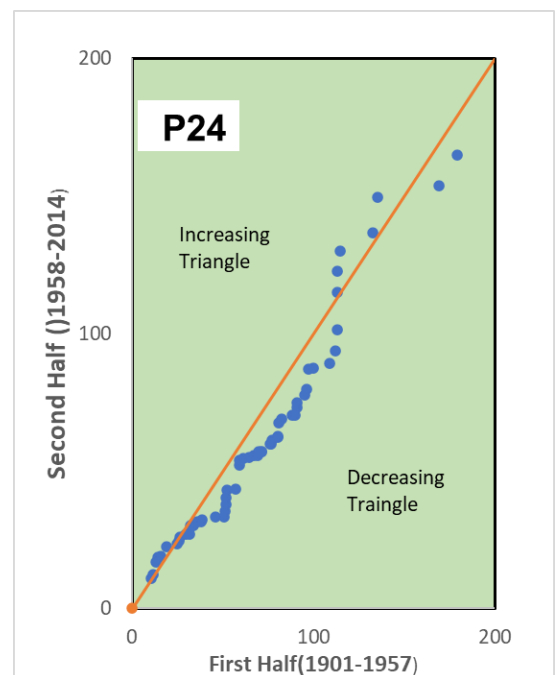
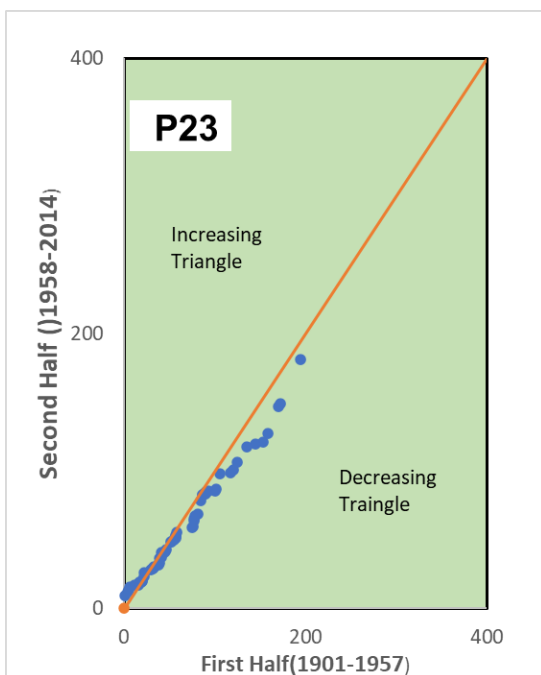
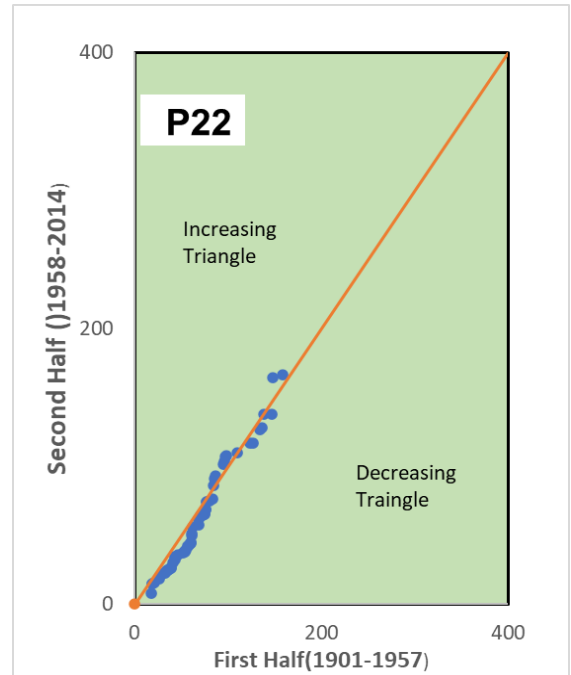
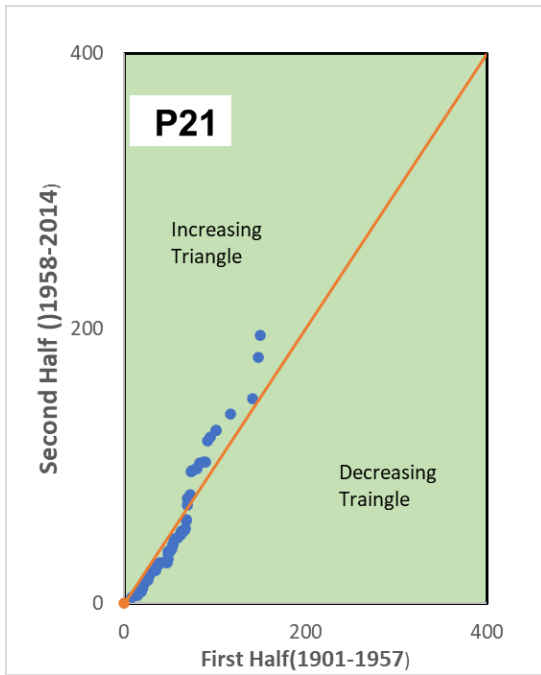


Fig 37: Trend Analysis of Points P21, P22, P23, P24

Result:

- Points P21, P22, P23, P24 are showing decreasing trend

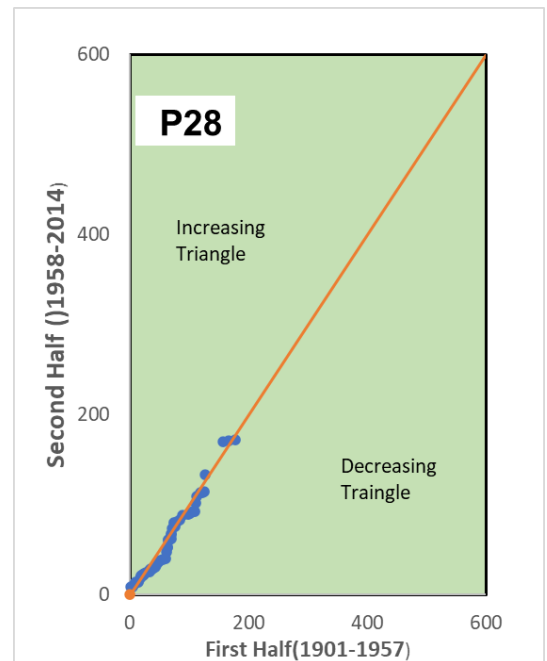
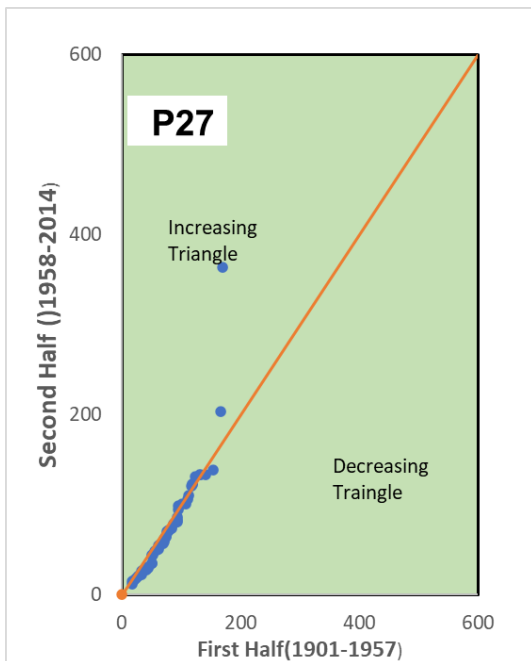
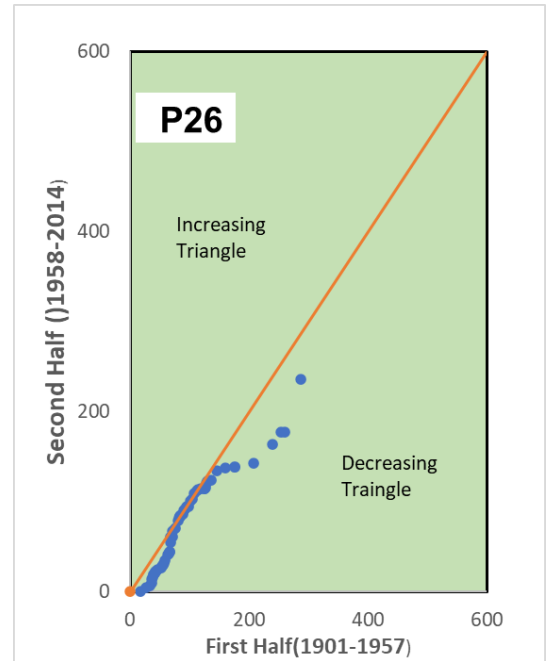
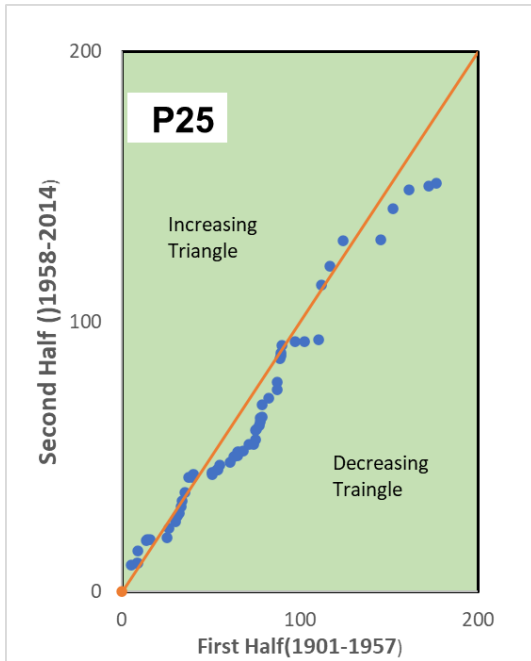


Fig 38: Trend Analysis of Points P25, P26, P27, P28

Result:

- Points P25, P26, P27, P28 are showing decreasing trend

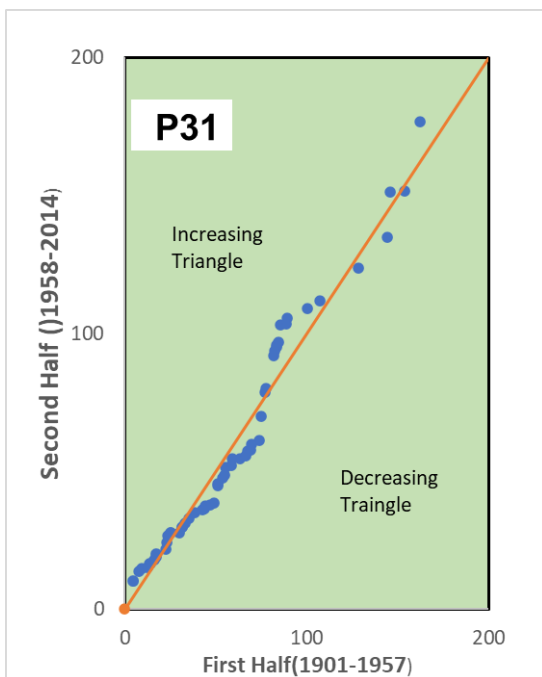
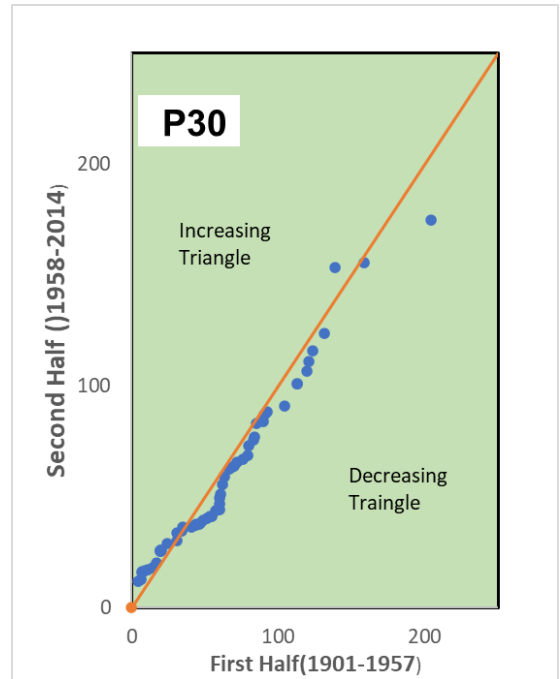
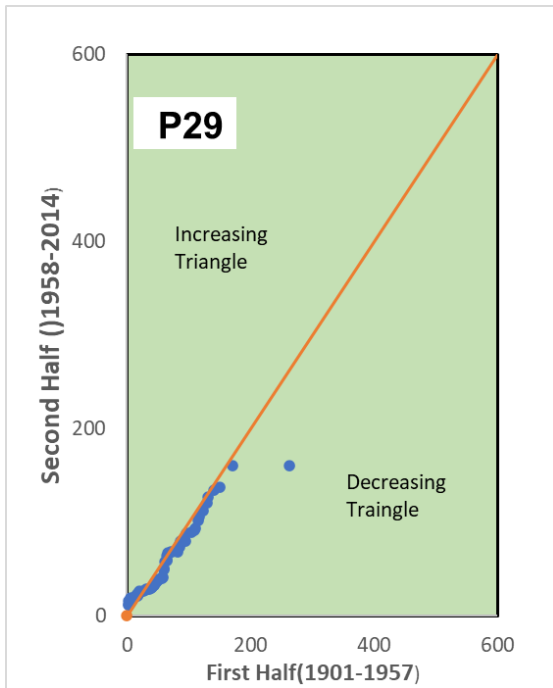


Fig 39: Trend Analysis of Points P29, P30, P31

Result:

- Points P29, P30 are showing decreasing trend
- Points P31 is showing increasing trend

Discussion

There is a decreasing trend in the post-monsoon season

18 stations are showing decreasing trend and 13 stations are showing increasing trend.

ANNUAL

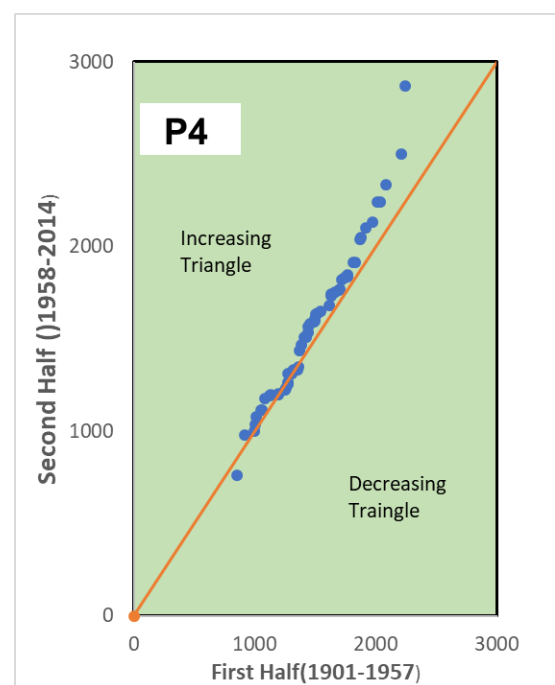
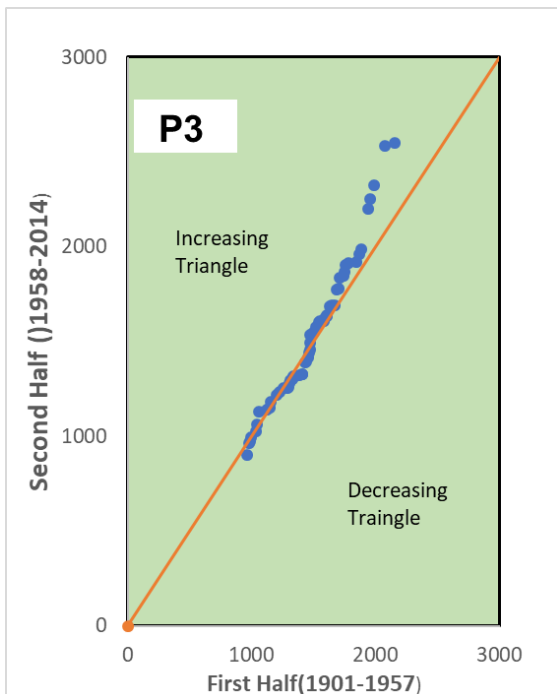
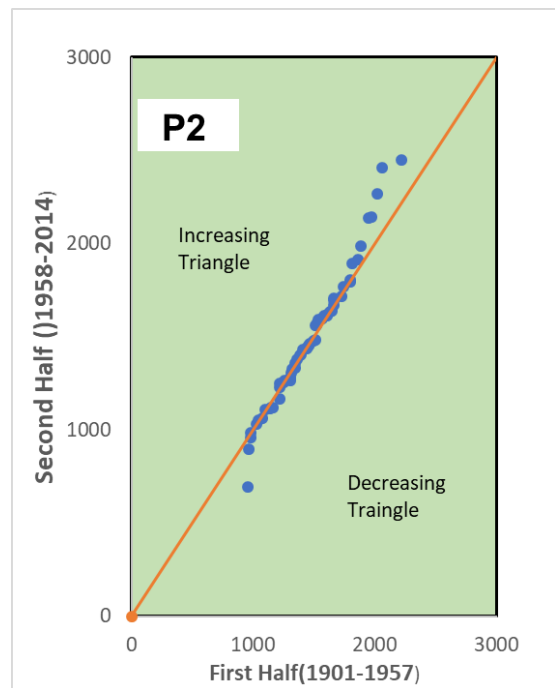
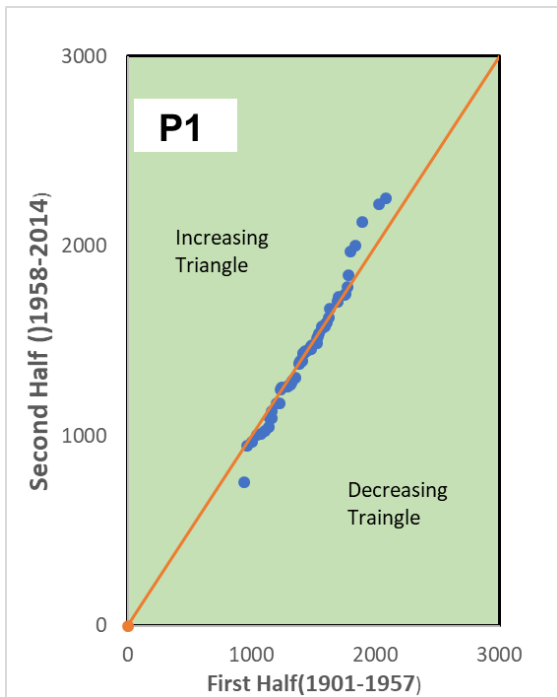


Fig 40: Trend Analysis of Points P1, P2, P3, P4

Result:

- Points P1, P2, P3, P4 are showing increasing trend

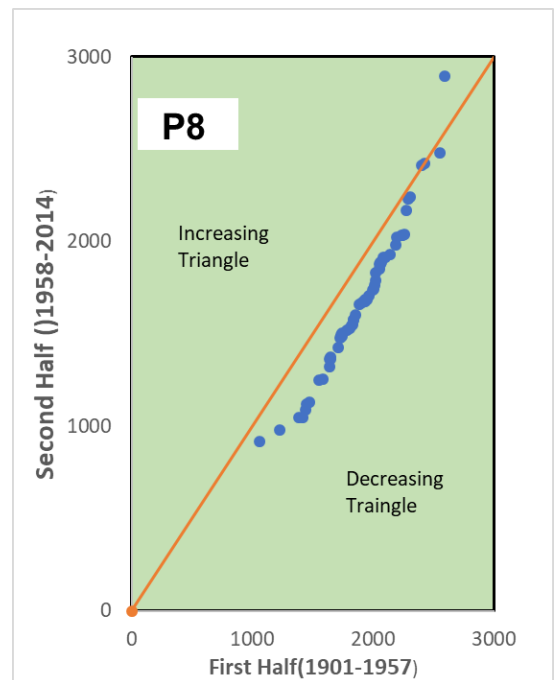
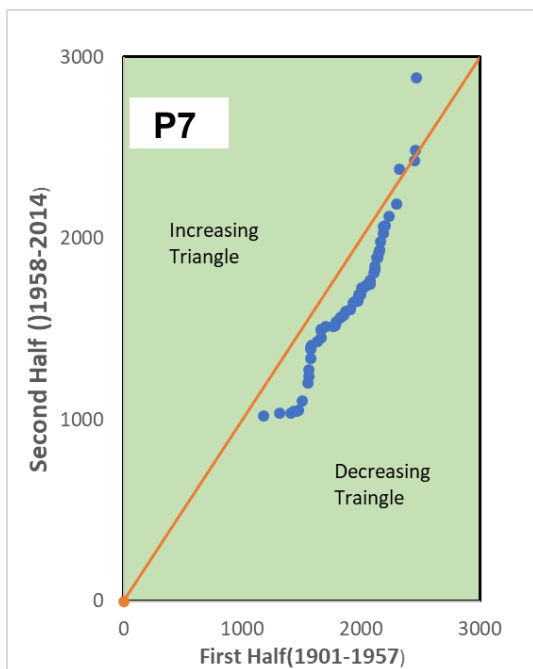
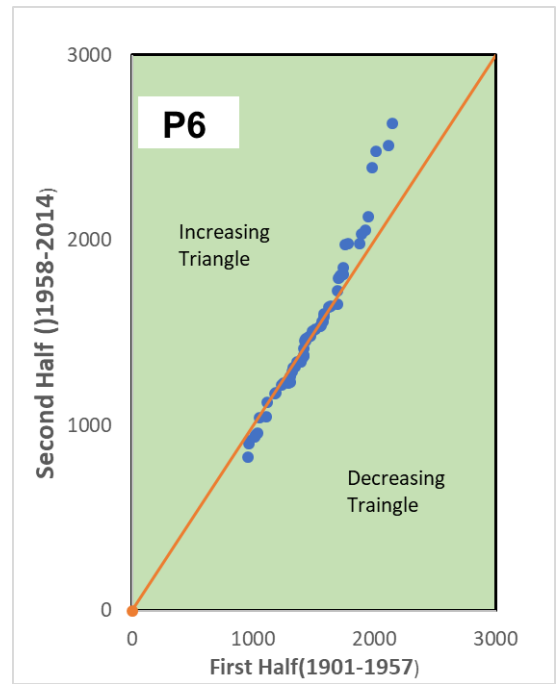
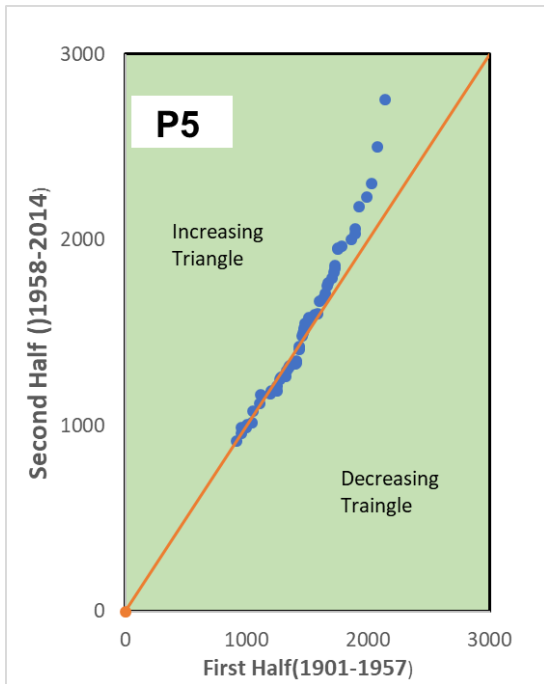


Fig 41: Trend Analysis of Points P5, P6, P7, P8

Result:

- Points P5, P6 are showing increasing trend
- Points P7, P8 are showing decreasing trend

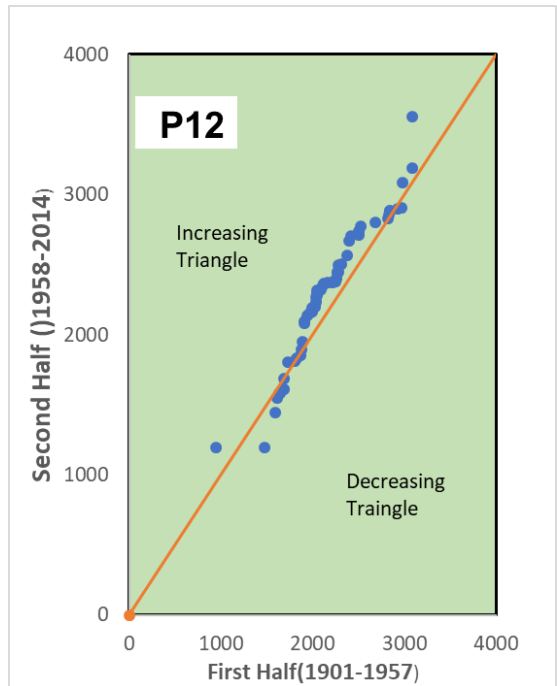
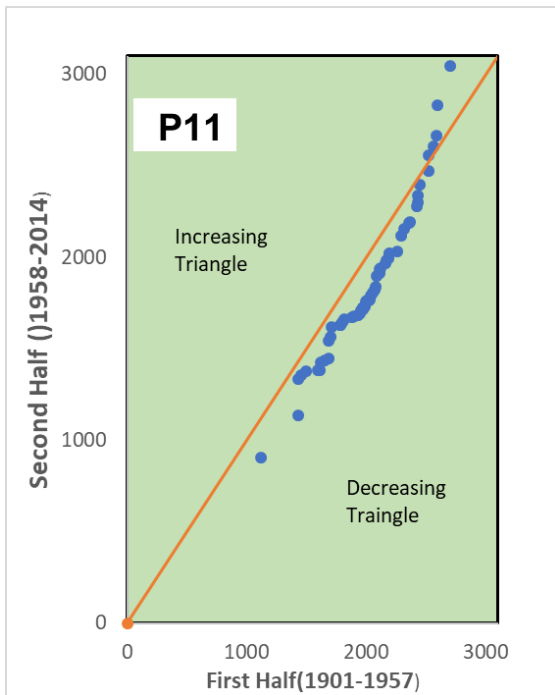
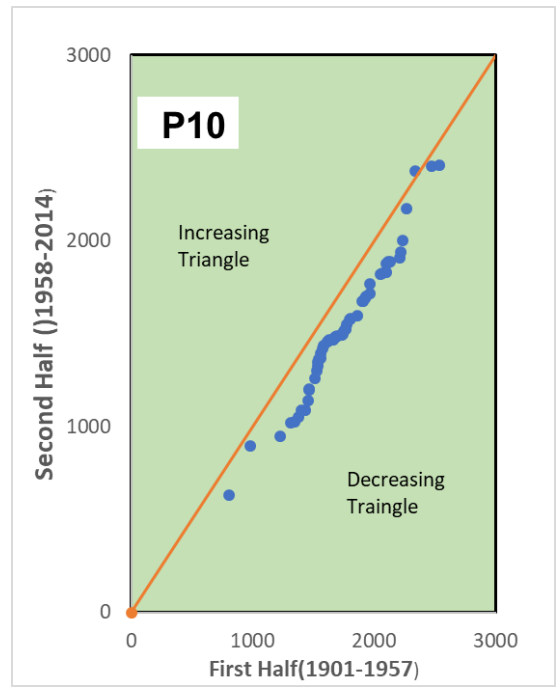
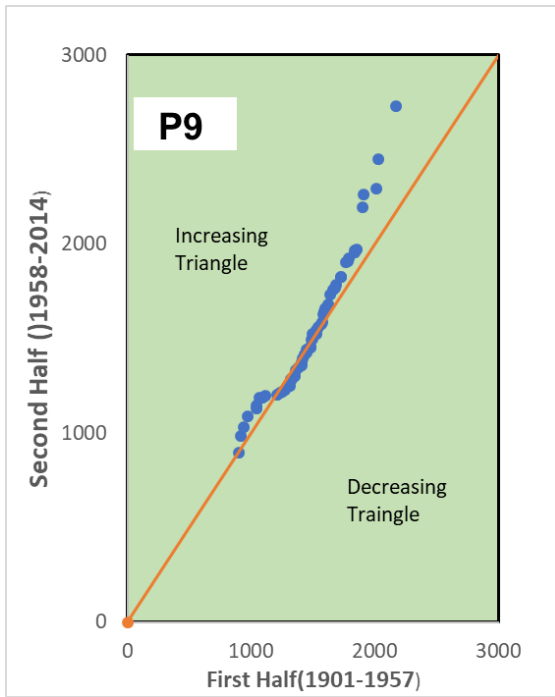


Fig 42: Trend Analysis of Points P9, P10, P11, P12

Result:

- Points P9, P12 are showing increasing trend
- Points P10, P11 are showing decreasing trend

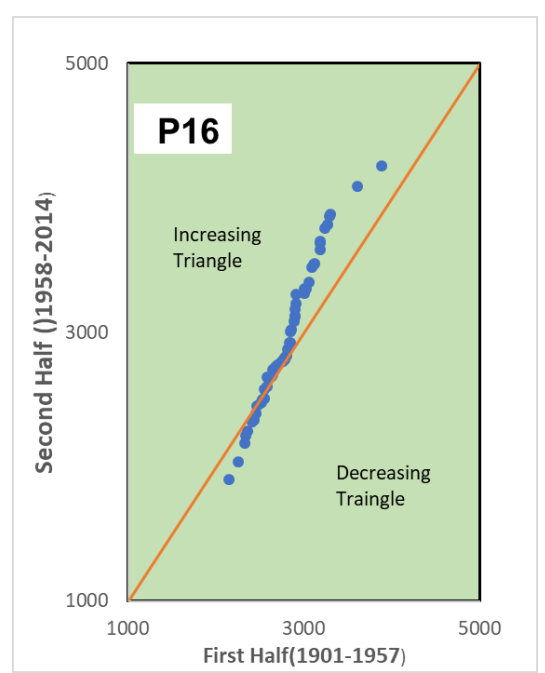
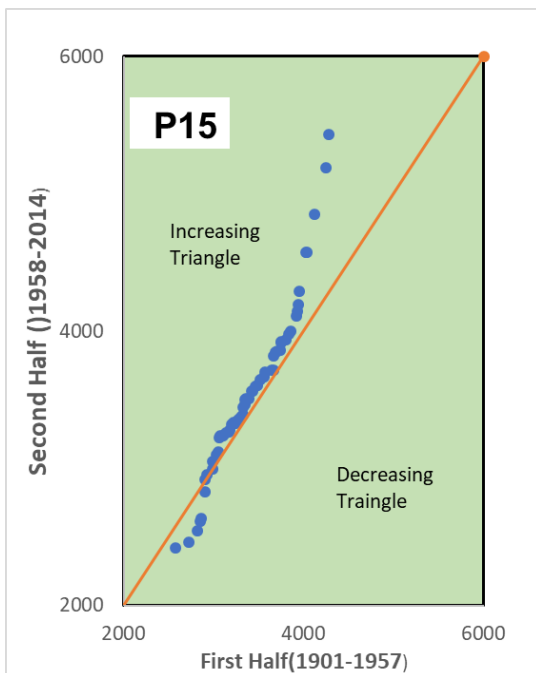
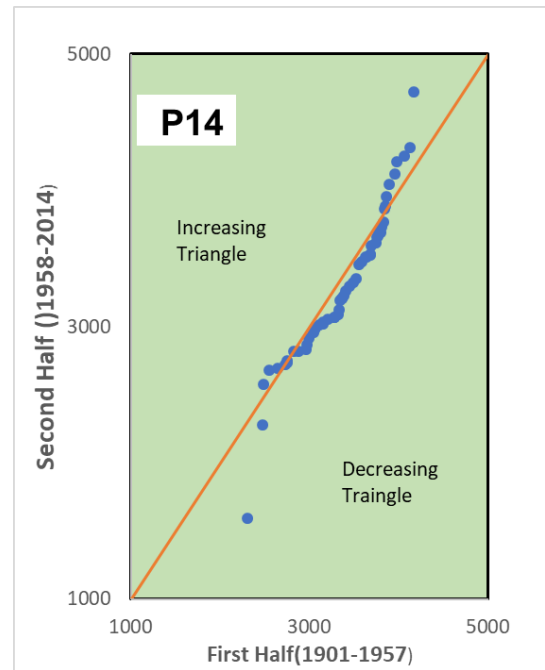
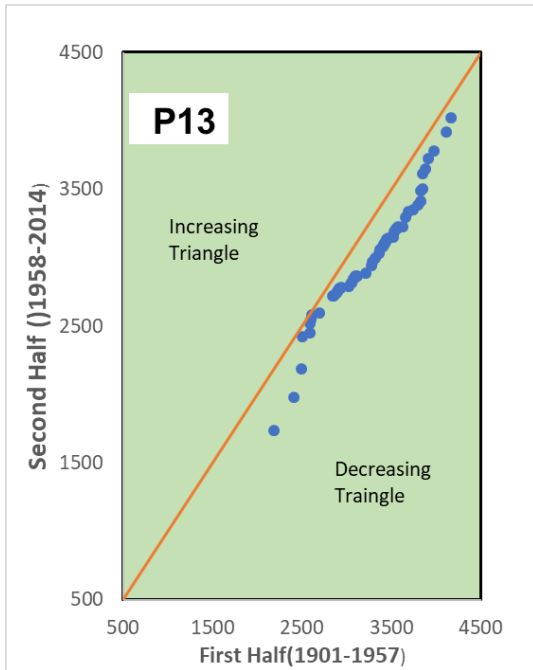


Fig 43: Trend Analysis of Points P13, P14, P15, P16

Result:

- Points P13, P14 are showing decreasing trend
- Points P15, P16 are showing increasing trend

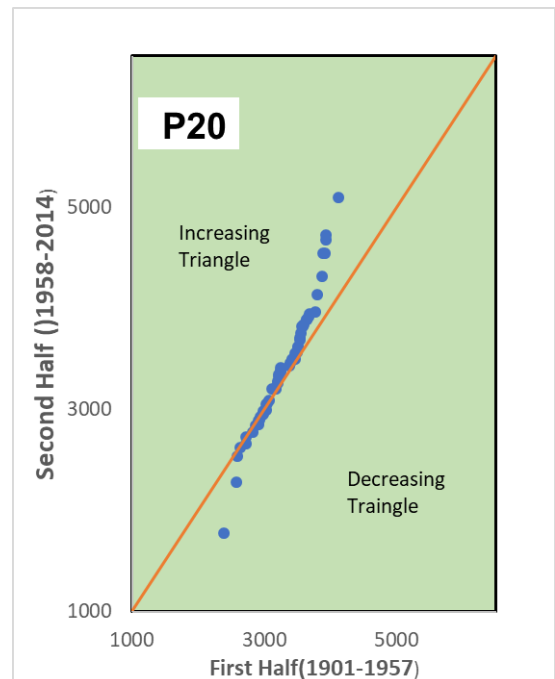
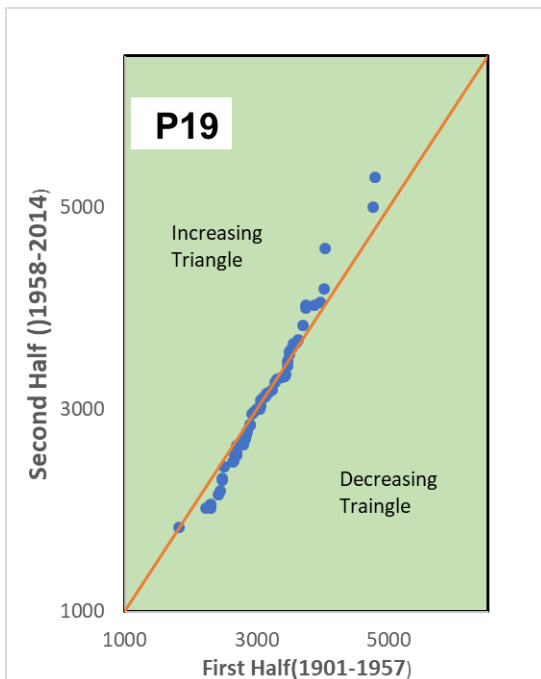
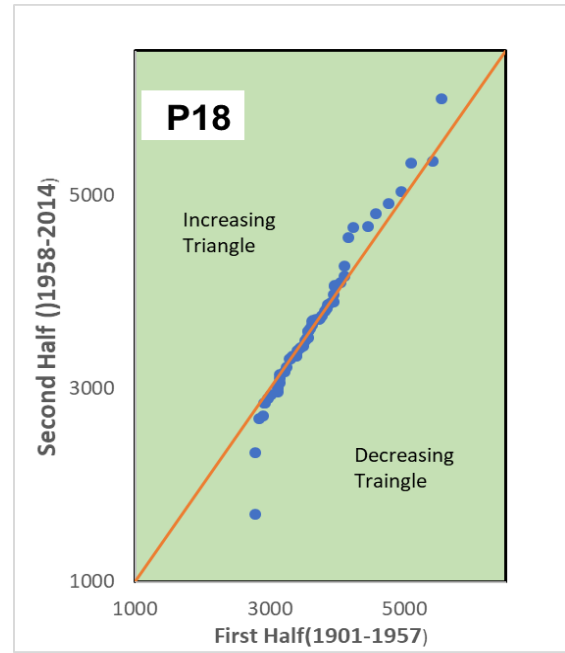
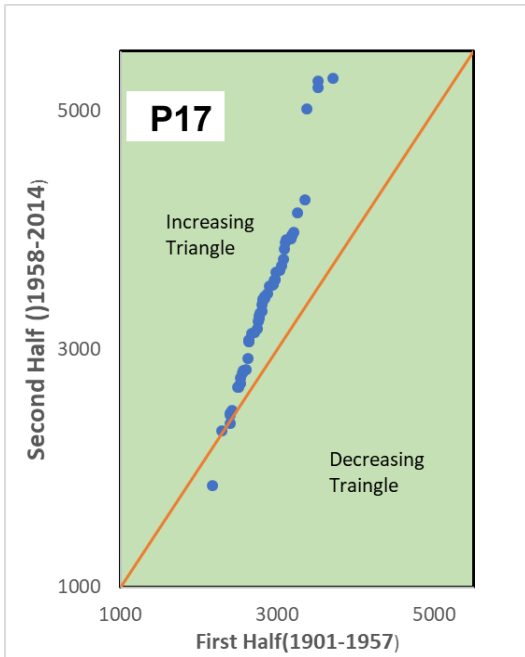


Fig 44: Trend Analysis of Points P17, P18, P19, P20

Result:

- Points P17, P18, P20 are showing increasing trend
- Points P19 are showing decreasing trend

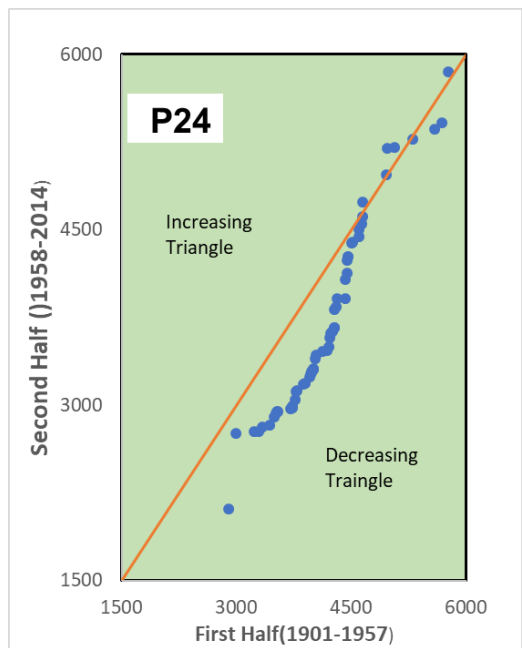
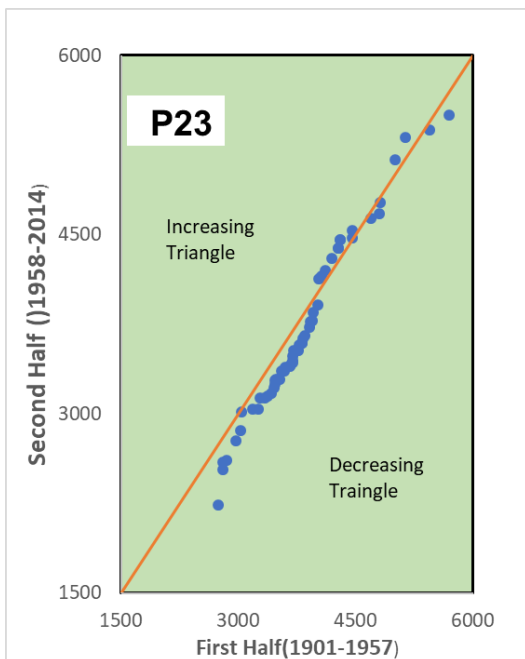
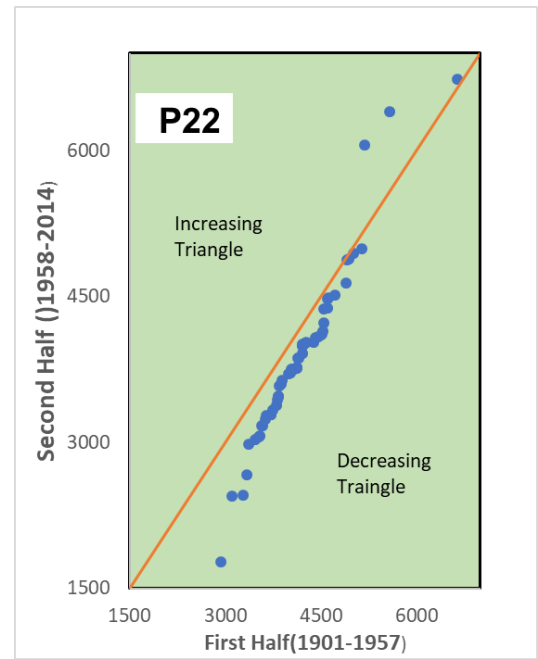
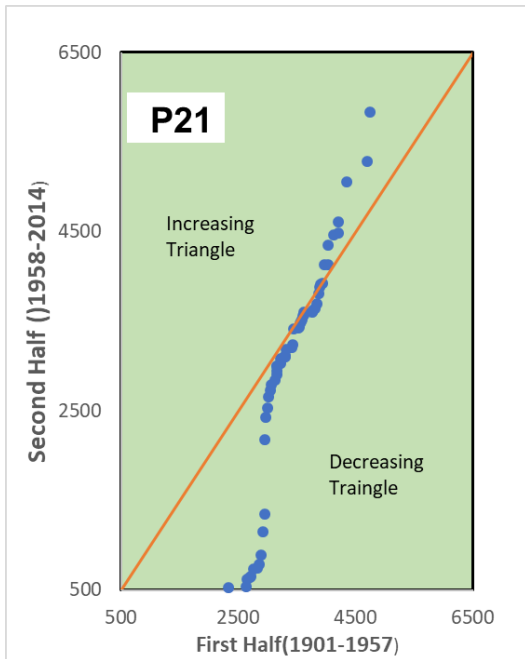


Fig 45: Trend Analysis of Points P21, P22, P23, P24

Result:

- Points P21, P22, P23, P24 are showing decreasing trend

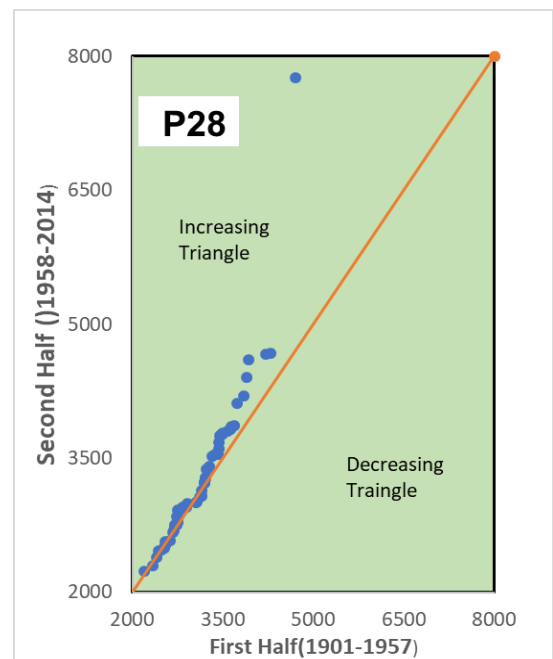
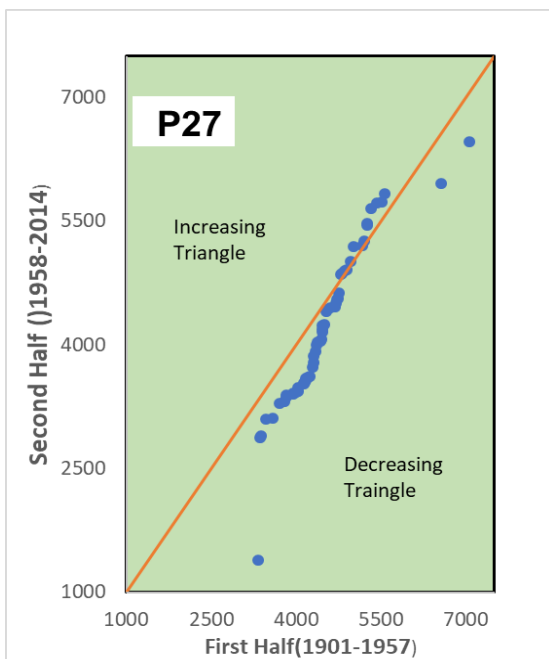
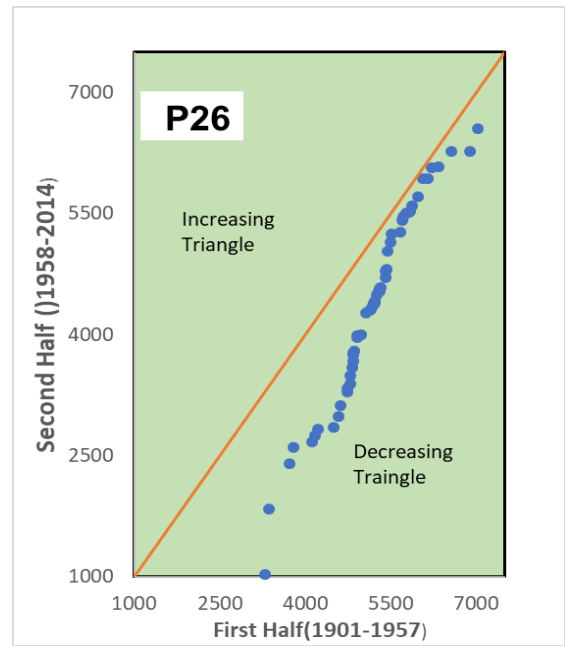
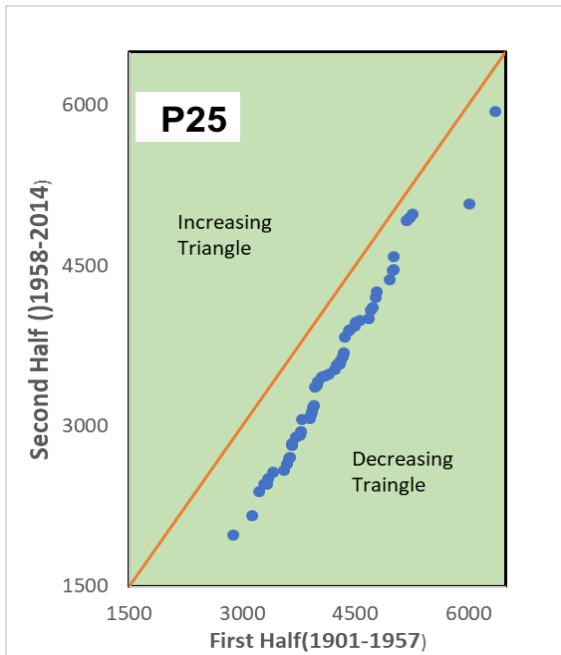


Fig 46: Trend Analysis of Points P25, P26, P27, P28

Result:

- Points P25, P26, P27 are showing decreasing trend
- Points P28 is showing increasing trend

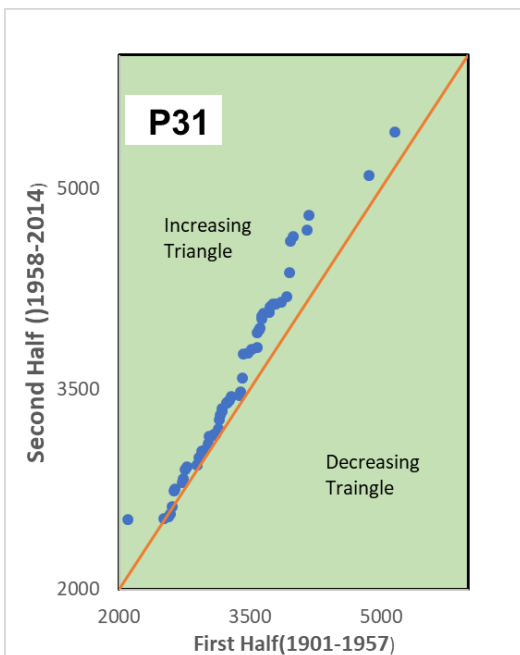
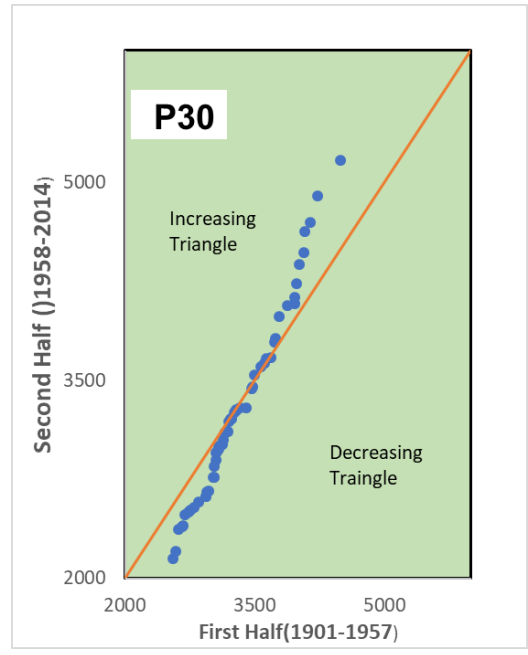
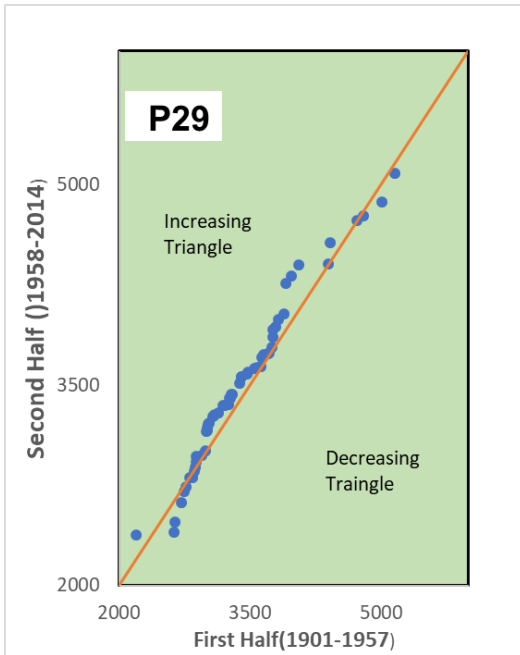


Fig 47: Trend Analysis of Points P29, P30, P31

Result:

- Points P29, P31 are showing increasing trend
- Points P30 is showing decreasing trend

Discussion

There is a mix trend in the Annual rainfall but

We can observe increasing trend in 16 stations and decreasing trend in 15 stations.

4.1.2 Sen's slope estimator method

To estimate the true slope of an existing trend (as change per year) the Sen's nonparametric method is used. The Sen's method can be used in cases where the trend can be assumed to be linear. If a linear trend is present in a time series, then the true slope (change per unit time) was estimated by using a simple nonparametric procedure developed by Sen (1968). This means that linear model $f(t)$ can be described as

$$f(t) = Q_t + B$$

Where,

Q_t = Slope

B = Constant.

To derive an estimate of the slope Q_t , the slopes of all data pairs were calculated

$$Q_t = \frac{x_j - x_k}{j - k}, i = 1, 2, 3 \dots N, j > k$$

If there was n values x_j in the time series get as many as $N = n(n-1)/2$ slope estimates Q_t . The Sen's estimator of slope is the median of these N values of Q_t . The N values of Q_t were ranked from the smallest to the largest and the Sen's estimator is

$$Q_t = \begin{cases} Q_{\frac{N+1}{2}} & \text{if } N \text{ is odd} \\ \frac{1}{2} \left(Q_{\frac{N}{2}} + Q_{\frac{N+2}{2}} \right) & \text{if } N \text{ is even} \end{cases}$$

Results and Discussion of Sen slope estimator

WINTER

POINT 1

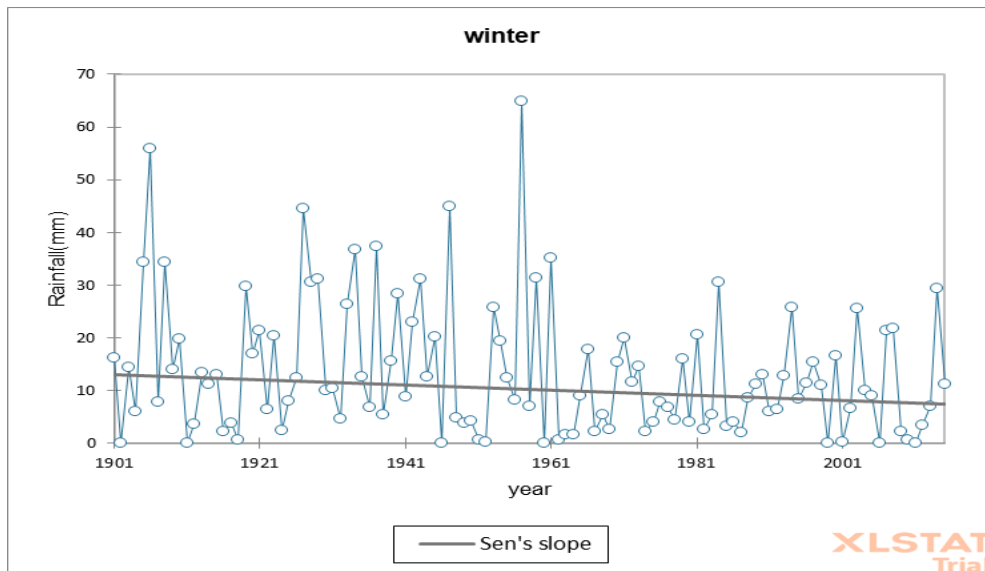


Fig 48. Trend Analysis of point 1

POINT 2

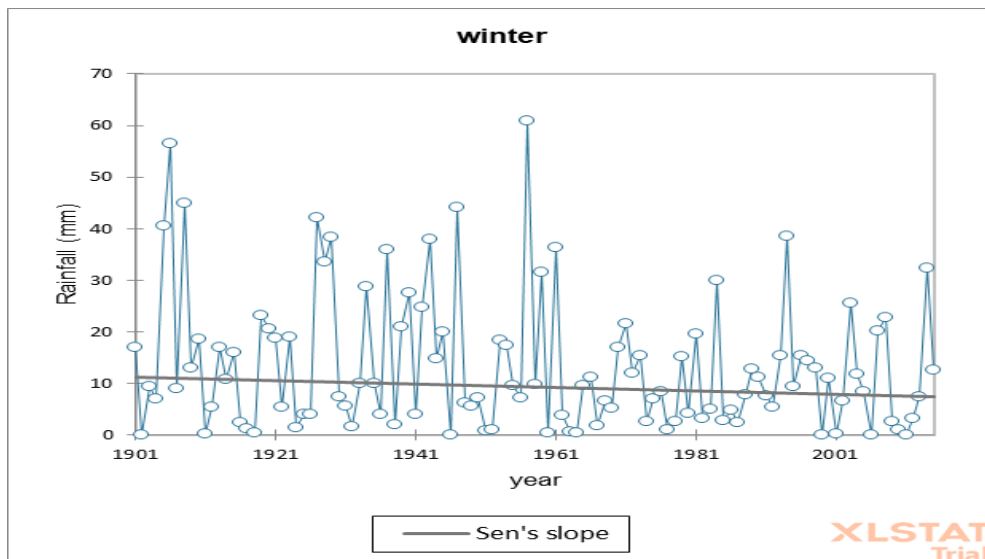


Fig 49. Trend Analysis of point 2

Result:

- Points P1, P2 are showing decreasing trend

POINT 3

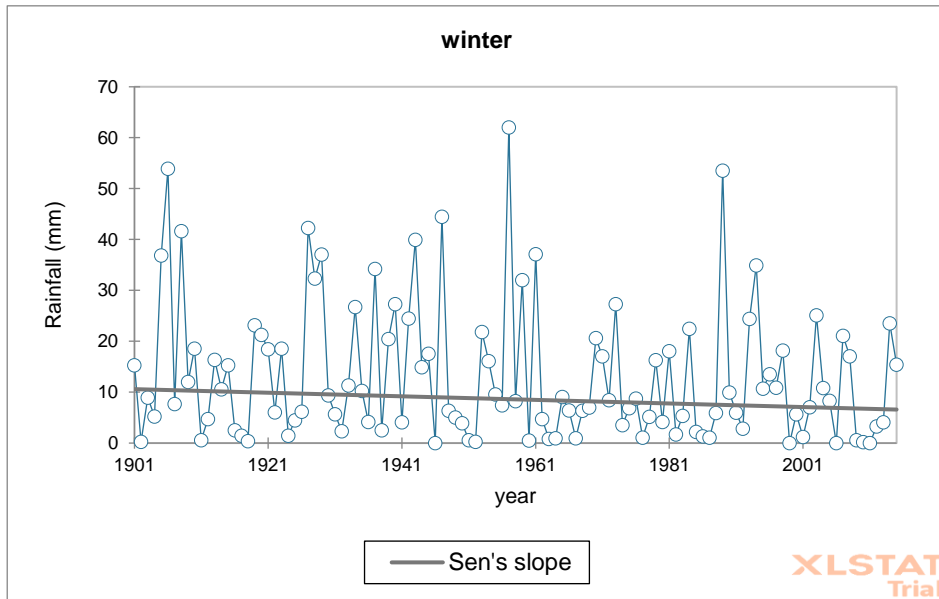


Fig 50. Trend Analysis of point 3

POINT 4

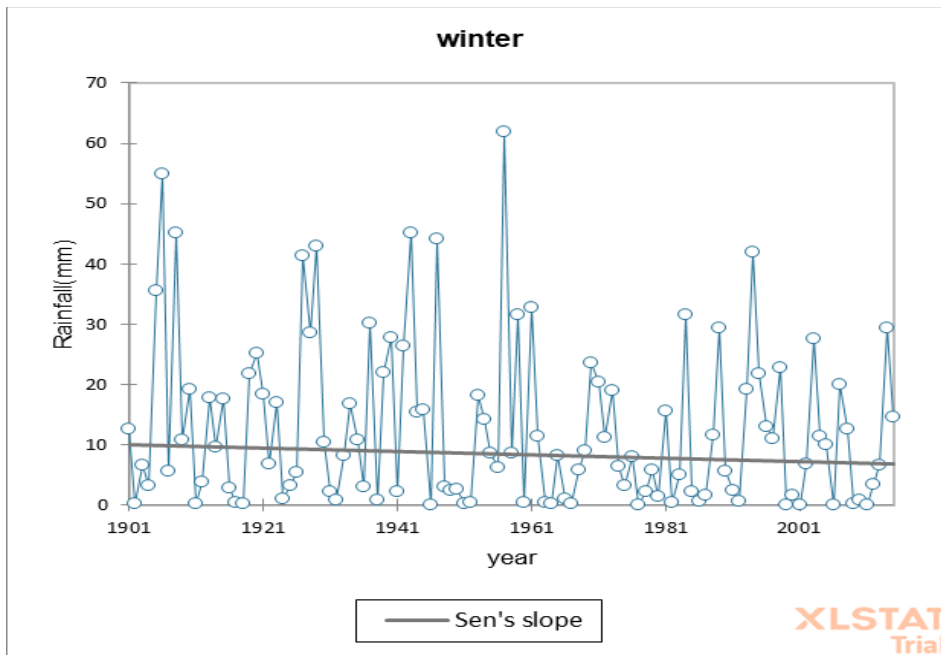


Fig 51. Trend Analysis of point 4

Result:

- Points P3, P4 are showing decreasing trend

POINT 5

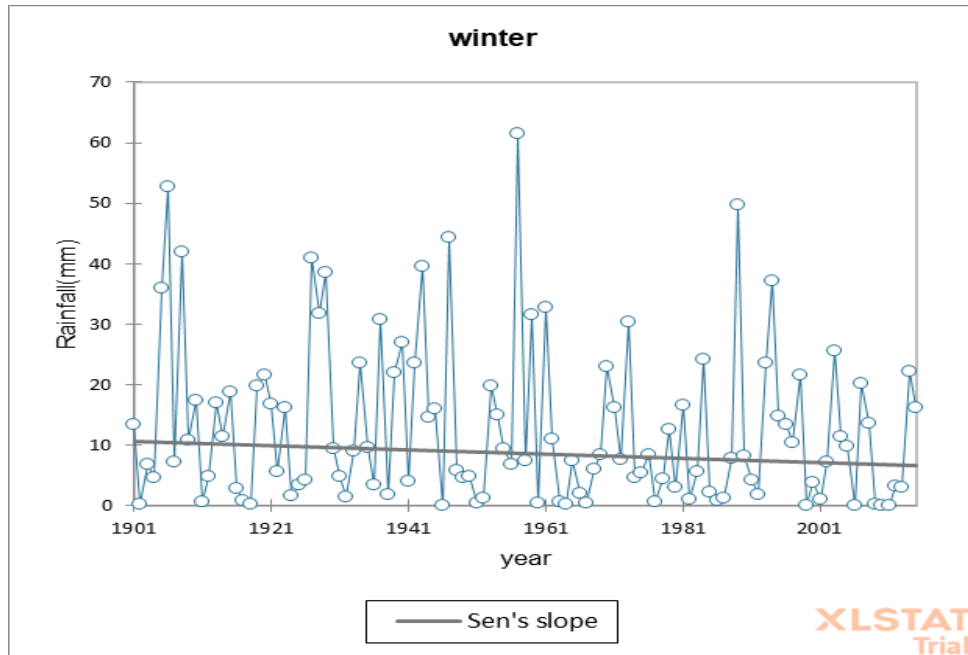


Fig 52. Trend Analysis of point 5

POINT 6

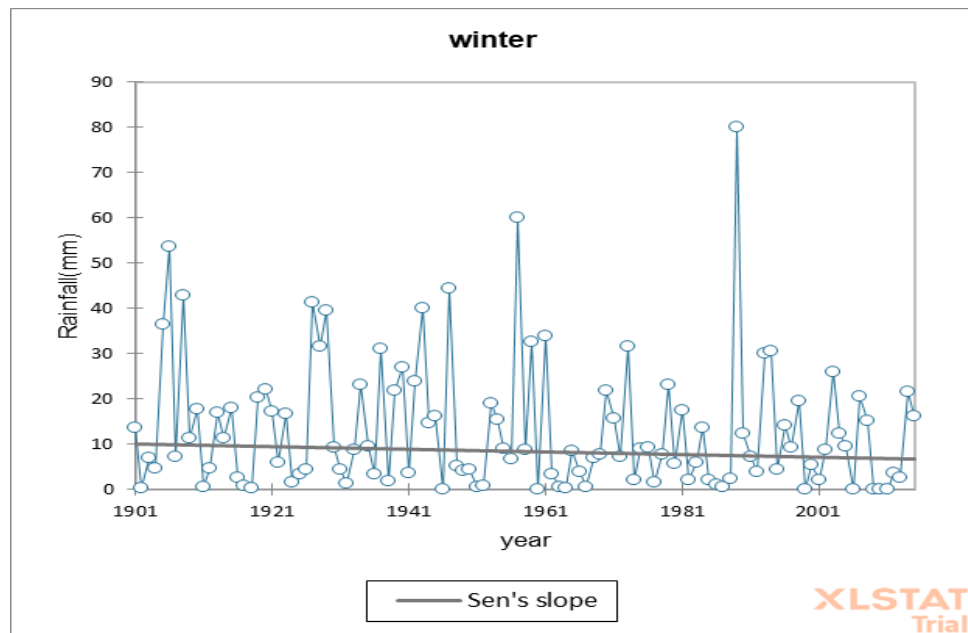


Fig 53. Trend Analysis of point 6

Result:

- Points P5, P6 are showing decreasing trend

POINT 7

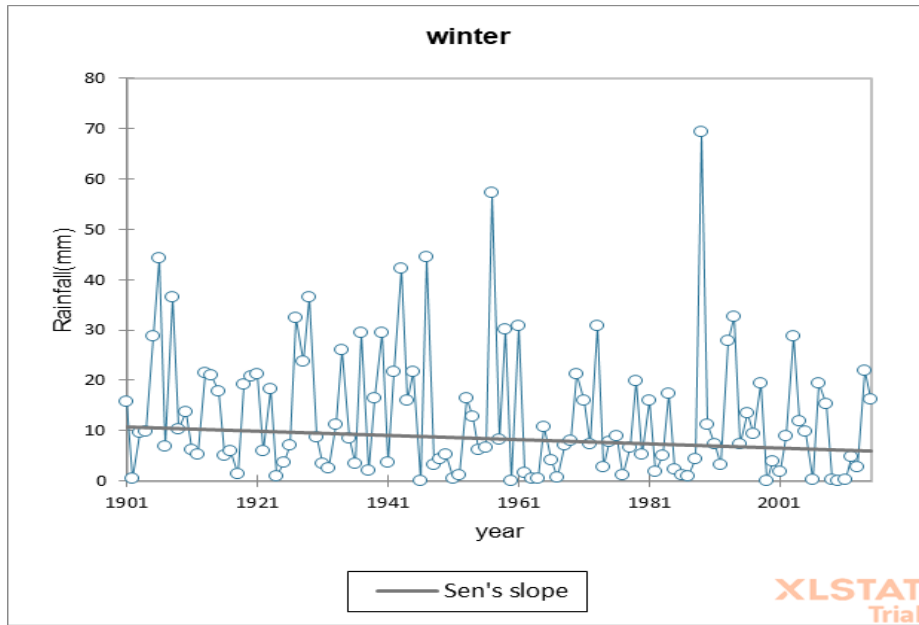


Fig 54. Trend Analysis of point 7

POINT 8

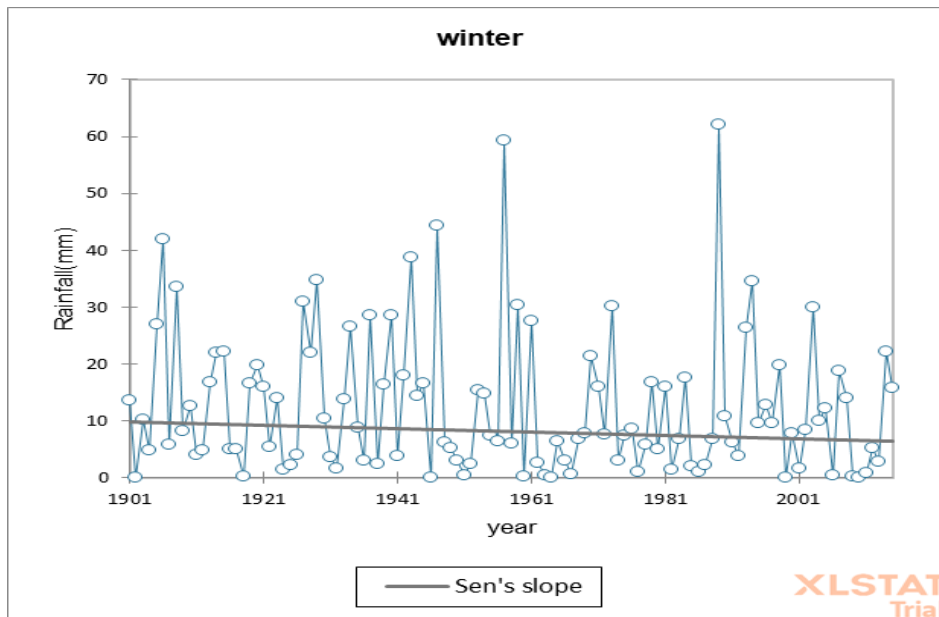


Fig 55. Trend Analysis of point 8

Result:

- Points P7, P8 are showing decreasing trend

POINT 9

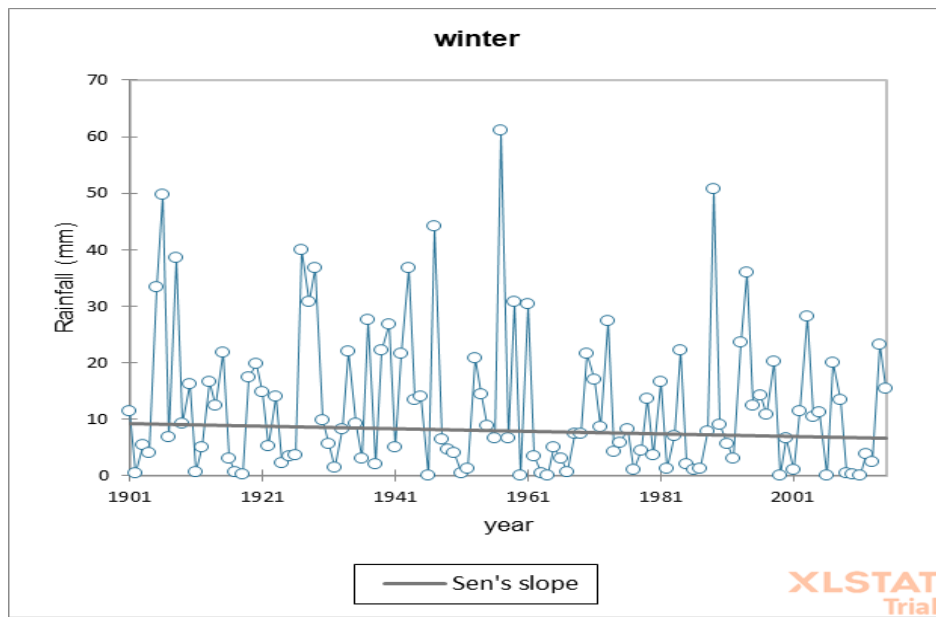


Fig 56. Trend Analysis of point 9

POINT 10

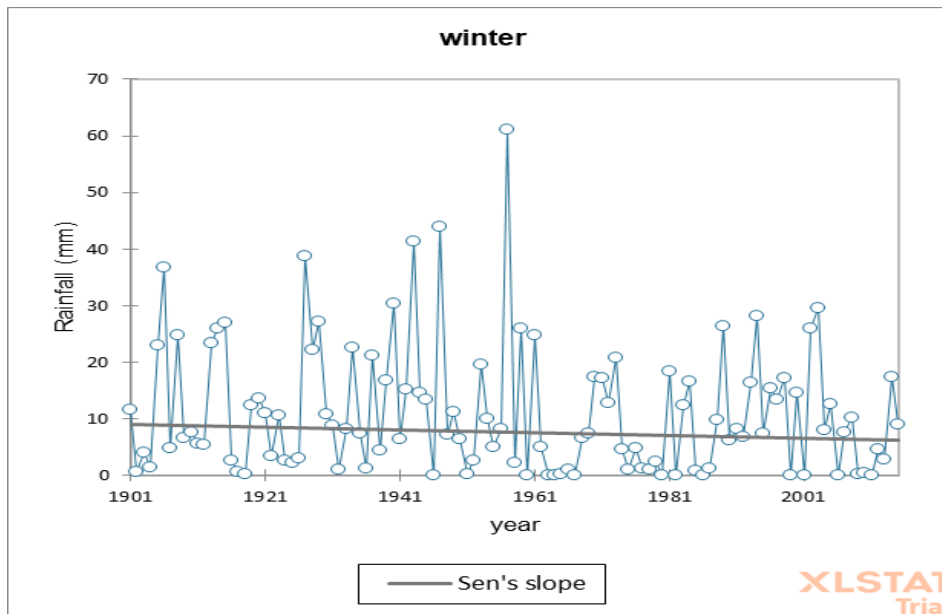


Fig 57. Trend Analysis of point 10

Result:

- Points P9, P10 are showing decreasing trend

POINT 11

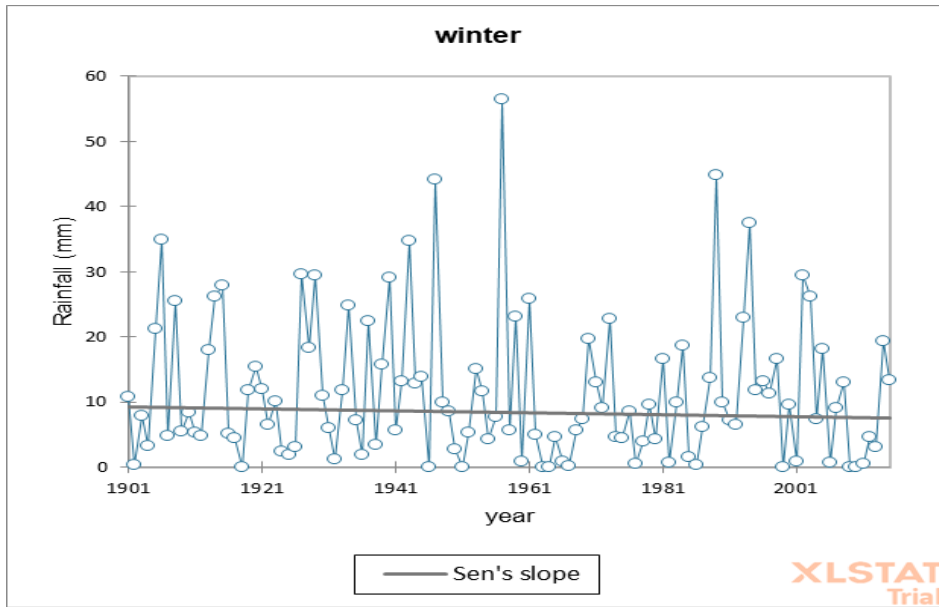


Fig 58. Trend Analysis of point 11

POINT 12

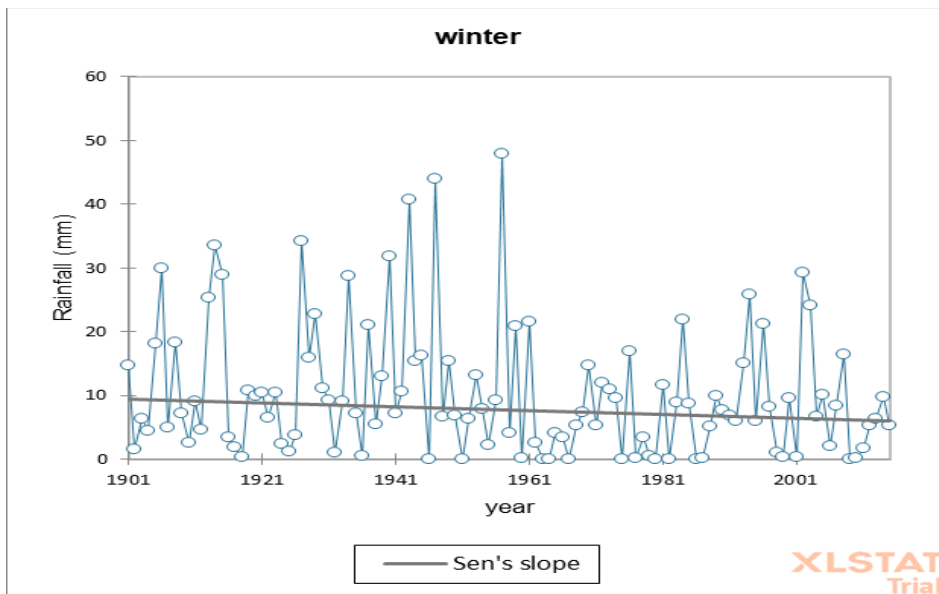


Fig 59. Trend Analysis of point 12

Result:

- Points P11, P12 are showing decreasing trend

POINT 13

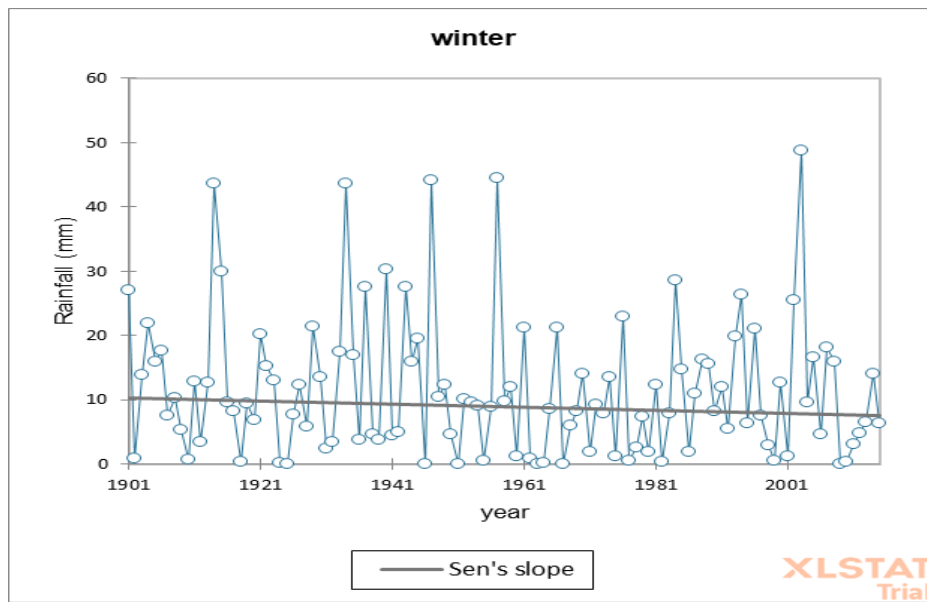


Fig 60. Trend Analysis of point 13

POINT 14

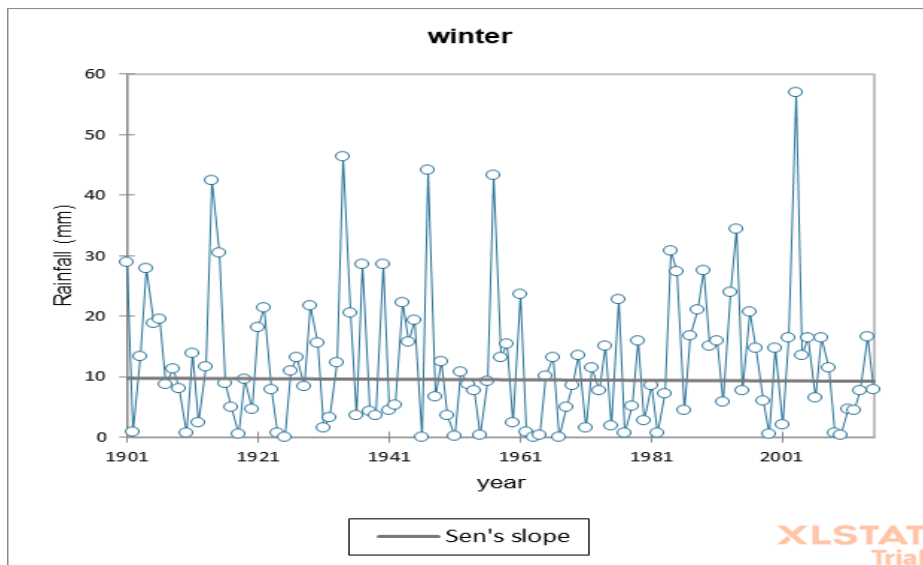


Fig 61. Trend Analysis of point 14

Result:

- Point P13 is showing decreasing trend
- Point P14 is not showing any change

POINT 15

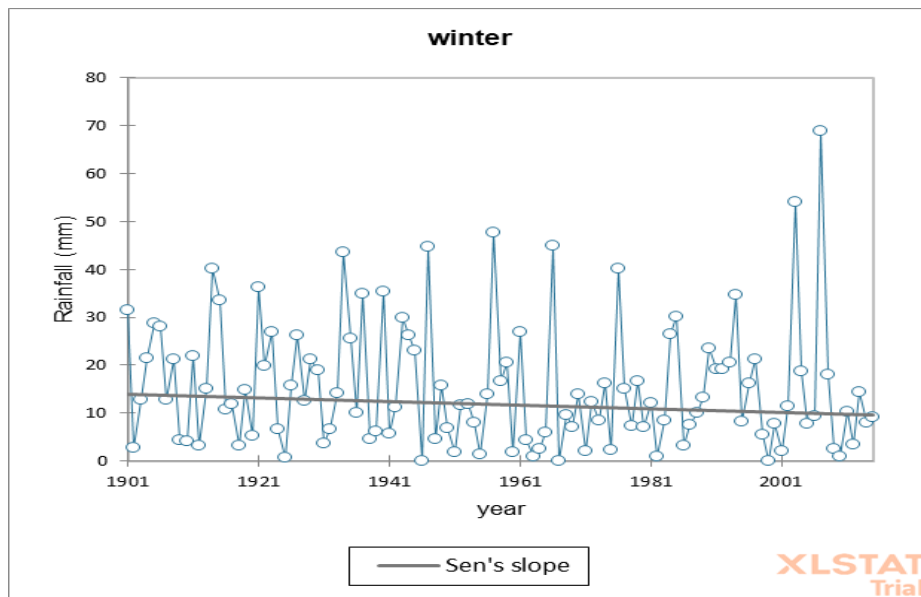


Fig 62. Trend Analysis of point 15

POINT 16

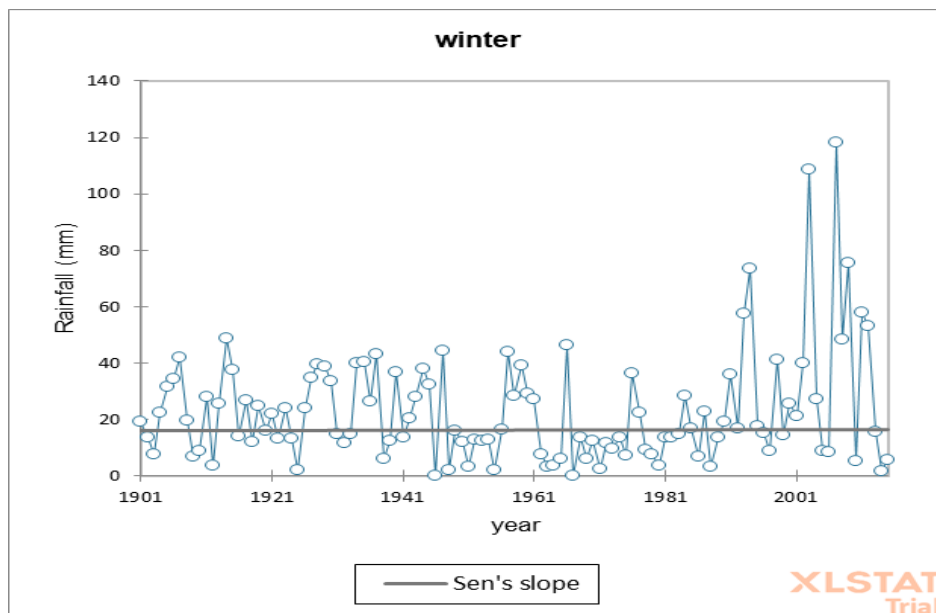


Fig 63. Trend Analysis of point 16

Result:

- Point P15 is showing decreasing trend
- Point P16 is showing slight increasing trend

Point 17

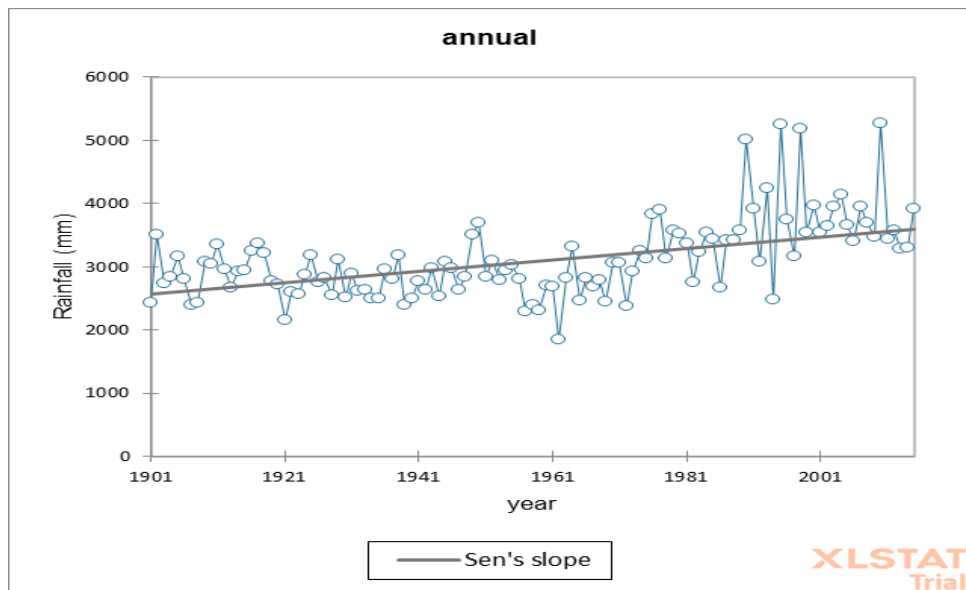


Fig 64. Trend Analysis of point 17

Point 18

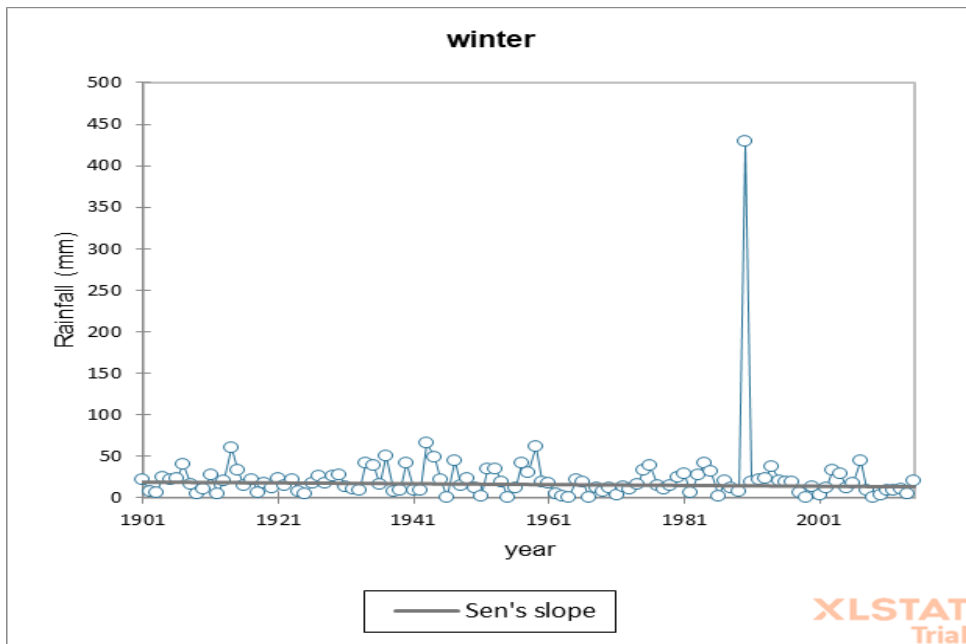


Fig 65. Trend Analysis of point 18

Result:

- Points P17, P18 are showing decreasing trend

Point 19

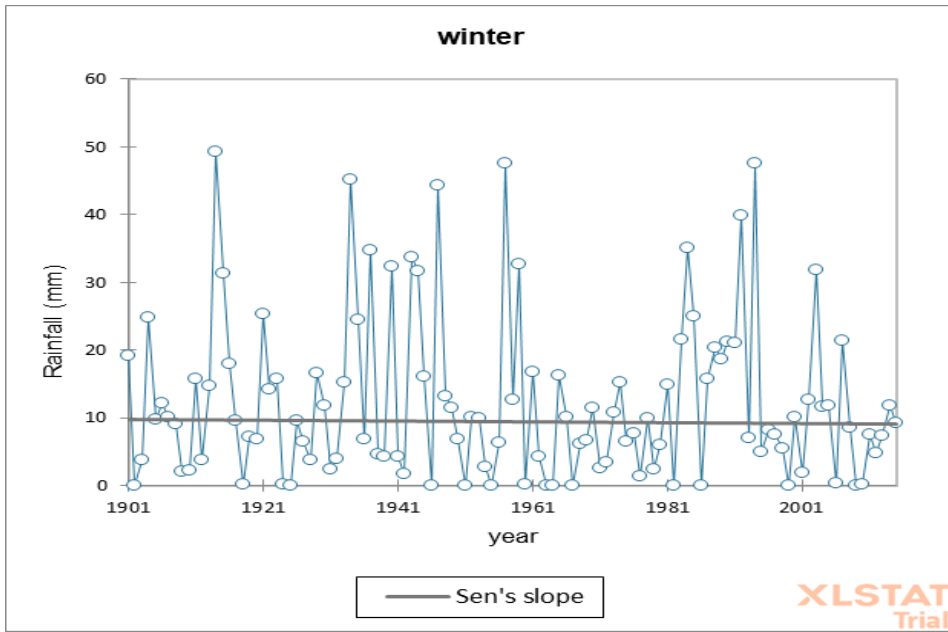


Fig 66. Trend Analysis of point 19

Point 20

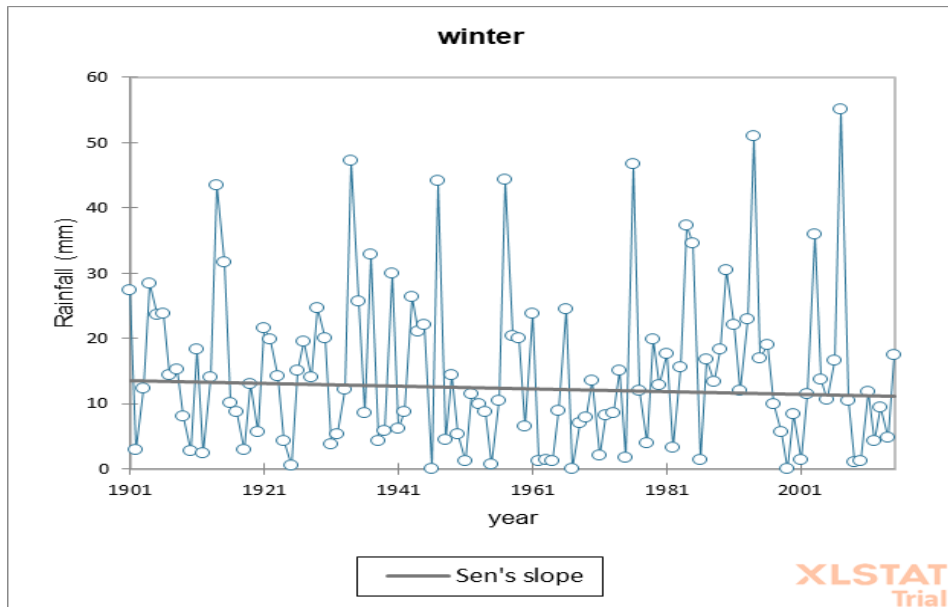


Fig 67. Trend Analysis of point 20

Result:

- Points P19, P20 are showing decreasing trend

Point 21

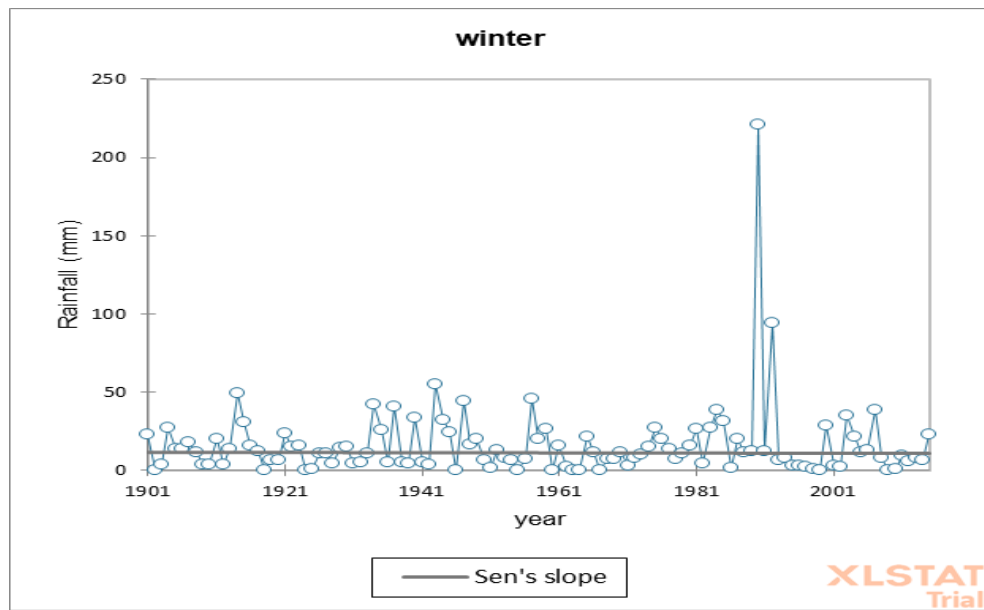


Fig 68. Trend Analysis of point 21

Point 22

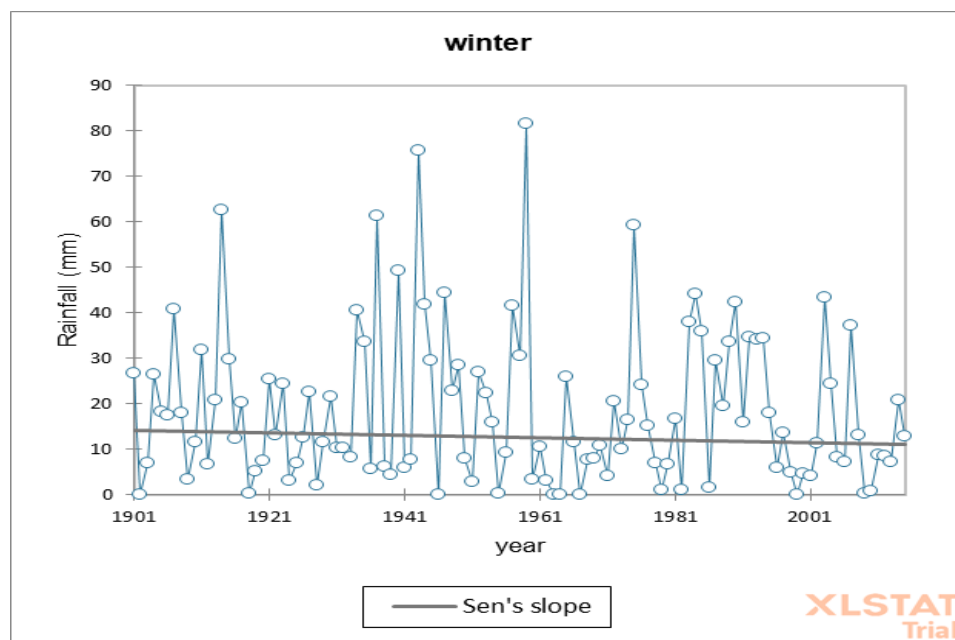


Fig 69. Trend Analysis of point 22

Result:

- Points P21, P22 are showing decreasing trend

Point 23

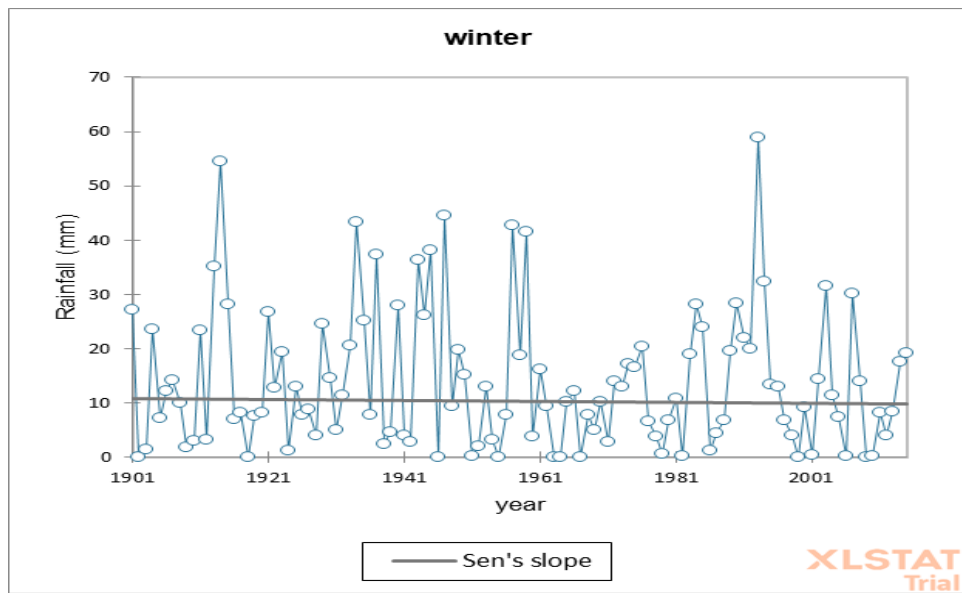


Fig 70. Trend Analysis of point 23

Point 24

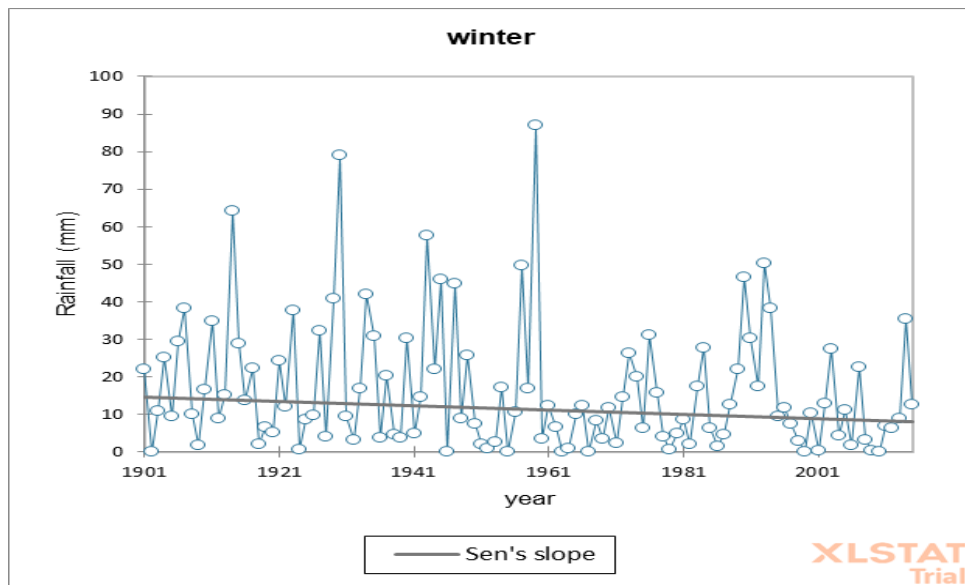


Fig 71. Trend Analysis of point 24

Result:

- Point P23, P24 are showing decreasing trend

Point 25

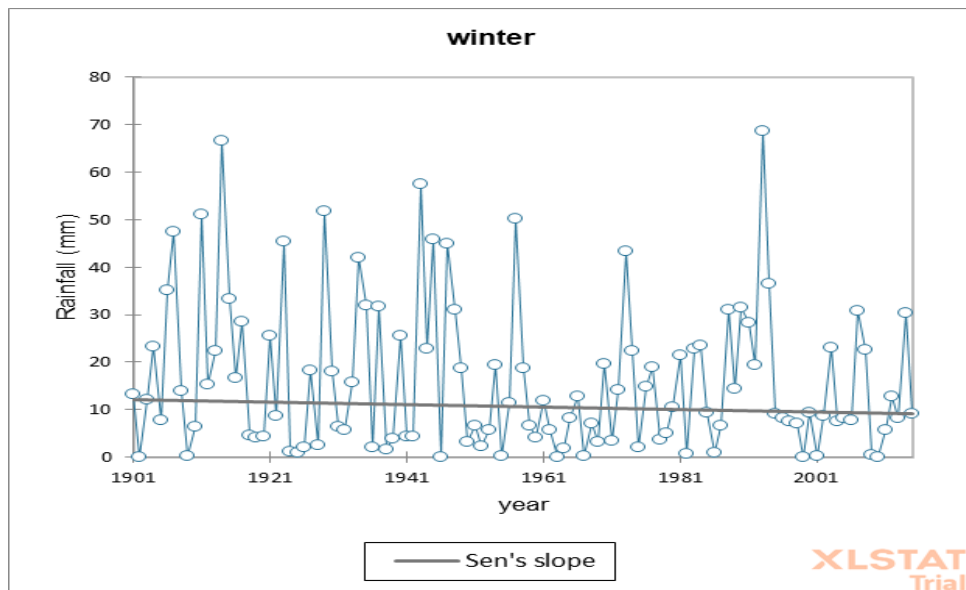


Fig 72. Trend Analysis of point 25

Point 26

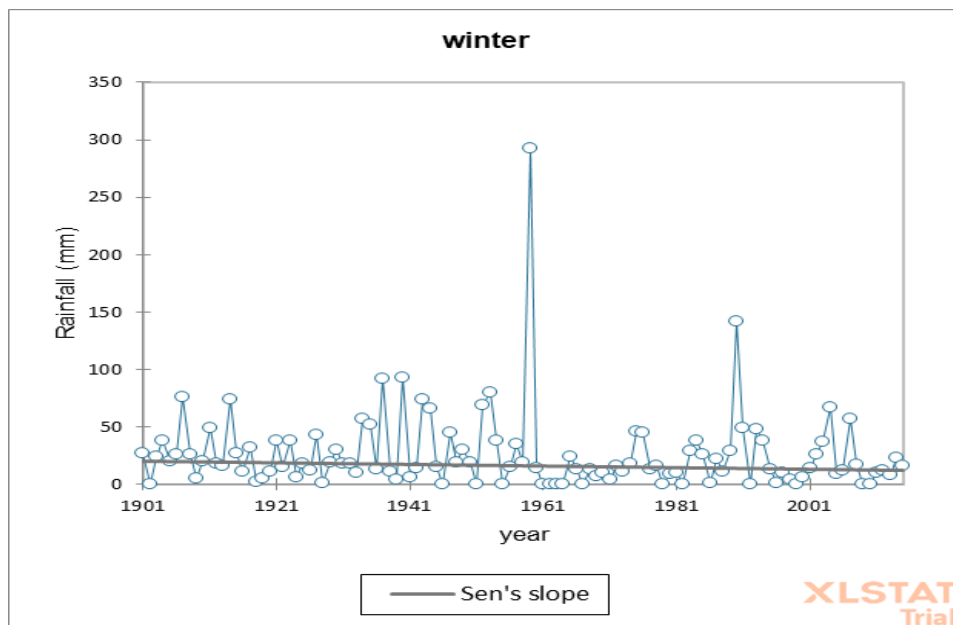


Fig 73. Trend Analysis of point 26

Result:

- Point P26, P26 are showing decreasing trend

Point 27

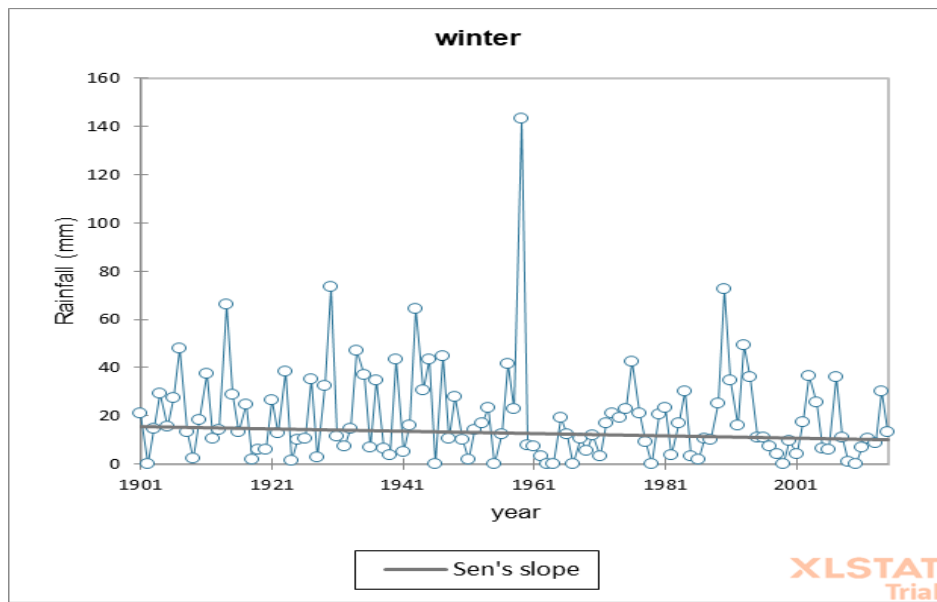


Fig 74. Trend Analysis of point 27

Point 28

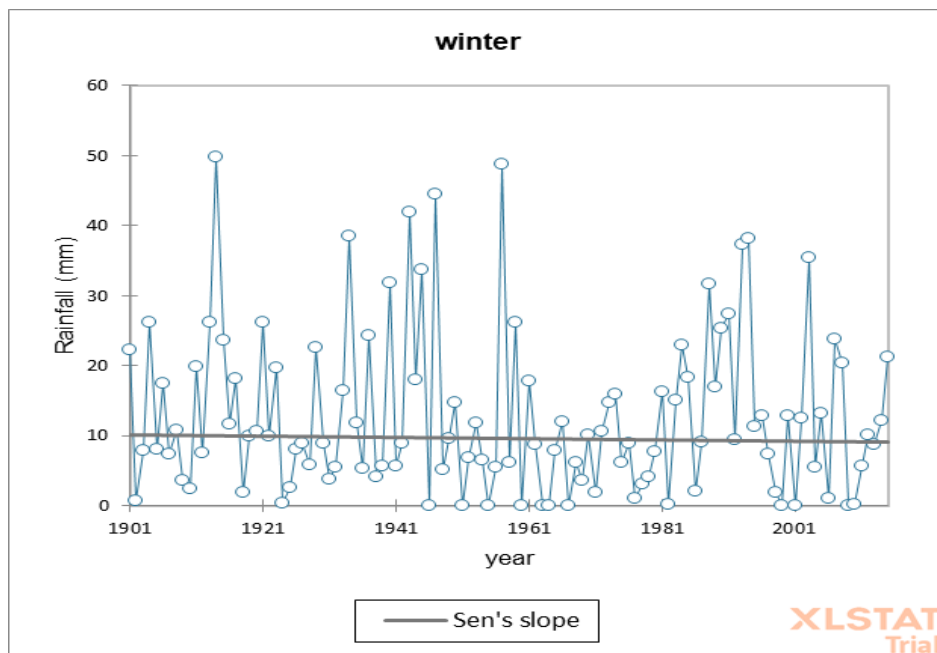


Fig 75. Trend Analysis of point 28

Result:

- Point P27, P28 are showing decreasing trend

Point 29

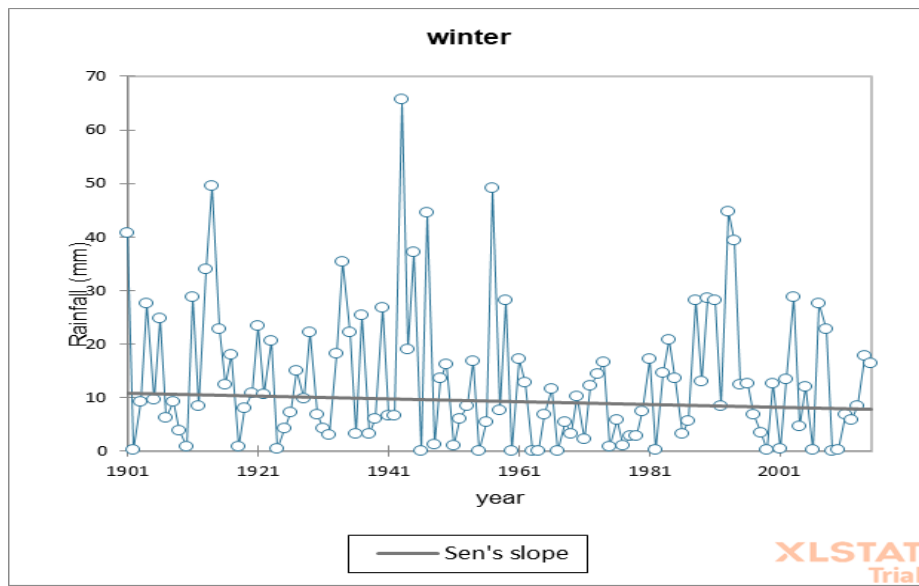


Fig 76. Trend Analysis of point 29

Point 30

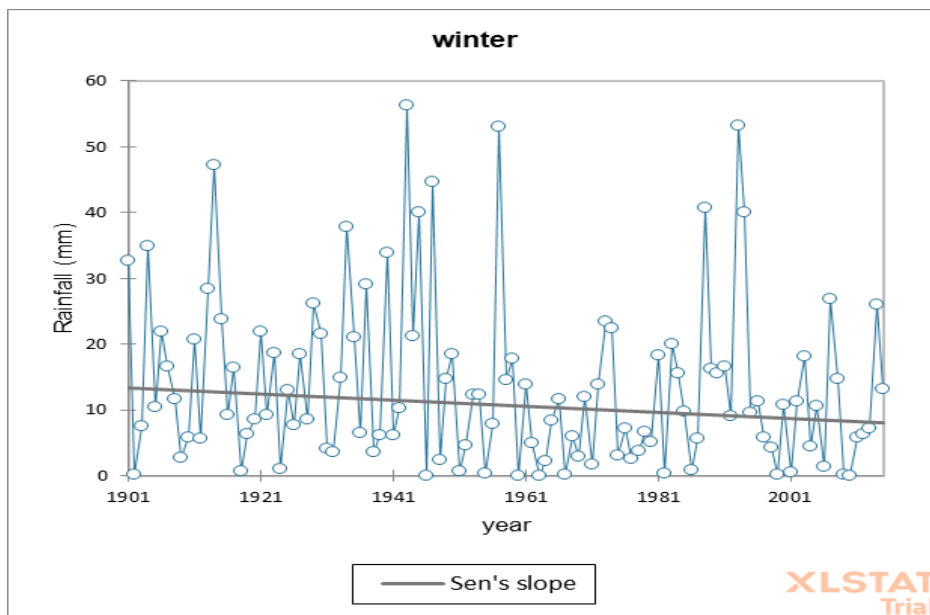


Fig 77. Trend Analysis of point 30

Result:

- Point P29, P30 are showing decreasing trend

Point 31

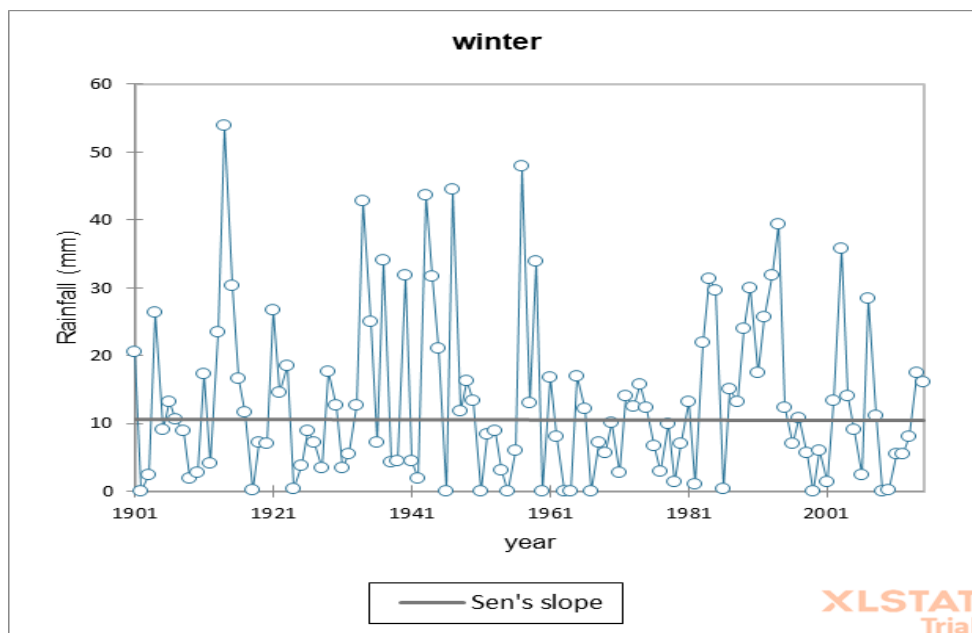


Fig 78. Trend Analysis of point 31

Result:

- Points P31 is showing increasing trend

Discussion

from the above pictorial representation of the Sen slope we can clearly observe a general decreasing trend in the rainfall over these 115 years of rainfall data.

In some of the stations we can see a non-decreasing trend such as P14, P16, P19, P21, P23, P31 are showing no change trend.

PRE-MONSOON

POINT 1

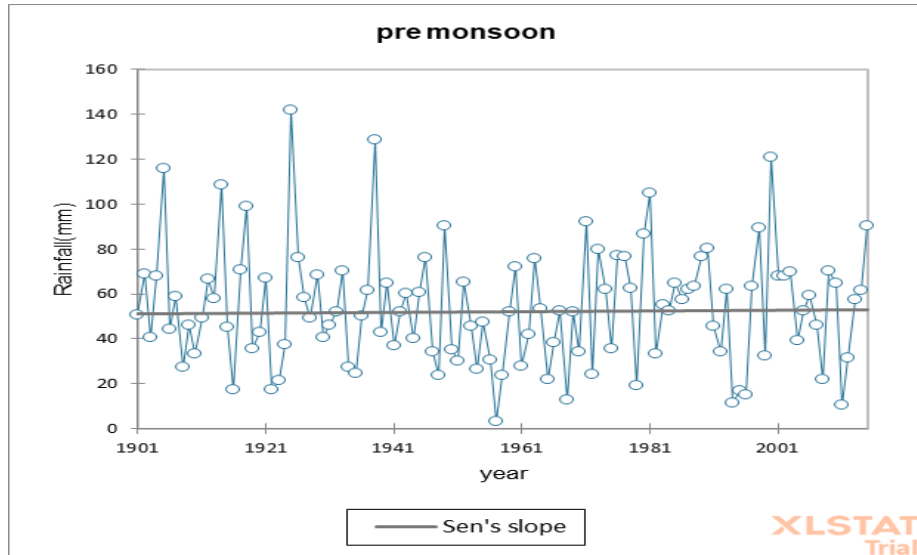


Fig 79. Trend Analysis of point 1

POINT 2

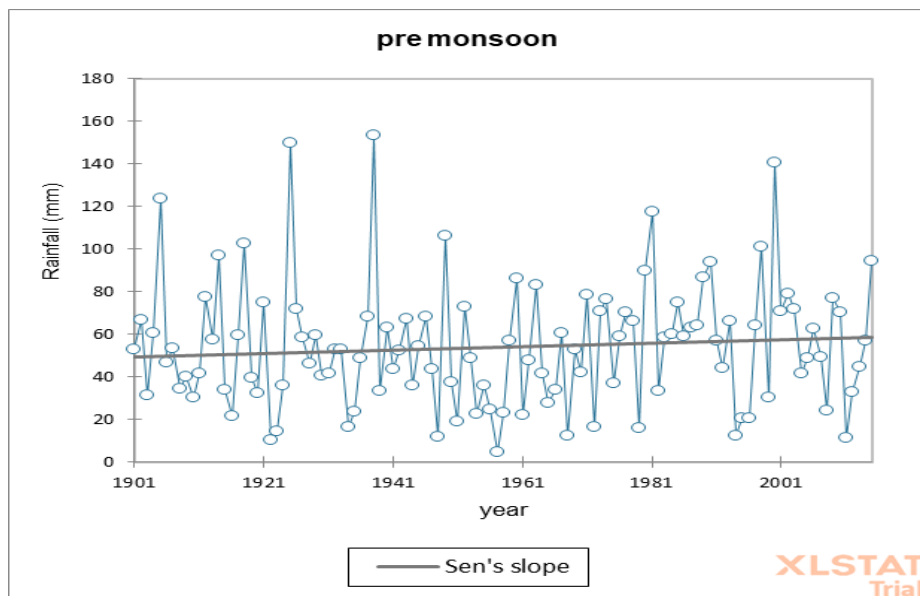


Fig 80. Trend Analysis of point 2

Result:

- Points P1, P2 are showing increasing trend

POINT 3

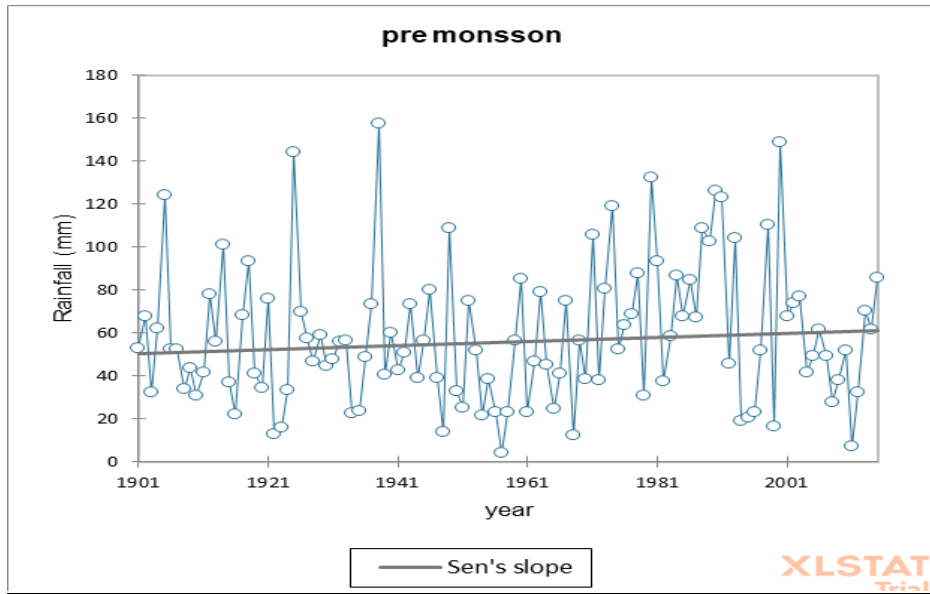


Fig 81. Trend Analysis of point 3

POINT 4

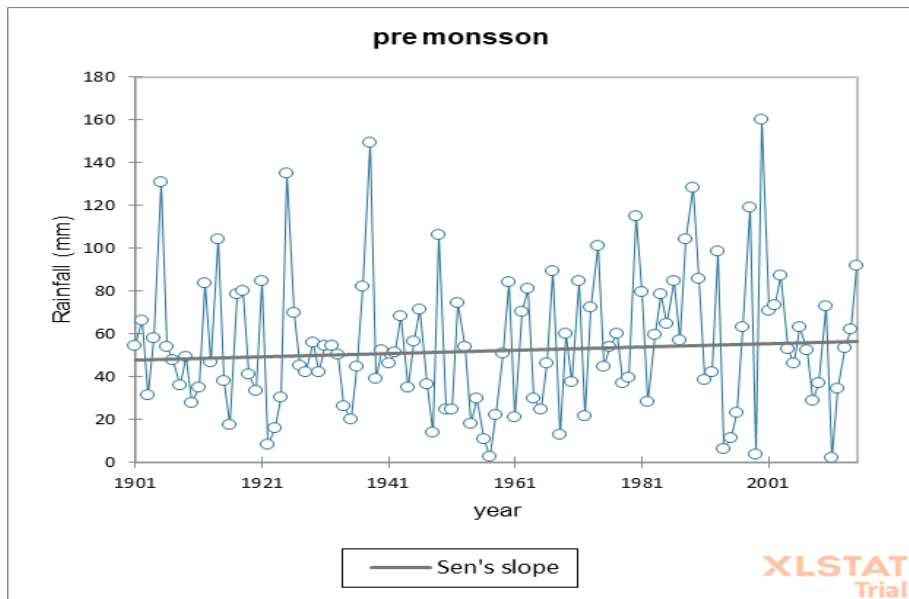


Fig 82. Trend Analysis of point 4

Result:

- Points P3, P4 are showing increasing trend

POINT 5

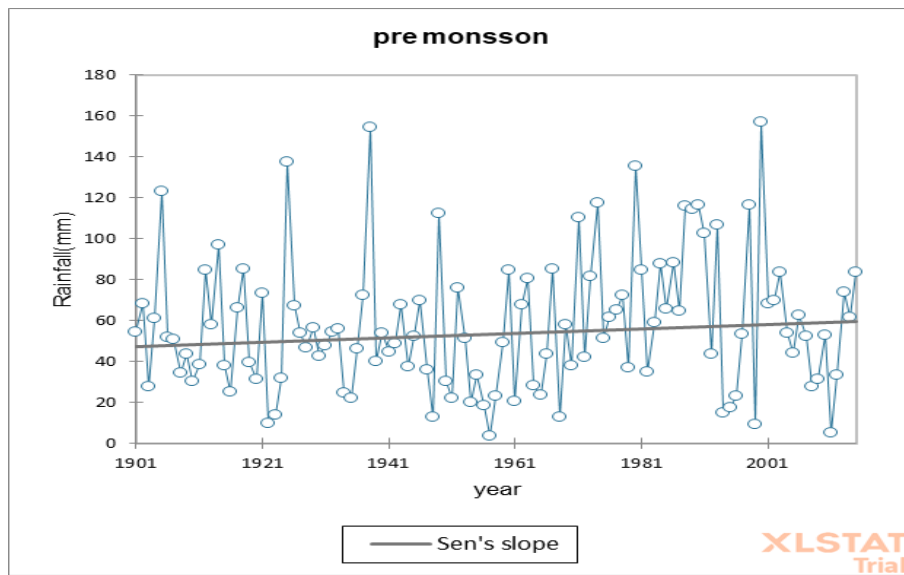


Fig 83. Trend Analysis of point 5

POINT 6

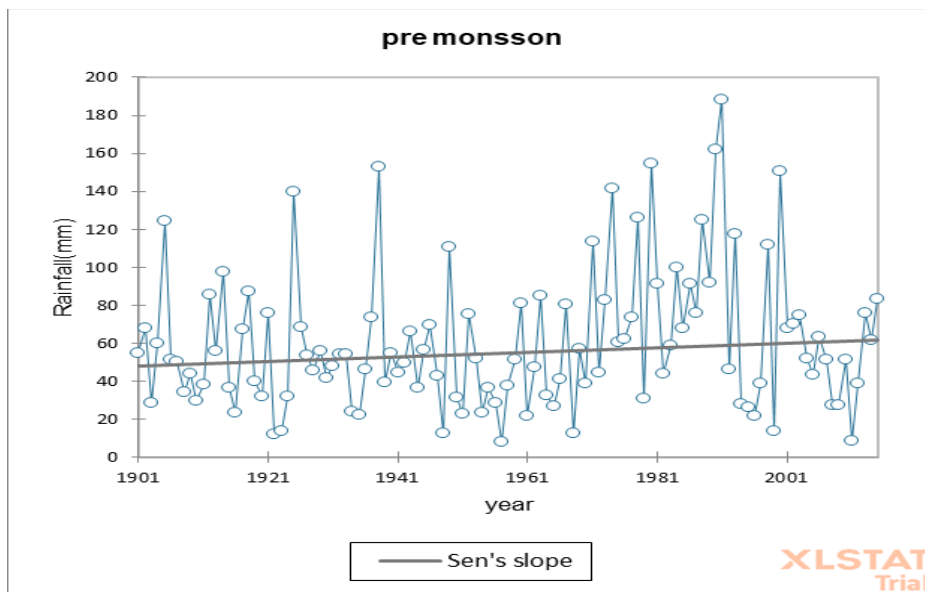


Fig 84. Trend Analysis of point 6

Result:

- Points P5, P6 are showing increasing trend

POINT 7

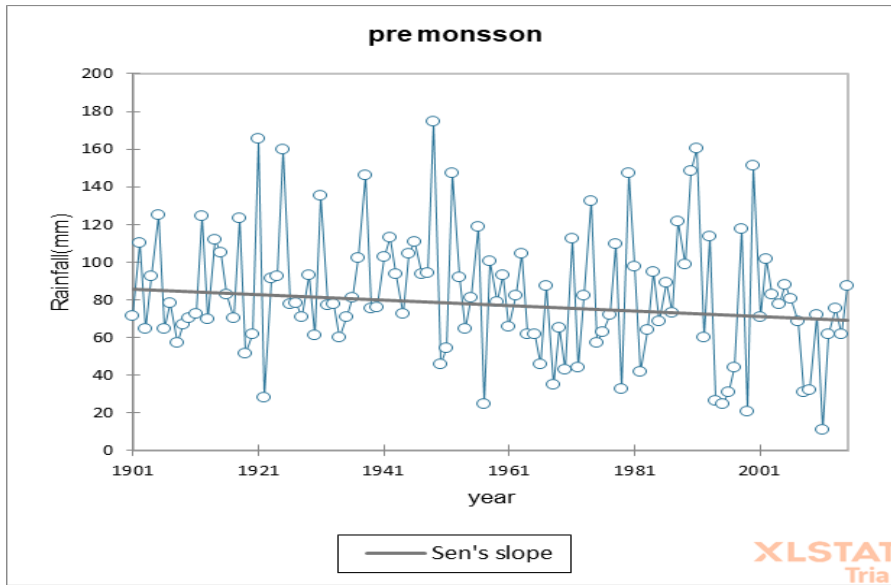


Fig 85. Trend Analysis of point 7

POINT 8

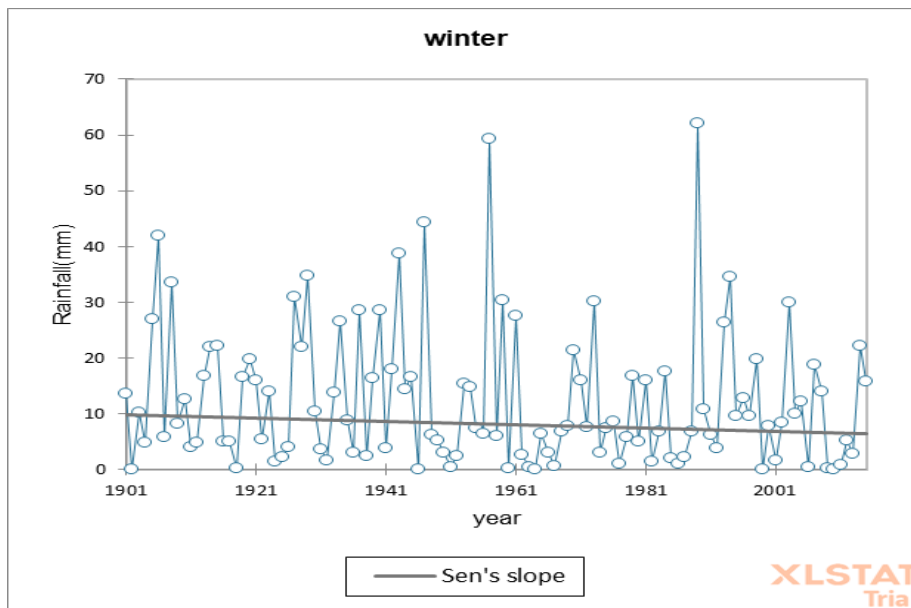


Fig 86. Trend Analysis of point 8

Result:

- Points P7, P8 are showing decreasing trend

POINT 9

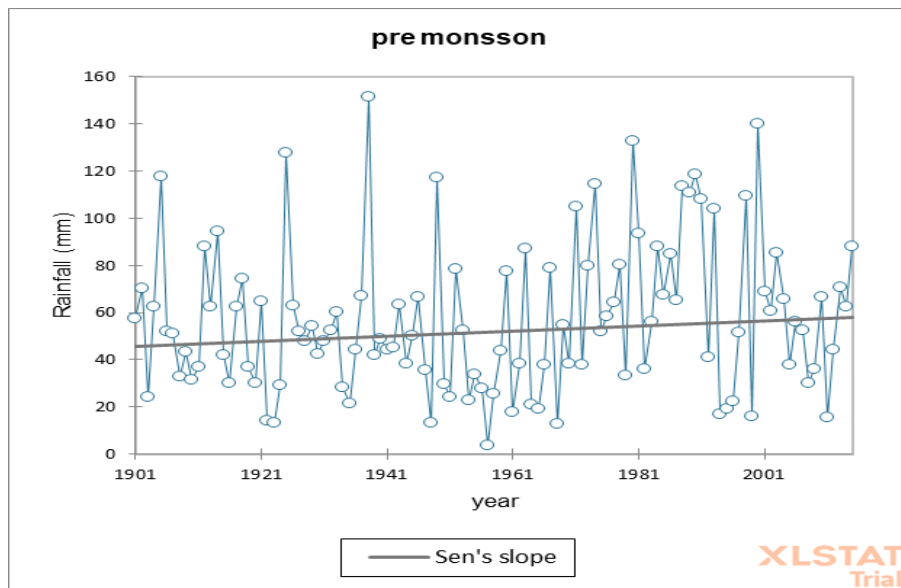


Fig 87. Trend Analysis of point 9

POINT 10

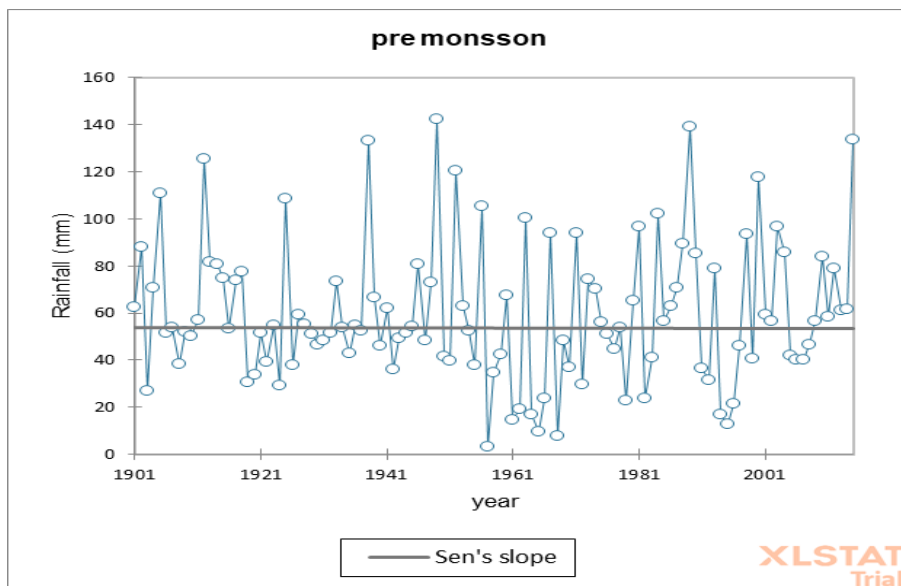


Fig 88. Trend Analysis of point 10

Result:

- Points P9, P10 are showing increasing trend

POINT 11

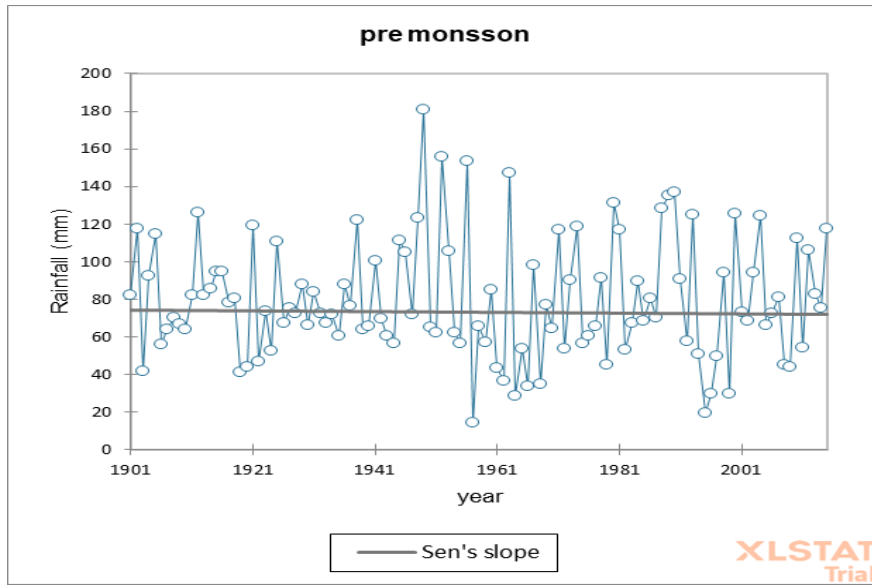


Fig 90. Trend Analysis of point 11

POINT 12

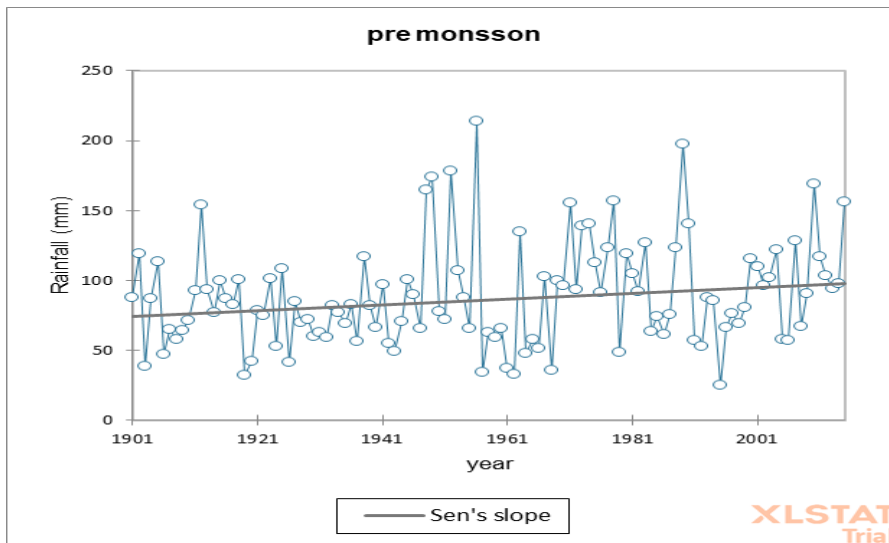


Fig 91. Trend Analysis of point 12

Result:

- Points P11, P12 are showing decreasing trend



POINT 13

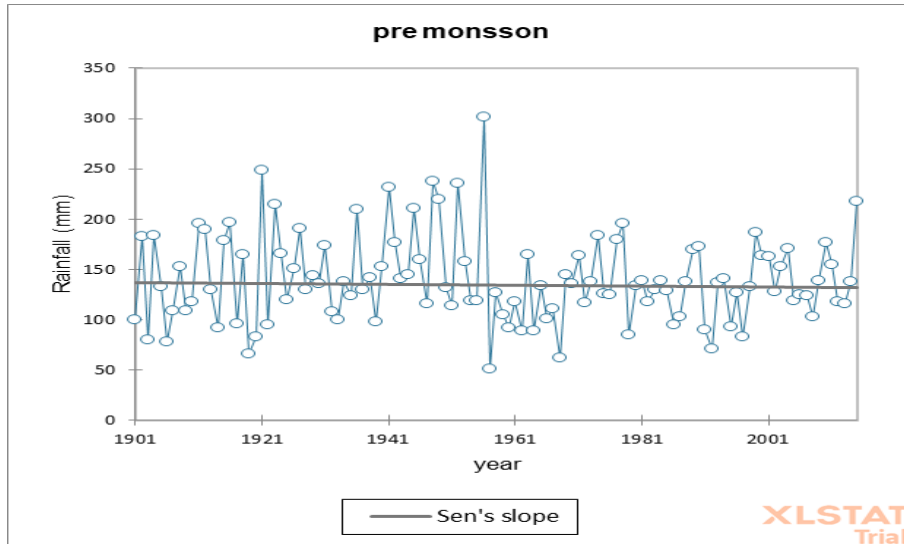


Fig 92. Trend Analysis of point 13

POINT 14

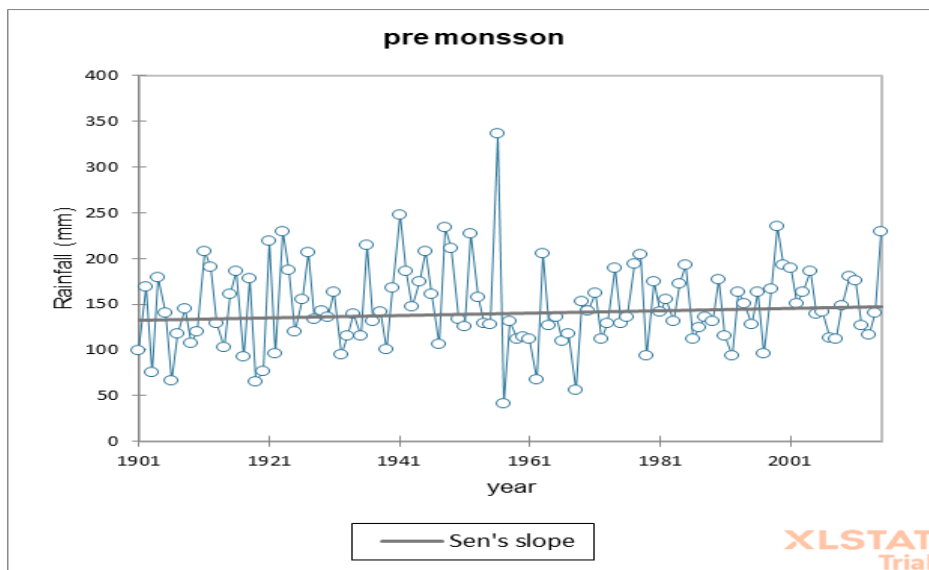


Fig 93. Trend Analysis of point 14

Result:

- Point P13, P14 is showing increasing trend

POINT 15

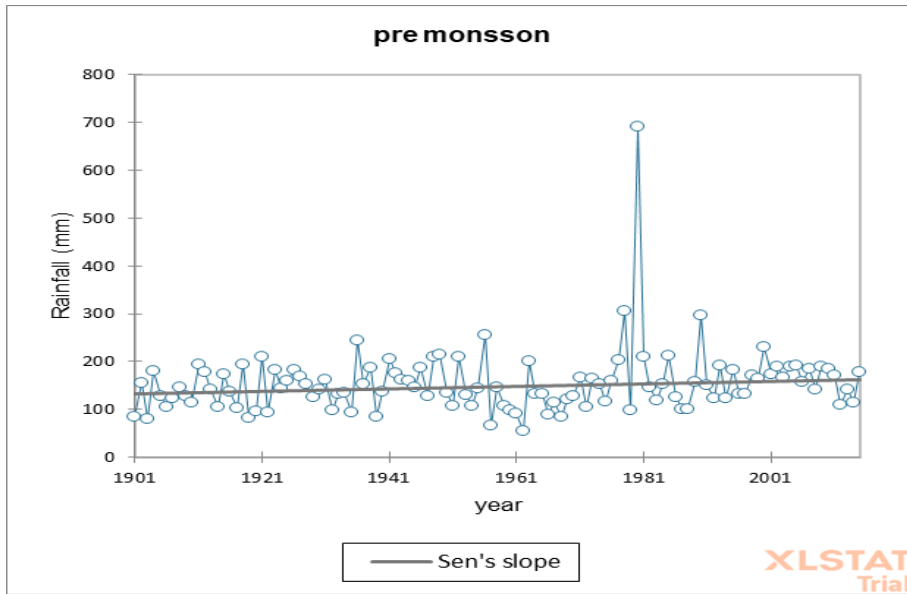


Fig 94. Trend Analysis of point 15

POINT 16

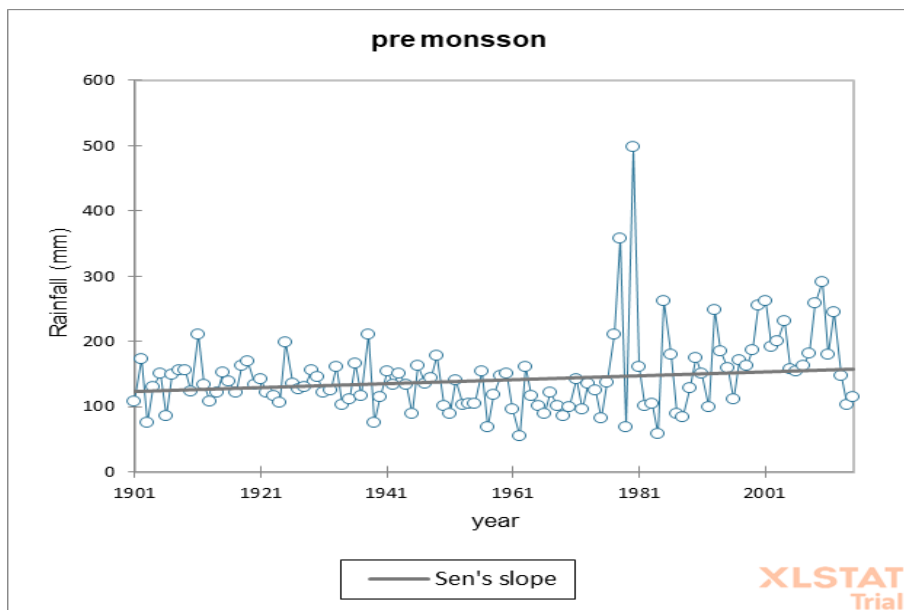


Fig 95. Trend Analysis of point 16

Result:

- Points P15, P16 are showing increasing trend

POINT 17

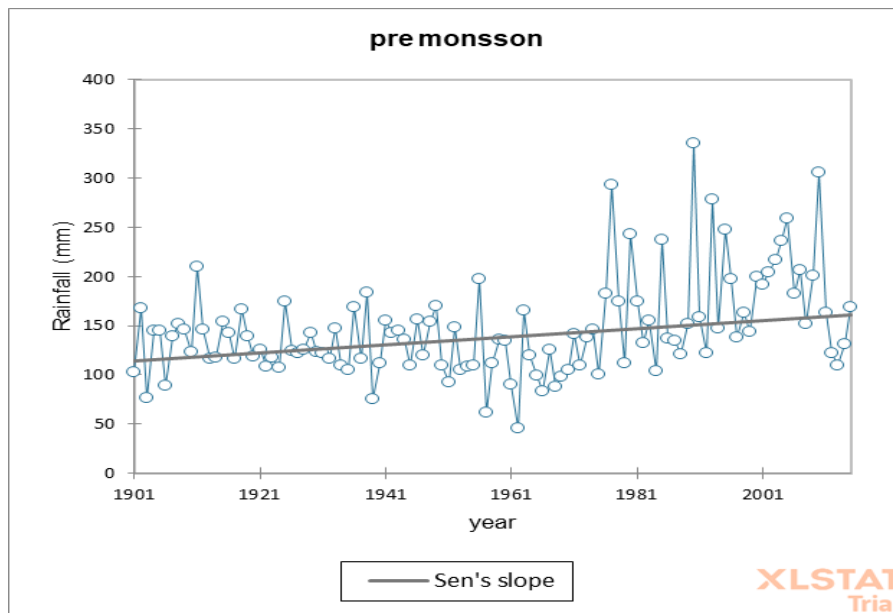


Fig 96. Trend Analysis of point 17

POINT 18

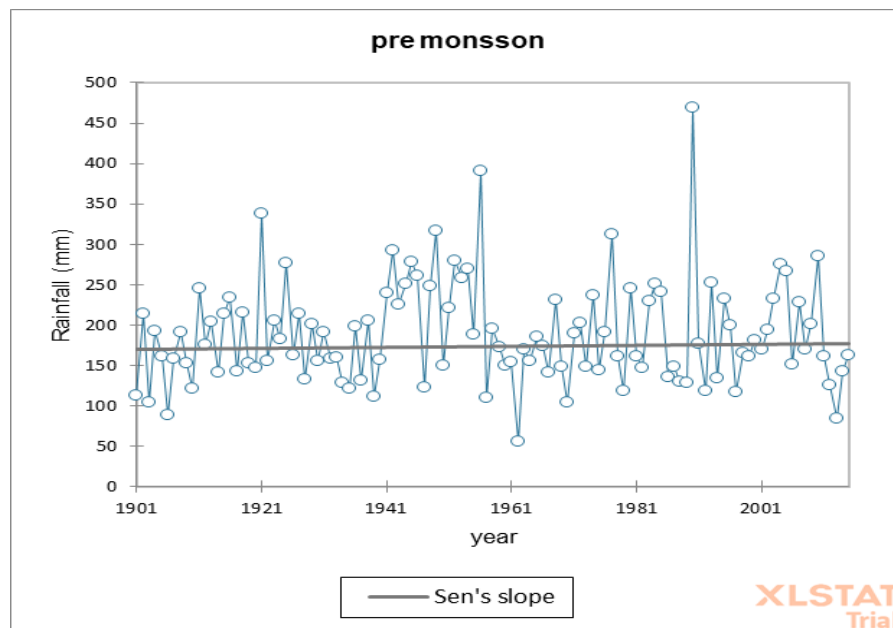


Fig 97. Trend Analysis of point 18

Result:

- Points P17, P18 are showing increasing trend

POINT 19

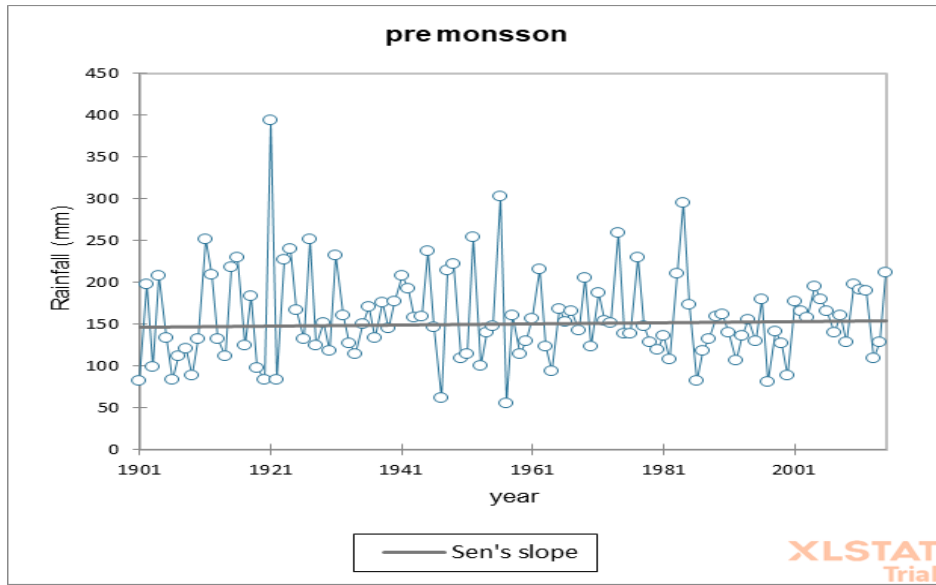


Fig 98. Trend Analysis of point 19

POINT 20

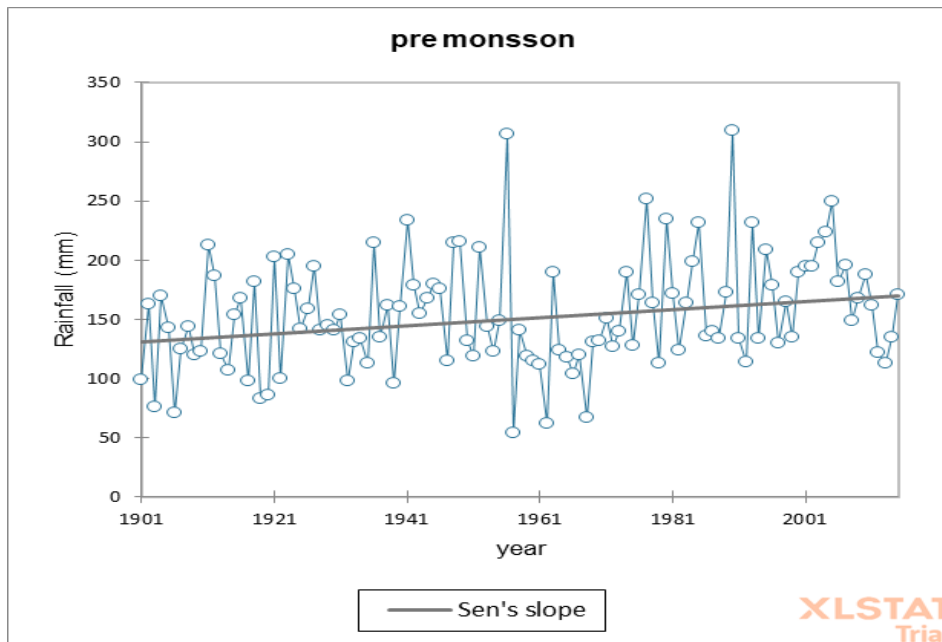


Fig 99. Trend Analysis of point 20

Result:

- Points P19, P20 are showing increasing trend

POINT 21

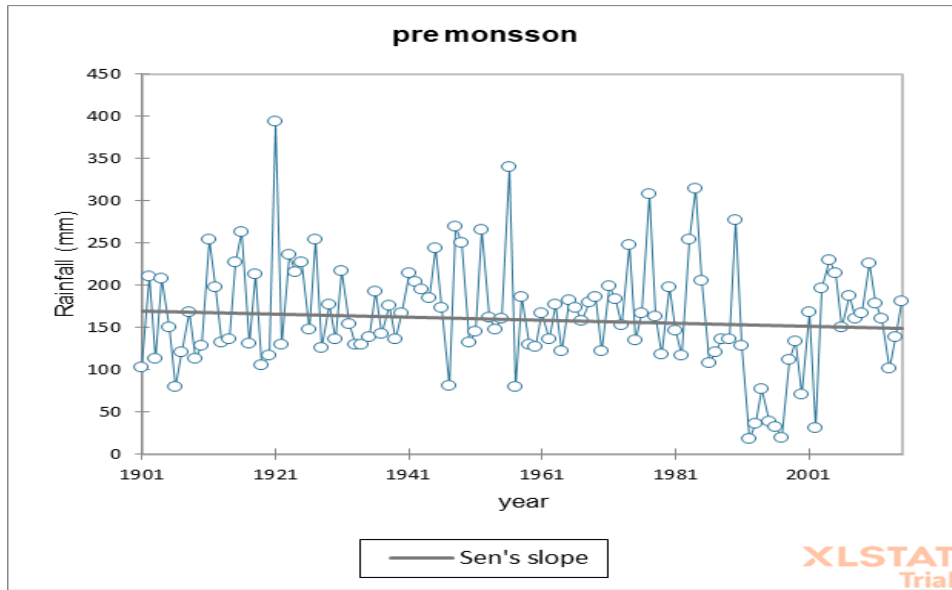


Fig 100. Trend Analysis of point 21

POINT 22

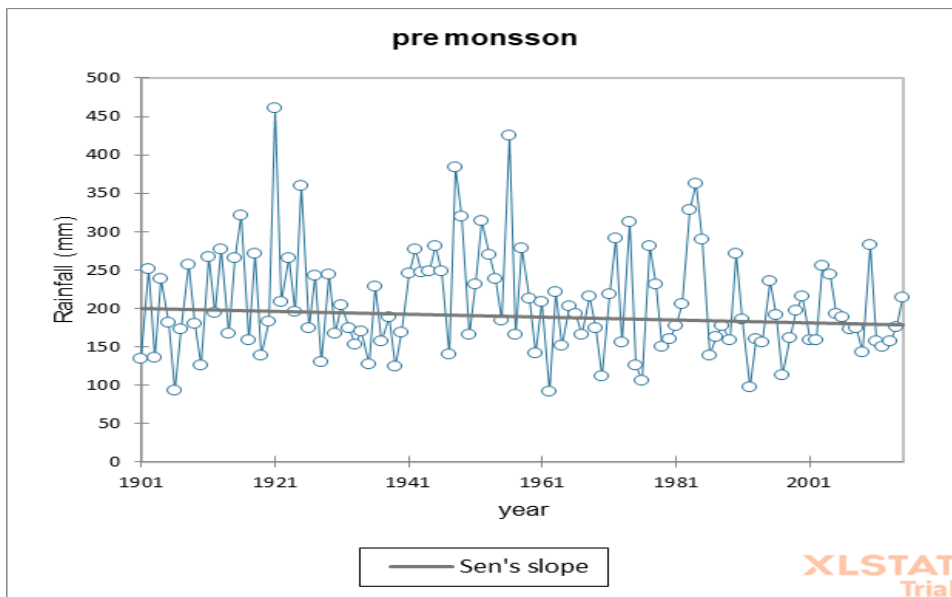


Fig 101. Trend Analysis of point 22

POINT 23

Result:

- Point P21 P22 are showing decreasing trend

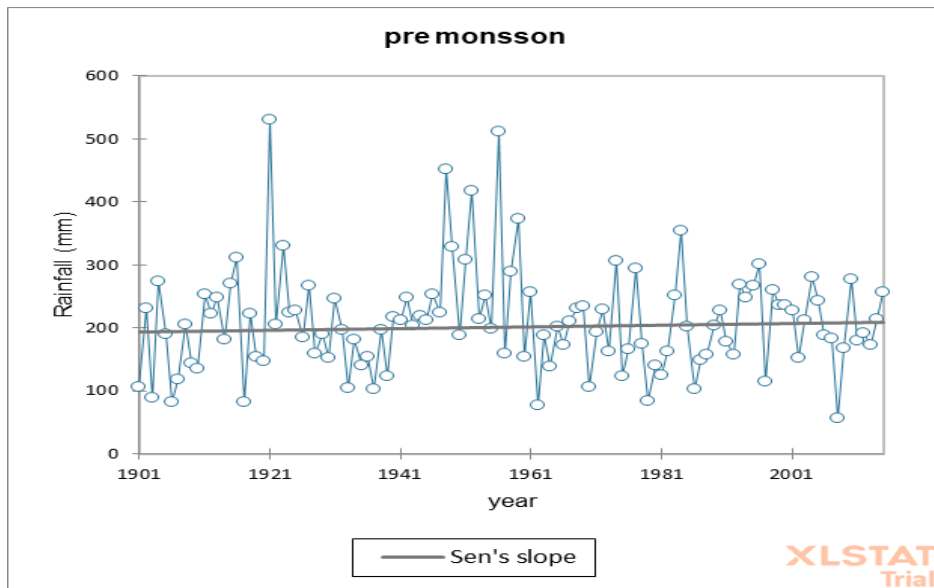


Fig 102. Trend Analysis of point 23

POINT 24

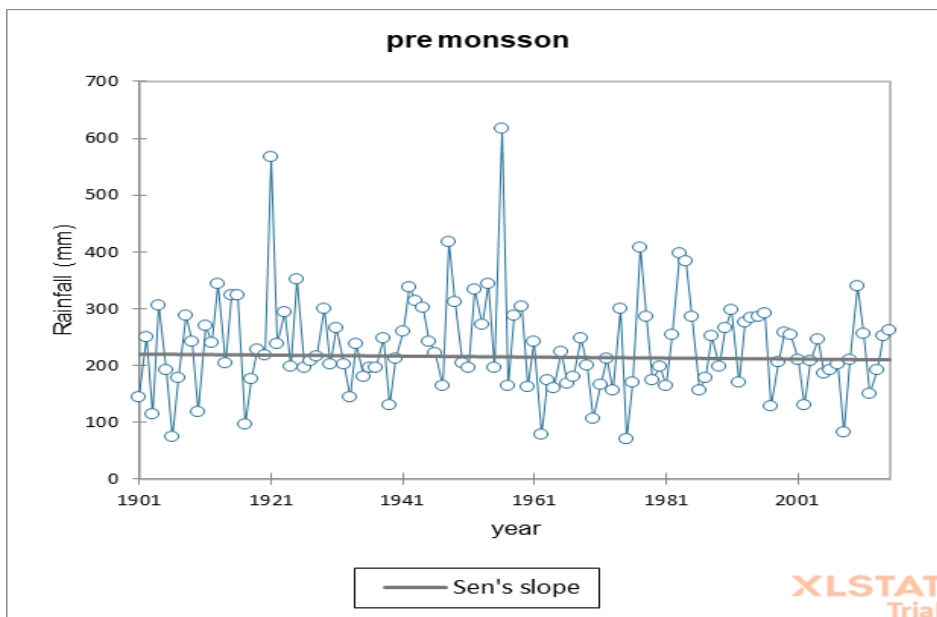


Fig 103. Trend Analysis of point 24

Result:

- Point P23 P24 are showing increasing trend

POINT 25

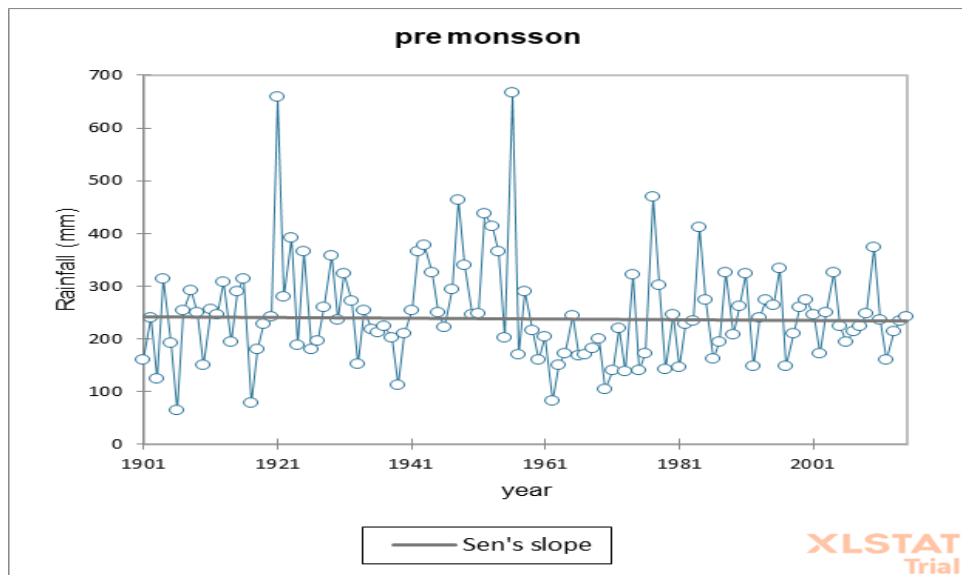


Fig 104. Trend Analysis of point 25

POINT 26

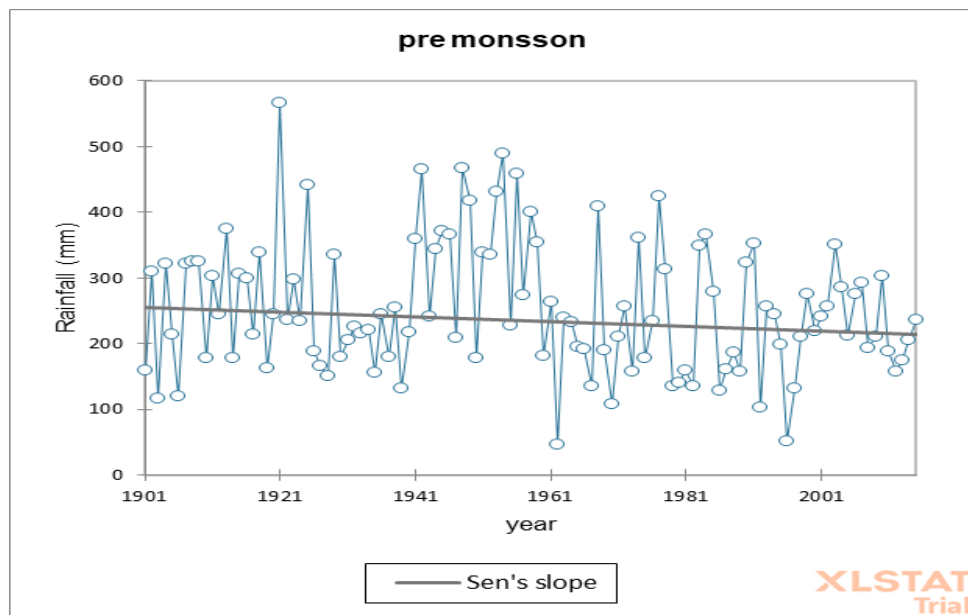


Fig 105. Trend Analysis of point 26

Result:

- Point P25 is showing increasing trend
- Point P26 are showing decreasing trend

POINT 27

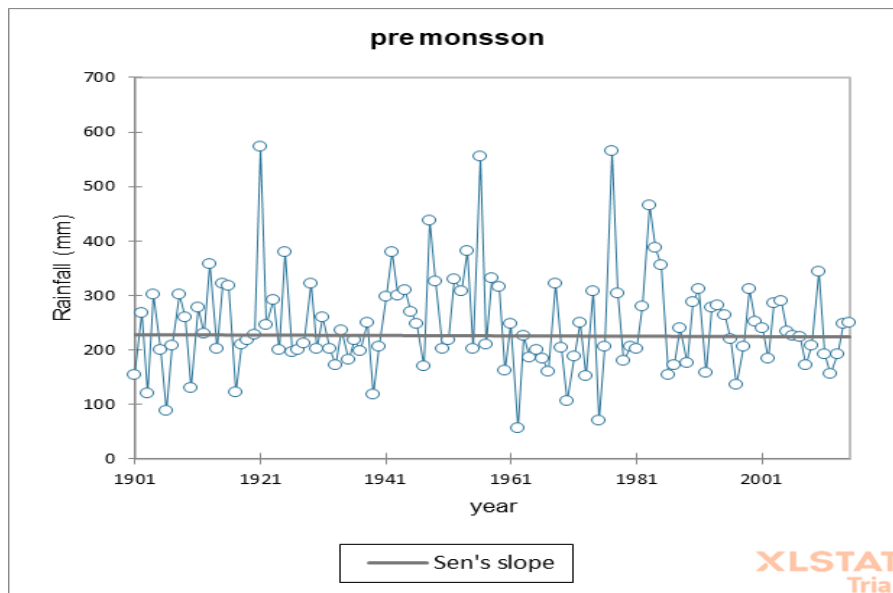


Fig 106. Trend Analysis of point 27

POINT 28

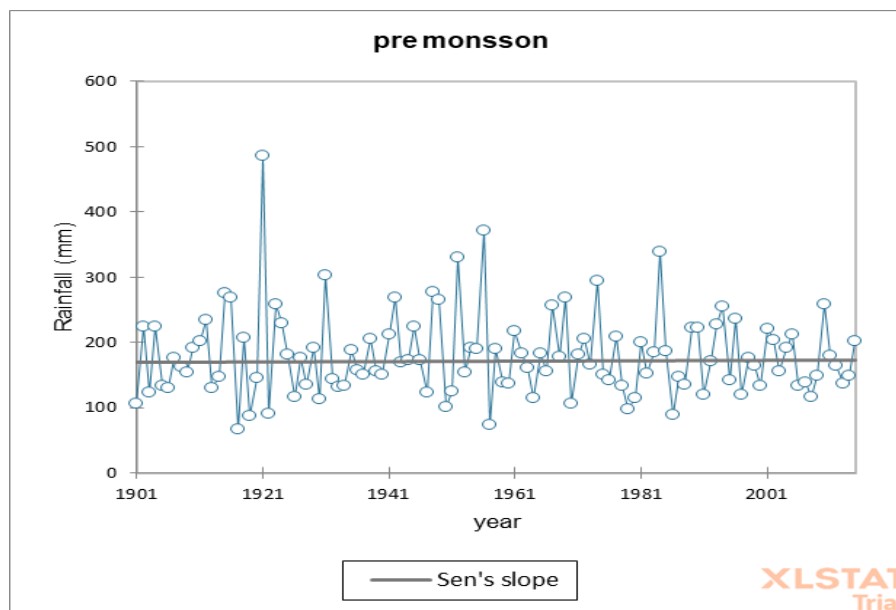


Fig 107. Trend Analysis of point 28

Result:

- Points P27, P28 are showing slight decreasing trend

POINT 29

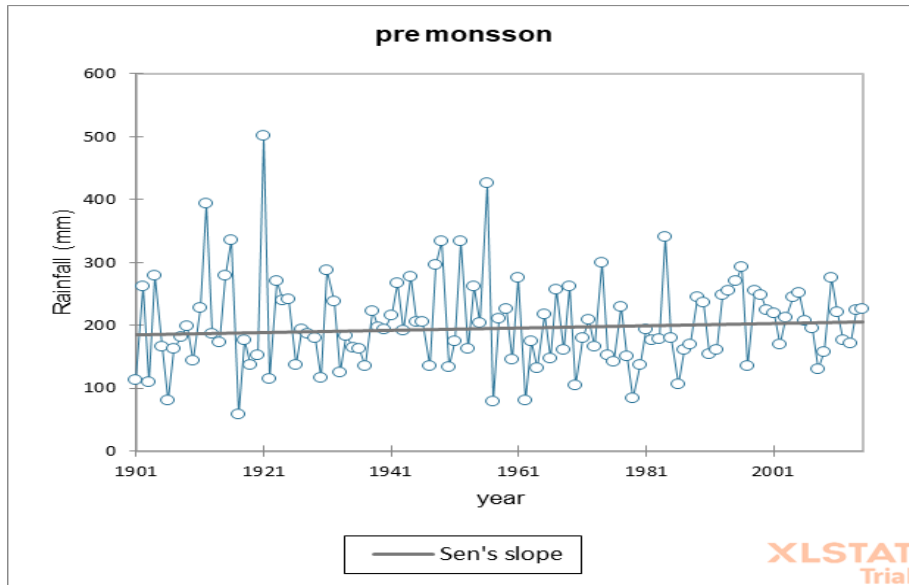


Fig 108. Trend Analysis of point 29

POINT 30

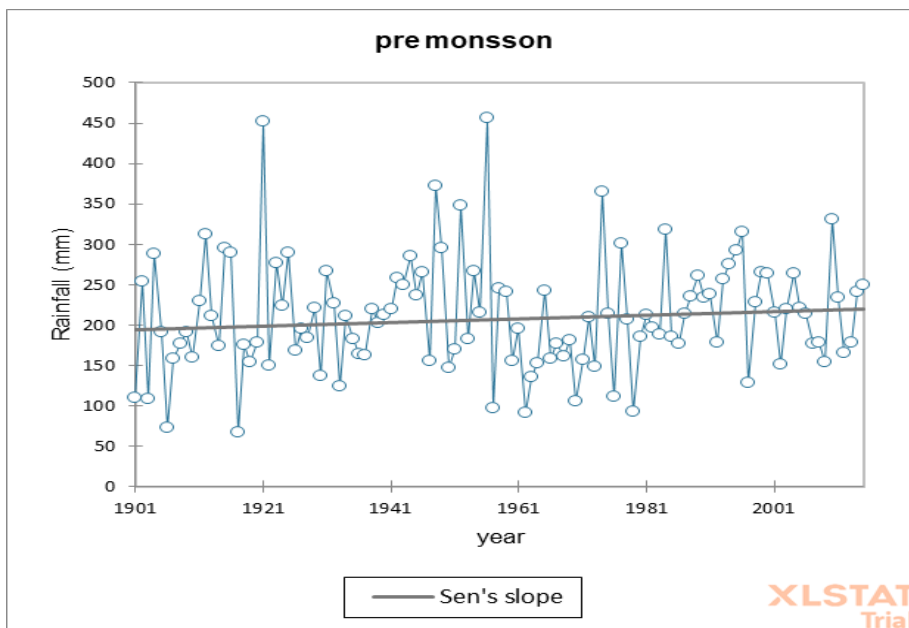


Fig 109. Trend Analysis of point 30

Result:

- Points P29, P30 are showing increasing trend

POINT 31

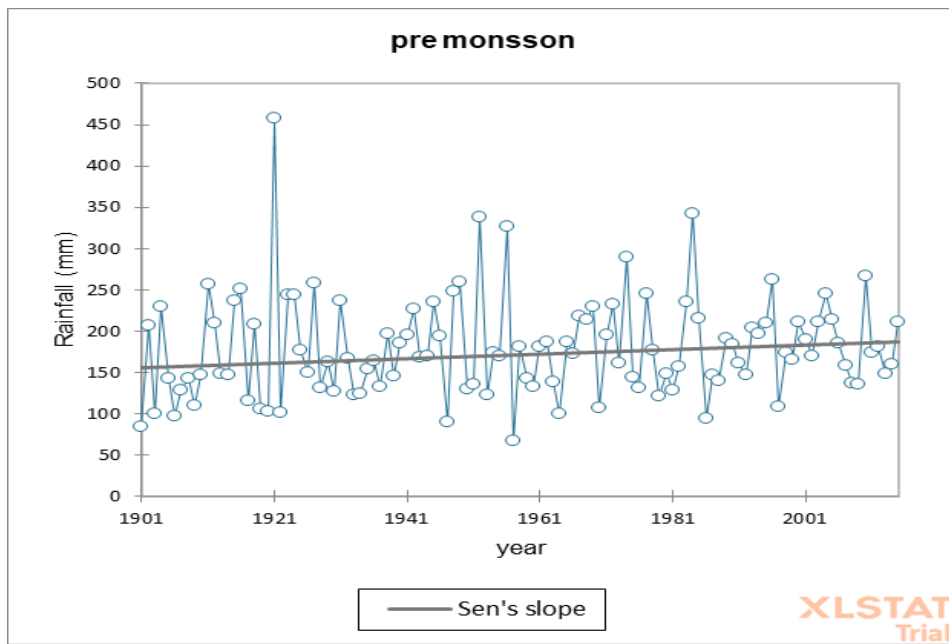


Fig 110. Trend Analysis of point 31

Result:

- Point P31 is showing increasing trend

Discussion

From the above graphical representation of the Sen Slope we can infer that there is increasing trend in the rainfall in the Pre-Monsoon season

However, some station such as P7, P8, P13, P21, P22, P25 P26 are showing decreasing trend in the rainfall pattern over the specified area.

MONSOON

POINT 1

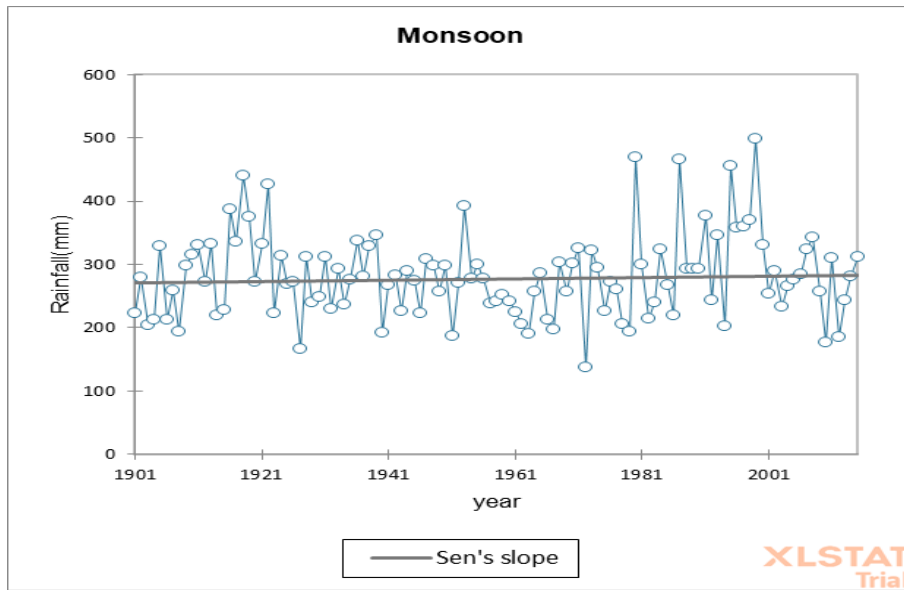


Fig 111. Trend Analysis of point 1

POINT 2

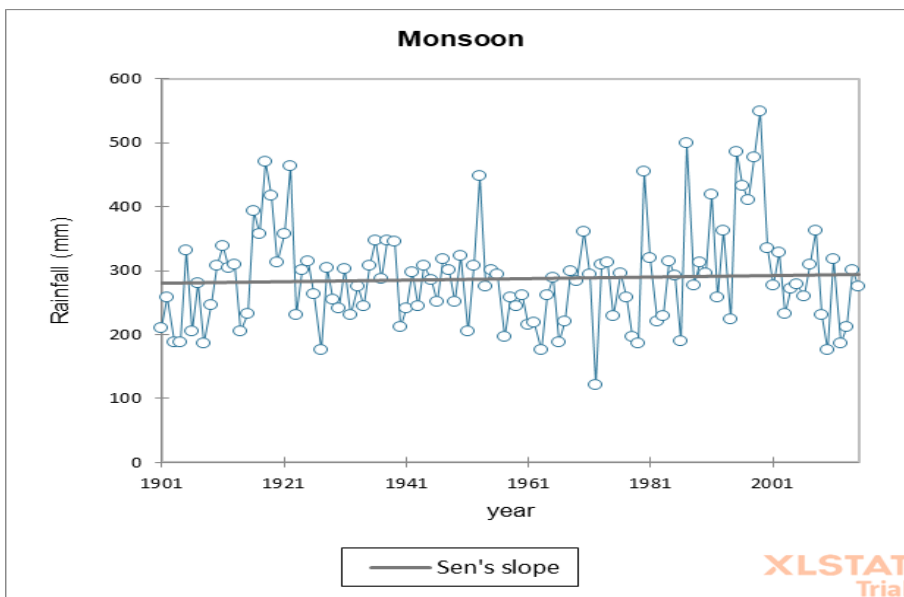


Fig 112. Trend Analysis of point 2

Result:

- Points P1, P2 are showing increasing trend

POINT 3

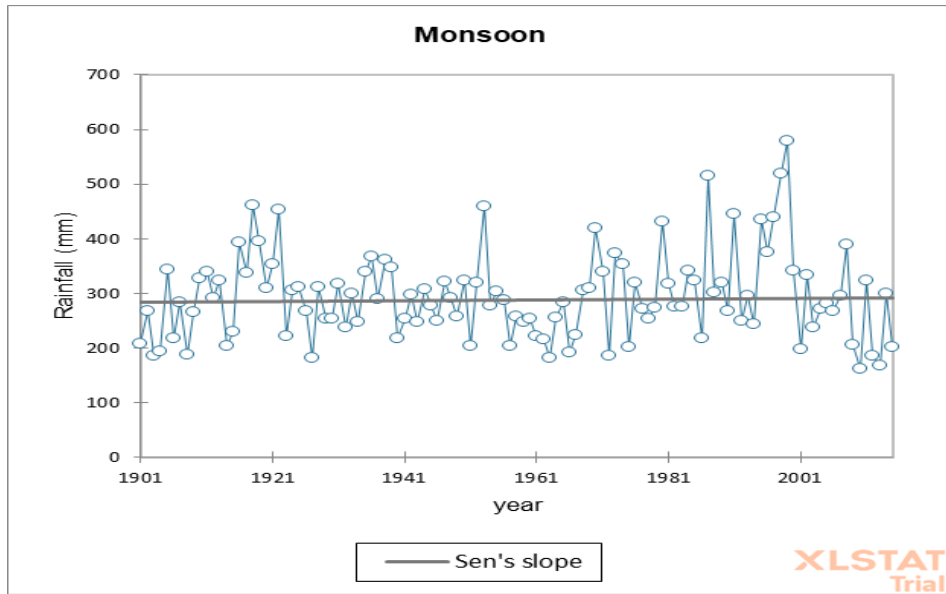


Fig 113. Trend Analysis of point 3

POINT 4

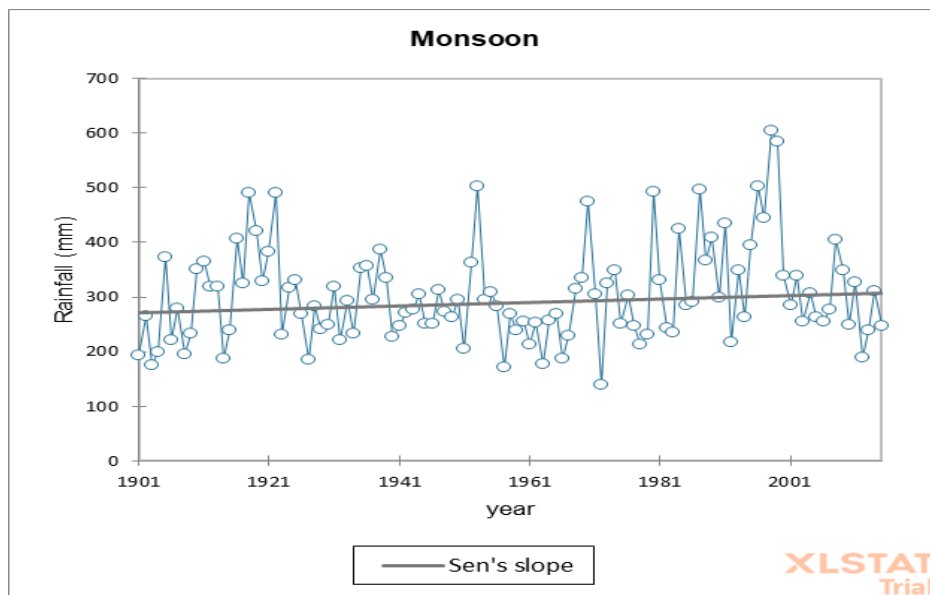


Fig 114. Trend Analysis of point 4

Result:

- Points P3, P4 are showing increasing trend

POINT 5

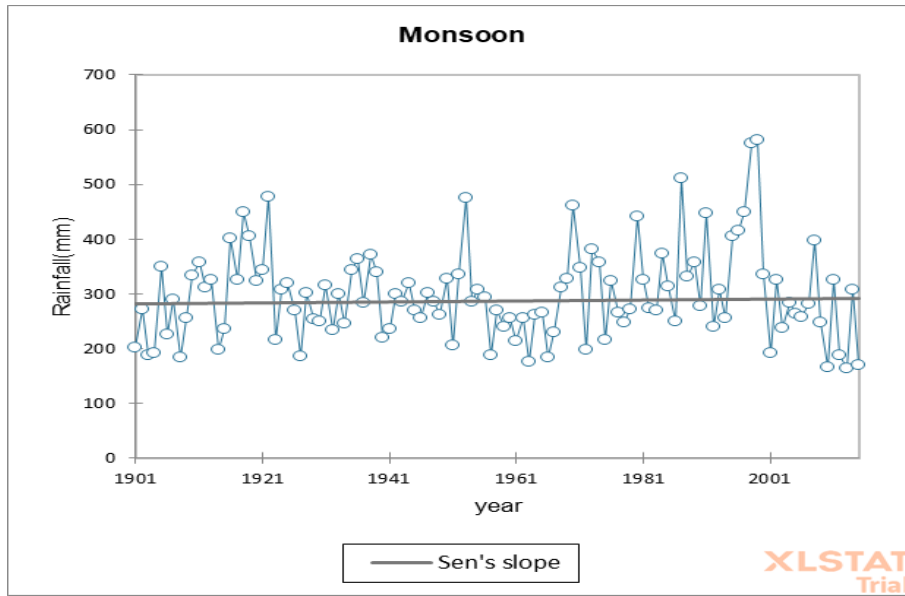


Fig 115. Trend Analysis of point 5

POINT 6

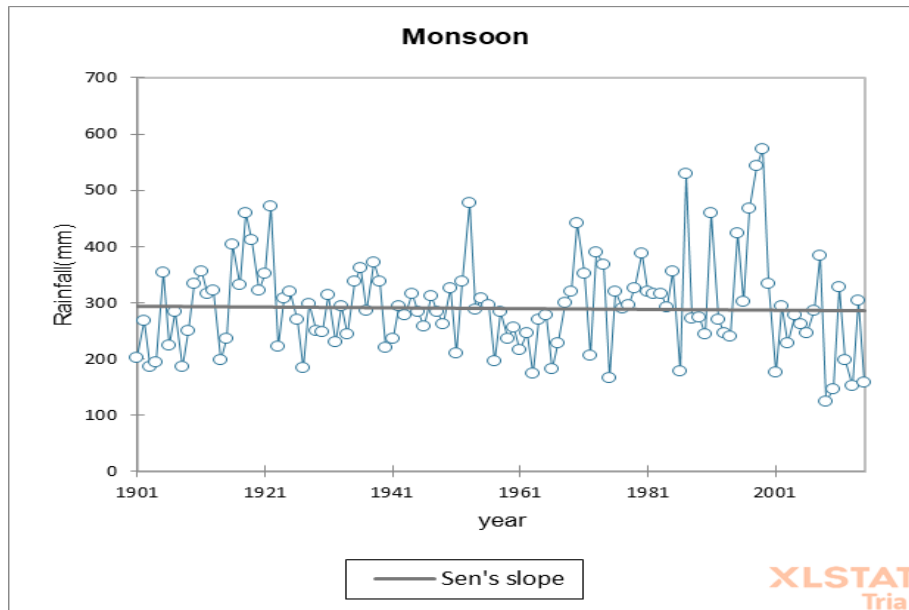


Fig 116. Trend Analysis of point 6

Result:

- Points P5, P6 are showing increasing trend

POINT 7

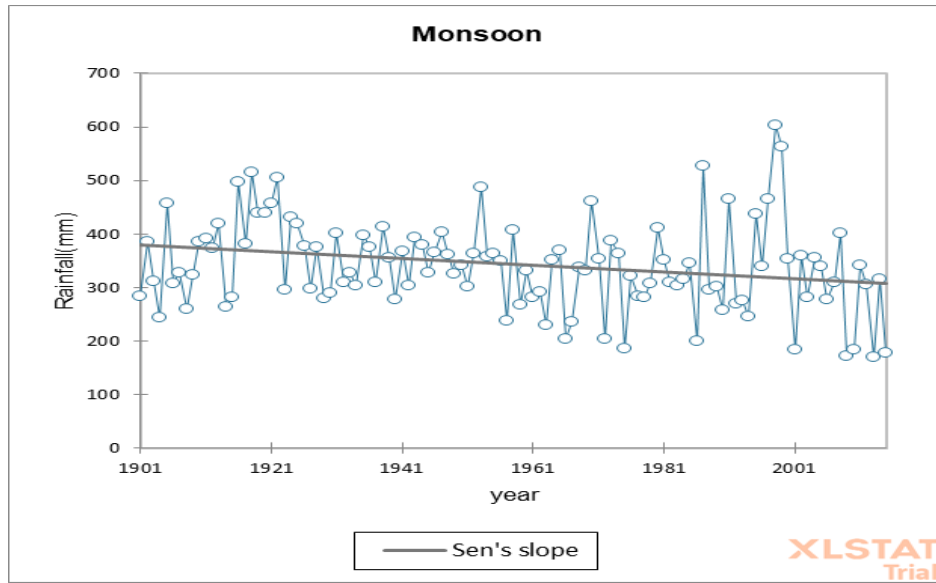


Fig 117. Trend Analysis of point 7

POINT 8

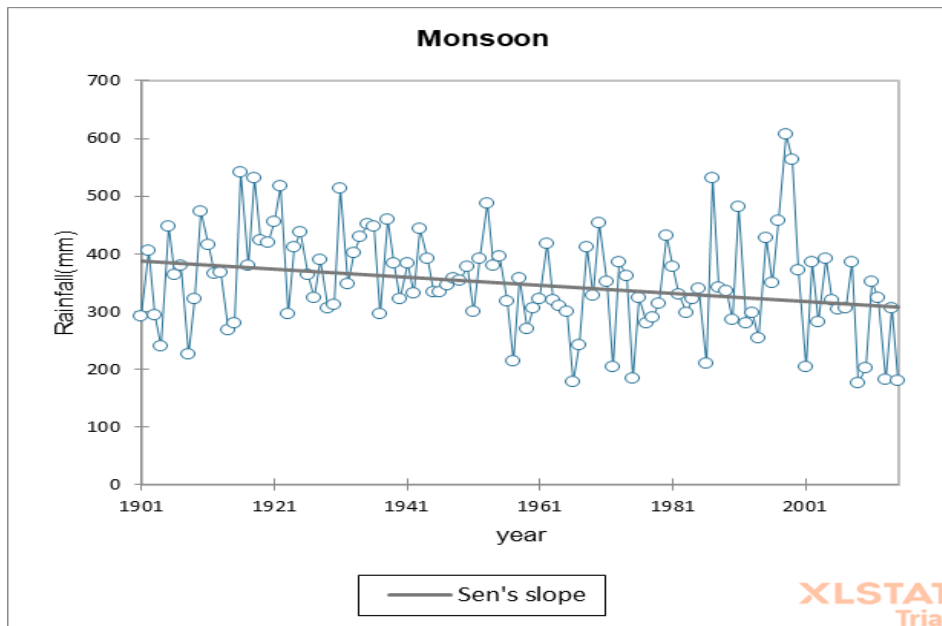


Fig 118. Trend Analysis of point 8

Result:

- Points P7, P8 are showing decreasing trend

POINT 9

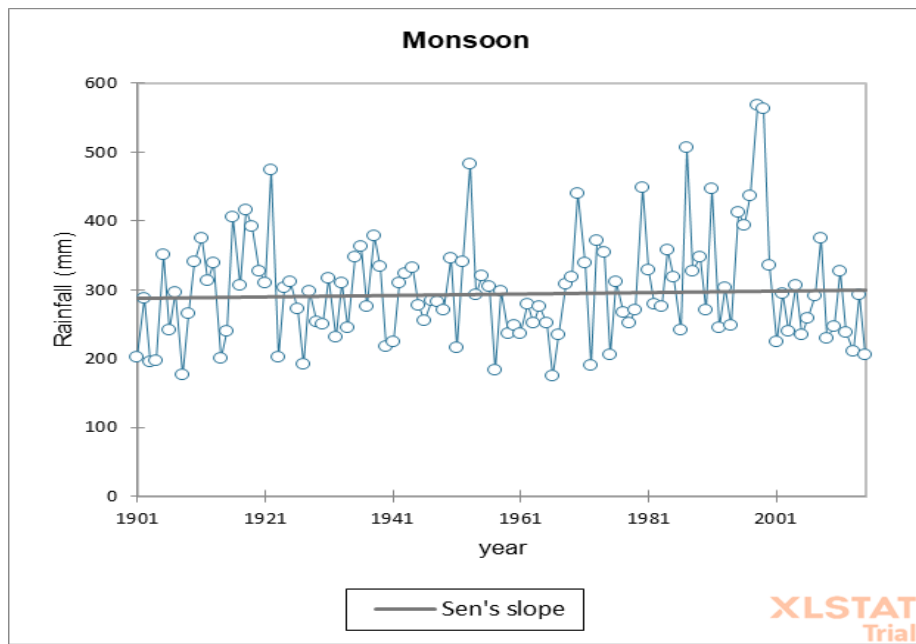


Fig 119. Trend Analysis of point 9

POINT 10

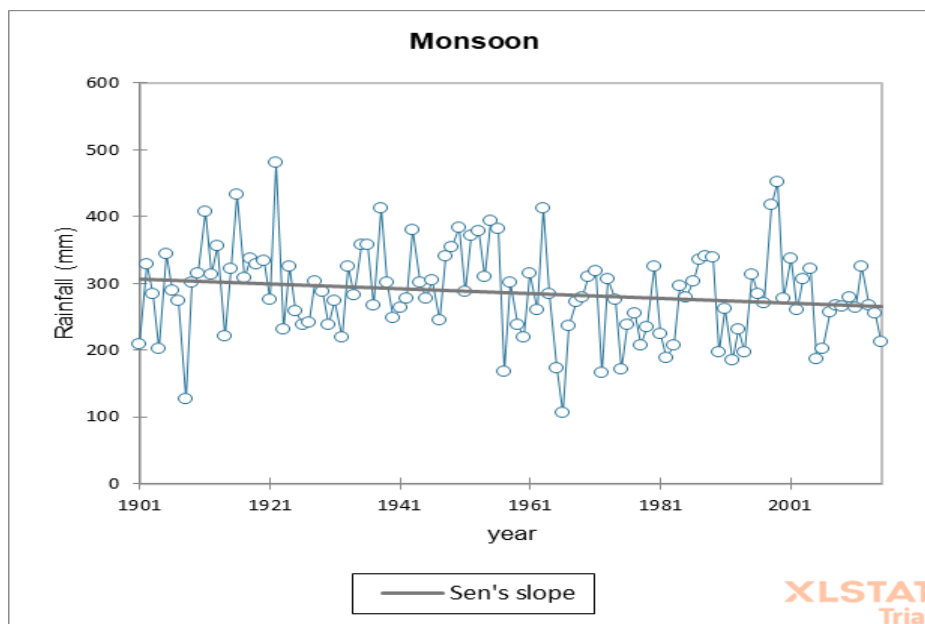


Fig 120. Trend Analysis of point 10

Result:

- Point P9 is showing increasing trend
- Point P10 is showing decreasing trend

POINT 11

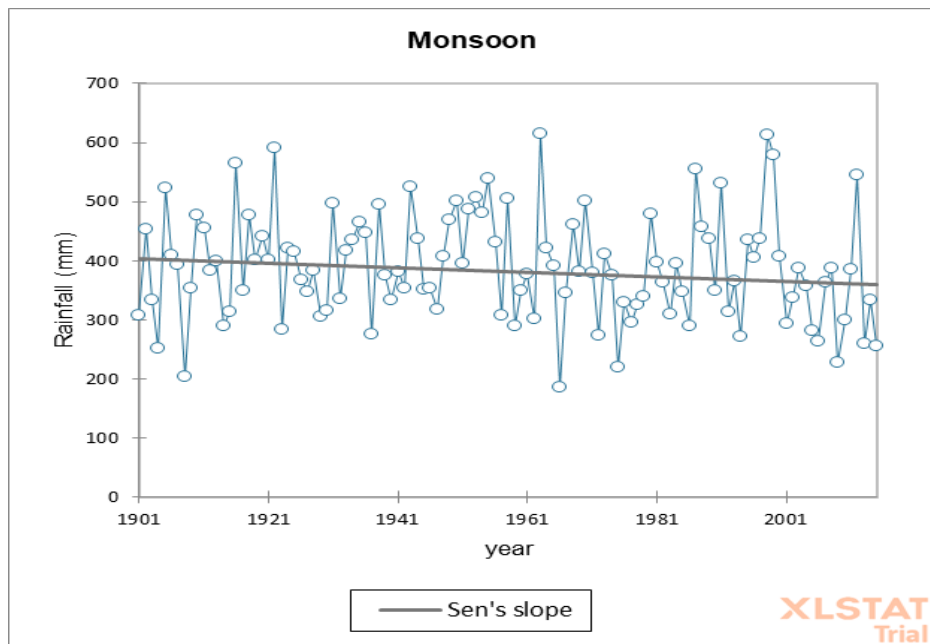


Fig 121. Trend Analysis of point 11

POINT 12

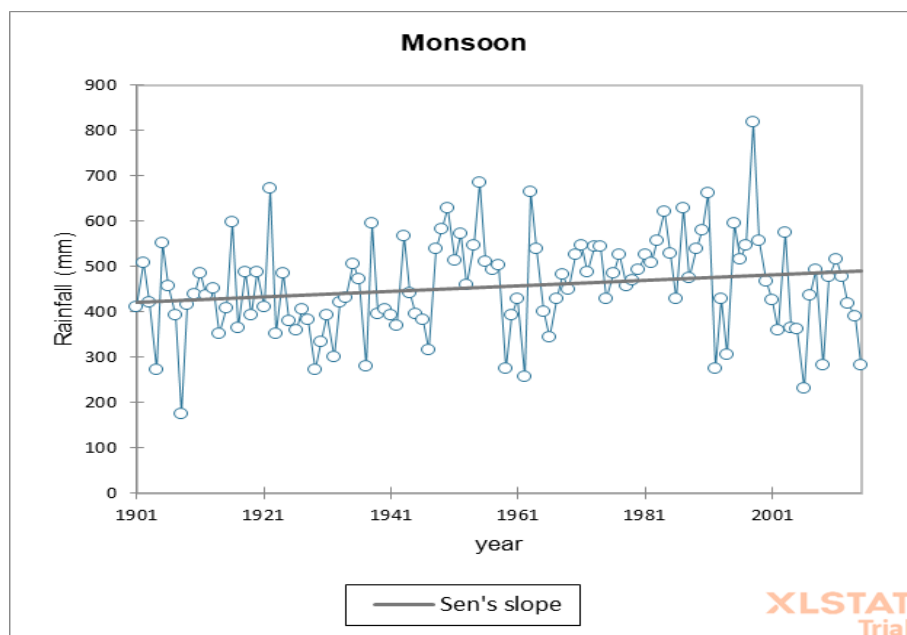


Fig 122. Trend Analysis of point 12

Result:

- Point P11 is showing decreasing trend
- Point P12 is showing increasing trend

POINT 13

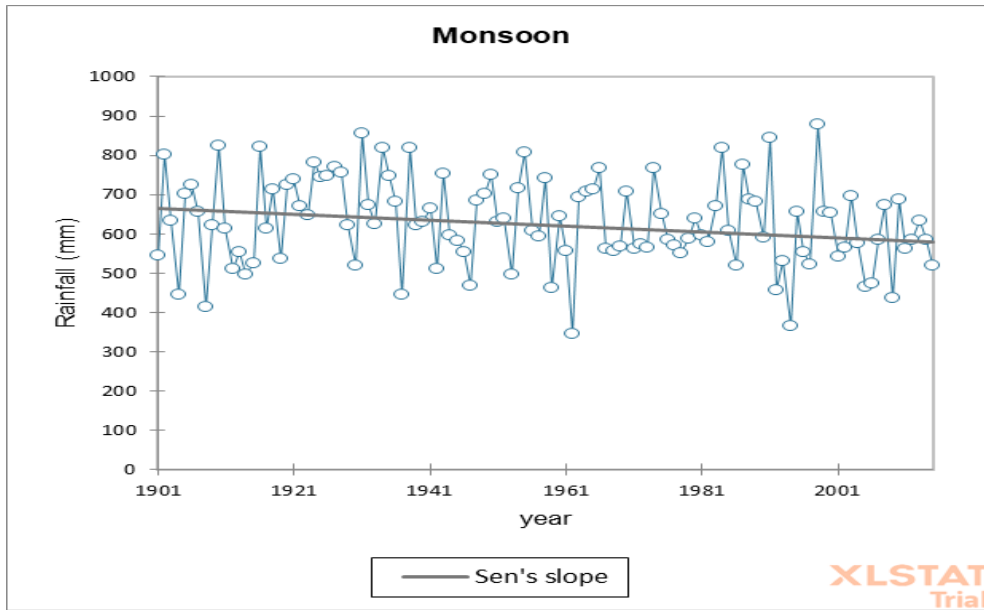


Fig 123. Trend Analysis of point 13

POINT 14

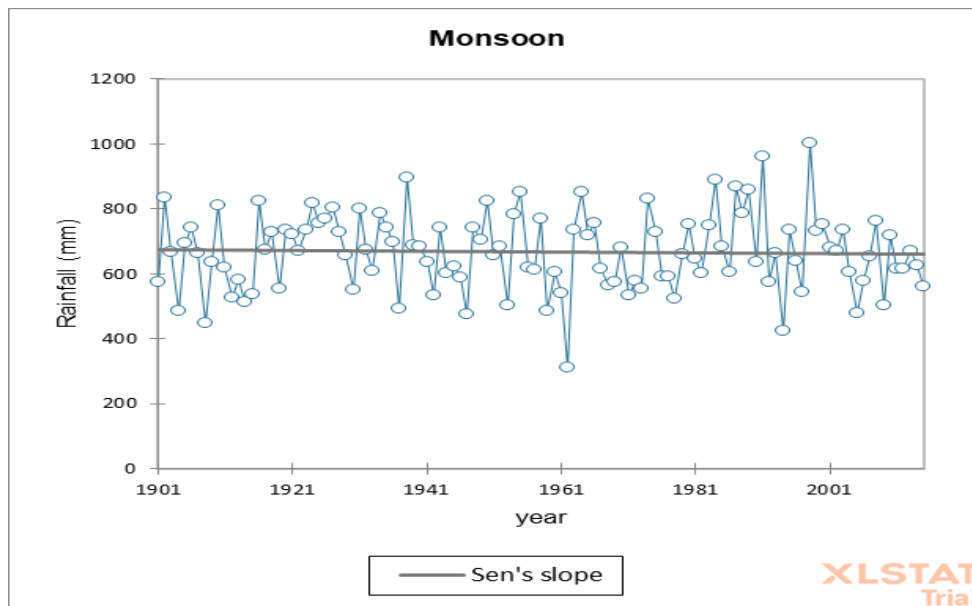


Fig 124. Trend Analysis of point 14

Result:

- Point P13 is showing decreasing trend
- Point P14 is showing increasing trend

POINT 15

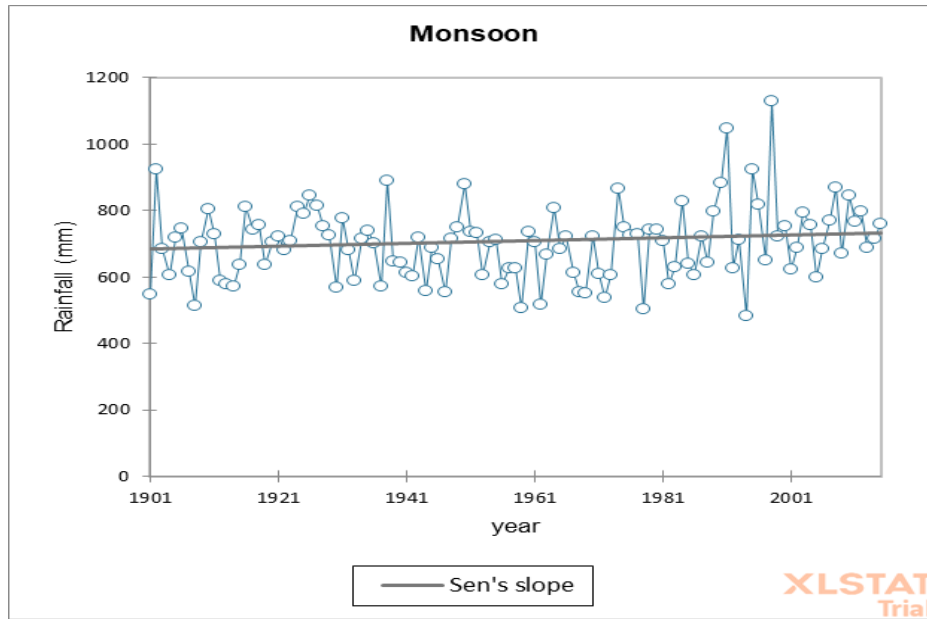


Fig 125. Trend Analysis of point 15

POINT 16

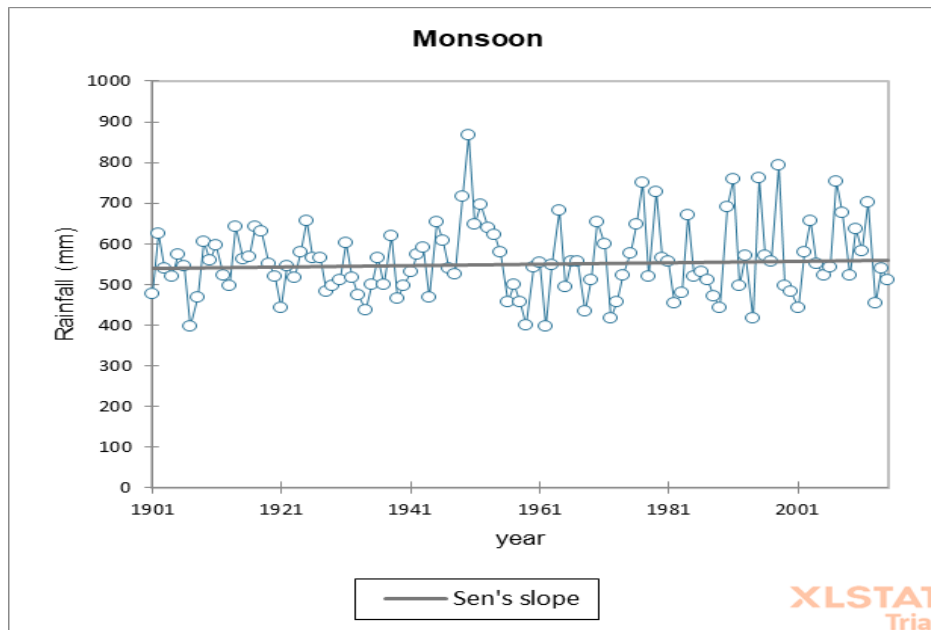


Fig 126. Trend Analysis of point 16

Result:

- Points P15, P16 are showing increasing trend

POINT 17

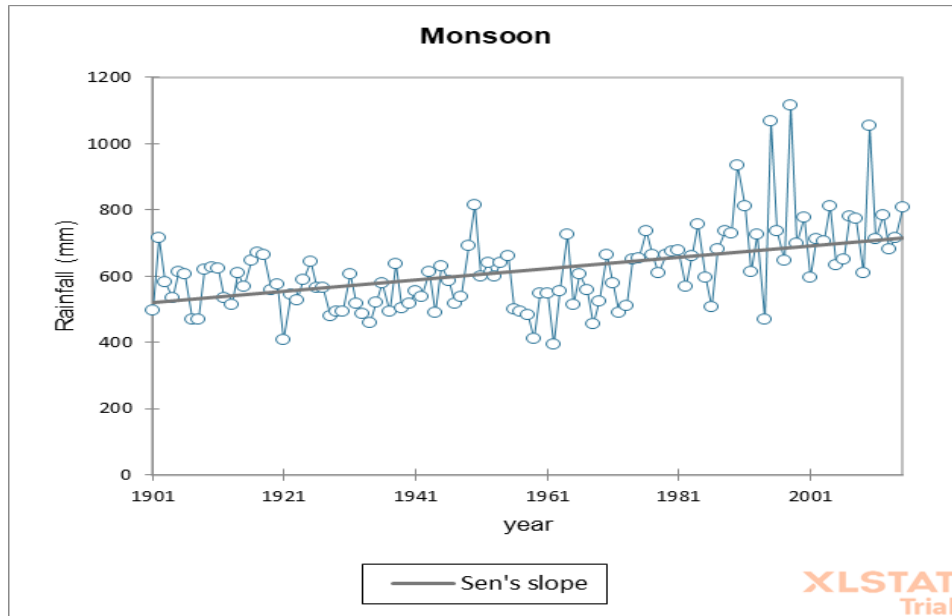


Fig 127. Trend Analysis of point 17

POINT 18

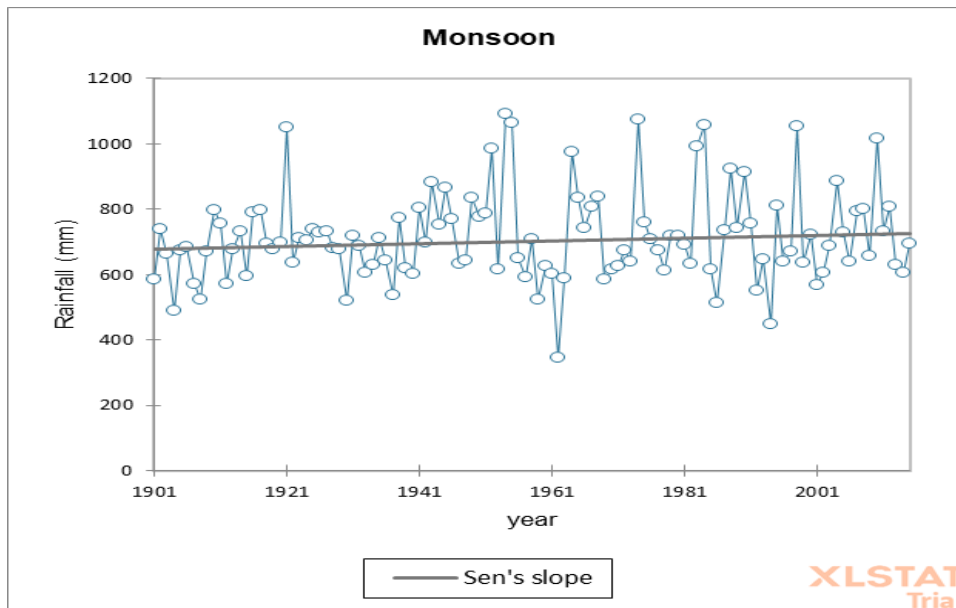


Fig 128. Trend Analysis of point 18

Result:

- Points P17, P18 are showing increasing trend

POINT 19

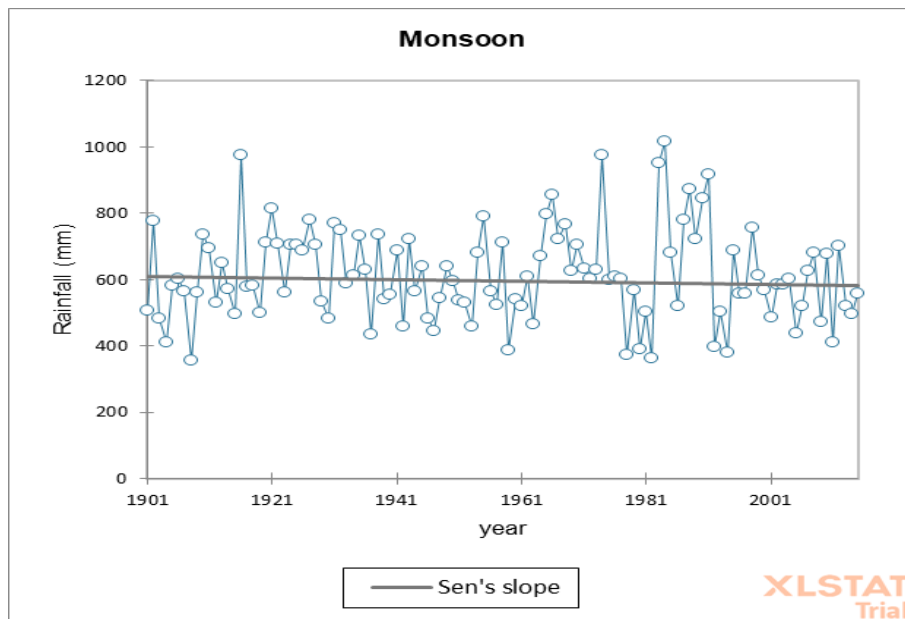


Fig 129. Trend Analysis of point 19

POINT 20

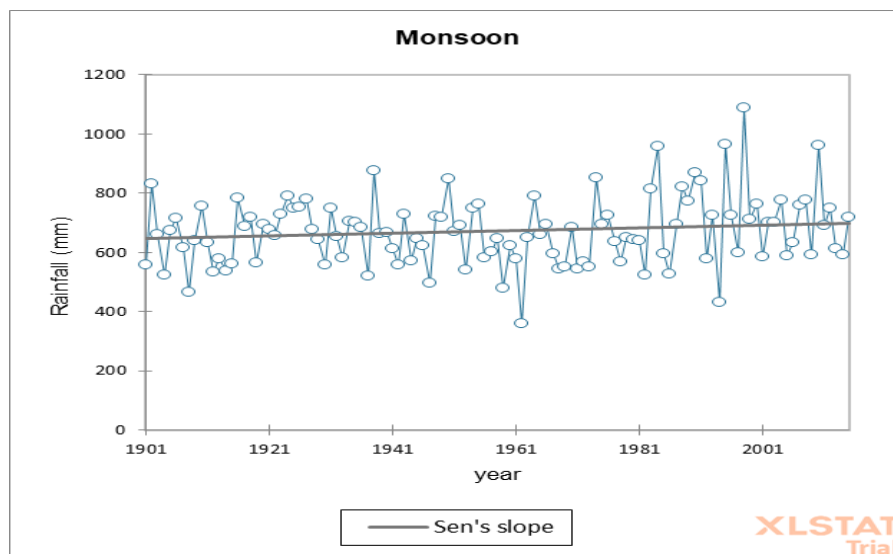


Fig 130. Trend Analysis of point 20

Result:

- Point P19 is showing decreasing trend
- Point P20 is showing increasing trend

POINT 21

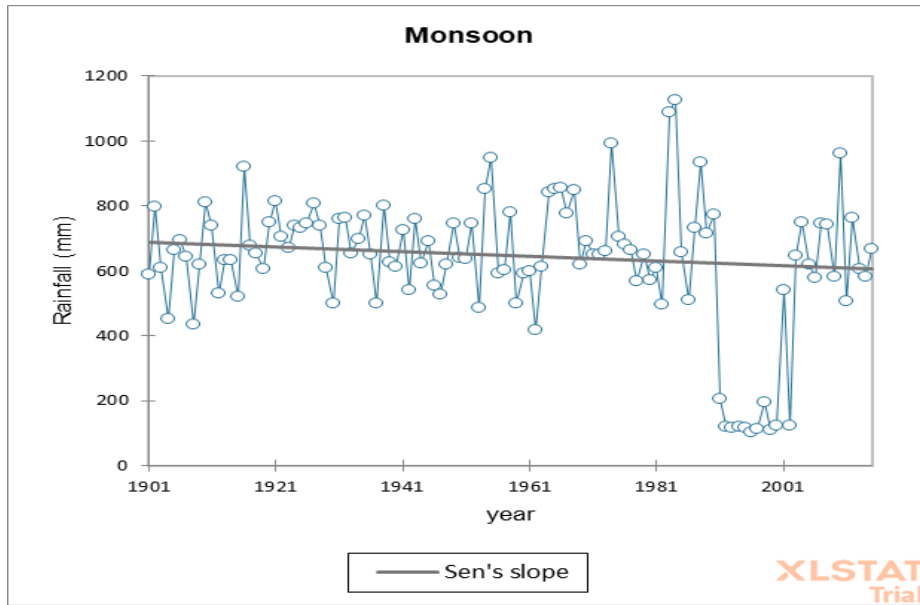


Fig 131. Trend Analysis of point 21

POINT 22

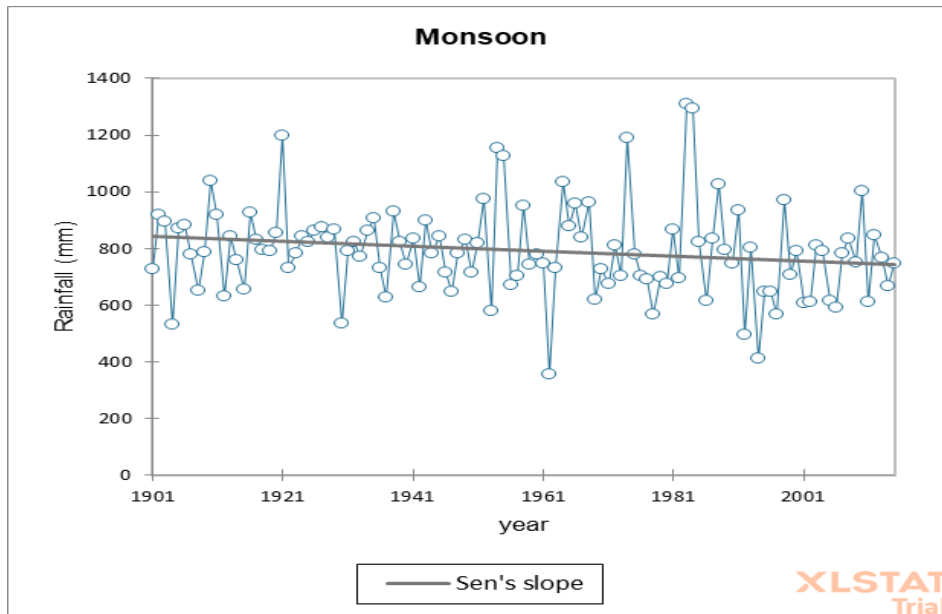


Fig 132. Trend Analysis of point 22

Result:

- Points P21, P22 are showing decreasing trend

POINT 23

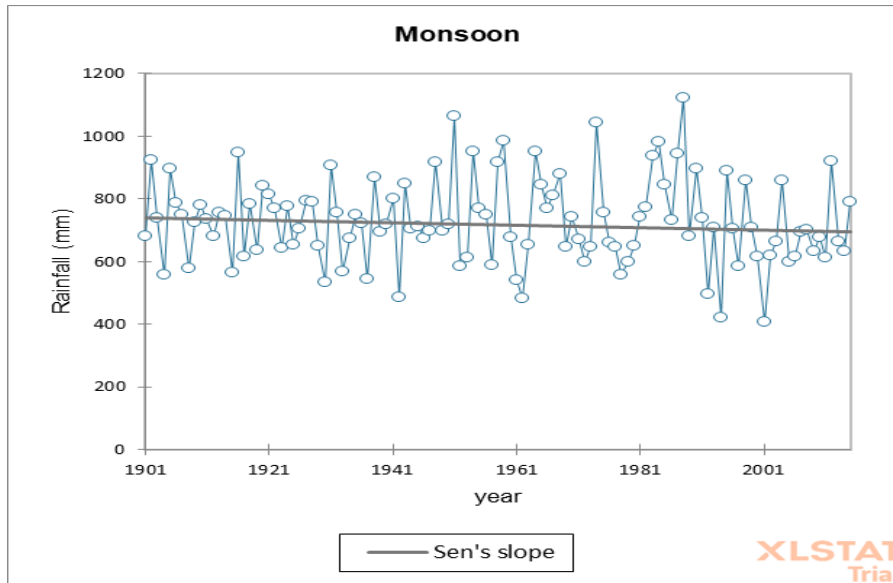


Fig 133. Trend Analysis of point 23

POINT 24

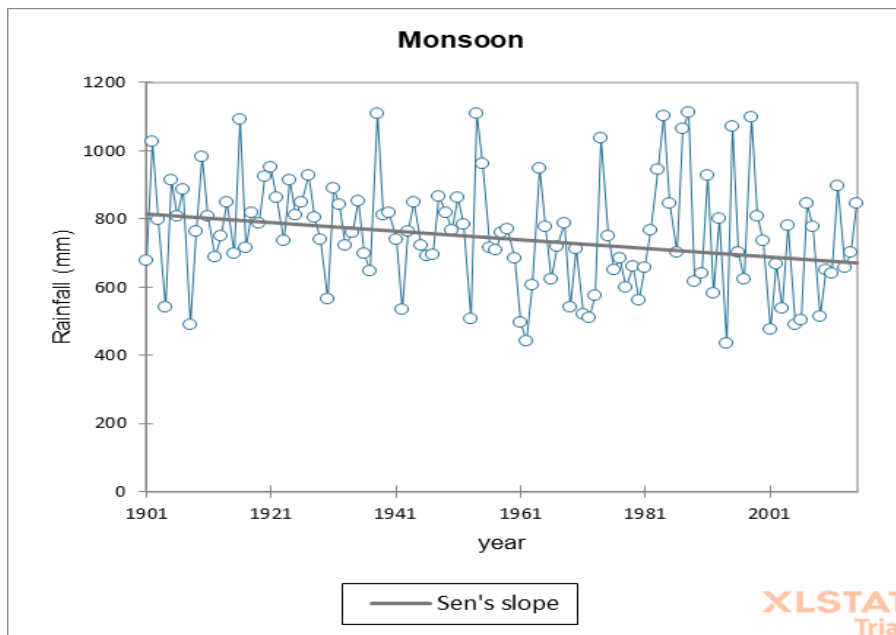


Fig 134. Trend Analysis of point 24

Result:

- Points P23, P24 are showing decreasing trend

POINT 25

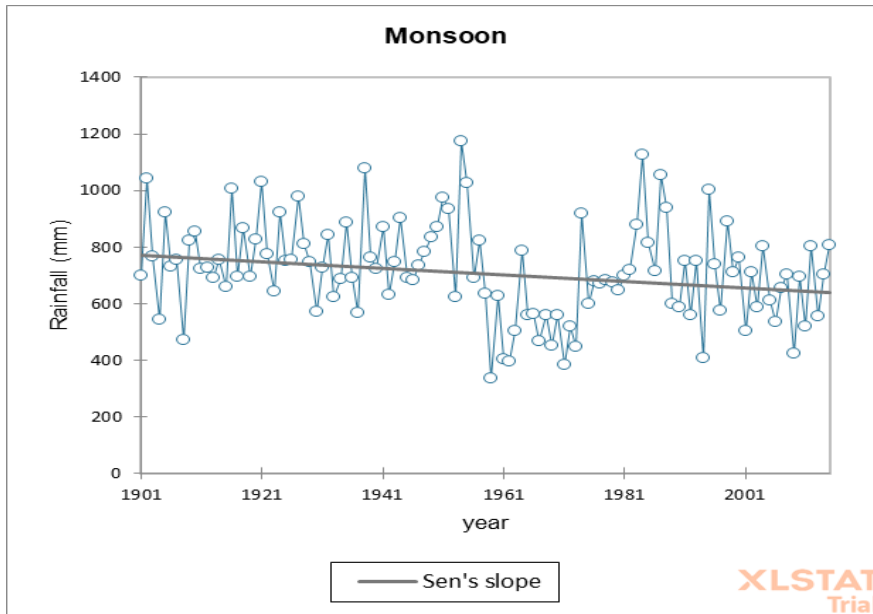


Fig 135. Trend Analysis of point 25

POINT 26

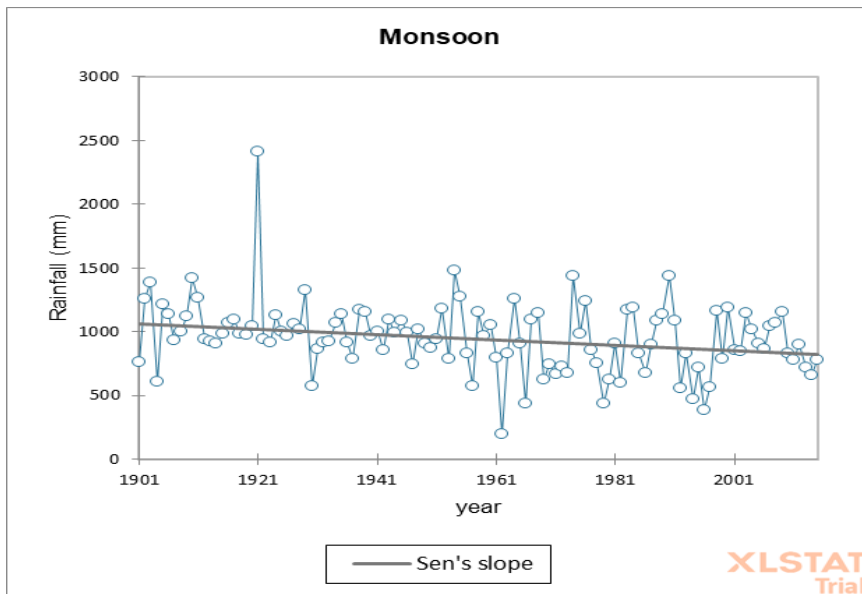


Fig 136. Trend Analysis of point 26

Result:

- Points P26, P26 are showing decreasing trend

POINT 27

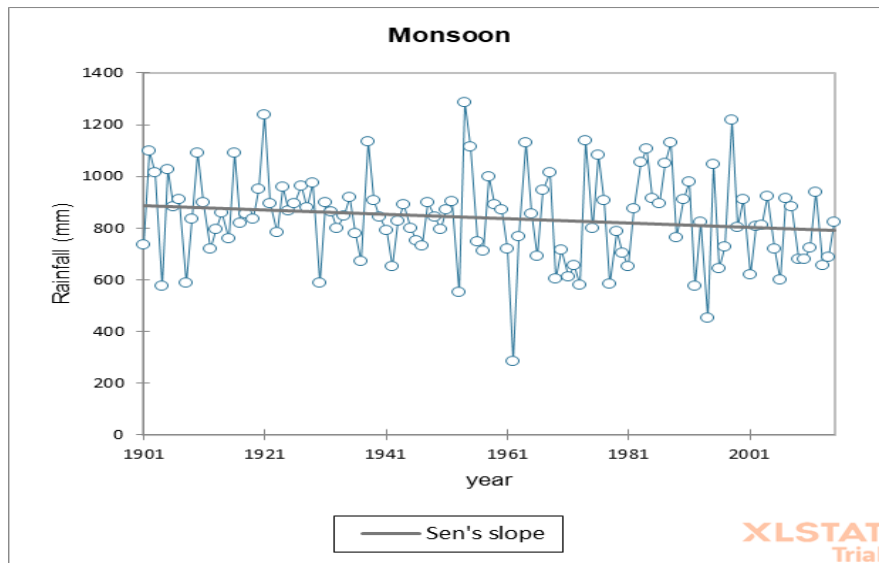


Fig 137. Trend Analysis of point 27

POINT 28

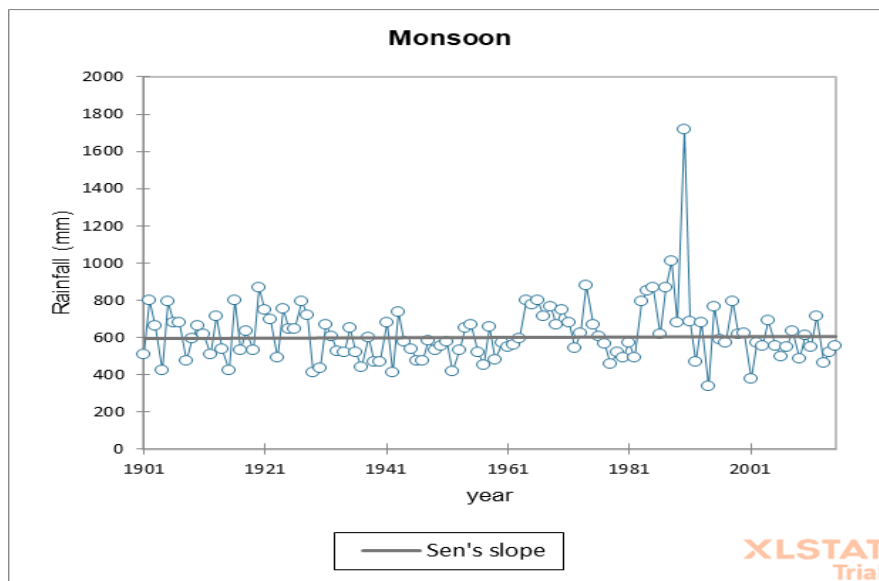


Fig 138. Trend Analysis of point 28

Result:

- Points P27, P28 are showing decreasing trend

POINT 29

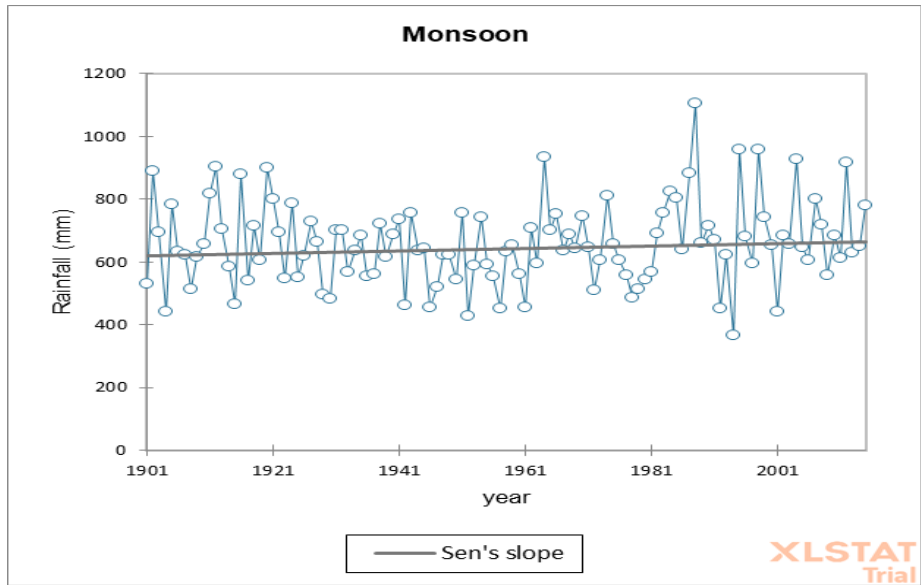


Fig 139. Trend Analysis of point 29

POINT 30

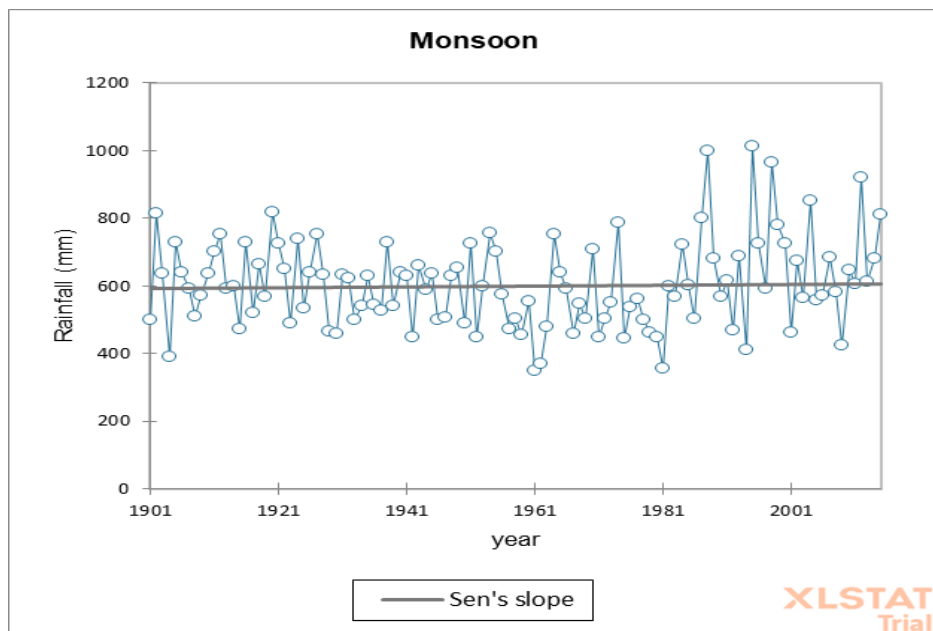


Fig 140. Trend Analysis of point 30

Result:

- Points P29, P30 are showing increasing trend

POINT 31

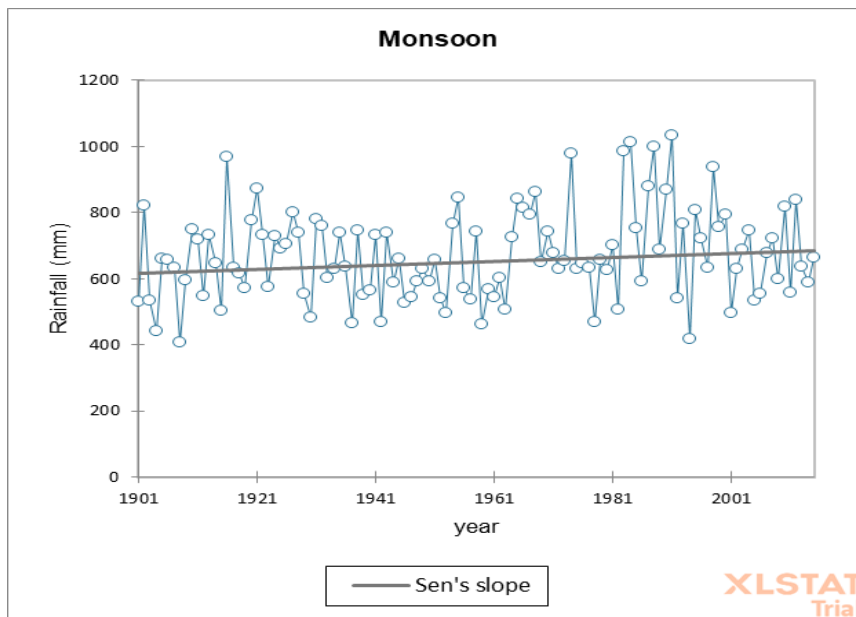


Fig 141. Trend Analysis of point 31

Result:

- Point P31 is showing increasing trend

Discussion

From the above graphical representation of the Sen slope we can conclude that Monsoon is exhibiting an increasing trend in the rainfall pattern over the years in the specified area of northern districts of north Bengal.

However, we can also observe decreasing trend in the rainfall over some stations such as

P7, P8, P10, P11, P13, P21, P22, P23, P24

POST MONSOON

Point 1

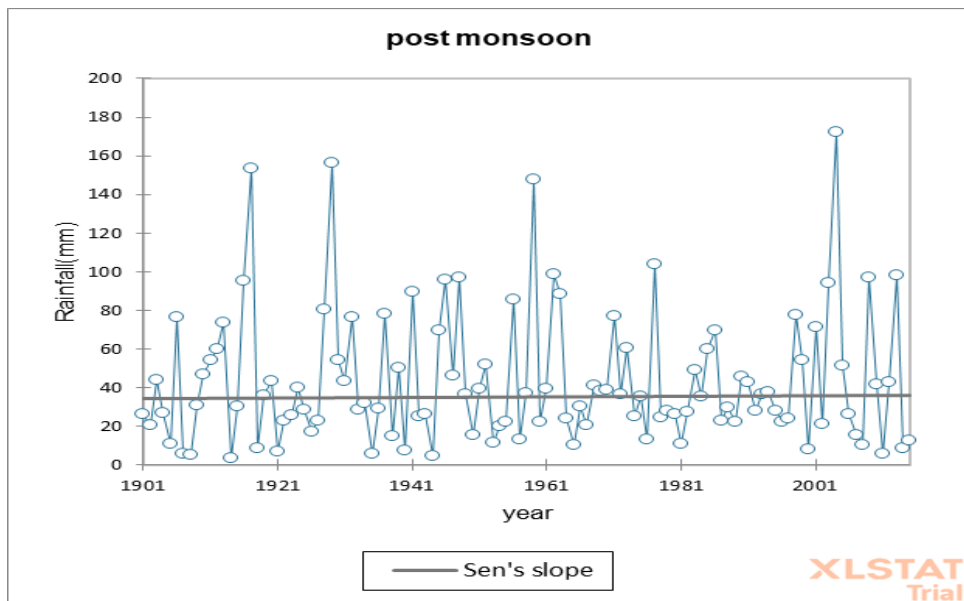


Fig 142. Trend Analysis of point 1

Point 2

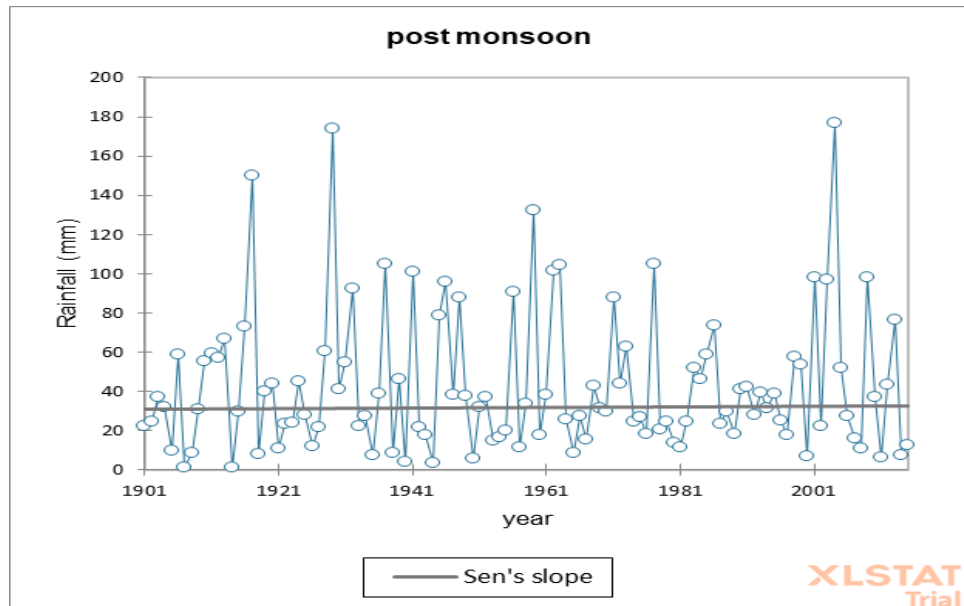


Fig 143. Trend Analysis of point 2

Result:

- Points P1, P2 are showing no change trend

Point 3

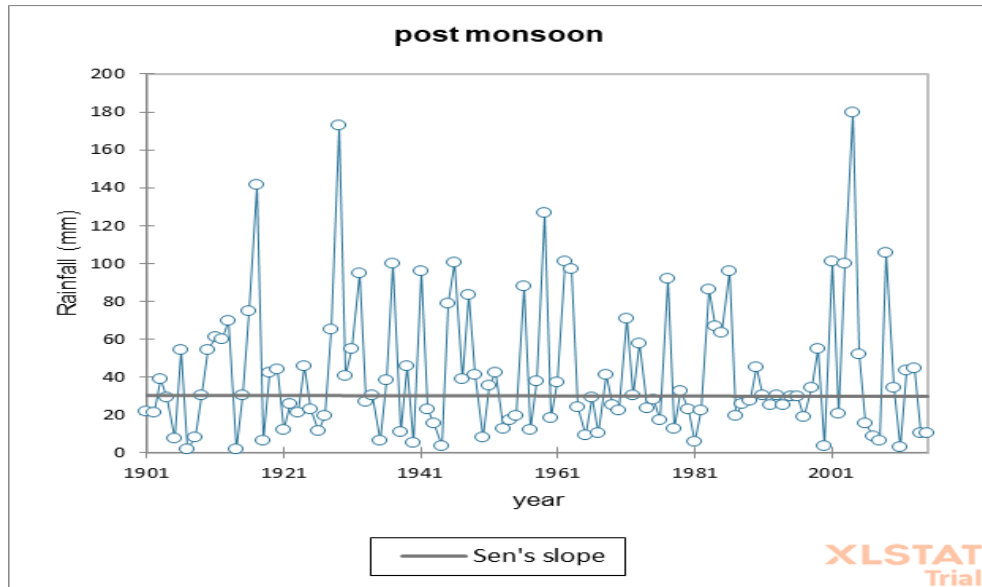


Fig 144. Trend Analysis of point 3

Point 4

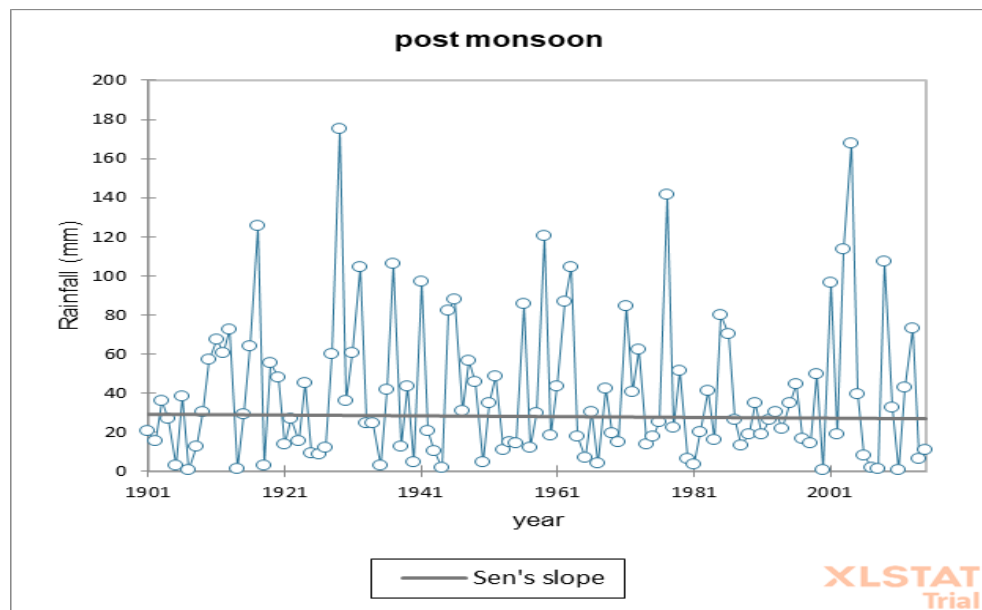


Fig 145. Trend Analysis of point 4

Result:

- Points P3, P4 are showing slight decreasing trend

Point 5

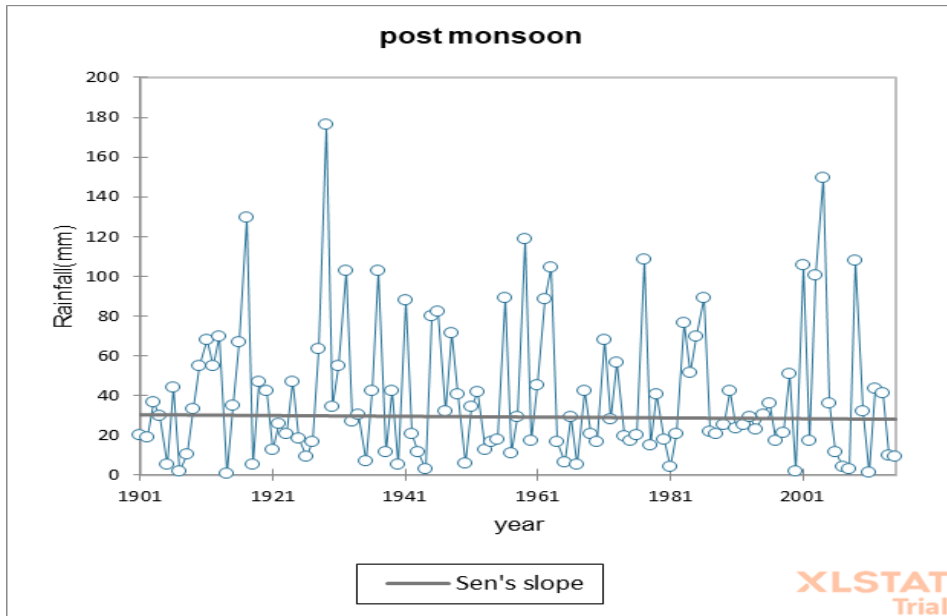


Fig 146. Trend Analysis of point 5

Point 6

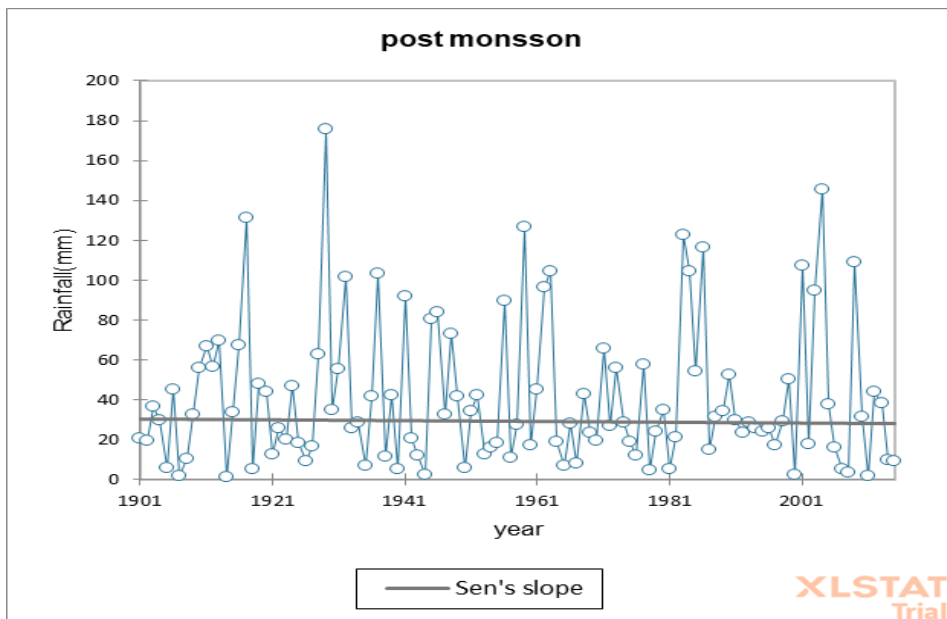


Fig 147. Trend Analysis of point 6

Result:

- Points P5, P6 are showing no change trend

Point 7

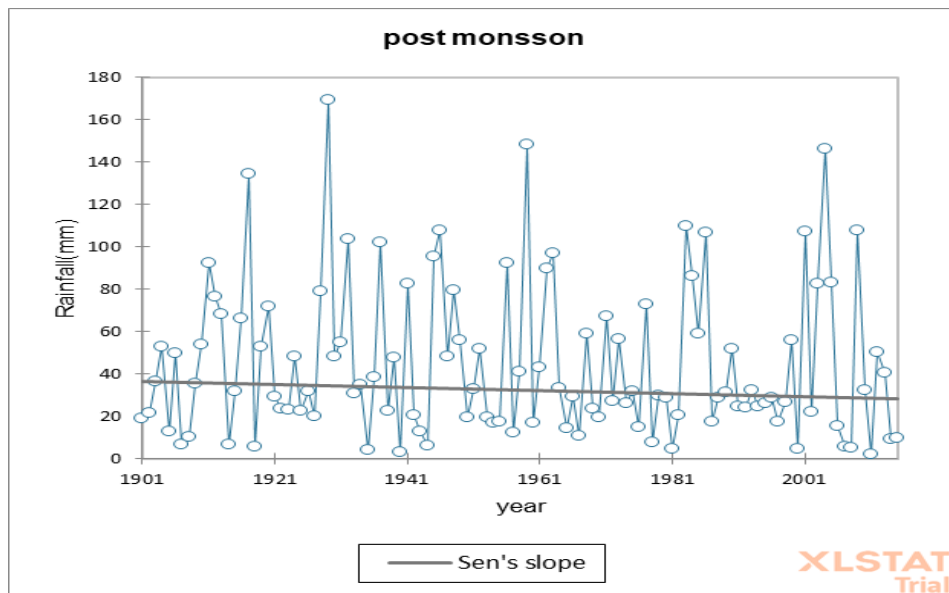


Fig 148. Trend Analysis of point 7

Point 8

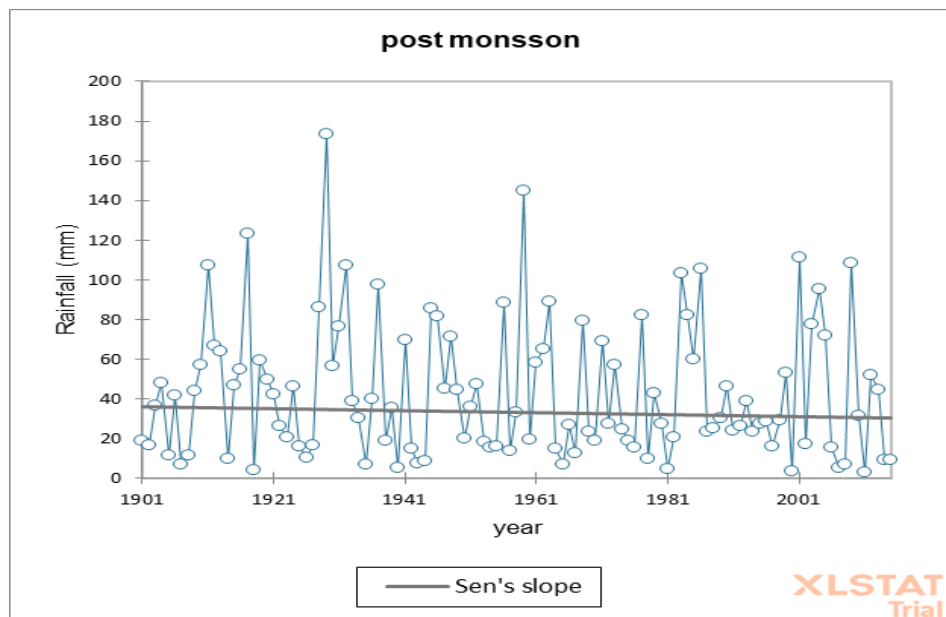


Fig 149. Trend Analysis of point 8

Result:

- Points P7, P8 are showing decreasing trend

Point 9

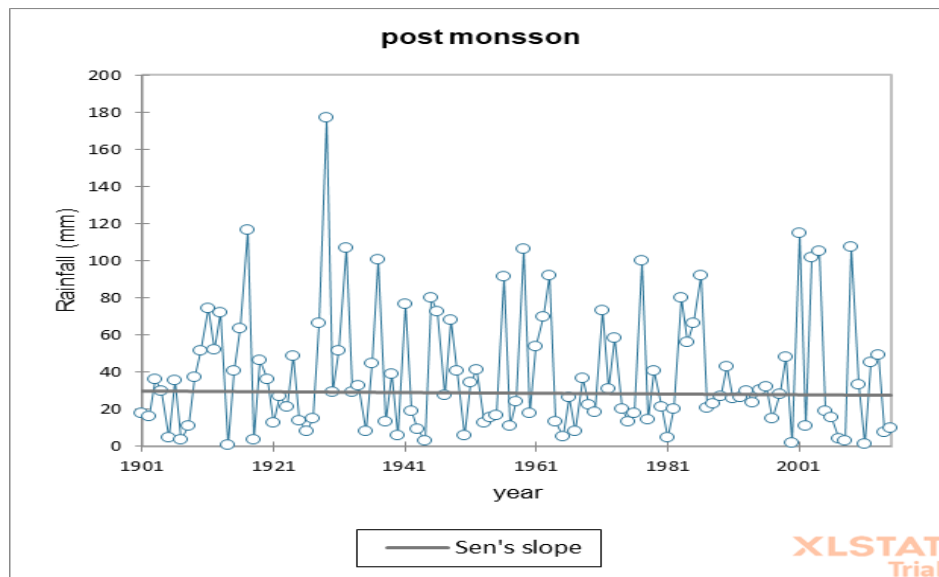


Fig 150. Trend Analysis of point 9

Point 10

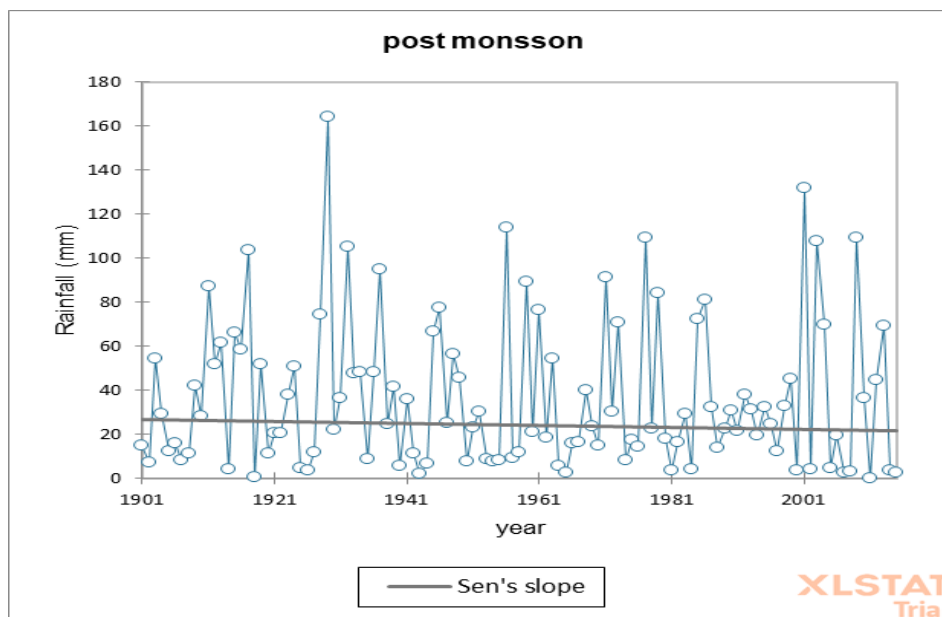


Fig 151. Trend Analysis of point 10

Result:

- Points P9, P10 are showing decreasing trend

Point 11

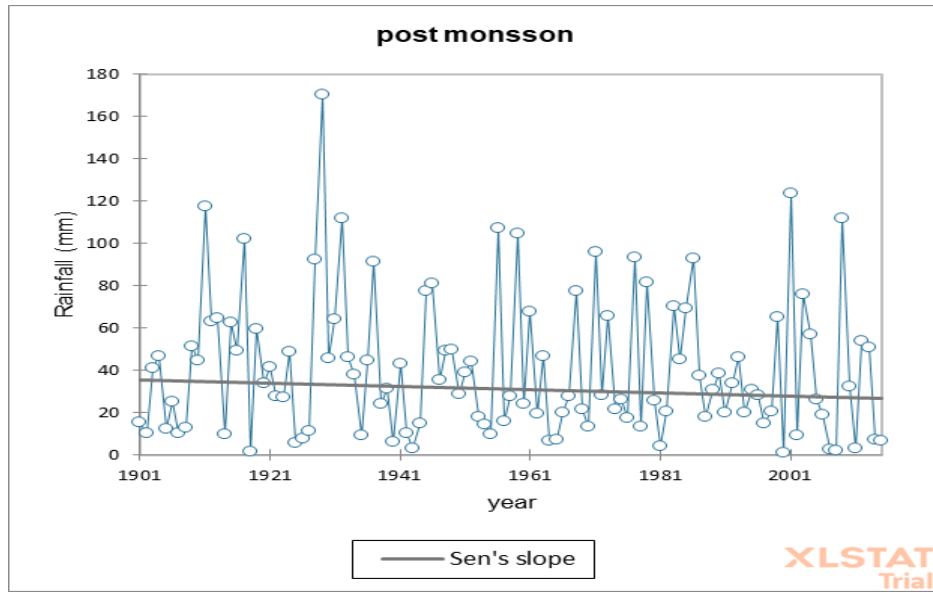


Fig 152. Trend Analysis of point 11

Point 12

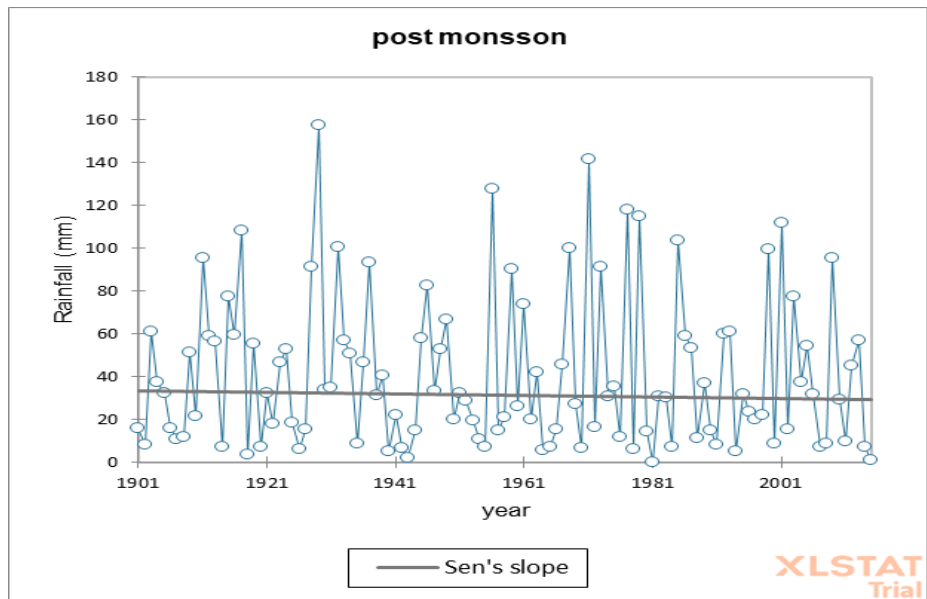


Fig 153. Trend Analysis of point 12

Result:

- Point P11 is showing no change in trend
- Point P12 is showing decreasing trend

Point 13

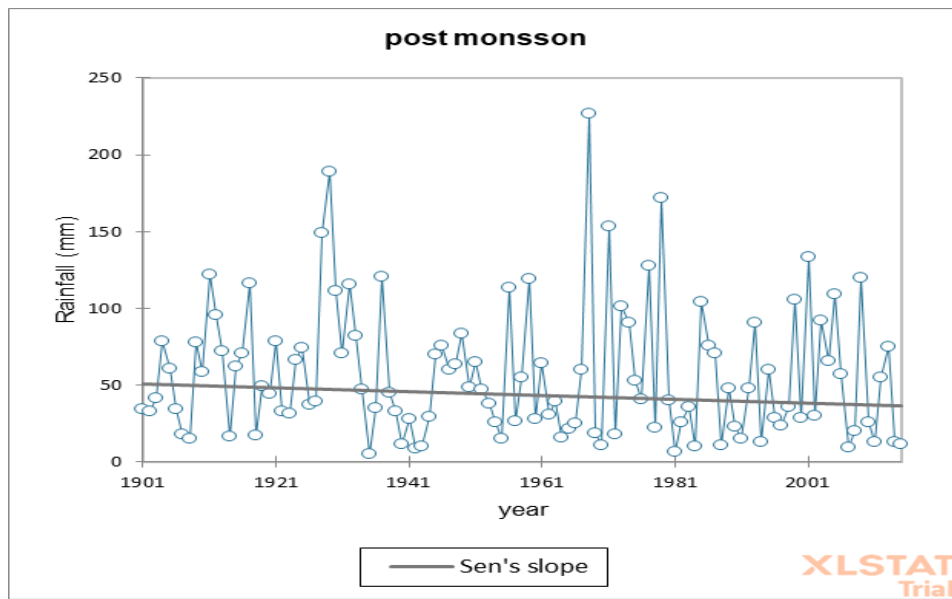


Fig 154. Trend Analysis of point 13

Point 14

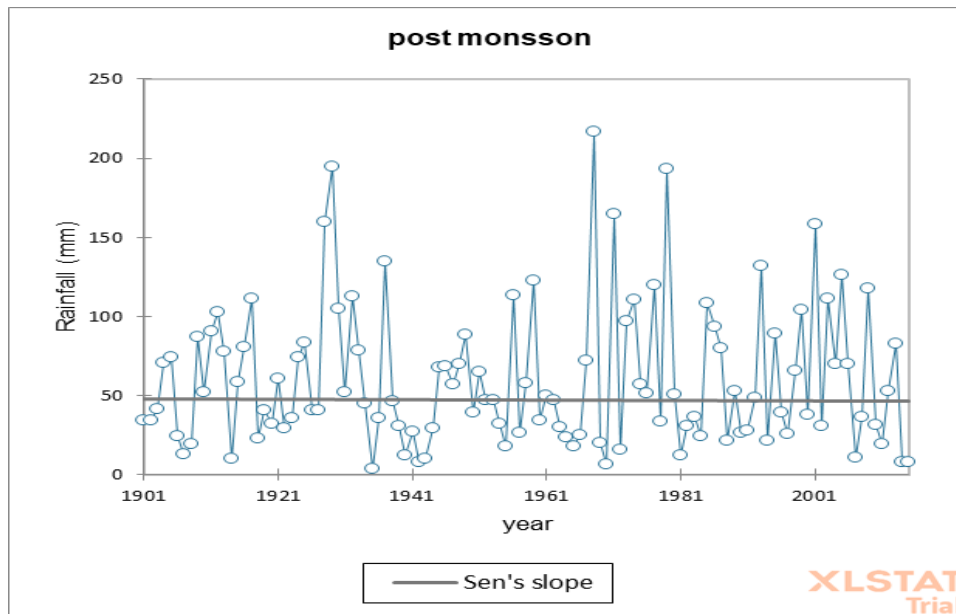


Fig 155. Trend Analysis of point 14

Result:

- Point P13 is showing decreasing trend
- Point P14 is not showing any change

Point 15

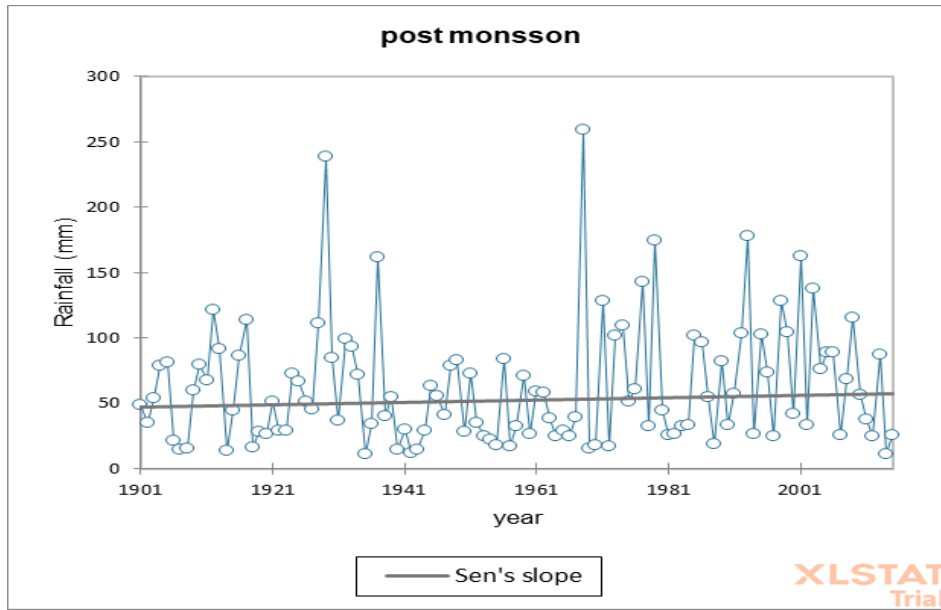


Fig 156. Trend Analysis of point 15

Point 16

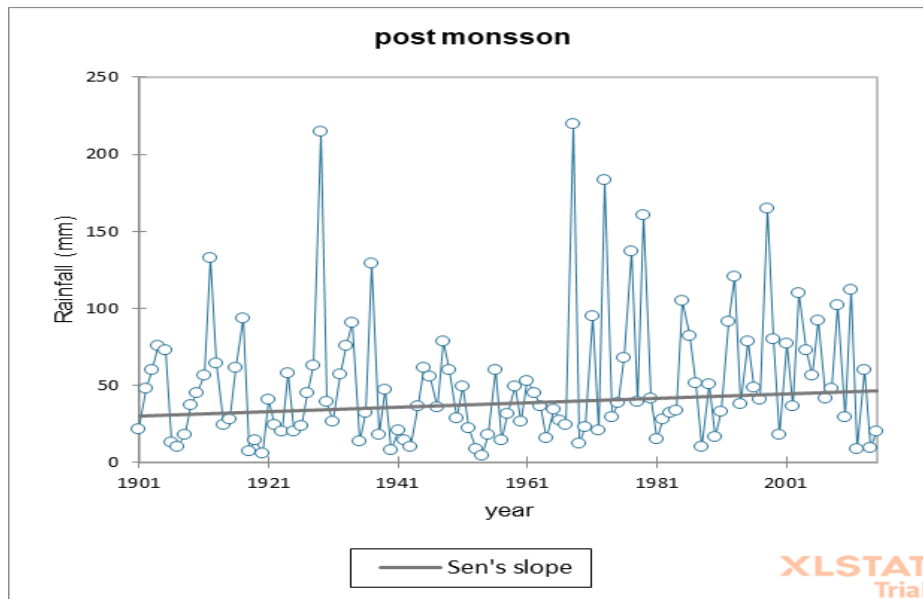


Fig 157. Trend Analysis of point 16

Result:

- Points P15, P16 are showing increasing trend

Point 17

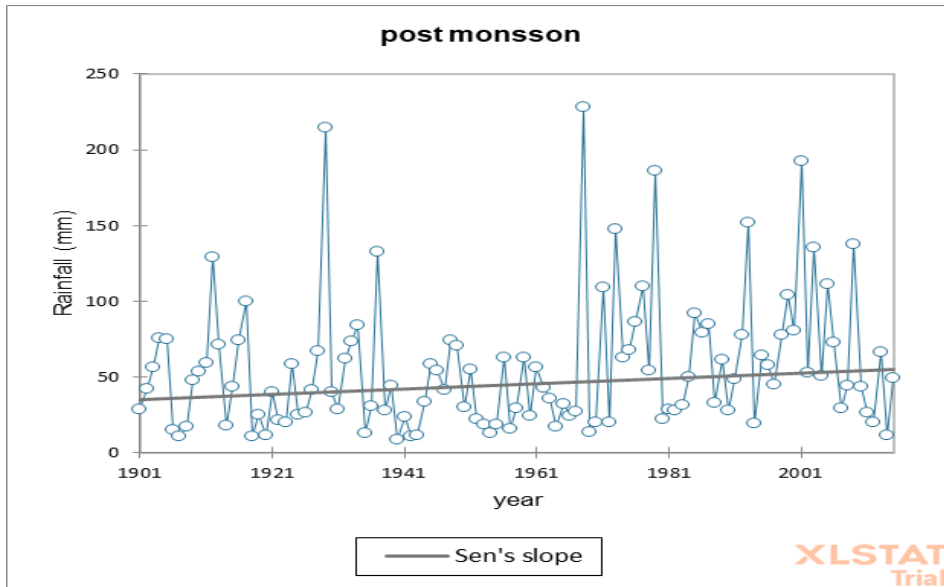


Fig 158. Trend Analysis of point 17

Point 18

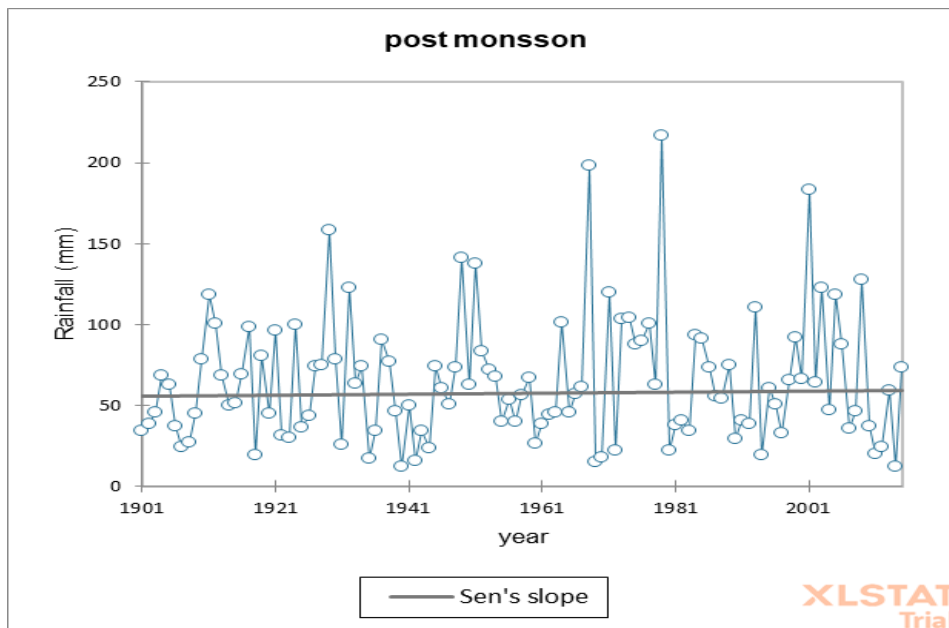


Fig 159. Trend Analysis of point 18

Result:

- Points P17, P18 are showing increasing trend

Point 19

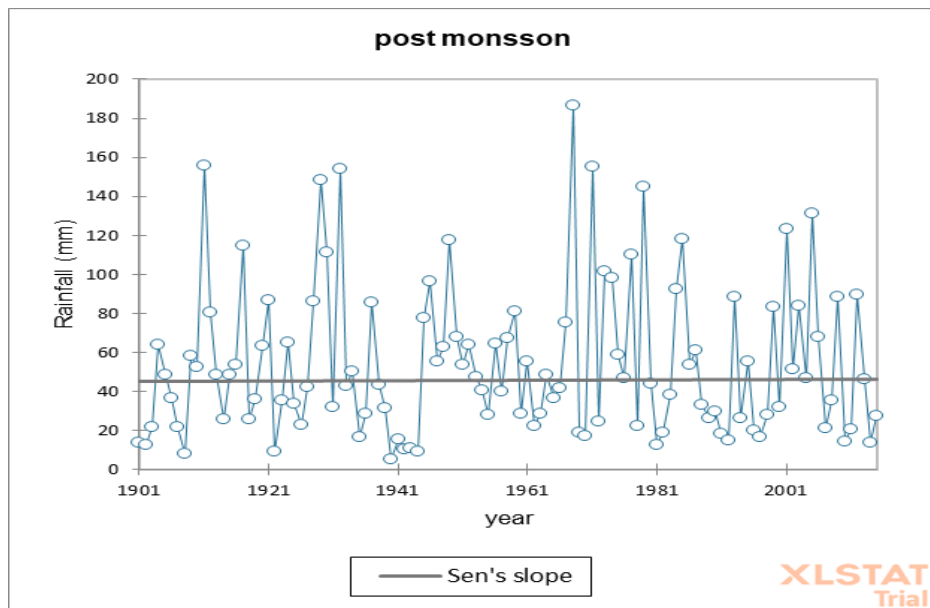


Fig 160. Trend Analysis of point 19

Point 20

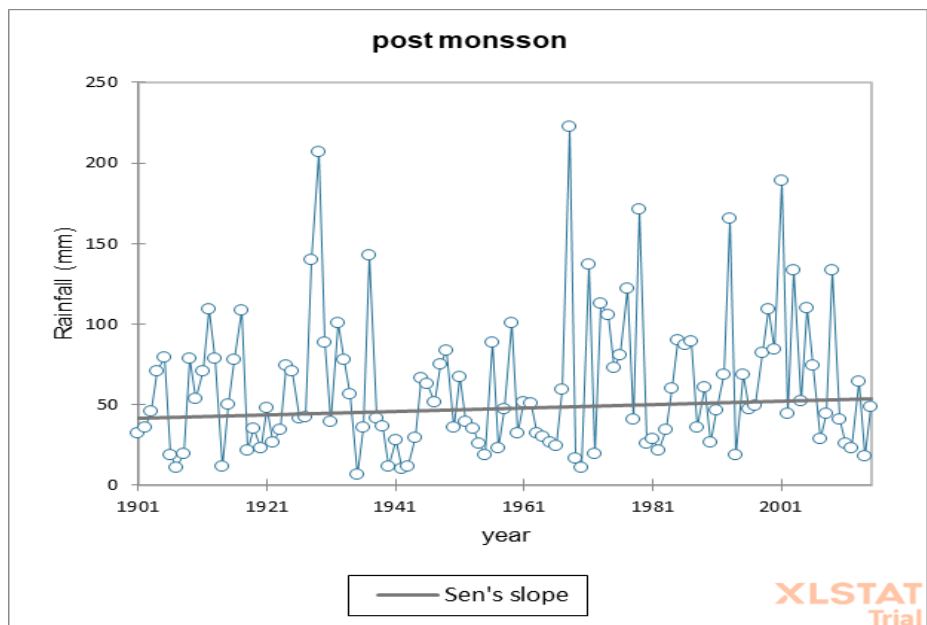


Fig 161. Trend Analysis of point 20

Result:

- Points P19, P20 are showing increasing trend

Point 21

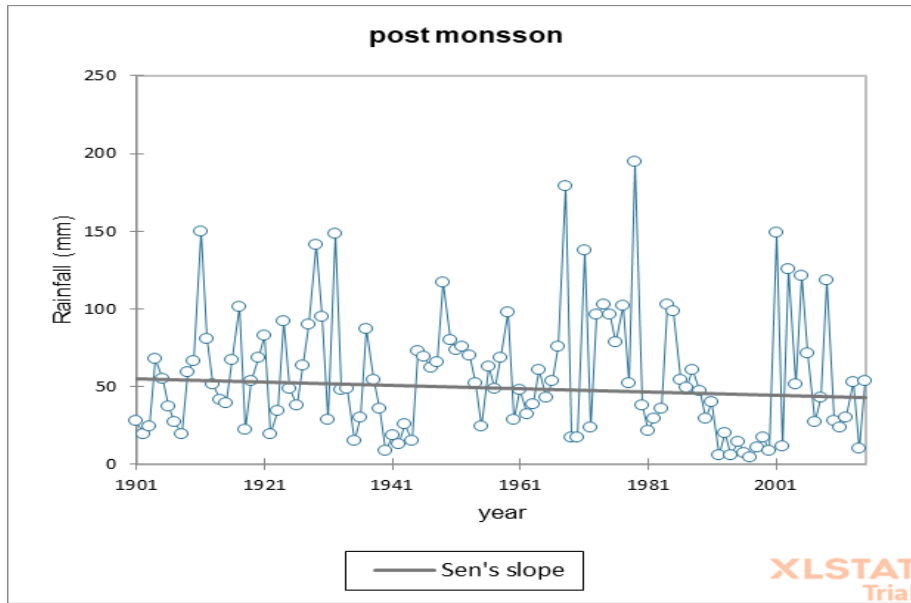


Fig 162. Trend Analysis of point 21

Point 22

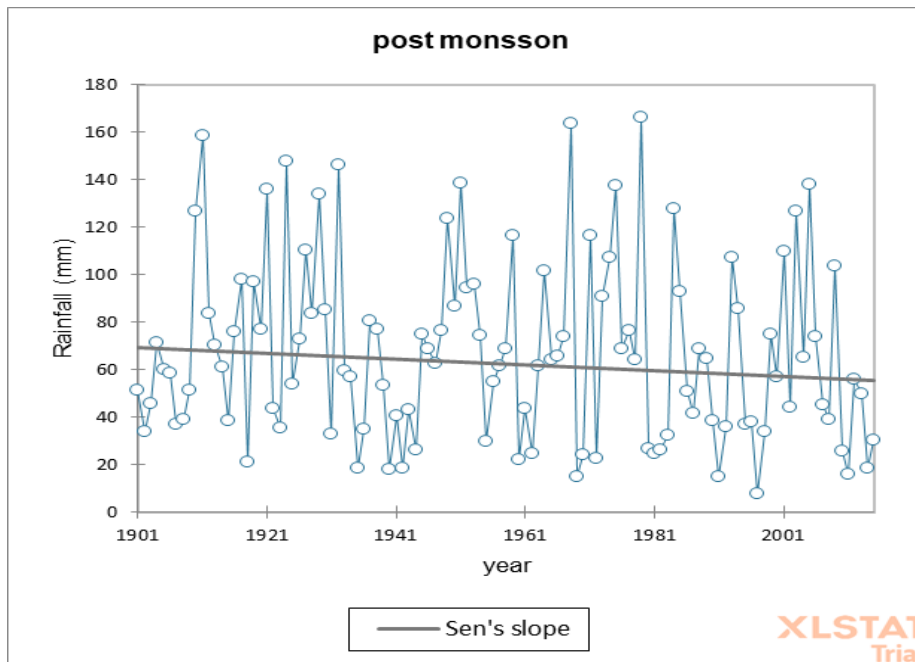


Fig 163. Trend Analysis of point 22

Result:

- Points P21, P22 are showing decreasing trend

Point 23

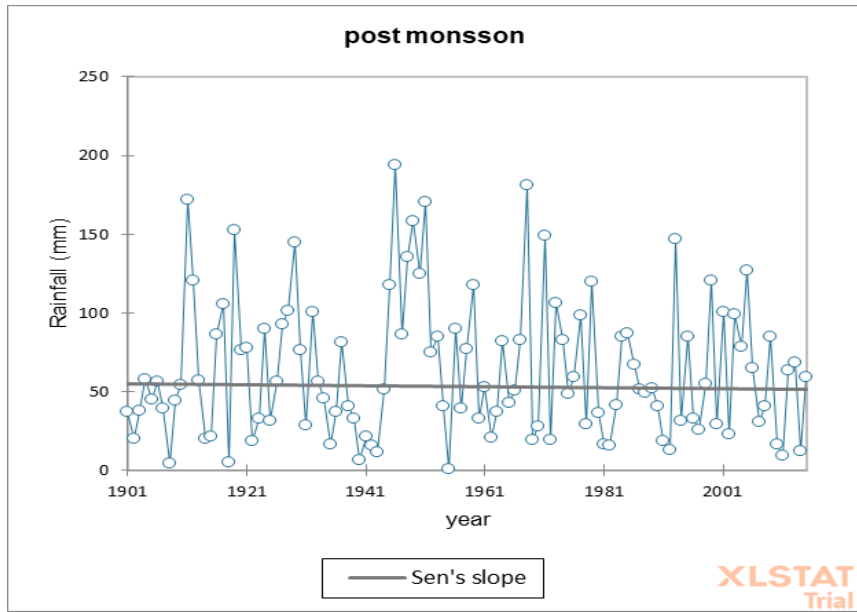


Fig 164. Trend Analysis of point 23

Point 24

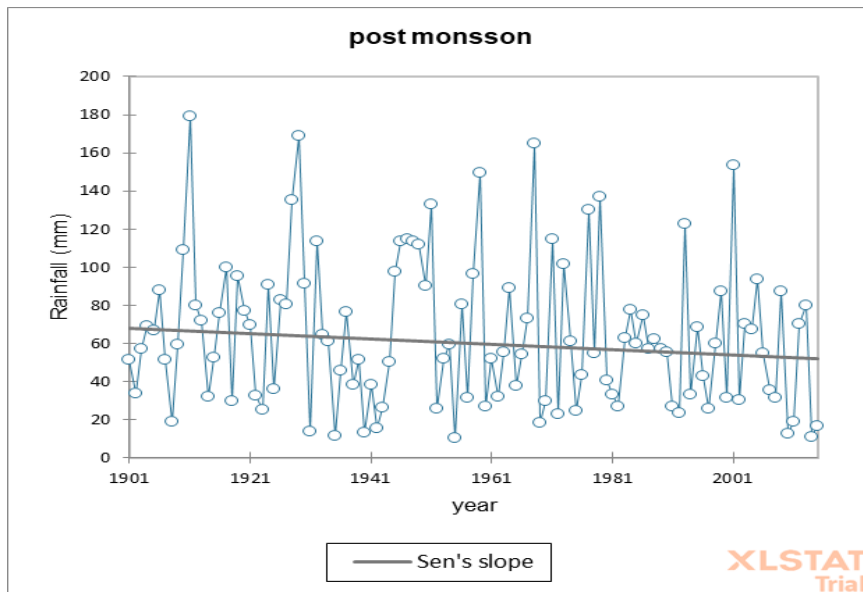


Fig 165. Trend Analysis of point 24

Result:

- Points P23, P24 are showing decreasing trend

Point 25

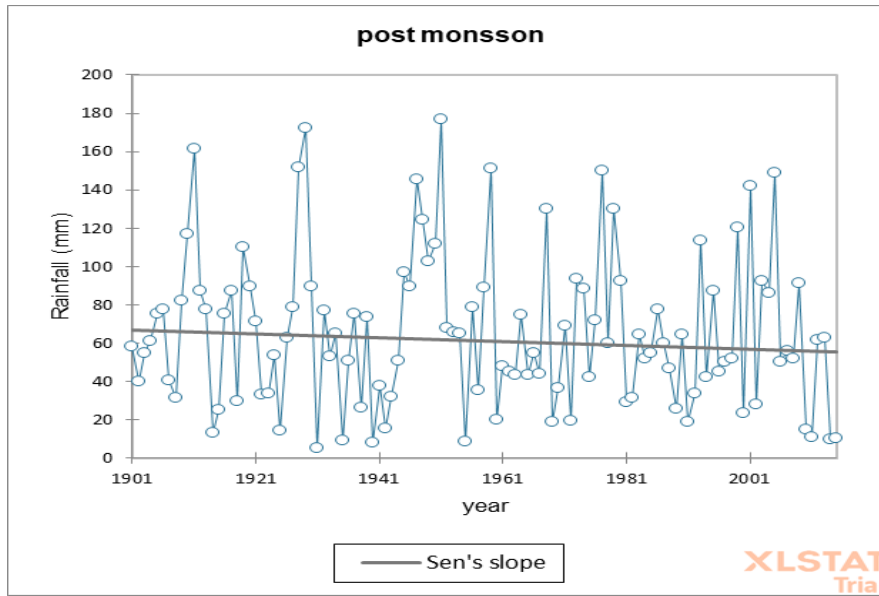


Fig 166. Trend Analysis of point 25

Point 26

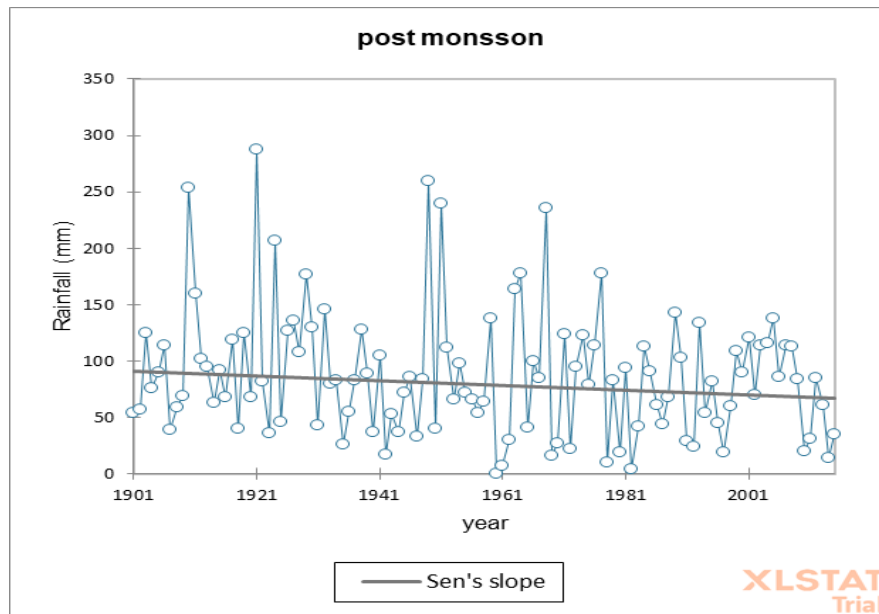


Fig 167. Trend Analysis of point 26

Result:

- Points P26, P26 are showing decreasing trend

Point 27

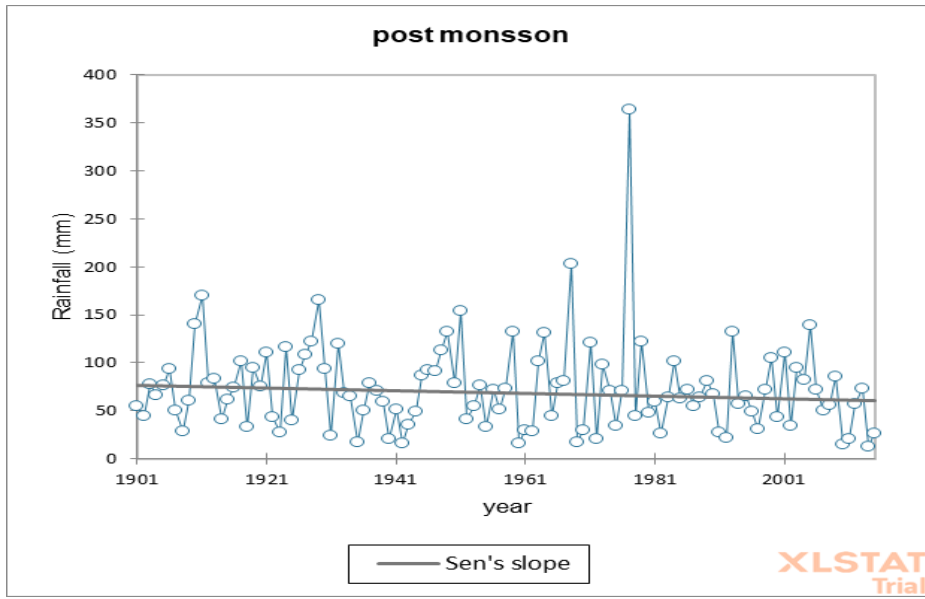


Fig 168. Trend Analysis of point 27

Point 28

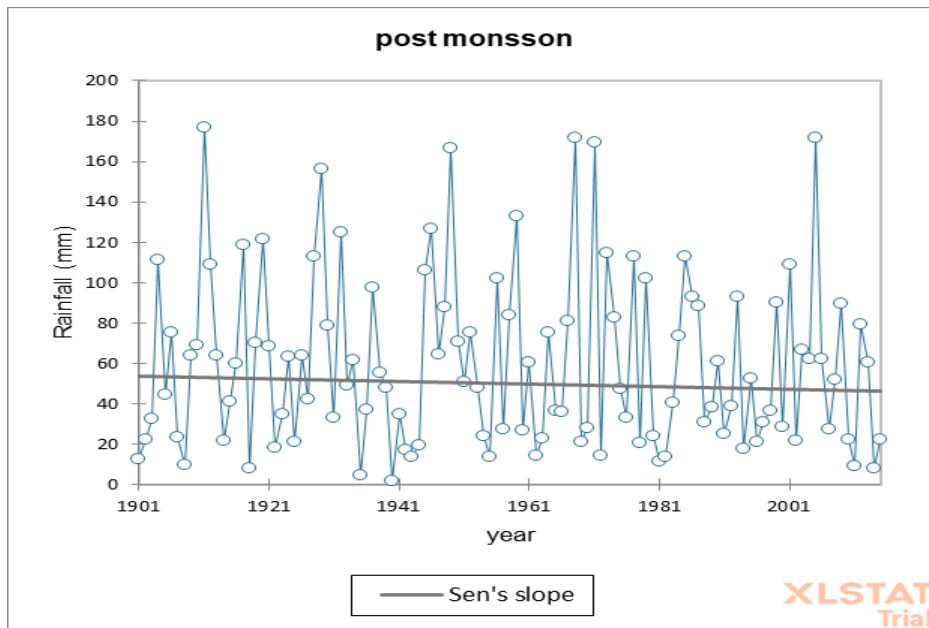


Fig 169. Trend Analysis of point 28

Result:

- Points P27, P28 are showing decreasing trend

Point 29

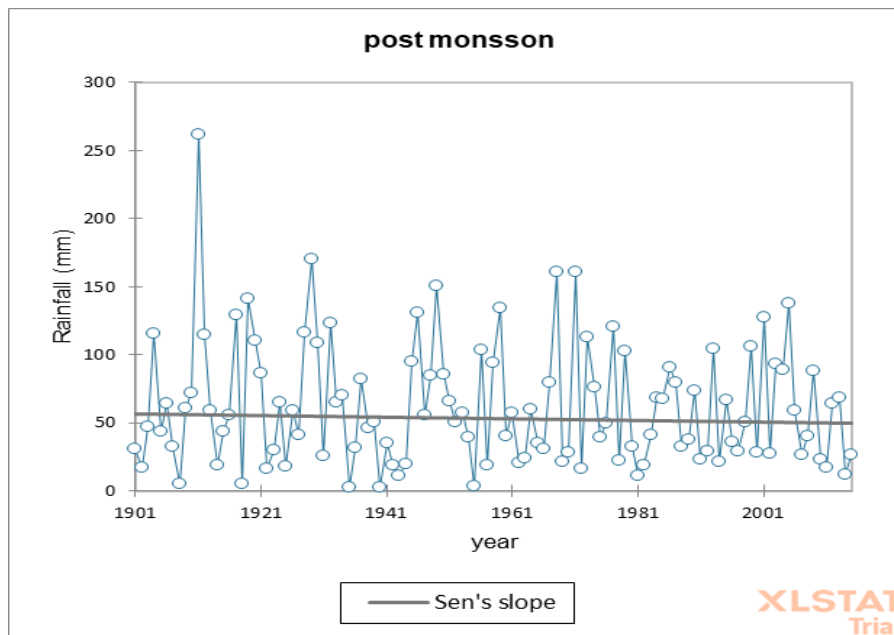


Fig 170. Trend Analysis of point 29

Point 30

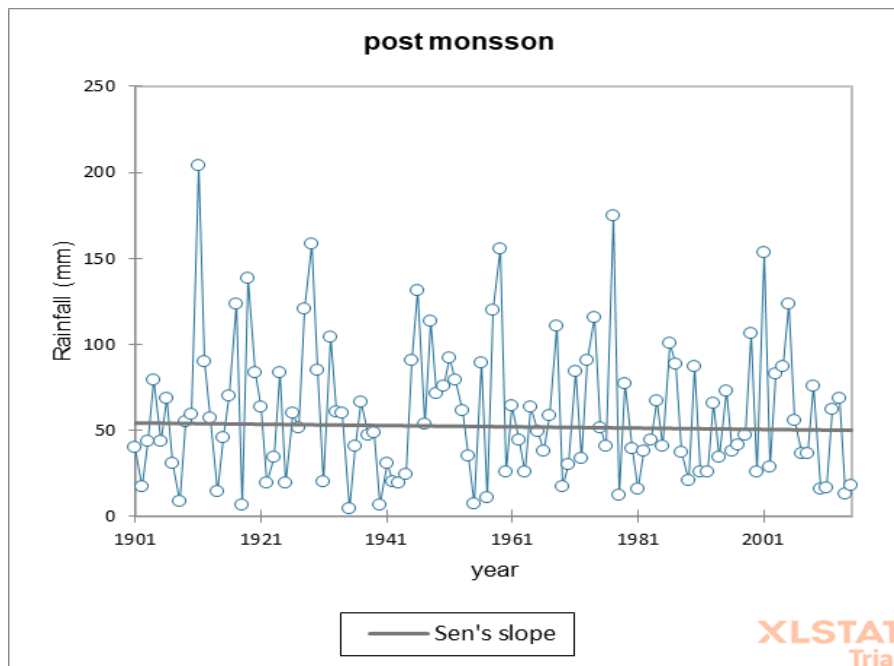


Fig 171. Trend Analysis of point 30

Result:

- Points P29, P30 are showing decreasing trend

Point 31

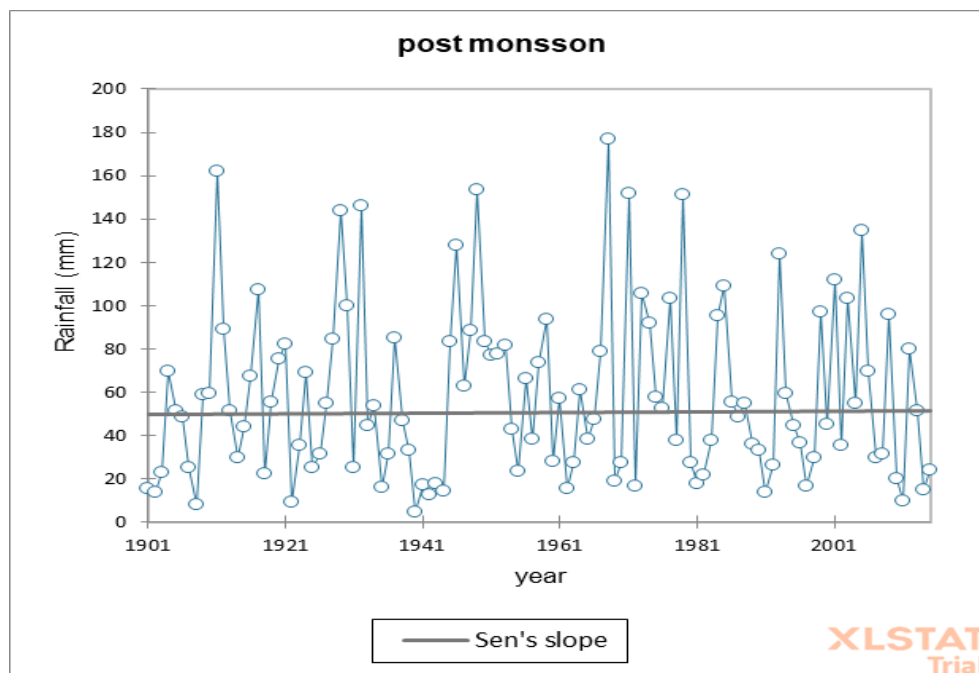


Fig 172. Trend Analysis of point 31

Result:

- Point P31 is showing increasing trend

Discussion

As observed from the graphs of Sen slope, generally Post-monsoon season is following a decreasing trend of rainfall. Decreasing trend can be seen on some stations such as P7, P8, P10, P11, P13, P21, P22, P24, P25, P26, P27, P28.

And increasing trend can be seen in some stations such as P16, P17, P20.

Rest of the stations are showing no change in the trend.

ANNUAL

Point 1

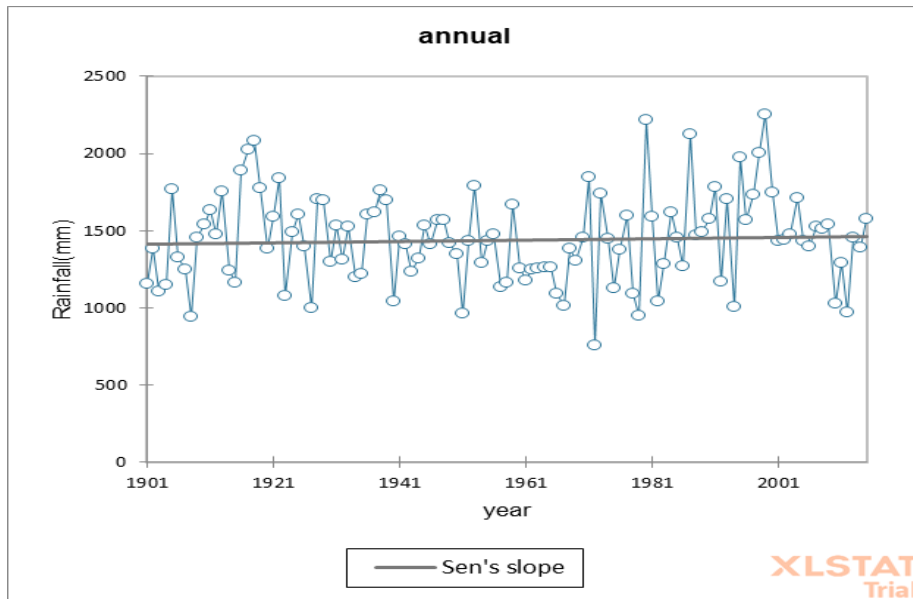


Fig 173. Trend Analysis of point 1

Point 2

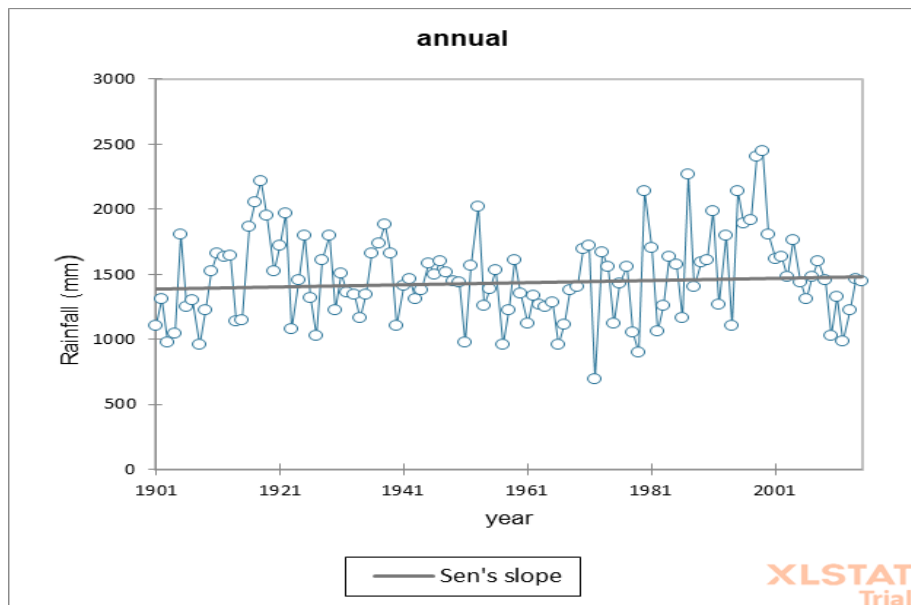


Fig 174. Trend Analysis of point 2

Result:

- Points P1, P2 are showing increasing trend

Point 3

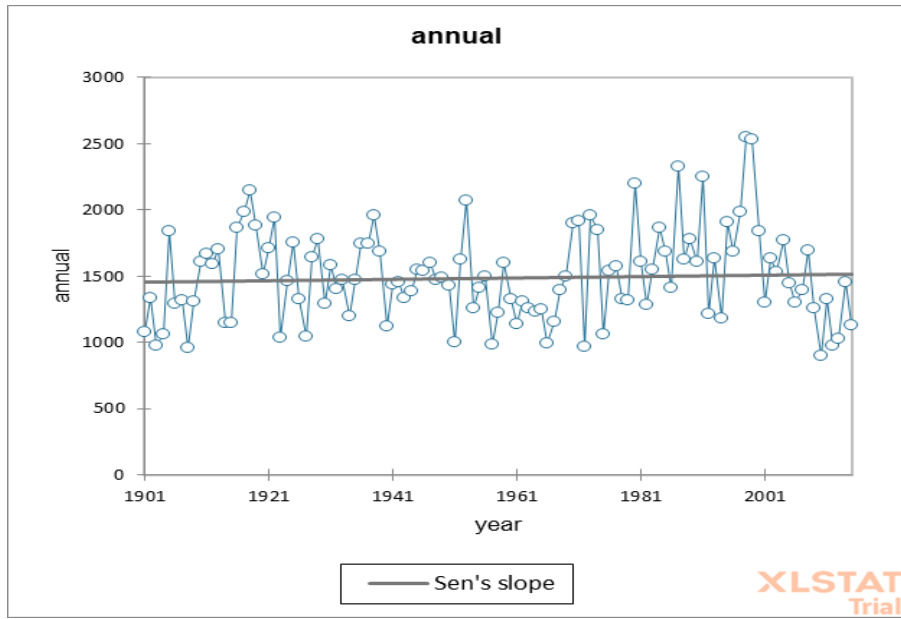


Fig 175. Trend Analysis of point 3

Point 4

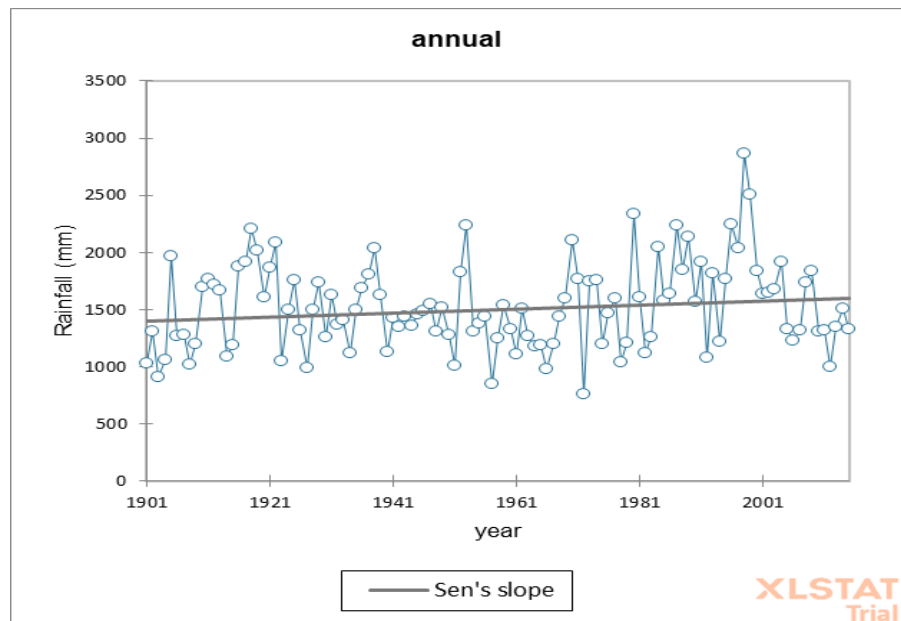


Fig 176. Trend Analysis of point 4

Result:

- Points P3, P4 are showing increasing trend

Point 5

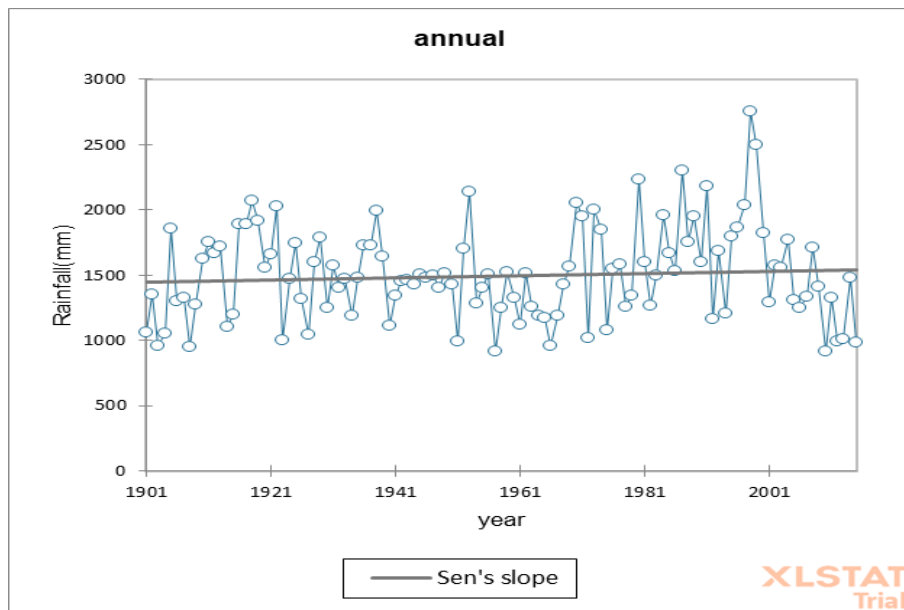


Fig 177. Trend Analysis of point 5

Point 6

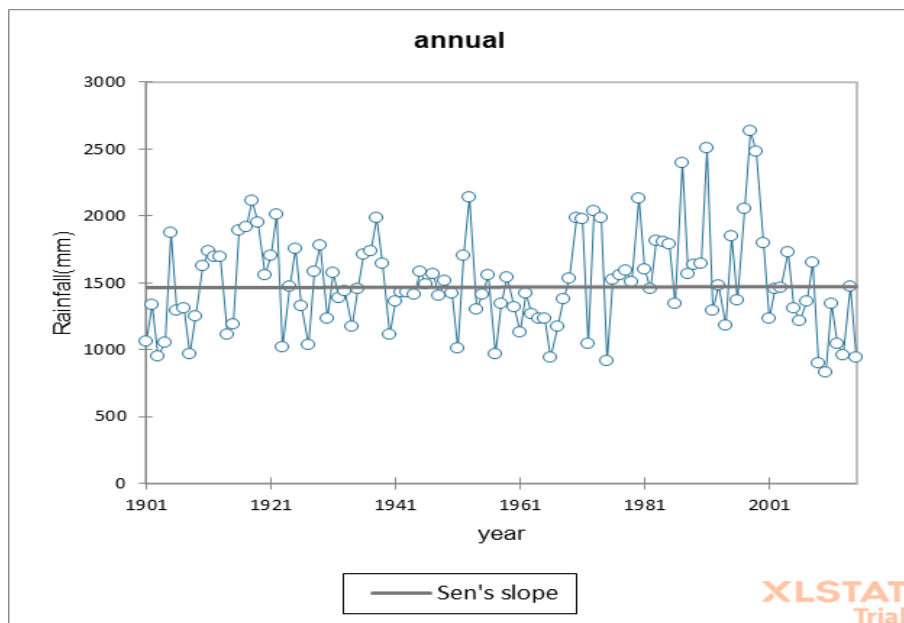


Fig 178. Trend Analysis of point 6

Result:

- Points P5, P6 are showing increasing trend

Point 7

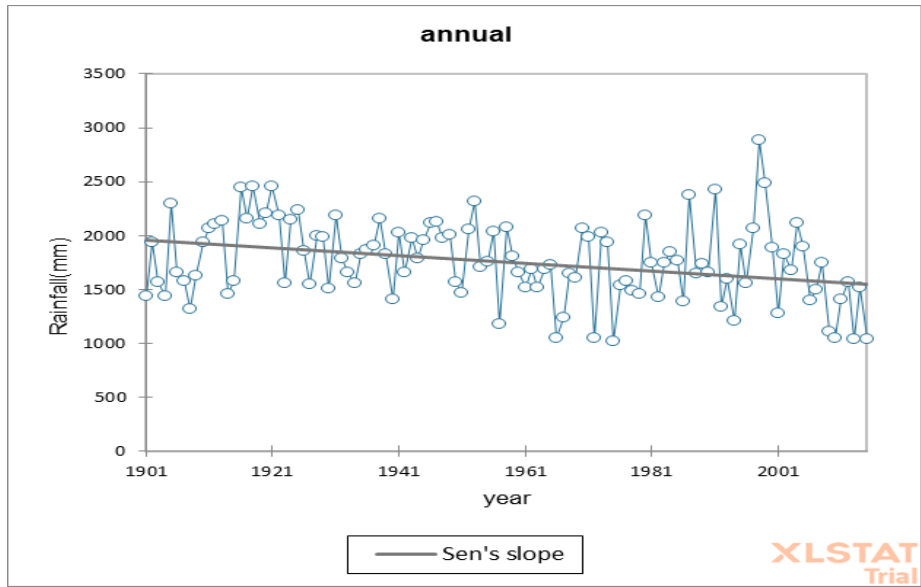


Fig 179. Trend Analysis of point 7

Point 8

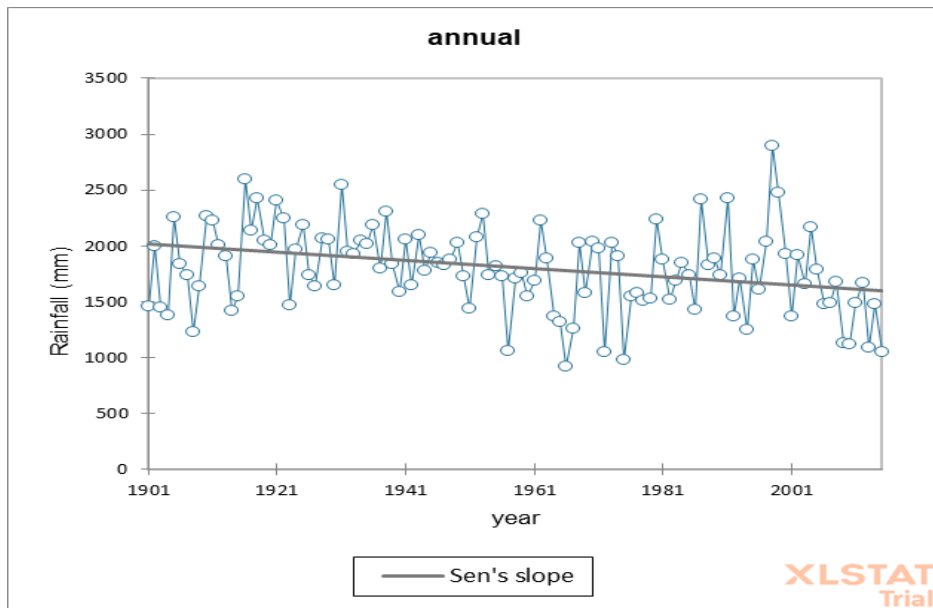


Fig 180. Trend Analysis of point 8

Result:

- Points P7, P8 are showing decreasing trend

Point 9

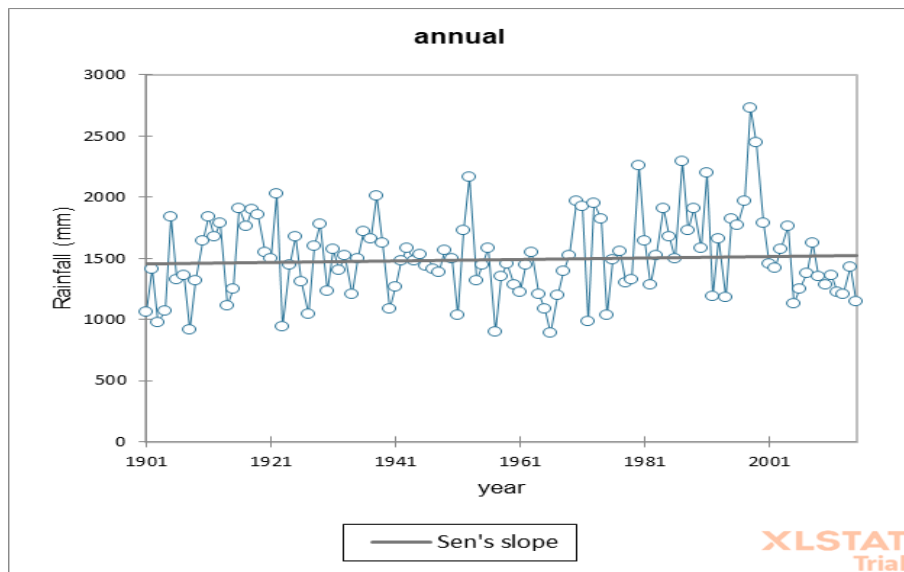


Fig 181. Trend Analysis of point 9

Point 10

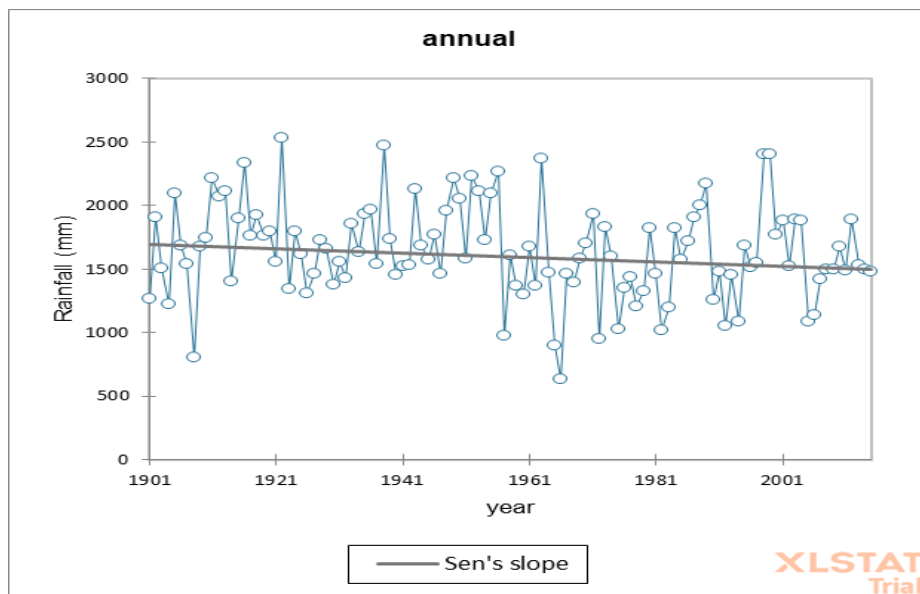


Fig 182. Trend Analysis of point 10

Result:

- Point P9 is showing increasing trend
- Point P10 is showing decreasing trend

Point 11

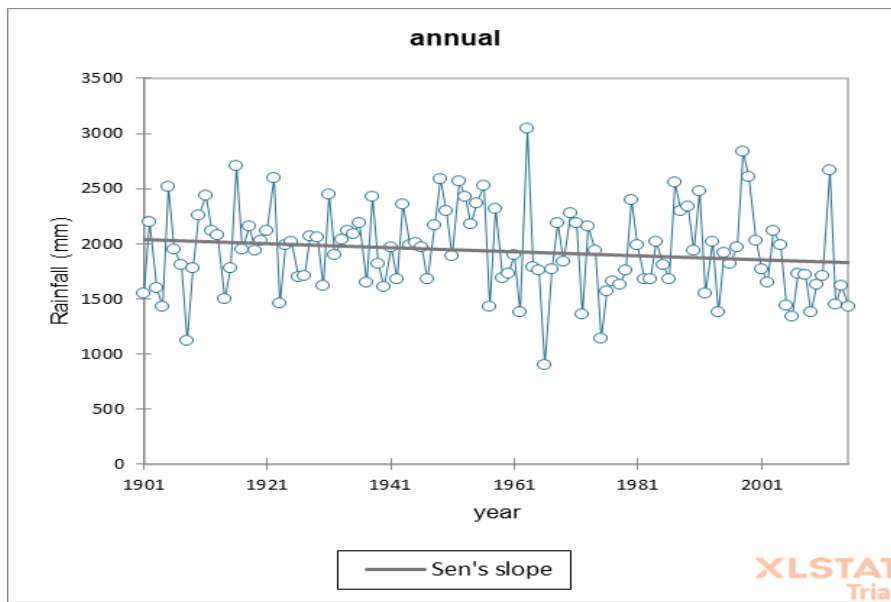


Fig 183. Trend Analysis of point 11

Point 12

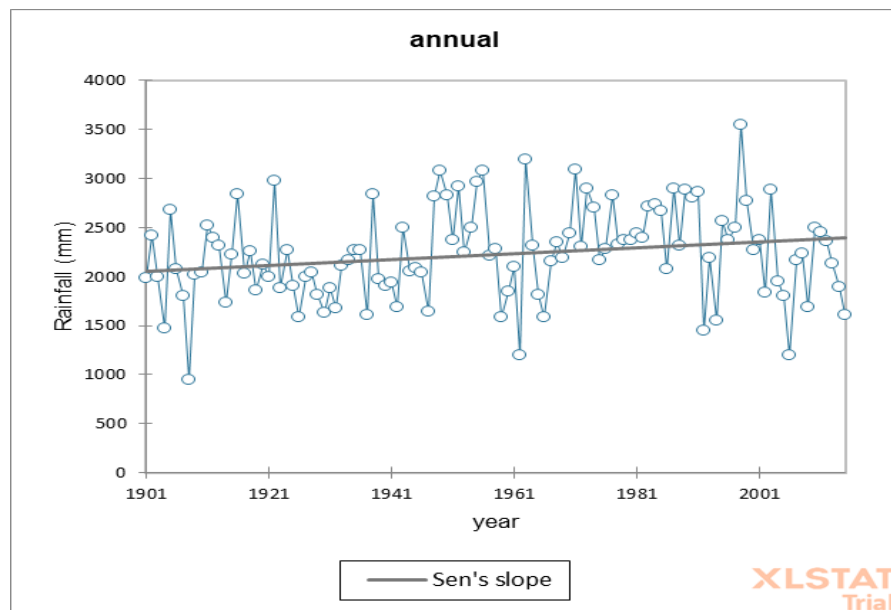


Fig 184. Trend Analysis of point 12

Result:

- Point P11 is showing decreasing trend
- Point P12 is showing increasing trend

Point 13

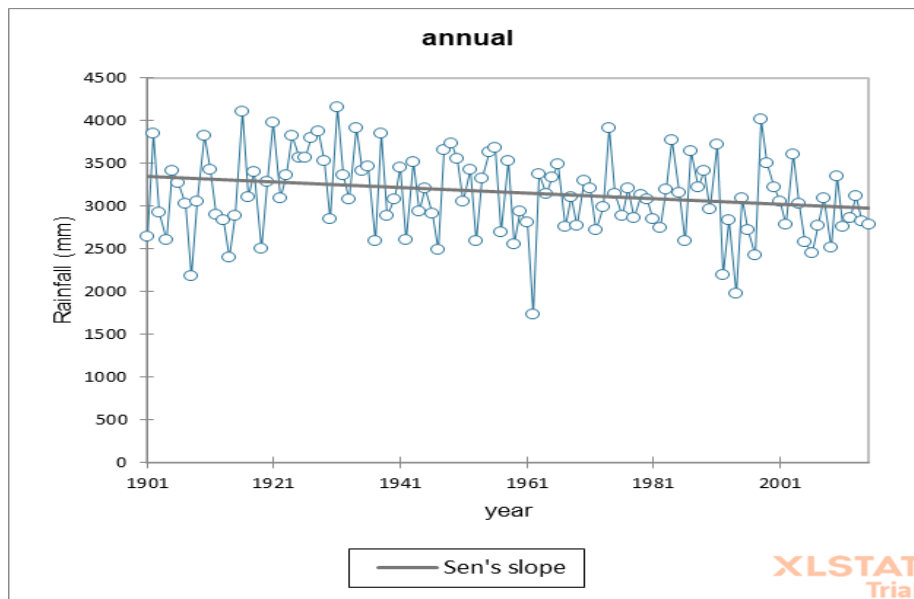


Fig 185. Trend Analysis of point 13

Point 14

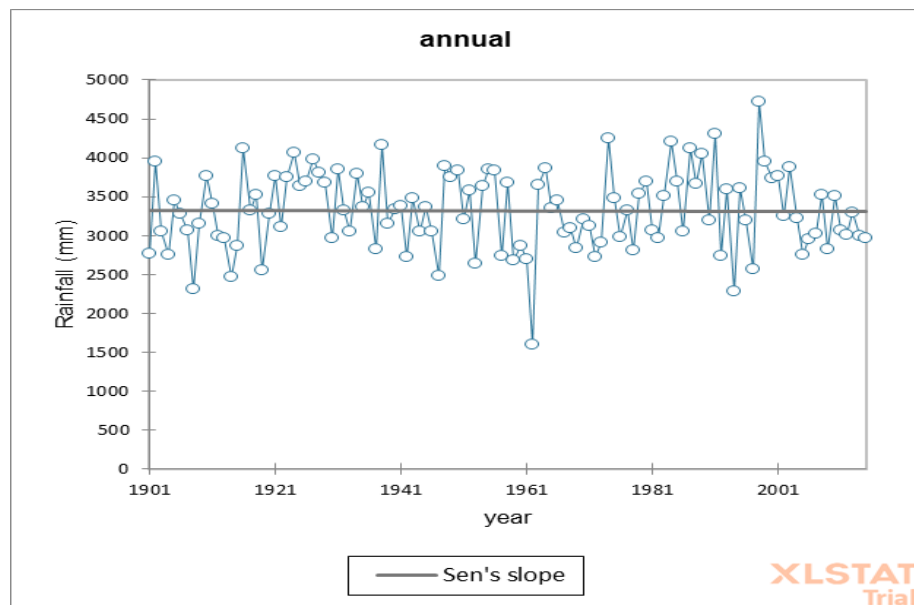


Fig 186. Trend Analysis of point 14

Result:

- Point P13 is showing decreasing trend
- Point P14 is showing increasing trend

Point 15

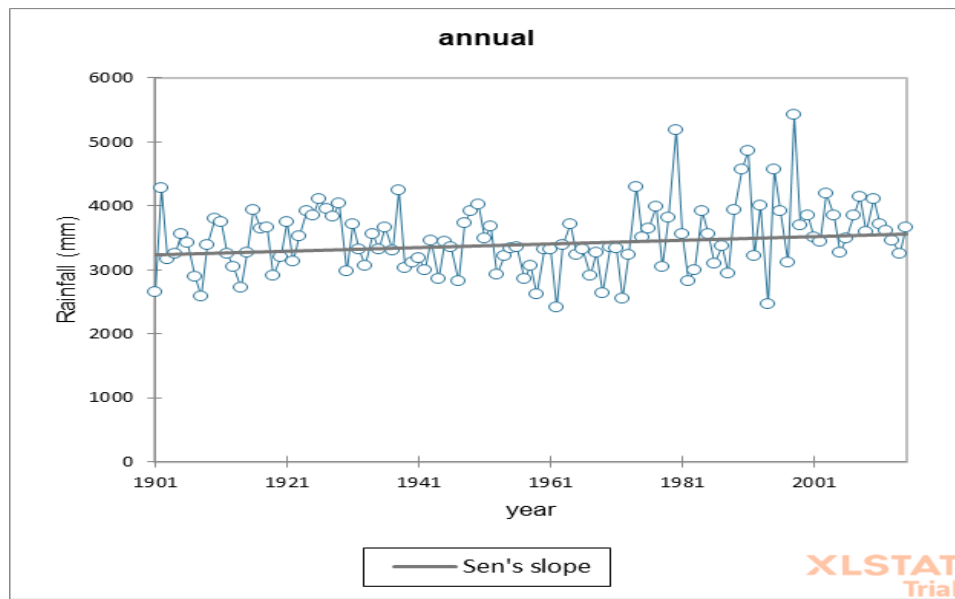


Fig 187. Trend Analysis of point 15

Point 16

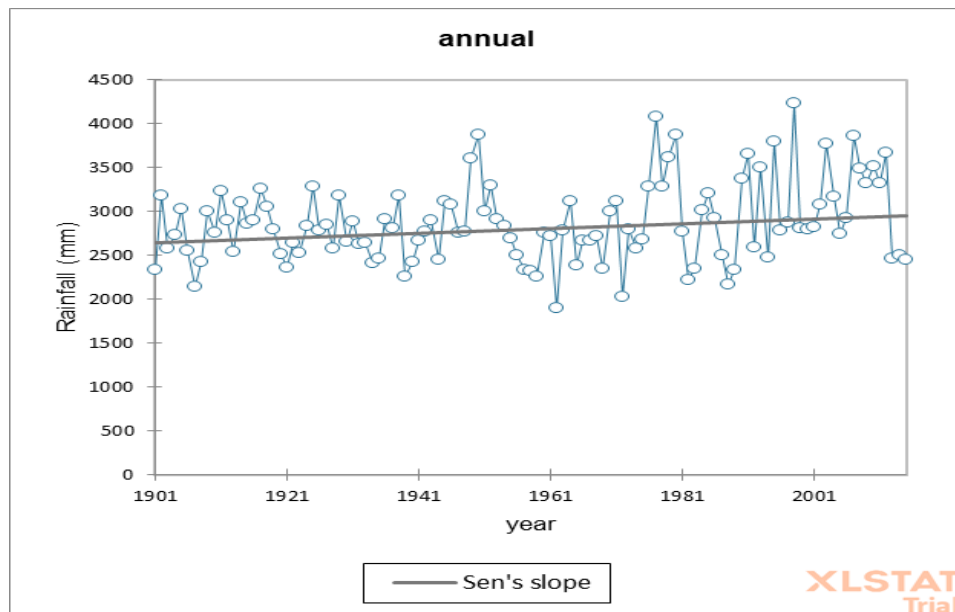


Fig 188. Trend Analysis of point 16

Result:

- Points P15, P16 are showing increasing trend

Point 17

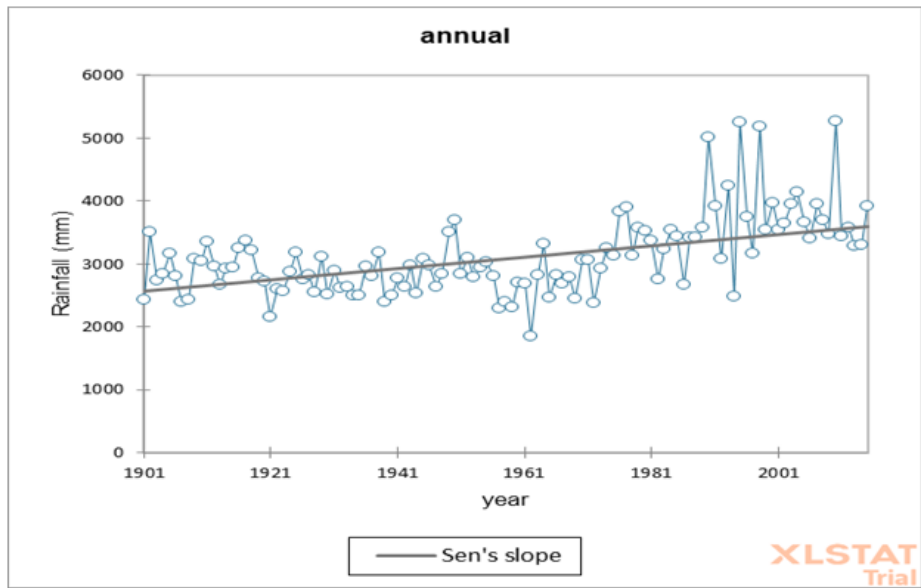


Fig 189. Trend Analysis of point 17

Point 18

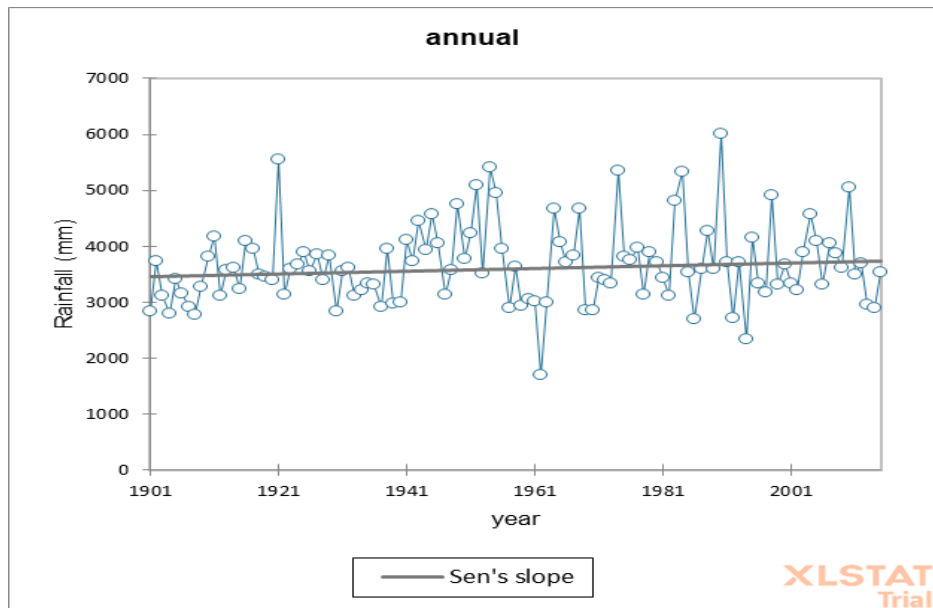


Fig 190. Trend Analysis of point 18

Result:

- Points P17, P18 are showing increasing trend

Point 19

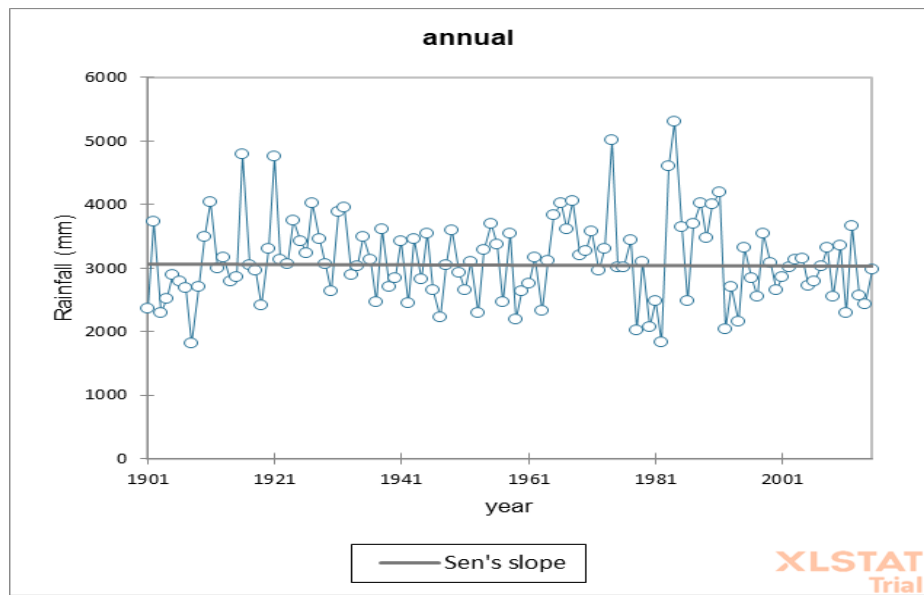


Fig 191. Trend Analysis of point 19

Point 20

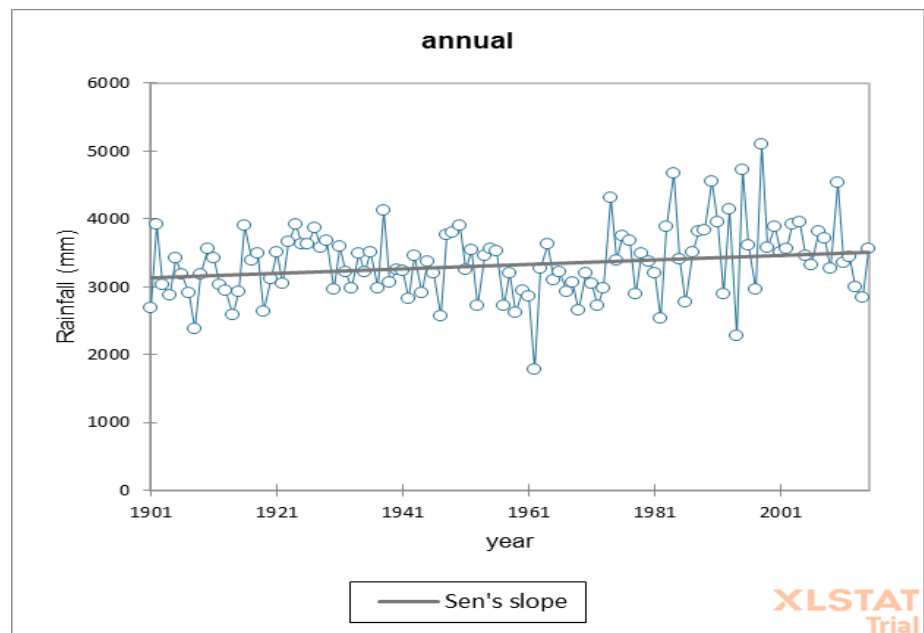


Fig 192. Trend Analysis of point 20

Result:

- Point P19 is showing decreasing trend
- Point P20 is showing increasing trend

Point 21

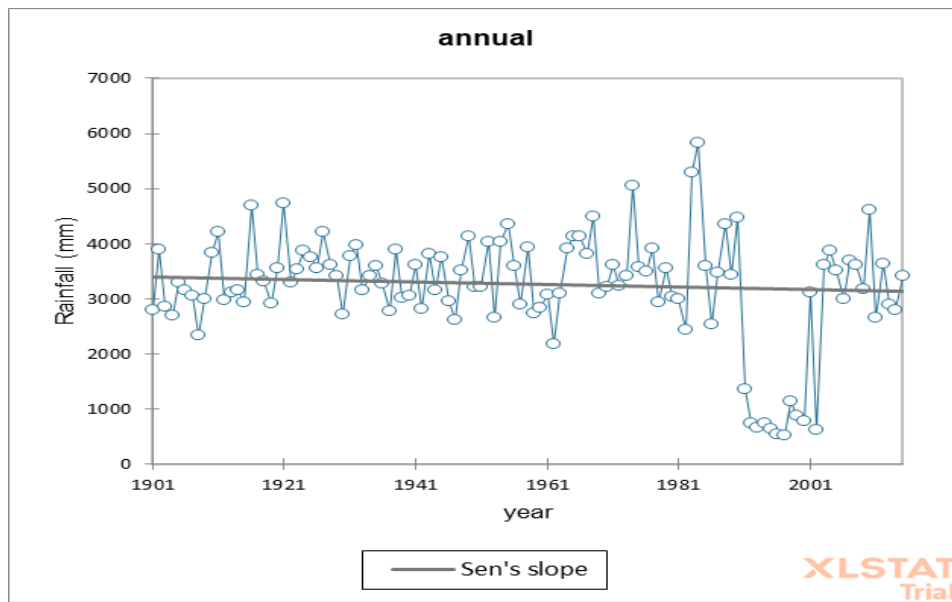


Fig 193. Trend Analysis of point 21

Point 22

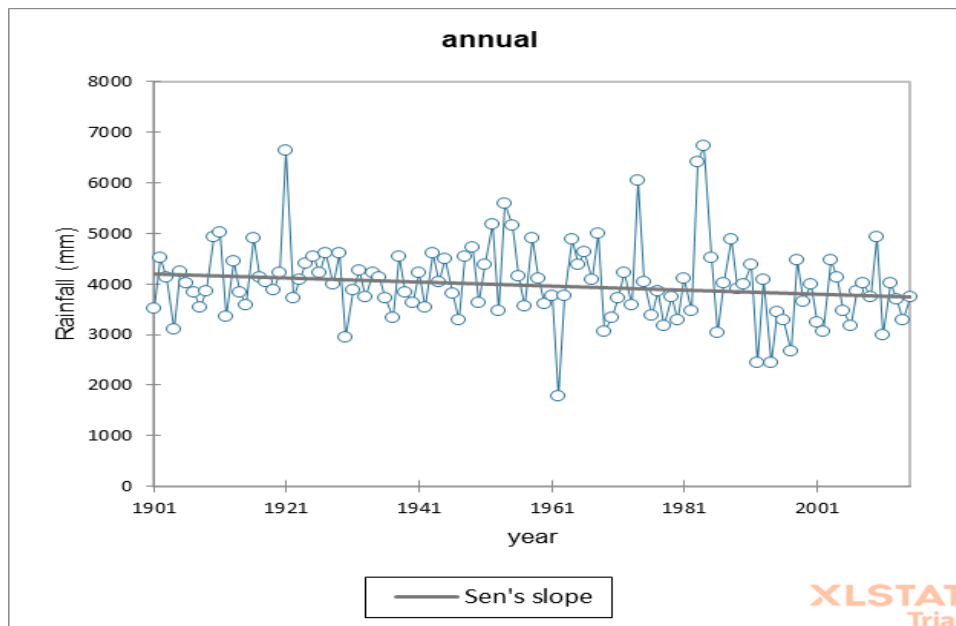


Fig 194. Trend Analysis of point 22

Result:

- Points P21, P22 are showing decreasing trend

Point 23

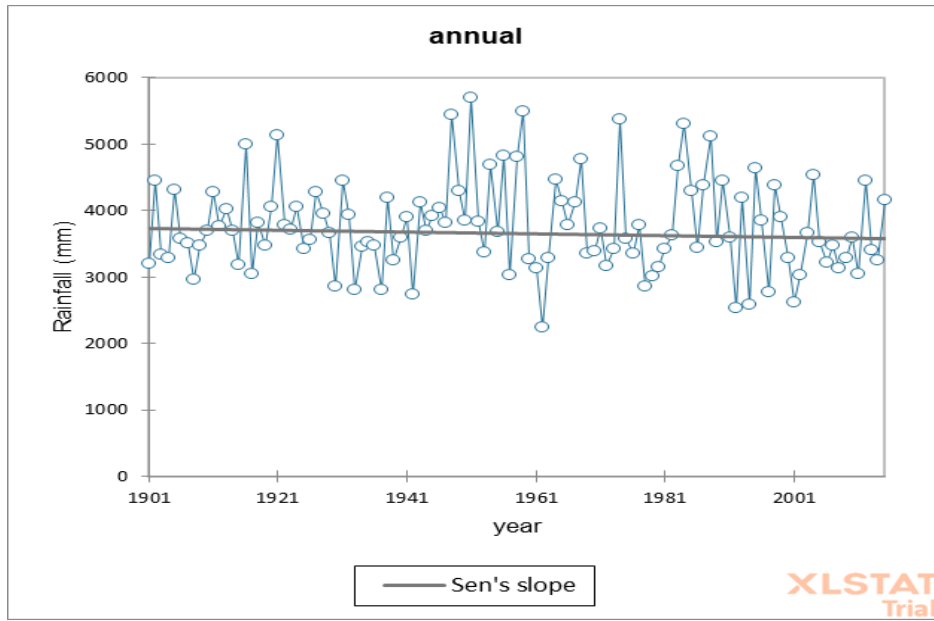


Fig 195. Trend Analysis of point 23

Point 24

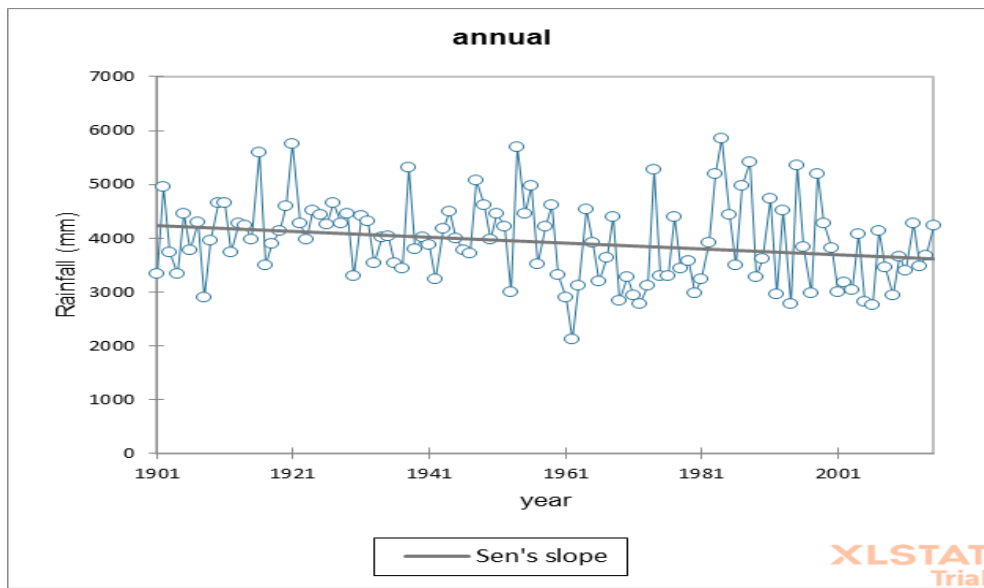


Fig 196. Trend Analysis of point 24

Result:

- Points P23, P24 are showing decreasing trend

Point 25

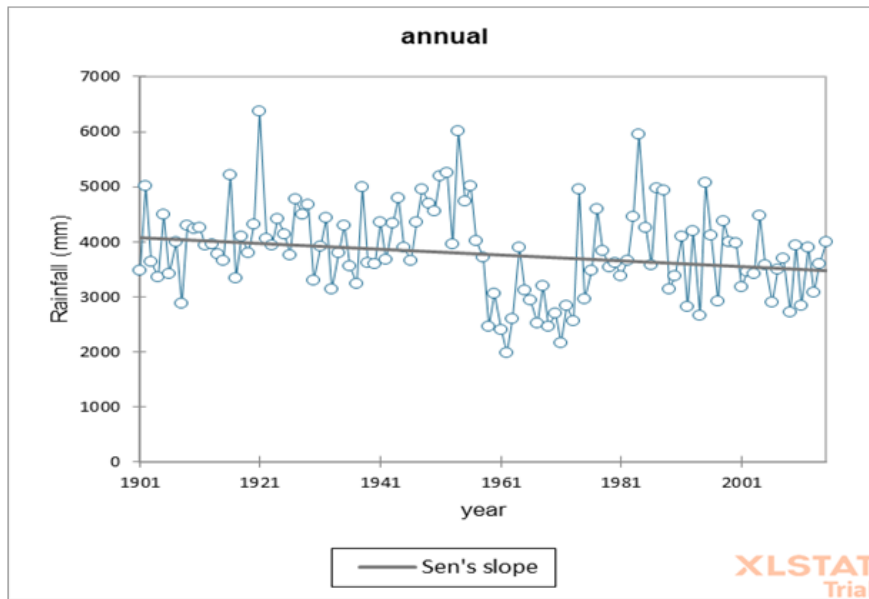


Fig 197. Trend Analysis of point 25

Point 26

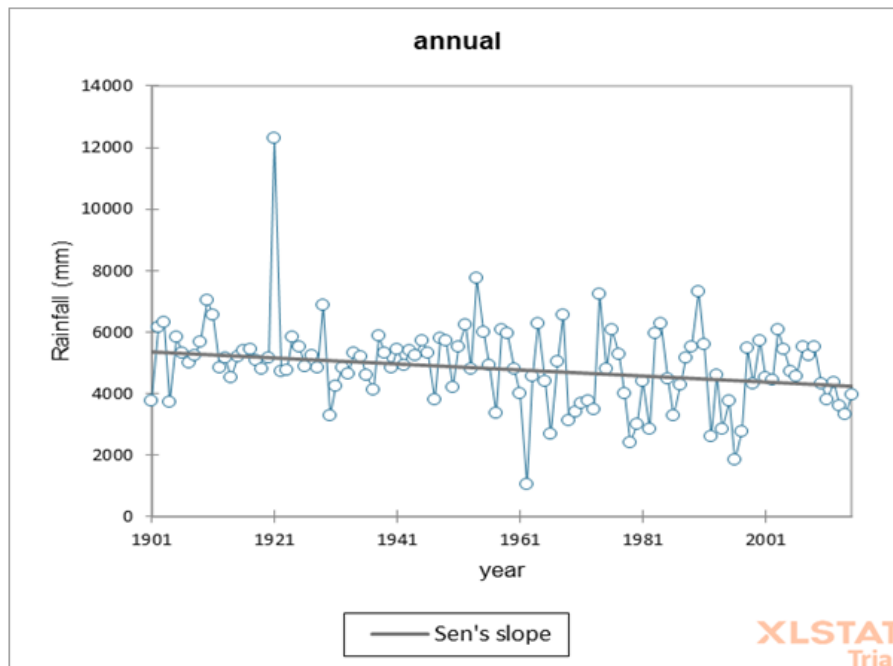


Fig 198. Trend Analysis of point 26

Result: Points P25, P26 are showing decreasing trend

Point 27

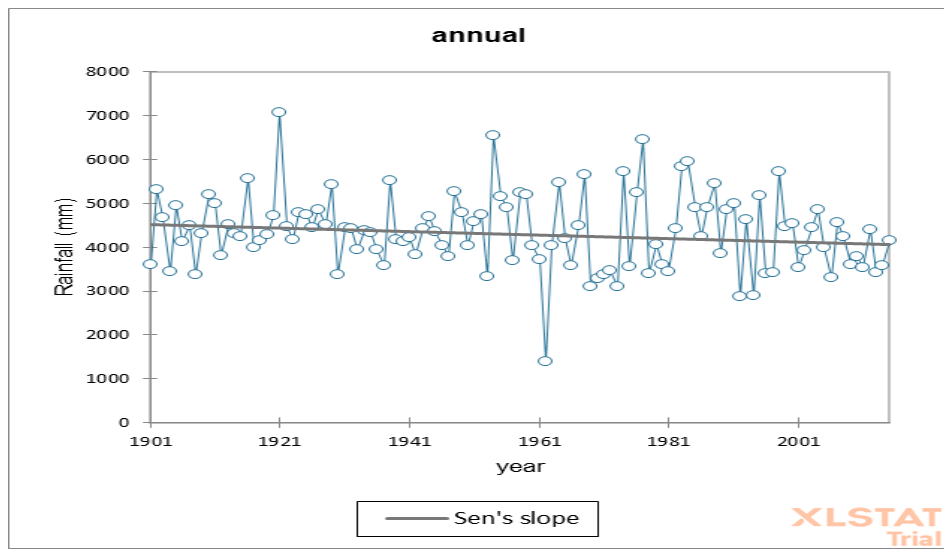


Fig 199. Trend Analysis of point 27

Point 28

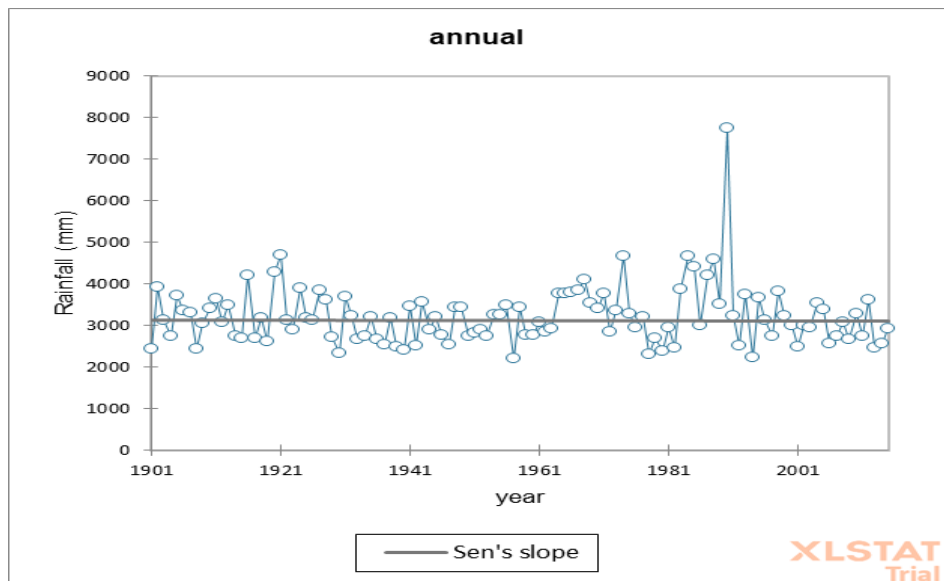


Fig 200. Trend Analysis of point 28

Result:

- Point P27 is showing decreasing trend
- Point P28 is showing increasing trend

Point 29

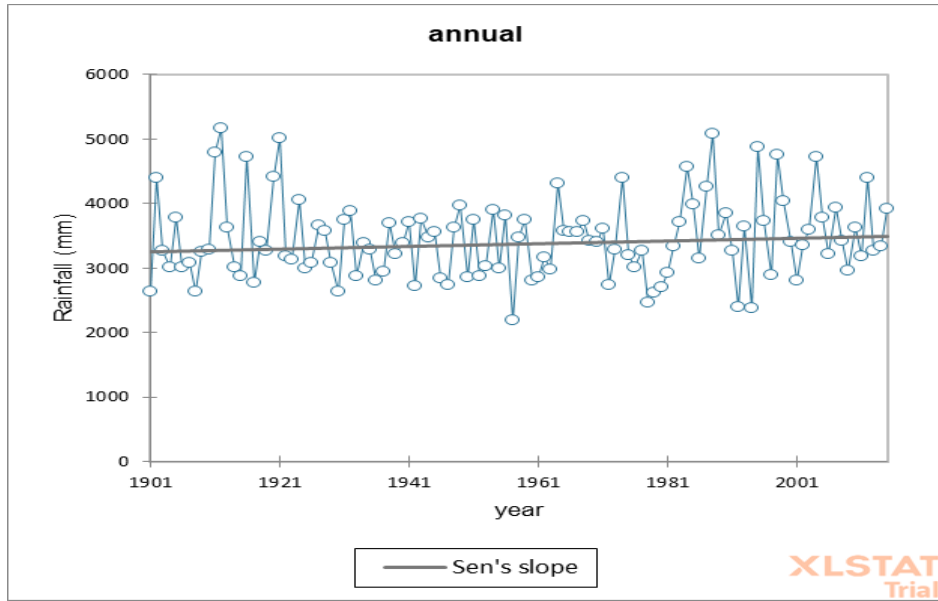


Fig 201. Trend Analysis of point 29

Point 30

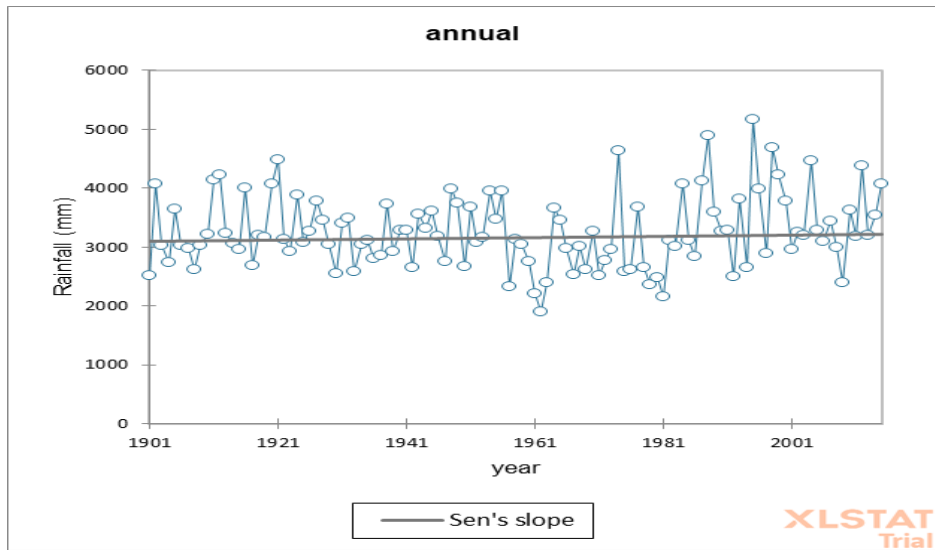


Fig 202. Trend Analysis of point 30

Point 31

Result:

- Points P29, P30 are showing increasing trend

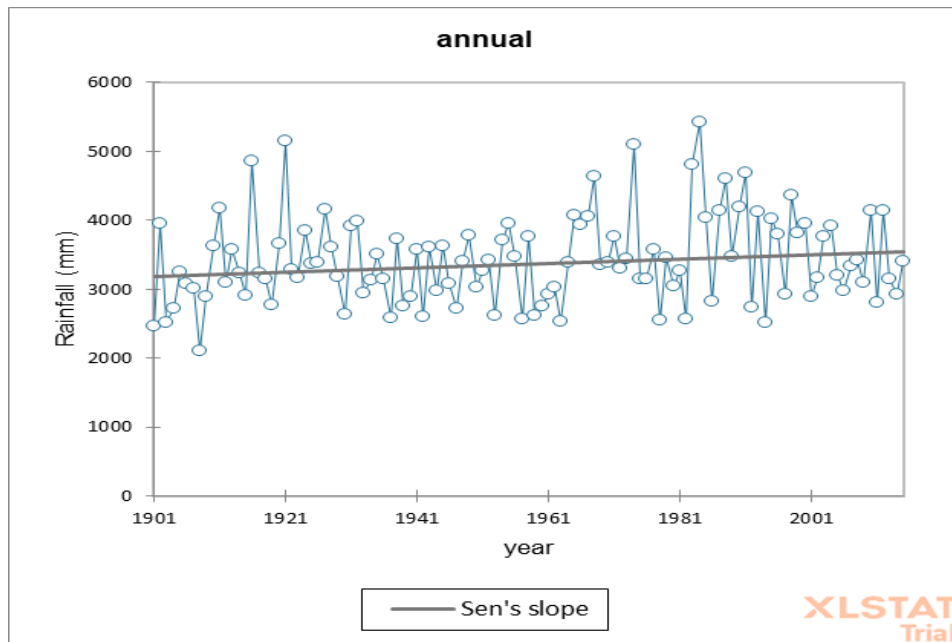


Fig 203. Trend Analysis of point 31

Result:

- Points P31 is showing increasing trend

Discussion

Graphical representation of the Sen-slope of annual rainfall pattern shows a mixed trend of increasing and decreasing rainfall overs different station in the specified areas.

Stations showing increasing rainfall trend are P2, P4, P5, P6, P9, P12, P14, P15, P16, P17, P18, P20, P29, P30, P31

Stations showing decreasing rainfall trend are P7, P8, P10, P11, P13, P21, P22, P23, P24, P25, P26, P27

4.1.3 Mann-Kendall Test

The data values were evaluated as ordered time series. Each data value was compared with all subsequent data values. The initial value of the Mann-Kendall statistic, S, is assumed to be 0 (e.g. no trend), if a data value from a later time period is higher than a data value from an earlier time period, S is incremented by 1. On the other hand, if a data value from a later time period is lower than a data value estimated earlier, S is decremented by 1. The net result of all such increments and decrements yields the final value of S (Drapela and Drapelova 2011). Let x_1, x_2, \dots, x_n represent n data points where x_j represents the data point at time j and x_k represent the data point at time k. Then the Mann-Kendall statistic (S) is given by the following formula:

$$S = \sum_{k=1}^{n-1} \sum_{j=k+1}^n \text{sign}(x_j - x_k)$$

$$\text{Sign}(x_j - x_k) = \begin{cases} 1 & \text{if } x_j - x_k > 0 \\ 0 & \text{if } x_j - x_k = 0 \\ -1 & \text{if } x_j - x_k < 0 \end{cases}$$

If n is 9 or less, the absolute value of S is compared directly to the theoretical distribution of S derived by Mann and Kendall (Gilbert, 1987). A very high positive value of S is an indicator of an increasing trend, and a very low negative value indicates a decreasing trend (Bihrat and Mehmetcik, (2003), Choudhury et al. (2012), Kazimierz and Leszek, 2012). If n is at least 10, the normal approximation test is used. For $n \geq 10$, the statistic S was approximately normally distributed with the mean (Drapela and Drapelova 2011) and variance as follows.

$$VAR(S) = \frac{1}{18} [n(n-1)(2n+5) - \sum_{p=1}^q t_p(t_p-1)(2t_p+5)]$$

Where, q = Number of tied groups, t_p = Number of data values in the pth group. The standard test statistic Z computed as follows

$$Z = \begin{cases} \frac{S-1}{\sqrt{VAR(S)}} & \text{if } S > 0 \\ 0 & \text{if } S = 0 \\ \frac{S+1}{\sqrt{VAR(S)}} & \text{if } S < 0 \end{cases}$$

The presence of a statistically significant trend was evaluated using the Z value. A positive value of Z indicates an upward trend and negative value of the Z indicates downward trend. In the present study, confidence level of 99, 95 and 90 % signify the positive ornegative trends determined bythe test

statistic. At the 99 % significance level, the null hypothesis of no trend is rejected if $|Z| > 2.575$; at the 95 % significance level, the null hypothesis of no trend is rejected if $|Z| > 1.96$; and at the 90 % significance level, the null hypothesis of no trend is rejected if $|Z| > 1.645$.

Table7: Mann-Kendall(M-K) test result (Winter)

Points	Minimum	Maximum	Mean	S	Var(S)	Slope	Z
P1	0	64.99998574	13.373129	-778	171130	-0.04973	-1.87827
P2	0	60.92981619	13.245829	-541	171149.7	-0.03306	-1.30529
P3	0	62.003	13.197	-631	171149.7	-0.035	-1.52283
P4	0	61.95	12.606	-603	171141.7	-0.029	-1.45519
P5	0	61.47	12.77	-633	171141.7	-0.034	-1.5277
P6	0	80.065	13.093	-588	171130	-0.031	-1.41898
P7	0	69.414	12.887	-769	171149.7	-0.044	-1.85641
P8	0.000	62.104	12.342	-470	171157.3	-0.029	-1.13364
P9	0.000	61.104	12.388	-467	171141.7	-0.024	-1.12644
P10	0.000	61.184	10.968	-572	170993.3	-0.025	-1.38085
P11	0.000	56.490	11.492	-301	171141.7	-0.014	-0.72518
P12	0.000	47.870	10.229	-728	171033.3	-0.031	-1.7579
P13	0.000	48.862	11.542	-417	171149.7	-0.023	-1.00555
P14	0.000	56.921	12.441	-100	171154.7	-0.004	-0.2393
P15	0.000	69.414	12.887	-769	171149.7	-0.044	-1.85641
P16	0.000	118.201	23.020	18	171157.3	0.002	0.041091
P17	0.000	94.774	18.451	-682	171157.3	-0.053	-1.64607
P18	0.000	428.892	22.291	-486	171157.3	-0.041	-1.17231
P19	0.000	49.239	12.329	-178	171033.3	-0.006	-0.42799
P20	0.000	55.112	14.848	-304	171154.7	-0.021	-0.7324
P21	0.000	220.750	16.072	-172	171130	-0.007	-0.41336
P22	0.000	81.573	18.440	-273	171149.7	-0.027	-0.65748
P23	0.000	58.995	13.790	-139	171093	-0.008	-0.33363
P24	0.000	87.124	16.282	-731	171141.7	-0.057	-1.76459
P25	0.000	68.684	16.072	-341	171141.7	-0.027	-0.82187
P26	0.000	292.525	25.923	-748	171033.3	-0.074	-1.80626
P27	0.000	143.188	19.382	-598	171114	-0.050	-1.44322
P28	0.000	49.821	12.760	-168	171130	-0.009	-0.4037
P29	0.000	65.794	13.386	-447	171149.7	-0.026	-1.07807
P30	0.000	56.390	13.575	-718	171154.7	-0.046	-1.7331
P31	0.000	53.888	13.295	-51	171093	-0.001	-0.12088

Table8: Mann-Kendall(M-K) test result (Pre-Monsoon)

Points	Minimum	Maximum	Mean	S	Var(S)	Slope	Z
P1	3.332	142.050	53.780	117	171158.3	0.017954	0.280388
P2	4.717854	153.3016	54.30827	433	171158.3	0.080	1.044202
P3	4.195	157.559	58.526	457	171158.3	0.094	1.102214
P4	1.860	160.160	55.393	369	171158.3	0.078	0.889506
P5	3.890	157.242	57.637	485	171158.3	0.107	1.169894
P6	8.189	188.234	60.321	583	171158.3	0.120	1.406773
P7	10.631	174.399	82.613	-705	171158.3	-0.148	-1.70166
P8	12.887	154.578	76.226	-389	171158.3	-0.082	-0.93785
P9	3.775	151.516	56.899	545	171158.3	0.109	1.314922
P10	3.420	142.297	59.670	-11	171158.3	-0.002	-0.02417
P11	14.203	181.058	79.742	-101	171158.3	-0.021	-0.24171
P12	24.749	213.756	88.936	899	171158.3	0.205	2.170588
P13	50.702	301.988	140.004	-145	171158.3	-0.041	-0.34807
P14	41.475	337.003	147.592	441	171158.3	0.133	1.06354
P15	10.631	174.399	82.613	-705	171158.3	-0.148	-1.70166
P16	54.173	497.414	146.381	863	171158.3	0.293	2.083571
P17	45.380	335.751	146.449	1449	171158.3	0.407	3.500012
P18	56.372	469.830	188.489	135	171158.3	0.051	0.323896
P19	55.032	393.745	158.008	201	171158.3	0.073	0.483427
P20	53.605	309.826	154.506	1085	171158.3	0.343	2.620175
P21	18.311	393.810	164.720	-407	171158.3	-0.180	-0.98136
P22	90.947	460.859	206.348	-499	171158.3	-0.198	-1.20373
P23	57.319	529.890	209.859	257	171158.3	0.138	0.618787
P24	69.165	617.324	232.732	-177	171158.3	-0.095	-0.42542
P25	64.370	666.185	247.011	-151	171158.3	-0.072	-0.36257
P26	46.206	566.820	253.349	-575	171158.3	-0.367	-1.38744
P27	56.514	573.879	245.446	-75	171158.3	-0.040	-0.17887
P28	67.201	486.156	180.347	65	171158.3	0.022	0.154697
P29	58.592	501.053	202.438	359	171158.3	0.190	0.865334
P30	66.638	457.008	212.084	523	171158.3	0.226	1.261745
P31	67.387	457.539	179.223	727	171158.3	0.272	1.75484

Table9: Mann-Kendall(M-K) test result (Monsoon)

Points	Minimum	Maximum	Mean	S	Var(S)	Slope	Z
P1	138.038	497.972	281.864	219	171158	0.108658	0.526936
P2	121.694	548.595	289.185	255	171158	0.110	0.613952
P3	161.046	579.583	294.466	127	171158	0.071	0.304559
P4	138.631	605.590	303.695	583	171158	0.311	1.406773
P5	163.663	580.982	298.369	175	171158	0.087	0.420582
P6	123.287	572.647	293.386	-117	171158	-0.066	-0.28039
P7	170.834	603.917	340.278	-1189	171158	-0.635	-2.87156
P8	175.840	606.402	352.368	-1181	171158	-0.715	-2.85222
P9	174.029	569.065	300.351	173	171158	0.101	0.415747
P10	106.538	481.716	286.011	-851	171158	-0.362	-2.05457
P11	185.362	615.571	389.064	-613	171158	-0.388	-1.47929
P12	175.142	819.370	456.670	809	171158	0.607	1.953045
P13	344.457	877.341	630.150	-853	171158	-0.751	-2.0594
P14	311.802	1003.474	667.705	-153	171158	-0.114	-0.3674
P15	170.834	603.917	340.278	-1189	171158	-0.635	-2.87156
P16	397.344	867.807	558.558	293	171158	0.160	0.705804
P17	394.128	1114.345	618.931	2341	171158	1.726	5.656097
P18	347.189	1090.859	714.889	489	171158	0.407	1.179562
P19	354.690	1016.530	615.127	-261	171158	-0.231	-0.62846
P20	359.946	1087.477	670.497	611	171158	0.441	1.474453
P21	102.186	1125.905	629.340	-713	171158	-0.733	-1.721
P22	354.513	1311.328	791.544	-949	171158	-0.889	-2.29144
P23	406.875	1122.355	729.460	-439	171158	-0.391	-1.05871
P24	435.992	1111.573	757.180	-1149	171158	-1.272	-2.77487
P25	336.857	1172.317	719.922	-1089	171158	-1.172	-2.62984
P26	200.939	2416.617	955.665	-1323	171158	-2.119	-3.19545
P27	282.950	1284.085	839.321	-691	171158	-0.862	-1.66782
P28	335.056	1714.883	619.005	59	171158	0.066	0.140194
P29	367.268	1105.116	658.753	437	171158	0.373	1.053871
P30	350.848	1012.840	605.994	151	171158	0.123	0.36257
P31	407.964	1033.043	671.765	665	171158	0.615	1.604978

Table10: Mann-Kendall(M-K)Test result (Post-Monsoon)

Points	Minimum	Maximum	Mean	S	Var(S)	Slope	Z
P1	3.432194	172.1554	43.41611	87	171158.3	0.014871	0.207874
P2	1.029	177.057	42.729	111	171158.3	0.018	0.265885
P3	1.812	179.915	41.765	-23	171158.3	-0.003	-0.05318
P4	0.342	175.126	39.622	-157	171158.3	-0.024	-0.37707
P5	0.904	176.195	39.666	-147	171158.3	-0.023	-0.3529
P6	0.939	175.567	40.644	-133	171158.3	-0.022	-0.31906
P7	2.127	169.421	44.451	-385	171158.3	-0.072	-0.92818
P8	2.935	173.429	42.704	-287	171158.3	-0.051	-0.6913
P9	0.835	176.971	38.579	-93	171158.3	-0.019	-0.22238
P10	0.264	164.201	36.255	-249	171158.3	-0.047	-0.59945
P11	1.140	170.364	40.449	-393	171158.3	-0.076	-0.94752
P12	0.155	157.519	40.747	-297	171158.3	-0.037	-0.71547
P13	4.948	226.841	56.688	-587	171158.3	-0.127	-1.41644
P14	3.855	216.835	60.011	-71	171158.3	-0.017	-0.1692
P15	2.127	169.421	44.451	-385	171158.3	-0.072	-0.92818
P16	4.130	219.452	51.598	675	171158.3	0.144	1.629149
P17	8.490	228.297	55.731	929	171158.3	0.176	2.243102
P18	11.904	216.489	64.867	163	171158.3	0.033	0.391576
P19	5.105	186.324	54.141	43	171158.3	0.010	0.10152
P20	6.689	222.857	60.814	457	171158.3	0.105	1.102214
P21	4.312	194.863	56.452	-479	171158.3	-0.112	-1.15539
P22	7.919	166.229	67.308	-503	171158.3	-0.121	-1.2134
P23	0.788	194.268	63.657	-117	171158.3	-0.031	-0.28039
P24	10.195	179.110	64.299	-573	171158.3	-0.137	-1.3826
P25	4.905	176.877	65.507	-387	171158.3	-0.098	-0.93301
P26	0.181	287.246	86.994	-601	171158.3	-0.207	-1.45028
P27	12.230	364.218	72.885	-577	171158.3	-0.141	-1.39227
P28	1.524	176.683	59.602	-243	171158.3	-0.066	-0.58495
P29	2.591	262.207	61.810	-227	171158.3	-0.060	-0.54627
P30	4.523	204.218	59.621	-181	171158.3	-0.043	-0.43508
P31	4.702	176.769	58.069	75	171158.3	0.016	0.178868

Table 11: Mann-Kendall(M-K) testresult (Annual)

Points	Minimum	Maximum	Mean	S	Var(S)	Slope	Z
P1	757.8632	2252.623	1445.79	183	171158.3	0.381124	0.439919
P2	692.899	2446.488	1474.345	331	171158.3	0.860	0.797655
P3	903.140	2549.689	1505.128	223	171158.3	0.542	0.536604
P4	763.201	2867.902	1525.041	617	171158.3	1.721	1.488955
P5	915.698	2754.122	1510.925	273	171158.3	0.792	0.657461
P6	829.769	2631.836	1502.628	27	171158.3	0.071	0.062846
P7	1022.618	2886.935	1768.076	-1337	171158.3	-3.535	-3.22929
P8	915.768	2893.912	1790.945	-1357	171158.3	-3.676	-3.27764
P9	894.623	2728.703	1512.615	215	171158.3	0.605	0.517267
P10	633.404	2533.697	1642.794	-743	171158.3	-1.735	-1.79351
P11	904.195	3044.955	1939.814	-671	171158.3	-1.758	-1.61948
P12	946.693	3554.382	2236.189	961	171158.3	3.023	2.32045
P13	1739.565	4160.603	3133.761	-1015	171158.3	-3.333	-2.45098
P14	1591.329	4722.709	3318.510	-19	171158.3	-0.044	-0.04351
P15	1022.618	2886.935	1768.076	-1337	171158.3	-3.535	-3.22929
P16	1903.435	4236.775	2874.207	895	171158.3	2.722	2.160919
P17	1850.621	5275.900	3119.166	2473	171158.3	8.987	5.975159
P18	1697.784	6007.667	3664.204	577	171158.3	2.398	1.39227
P19	1822.640	5300.590	3121.613	-69	171158.3	-0.366	-0.16437
P20	1778.356	5102.094	3357.644	975	171158.3	3.439	2.35429
P21	526.082	5832.280	3213.018	-449	171158.3	-2.261	-1.08288
P22	1771.804	6729.252	4024.020	-933	171158.3	-4.006	-2.25277
P23	2235.839	5700.314	3765.967	-307	171158.3	-1.464	-0.73964
P24	2113.637	5853.271	3952.376	-1099	171158.3	-5.448	-2.65401
P25	1979.992	6364.036	3849.385	-925	171158.3	-5.139	-2.23343
P26	1032.422	12304.82	4895.536	-1217	171158.3	-9.698	-2.93924
P27	1393.487	7063.812	4351.038	-711	171158.3	-4.081	-1.71617
P28	2197.304	7763.626	3221.391	-23	171158.3	-0.069	-0.05318
P29	2197.032	5161.165	3454.526	453	171158.3	2.020	1.092545
P30	1898.629	5168.479	3266.241	297	171158.3	1.141	0.715472
P31	2100.835	5423.578	3425.528	785	171158.3	3.194	1.895034

4.2 District-wise discussion of the results

WINTER SEASON

District	Stations	Mann-Kendall	Sen-slope	ITA
MALDA	P1, P2, P3, P4, P5	Decreasing	Decreasing	Decreasing
DAKSHIN DINAJPUR	P6, P7, P8	Decreasing	decreasing	Decreasing
UTTAR DINAJPUR	P9, P10, P11, P12, P13	Decreasing	Decreasing	Decreasing
DARJELLING	P14, P15, P16	Decreasing	Decreasing	Decreasing
KALIMPONG	P17, P18	Decreasing	Decreasing	No Change
JALPAIGURI	P19, P20, P21, P22	Decreasing	Decreasing	Decreasing
ALIPURDUAR	P23, P24, P25, P26, P27	Decreasing	Decreasing	Decreasing
COOCH BEHAR	P28, P29, P30, P31	Decreasing	Decreasing	Decreasing

PRE-MONSOON SEASON

District	Stations	Mann-Kendall	Sen-slope	ITA
MALDA	P1, P2, P3, P4, P5	Increasing	Increasing	Increasing
DAKSHIN DINAJPUR	P6, P7, P8	Decreasing	Decreasing	Decreasing
UTTAR DINAJPUR	P9, P10, P11, P12, P13	Increasing	Increasing	Decreasing
DARJELLING	P14, P15, P16	Increasing	Increasing	Increasing
KALIMPONG	P17, P18	Increasing	Increasing	Increasing
JALPAIGURI	P19, P20, P21, P22	Increasing	Increasing	Decreasing
ALIPURDUAR	P23, P24, P25, P26, P27	Decreasing	Decreasing	Decreasing
COOCH BEHAR	P28, P29, P30, P31	Increasing	Increasing	Decreasing

MONSOON SEASON

District	Stations	Mann-Kendall	Sen-slope	ITA
MALDA	P1, P2, P3, P4, P5	Increasing	Increasing	Increasing
DAKSHIN DINAJPUR	P6, P7, P8	Decreasing	Decreasing	Decreasing
UTTAR DINAJPUR	P9, P10, P11, P12, P13	Decreasing	Decreasing	Decreasing
DARJELLING	P14, P15, P16	Decreasing	Increasing	Increasing
KALIMPONG	P17, P18	Increasing	Increasing	Increasing
JALPAIGURI	P19, P20, P21, P22	Decreasing	Decreasing	Decreasing
ALIPURDUAR	P23, P24, P25, P26, P27	Decreasing	Decreasing	Decreasing
COOCH BEHAR	P28, P29, P30, P31	Increasing	Increasing	Increasing

POST-MONSOON SEASON

District	Stations	Mann-Kendall	Sen-slope	ITA
MALDA	P1, P2, P3, P4, P5	Decreasing	No change	Increasing
DAKSHIN DINAJPUR	P6, P7, P8	Decreasing	Decreasing	Decreasing
UTTAR DINAJPUR	P9, P10, P11, P12, P13	Decreasing	Decreasing	Decreasing
DARJELLING	P14, P15, P16	Decreasing	Increasing	Increasing
KALIMPONG	P17, P18	Increasing	Increasing	Increasing
JALPAIGURI	P19, P20, P21, P22	No change	Decreasing	Increasing
ALIPURDUAR	P23, P24, P25, P26, P27	Decreasing	Decreasing	Decreasing
COOCH BEHAR	P28, P29, P30, P31	Decreasing	Decreasing	Decreasing

ANNUAL

District	Stations	Mann-Kendall	Sen-slope	ITA
MALDA	P1, P2, P3, P4, P5	Increasing	Increasing	Decreasing
DAKSHIN DINAJPUR	P6, P7, P8	Decreasing	Decreasing	Decreasing
UTTAR DINAJPUR	P9, P10, P11, P12, P13	Decreasing	Decreasing	Decreasing
DARJELLING	P14, P15, P16	Decreasing	Increasing	Increasing
KALIMPONG	P17, P18	Increasing	Increasing	Increasing
JALPAIGURI	P19, P20, P21, P22	Decreasing	Decreasing	Decreasing
ALIPURDUAR	P23, P24, P25, P26, P27	Decreasing	Decreasing	Decreasing
COOCH BEHAR	P28, P29, P30, P31	Increasing	Increasing	Increasing

CHAPTER 5

5.1 CONCLUSION

Being an agriculture-based economy like India and so West-Bengal, understanding of rainfall trend becomes important. In this thesis we tried to understand rainfall trend of **Northern West-Bengal** over a period of time (1901-2015) using three different methods

1. Innovative trend analysis
2. Mann-Kendall analysis
3. Sen slope estimation

and came on few conclusions such as

- **Winter season** is exhibiting a Decreasing trend in rainfall over the given period of time.
 - **Pre-Monsoon season** is showing a mixed trend in rainfall change but in extreme north (Himalayan region) as Kalimpong and Darjeeling, increasing trend can be seen.
 - **Monsoon season** also exhibit a mixed or No change trend in rainfall pattern but again we can see increasing trend in Himalayan districts.
 - **Post-Monsoon season** is also showing Decreasing trend in general over the study area but again we can see increasing trend in the Himalayan districts (Darjeeling and Kalimpong).
 - **Annual** change in the rainfall also shows a mixed or No change in the trend in general but we can see increasing trend in Himalayan districts (Kalimpong and Darjeeling).
-
- **Malda** district is always showing an increasing trend except in winter season.
 - **Dakshin Dinajpur** is always showing a decreasing trend.
 - **Uttar Dinajpur** is always showing a decreasing trend except in winter season.
 - **Alipurduar** is always showing a decreasing trend.

CHAPTER 6

6.1 FUTURE SCOPE

This whole thesis is done to understand the rainfall pattern and the change in its trend over the years.

We have used monthly rainfall data of 31 stations of eight districts in northern part of west Bengal.

These districts include Malda, Dakshin Dinajpur, Uttar Dinajpur, Darjeeling, Kalimpong, Alipurduar, Cooch Behar, Jalpaiguri.

We used three methods to analyse the trend

- Innovative trend analysis
- Sen slope method
- Mann-Kendall analysis

In the same way we can analyse whole west Bengal or whole India too.

We can use also some other methods such as

- Modified Mann-Kendall analysis
- Regression test
- Kendall rank correlation
- Spearman rank correlation test etc.

CHAPTER 7

7.1 REFERENCES

Anurag Malik & Anil Kumar & Quoc Bao Pham & Senlin Zhu & Nguyen Thi Thuy Linh & Doan Quang Tri, Identification of EDI trend using Mann-Kendall and Sen-Innovative Trend methods (Uttarakhand, India).

Ay M, Kisi O (2015) Investigation of trend analysis of monthly total precipitation by an innovative method. *Theor Appl Climatol* 120: 617–629.

Bihrat O. and B. Mehmetcik. 2003. Power of statistical tests for trend detection. *Turkish J. Eng. Env. Sci.* 27:247 - 251.

Centre-Research report, India Meteorological Department, Pune, India.

Chung CE, Ramanathan V. (2006), Weakening of North Indian SST Gradients and the Monsoon Rainfall in India and the Sahel. *Journal of Climate*, Vol. 19, pp. 2036-2045.

Cui L, Wang L, Lai Z, Tian Q, Liu W, Li J (2017) Innovative trend analysis of annual and seasonal air temperature and rainfall in the Yangtze River basin, China during 1960-2015. *J Atmos Sol Terr Phys* 164:48–59

Choudhury B U, D Anup, S V Ngachan, A Slong, L J Bordoloi and P Chowdhury. 2012. Trend analysis of long-term weather variables in mid-altitude Meghalaya, north-east India. *Jour. of Agricultural Physics*, 12, (1):12-22.

Das, S., Dey, S. and Dash, S.K. (2016) Direct radiative effects of anthropogenic aerosols on Indian summer monsoon circulation. *Theoretical and Applied Climatology*, 124(3–4), 629–639.

Dabanli I, Şen Z, Yeleğen MÖ, Şişman E, Selek B, Güçlü YS (2016) Trend assessment by the innovative Sen method. *Water Resour Manag* 30(14):5193–5203

Drapela K and I Drapelova. 2011. Application of Mann-Kendall test and the Sen's slope estimates for trend detection in deposition data from Bily Kriz (Beskydy Mts., the Czech Republic) 1997-2010.

Guhathakurta P, Rajeevan M. (2008), Trends in rainfall pattern over India. *International Journal of Climatology*, Vol. 28, pp. 1453-1469.

Guhathakurta, P. and Rajeevan, M. (2006) Trends in Rainfall Patterns over India, National Climate.

Guhathakurta, P. and Saji, E. (2012) Trends and Variability of Monthly, Seasonal and Annual Rainfall for the Districts of Maharashtra and Spatial Analysis of Seasonality Index in Identifying the Changes in Rainfall Regime, NCC research report.

Güçlü YS, Dabanli I, Şişman E, Şen Z (2018) Air quality (AQ) identification by innovative trend diagram and AQ index combinations in Istanbul megacity. *Atmos Pollut Res.* <https://doi.org/10.1016/j.apr.2018.06.011>

Gilbert R O. 1987. Statistical methods for environmental pollution monitoring. Van Nostrand Reinold, ISBN 0-471-28878-0, New York

Jeffrey Denzil K. Marak & Arup Kumar Sarma & Rajib Kumar Bhattacharjya, Innovative trend analysis of spatial and temporal rainfall variations in Umiam and Umtru watersheds in Meghalaya, India.

Kisi O (2015) An innovative method for trend analysis of monthly panevaporations. J Hydrol 527:1123–1129.

Kisi O, Santos CAG, Silva RMD, Zounemat-Kermani M (2018) Trendanalysis of monthly treamflows using Sen’s innovative trend method.Geofizika 35(1):53–68

Kisi O, AyM (2014) Comparison of Mann–Kendall and innovative trendmethod for water quality parameters of the KizilirmakRiver,Turkey. J Hydrol 513:362–375

Kazimierz B. and H. Leszek. 2012. Long-term changes in runofffrom a small agricultural catchment. Soil and Water Res.,7, (2):64-72.

Mohorji AM, Şen Z, Almazroui M (2017) Trend analyses revision andglobal monthly temperature innovative multi-duration analysis.Earth Syst Environ. <https://doi.org/10.1007/s41748-017-0014-x>

Pathak, A., Ghosh, S., Kumar, P. and Murtugudde, R. (2017) Role of oceanic and terrestrial atmospheric moisture sources in intraseasonal variability of Indian summer monsoon rainfall. Scientific Reports, 7(1), 1–11.

Shastri, H., Paul, S., Ghosh, S. and Karmakar, S. (2015) Impacts of urbanization on Indian summer monsoon rainfall extremes. Journal of Geophysical Research: Atmospheres, 120(2), 496–516.

Salvi, K. and Ghosh, S. (2019) A kaleidoscopic research memoir on Indian summer monsoon rainfall. Mausam, 70(2), 293–298.

Şen Z (2012) An innovative trend analysis methodology. J HydrolEng 17(9):1042–1046

Şen Z (2014) Trend identification simulation and application. J HydrolEng 19(3):635–642

Şen Z (2017) Innovative trend significance test and applications. TheorApplClimatol 127:939–947

Şen Z (2018) Crossing trend analysis methodology and application forTurkish rainfall records. TheorApplClimatol 131:285–293

Wu H, Qian H (2017) Innovative trend analysis of annual and seasonalrainfall and extreme values in Shaanxi, China, since the 1950s. Int JClimatol 37:2582–2592

Wu H, Li X, Qian H (2018) Detection of anomalies and changes ofrainfall in the Yellow River basin, China, through two graphicalmethods. Water. <https://doi.org/10.3390/w10010015>

Zhou Z, Wang L, Lin A, Zhang M, Niu Z (2018) Innovative trend analysisof solar radiation in China during 1962–2015. Renew Energy119:675–689

Choudhury, B.U., Anup, D., Ngachan, S.V., Slong, A., Bordoloi, L.J. and Chowdhury, P. (2012) ‘Trend analysis of long-term weather variables in mid-altitude Meghalaya, north-east India’, Jour.of Agricultural Physics, Vol. 12, No. 1, pp.12–22.

de Luís, M., Raventós, J., González-Hidalgo, J.C., Sánchez, J.R. and Cortina, J. (2000) ‘Spatial analysis of rainfall trends in the region of Valencia (East Spain)’, Int. J. Climatol., Vol. 20, No. 12, pp.1451–1469.

Guhathakurta, P. and Saji, E. (2013) ‘Detecting changes in rainfall pattern and seasonality index vis-à-vis increasing water scarcity in Maharashtra’, J. Earth Syst. Sci., Vol. 122, No. 3,pp.639–649.

Jagadeesh, P. and Agrawal, S. (2015) ‘Investigation of trends and its magnitude by non-parametric

Mann-Kendall and Sen's slope methods', Int. J. Hydrology Science and Technology, Vol. 5,
No. 1, pp.83–94.